AFDELINGEN FOR

BÆRENDE KONSTRUKTIONER

DANMARKS TEKNISKE HØJSKOLE

STRUCTURAL RESEARCH LABORATORY

TECHNICAL UNIVERSITY OF DENMARK

H. Daniel Ramirez

BUCKLING OF PLATES BY THE RITZ METHOD USING PIECEWISE-DEFINED FUNCTIONS

RAPPORT NR. R 28 1972

PREFACE

The work reported here has been carried out during my stay at the Structural Research Laboratory headed by Prof. K.W. Johansen. This thesis is to be submitted to the Technical University of Denmark as partial requirement for the "Lic. Techn." degree.

May 1972

H. Daniel Ramirez B.

CONTENTS

INTRODUCTION

The readers who are interested mainly in the numerical computations are advised to skip the first two chapters with the exception of Art. 2.9, which contains a summary of previous numerical calculations of buckling loads for plates.

In Charpter 1 a discussion is given of the buckling equations for plates by means of a two dimensional theory. The purpose was not to find new equations but to look into the assumptions included in the derivation of the classical buckling equations. The buckling equations for initially flat plates decouple into two systems: 1) lateral buckling, where the increment of in-plane displacements is zero and 2) in-plane buckling, where the plate remains flat. The use of general nonlinear strain measures leads to the classical equations of lateral buckling of plates. Such equations include as a known quantity the initial nonlinear plane stress field at the bifurcation point and also include a linear bending measure. A further simplification is made by assuming a geometrically linear initial stress state. The resulting buckling equations can be extended for dynamic and follower forces.

Chapter 2 presents a summary of the trial function methods in common use. This material has been collected from diverse sources in the literature and includes some consideration of the boundary and continuity conditions which trial functions ought to satisfy.

It is not widely known that trial functions for the Galerkin method in many cases need only satisfy the same boundary conditions as the Ritz method. As for example, the application of Green's formula to Galerkin's orthogonality conditions, in the case of dynamic buckling of plates, leads to expressions which accept trial functions that only satisfy the specified homogeneous deflections and slopes.

The convergence in energy of the Ritz method is extended to inhomogeneous boundary conditions for boundary value problems and also extended to eigenvalue problems where the functions satisfy only homogeneous geometrical boundary conditions. The Ritz convergence is investigated in a closer way for the plane stress and lateral buckling plate problems. It turns out that in the plane stress problem the stresses and displacements converge in the mean to their exact values. In the buckling problem, the flexural moments and first derivatives obtained from the normalized Ritz solution converge in the mean to the values obtained by using the normalized exact solution. The normalized Ritz solution converges uniformly to the normalized exact solution.

In Chapter 2 it is also established that when expanding the exact solution in terms of an infinite number of coordinate functions, the Ritz parameters converge uniformly to the "exact" parameters of the expansion.

The method employed in Chapter 4 has been called Ritz-Subdomain method since local trial functions are defined on subdomains in such a way as to satisfy the continuity and boundary conditions required by the Ritz method for the entire domain. This particular case of the Ritz method has been termed "conforming finite element" elsewhere in the literature. In the finite element a structure is divided up in a finite number of parts which are interconnected at points called nodal points where continuity conditions are enforced. Consequently a stiffened plate may be analysed by connecting plate and beam elements at nodal points. On the other hand in the Ritz-Subdomain method, the displacement field is expressed in a piecewise form satisfying the continuity and geometrical boundary condition everywhere in the problem's domain of definition. In the Ritz-Subdomain's analysis of plates it is not possible to speak of beam elements by themselves since stiffeners are assumed to follow the plate's displacement pattern.

The trial functions in the Ritz-Subdomain method contain parameters which have physical significance. The application of the convergence criterion to such parameters leads to the conclusion that the physical quantities represented by the parameters converge uniformly towards their exact nodal values. The use of nodal parameters which represent in-plane displacements and their first derivatives when solving a plane stress analysis leads to uniform convergence of nodal stresses and nodal displacements towards their exact nodal values. Similarly the use of nodal parameters which represent normal deflections w together with their first and second mixed derivatives when solving lateral buckling problems leads to uniform convergence of the nodal quantities w, $w_{,\alpha}$ and $w_{,12}$ towards their exact nodal values (in a normalized form).

In Chapter 4 various numerical comparisons for rectangular plates are performed between the Ritz-Subdomain's results and other analytical or approximate results. The alternative results are given in Chapter 5. A Ritz-Subdomain's solution which gives discontinuous shearing forces only along intermediate stiffeners results in very accurate stresses when compared to an analytical solution of the same problem. When the plate does not have intermediate stiffeners the Ritz-Subdomain provides a continuous stress field. This is a very convenient result when the distribution of in-plane stresses for rectangular plates is sought.

Buckling loads for stiffened plates analysed by the Ritz-Subdomain method and analytical results are also in close agreement for non-complicated but discontinuous in-plane stresses. The buckling loads obtained by the Ritz method for more complicated discontinuous in-plane stresses were more accurate than the buckling loads obtained by a usual Ritz method which employs the exact in-plane stress distribution.

The conclusion is that the Ritz-Subdomain method presented in Chapter 3 gives very accurate plane stresses and buckling loads for rectangular stiffened plates (or unstiffened) for any in-plane load distribution and geometrical boundary condition. The discontinuous character of exact eigenvalue solutions to stiffened plates is better represented by the Ritz-Subdomain's discontinuous solutions than the usual Ritz continuous solutions.

1. BUCKLING EQUATIONS FOR PLATES.

1.1. Bifurcation Problem of Stability.

A mechanical system is assumed to be subjected to external loads which are the product of a unit load system and a single parameter P. When the loads are conservative nongyroscopic (Ziegler [1]), there exists a potential energy π consisting of the elastic strain energy and the work of the external loads.

Those structures whose behavior under loading is characterized by a bifurcation point (Koiter [2]) will be considered. Fig. 1.1 shows a typical graph of the parameter P versus the displacement component V at an unrestrained point of a mechanical system, which exhibits a bifurcation phenomena when $P = P_c$. In the figure, the displacements V, U* and U are supposed to be components of the vectors $\vec{V}$, $\vec{U}^*$ and $\vec{U}$ respectively.

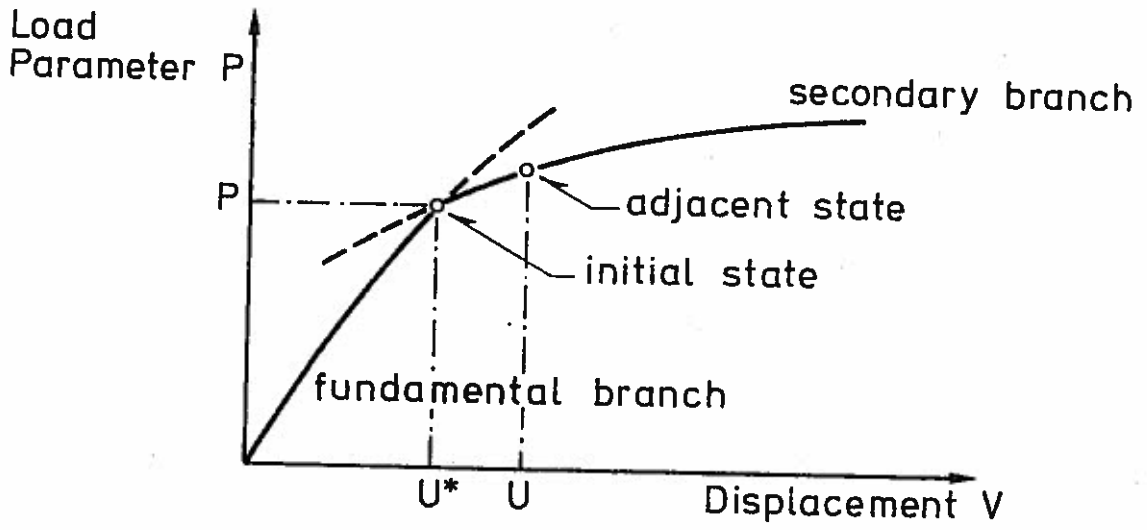

Fig. 1.1. Bifurcation Problem of Elastic Bodies.

In the fundamental branch of equilibrium (Fig. 1.1), the displacement vector $\vec{V}$ is a single-valued continuously differentiable function of the load parameter P in the range $0 \leq P \leq P_c$ and vanishes for P = 0. However, at the critical value of the parameter, $P = P_c$, a qualitative change in the deformation pattern

occurs; an alternative solution to the equations of equilibrium branches off. This new branch has been termed secondary branch in Fig. 1.1.

To the adjacent state of equilibrium $\vec{U}^* + \vec{U}$ (Fig. 1.1) corresponds a potential energy $\pi(\vec{U}^* + \vec{U})$, while to the initial state of equilibrium $\vec{U}^*$ corresponds the potential energy $\pi(\vec{U}^*)$. For continuous bodies and loads, π is a functional consisting of several definite integrals; therefore if $\vec{U}$ is sufficiently small, the integrands of $\pi\ (\vec{U}^* + \vec{U})$ may be expanded in power series of the displacements $\vec{U}$ and its derivatives, as follows:

$$\pi(\vec{U}^* + \vec{U}) = \pi(\vec{U}^*) + \pi_1(\vec{U}) + \pi_2(\vec{U}) + \cdots \tag{1.1}$$

where the subscript of the right hand indicates the order of the derivatives included in each term.

Following Koiter [2], the critical point of equilibrium is defined when a small nonvanishing displacement $\vec{U}$ satisfies the condition:

$$\min\ \pi_2(\vec{U}) = 0 \tag{1.2}$$

or in the notation of variational calculus

$$\delta\pi_2(\vec{U}) = 0 \tag{1.3}$$

The expression (1.3) defines a variational problem which leads to the determination of the critical value of the parameter P_c.

The Euler Method of Stability, as explained by Washizu [3], consists in the application of the principle of virtual work to the adjacent position of equilibrium $\vec{U}^* + \vec{U}$, neglecting terms which involve expressions of $\vec{U}$ and its derivatives of order higher than quadratic. For conservative systems, this means neglecting in (1.1) all terms with subscript greater than two

and afterwards applying the principle of stationary potential energy to the state $\vec{U}^* + \vec{U}$, which results in:

$$\delta\pi(\vec{U}^* + \vec{U}) = \delta\pi_2(\vec{U}) = 0 \qquad (1.4)$$

given the fact that the initial state is in equilibrium and therefore $\delta\pi_1(\vec{U}) = 0$.

Eq. (1.4) shows that the Euler Method of Stability and the criterium (1.3) are equivalent for censervative systems. However, when the loads are nonconservative, the Euler Method can still be applied. For this reason it appears convenient to use Euler's Method for the study of stability problems at the critical point.

1.2 Nonlinear Theory of Plates.

Introduction.

A nonlinear theory for plates is presented, which meets the following requirements:

a) The statical and geometrical field equations allow the definition of a virtual work equation.

b) The laws of Nature, such as Newton's law (i.e. equilibrium equations) are satisfied.

c) The theory is two dimensional in the sense that the middle surface of the plate determines the properties of the plate.

Using nonlinear axial and bending measures a virtual work expression is established. However, geometrical simplifications are later introduced for linearizing the bending measure and thus resulting in simpler field equations.

Geometrical considerations.

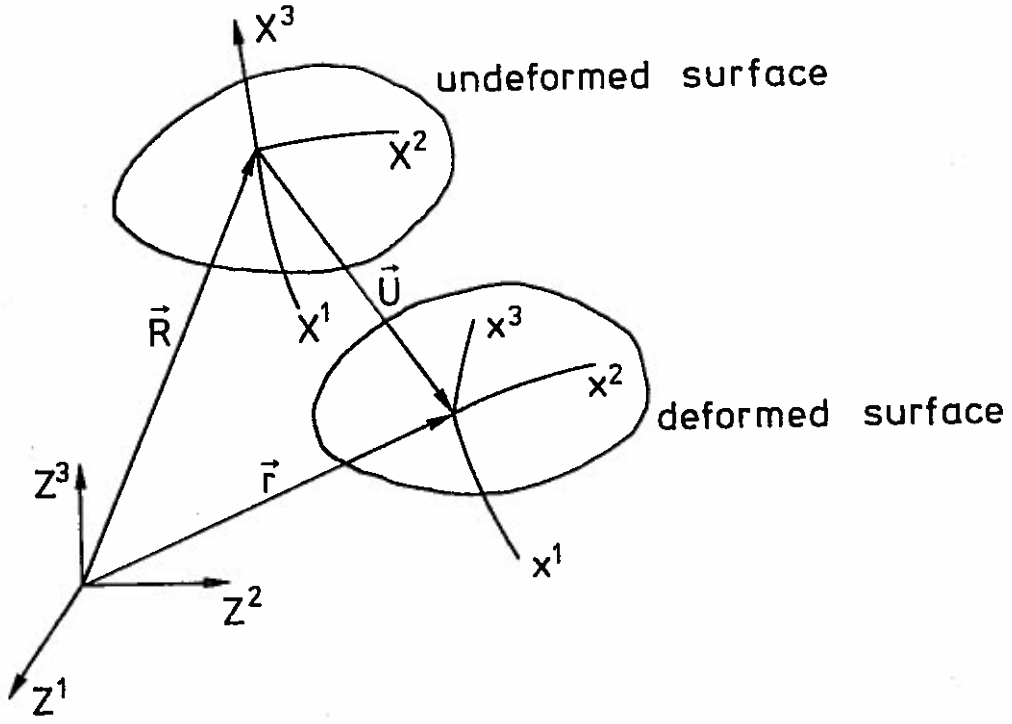

Fig. 1.2. Coordinate Systems for a Surface.

The following notation is used:

- Latin indices can take values 1, 2, 3. Greek indices take values 1,2.
- The summation convention indicates that repeated indices in a term are equivalent to the sum in the range of the index.

  Two sets of coordinates are shown in Fig. 1.2: The material coordinates X^I on the undeformed configuration, and the spatial coordinates x^i on the deformed configuration; both refer to the fixed cartesian frame Z^I.
- Any quantity refered to the material coordinates is written in majuscules, and components of vectors and tensors

by indices also in majuscules. In analogous manner for spatial coordinates, the quantities are denoted by minuscules, and the component of vectors and tensors by indices also in minuscules.

- Convected coordinates are adopted for the spatial coordinate system. Which means that the parameters designating a point in material coordinates in the undeformed configuration have the same values as the parameters which locate that point in the deformed configuration in spatial coordinates ($x^i = X^I$)

- Differentiation is abreviated by a comma $w_{,I} = \frac{\partial w}{\partial X^I}$

- The base vectors and fundamental metric tensors for three dimensions are (see Green and Zerna [4])

$$\vec{G}_I = \vec{R}_{,I} \tag{1.5}$$

$$G_{IJ} = \vec{G}_I \cdot \vec{G}_J \tag{1.6}$$

$$\vec{G}^R \cdot \vec{G}_S = \delta^R_S \tag{1.7}$$

$$G^{RS} = \vec{G}^R \cdot \vec{G}^S \tag{1.8}$$

where δ^R_S is the Kronecker's delta tensor and (1.7) defines the covariant base vectors.

- The components of $\vec{G}_{I,J}$ define the Christoffel symbols by:

$$\vec{G}_{I,J} = \left\{ \begin{matrix} K \\ I\,J \end{matrix} \right\} \vec{G}_K \tag{1.9}$$

- Covariant differentiation is denoted by a vertical line:

$$V^I\big|_J = V^I{}_{,J} + \left\{ \begin{matrix} I \\ K\,J \end{matrix} \right\} V^K \tag{1.10}$$

$$V_I\big|_J = V_{I,J} - \left\{ \begin{matrix} K \\ I\,J \end{matrix} \right\} V_K \tag{1.11}$$

$$\vec{V}_{,I} = V^K\big|_I \vec{G}_K = V_K\big|_I \vec{G}^K \tag{1.12}$$

- For spatial coordinates, minuscules are used to obtain analogous formulas to (1.5) .... (1.12).

- In order to define surface tensors, the X^3 axis is made parallel to the Z^3 axis.

The surface base vectors on the undeformed state are denoted $\vec{A}_\alpha$, $\vec{A}_3$, where $\vec{A}_3$ is a unit vector parallel to Z^3 axis. On the deformed surface the base vectors are $\vec{a}_\alpha$, $\vec{a}_3$, where $\vec{a}_3$, is a unit vector normal to $\vec{a}_\alpha$.

The space and surface base vectors are related as follows:

$$\vec{A}_3 = \vec{G}_3 \tag{1.13}$$

$$\vec{A}_\alpha = \vec{G}_\alpha$$

$$A_{\alpha\beta} = \vec{A}_\alpha \cdot \vec{A}_\beta = \vec{G}_\alpha \cdot \vec{G}_\beta = G_{\alpha\beta}$$

$$A_{33} = G_{33} = 1$$

- For a surface of area Ω delimited by a contour C, Greens formula (Green and Zerna [4]) reads

$$\int\int_\Omega V^\alpha|_\alpha \, d\Omega = \int\int_\Omega (V^\alpha \sqrt{A})_{,\alpha} \frac{d\Omega}{\sqrt{A}} = \int_C V^\alpha N_\alpha \, dC \tag{1.14}$$

where N_α are components of the outward unit vector to the contour and

$$A = A_{11} A_{22} - A_{12}^2$$

- The displacement vector $\vec{U}$ of Fig. 1.2 can be written as:

$$\vec{U} = U^I \vec{G}_I = U^\alpha \vec{A}_\alpha + U^3 \vec{A}_3$$

$$\vec{U} = U^\alpha \vec{A}_\alpha + w \vec{A}_3 \tag{1.15}$$

From Fig. 1.2, it is obtained

$$\vec{r} = \vec{R} + \vec{U}$$

$$\vec{g}_J = \vec{r}_{,J} = \vec{G}_J = \vec{U}_{,J} = \vec{G}_J + U^I|_J \vec{G}_I$$

Substituting (1.13) into the last equation, it is found

$$\begin{aligned} \vec{a}_\alpha &= \vec{A}_\alpha + U^\beta|_\alpha \vec{A}_\beta + \omega|_\alpha \vec{A}_3 \\ &= (\delta^\beta_\alpha + U^\beta|_\alpha) \vec{A}_\beta + \omega|_\alpha \vec{A}_3 \end{aligned} \tag{1.16}$$

- The normal vector to the deformed surface is defined by the relation:

$$\vec{a}_3 \, e_{\alpha\beta} = \vec{a}_\alpha \times \vec{a}_\beta \tag{1.16}_3$$

where $e_{\alpha\beta}$ is the surface permutation tensor.

Equilibrium Equations - Strain Measures

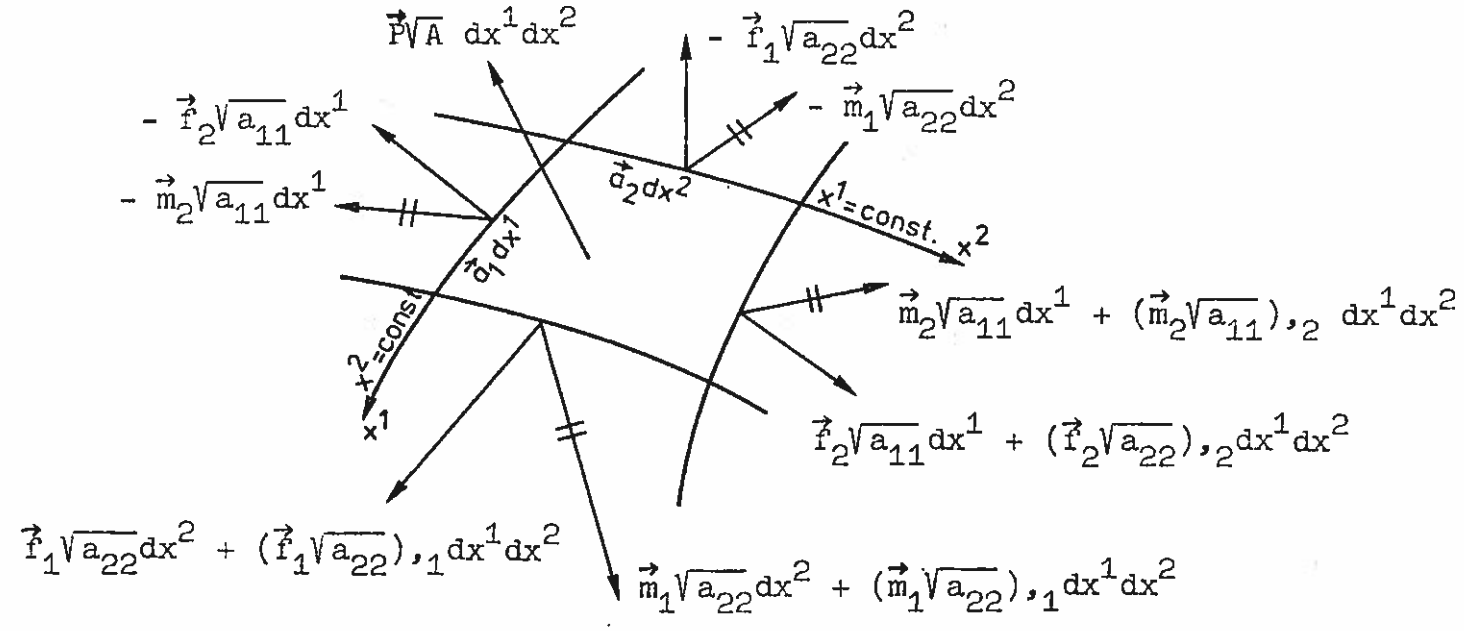

Fig. 1.3. Forces and Moments Acting on a Deformed Surface Element.

In Fig. 1.3 the forces in normal sections of the deformed slab are described by the moment tensor $m^{\alpha\beta}$, the normal force tensor $f^{\alpha\beta}$, and the tensor of shear forces q^{α}. By means of these tensors, the forces and moments per unit length in normal sections with the outward-directed unit normal, n_{β}, are calculated by

$$m_{\lambda} = e_{\beta\lambda}\, m^{\alpha\beta}\, n_{\alpha} \tag{1.17}$$

$$f^{\beta} = f^{\alpha\beta}\, n_{\alpha}$$

$$q = q^{\alpha}\, n_{\alpha}$$

or in vector notation

$$\vec{m}_{(n)} = m^{\alpha\beta}\, n_{\alpha}\, (\vec{a}_3 \times \vec{a}_{\beta}) = e_{\beta\lambda}\, m^{\alpha\beta}\, n_{\alpha}\, \vec{a}^{\lambda} \tag{1.18}$$

$$\vec{f}_{(n)} = f^{\alpha\beta}\, n_{\alpha}\, \vec{a}_{\beta} + \vec{q}_{(n)}$$

$$\vec{q}_{(n)} = q^{\alpha}\, n_{\alpha}\, \vec{a}_3$$

The prescribed loads defined with respect to the undeformed state are the load $\vec{P}$ per unit surface, and on the boundary C_1, the moments $\vec{M}^{*}_{(n)}$ and forces $\vec{F}^{*}_{(n)}$ per unit length of contour. On the remaining boundary, geometrical constraints are prescribed.

In the undeformed state the area of the plate is Ω with a boundary $C = C_1 + C_2$. For the deformed state, the area of the plate is Ω_o delimited by a boundary c_o.

The prescribed load per unit can be represented as

$$\vec{P} = p^{\alpha}\vec{a}_{\alpha} + p^{3}\, \vec{a}_3 \tag{1.19}$$

The equilibrium equations are:

$$\sum_{\gamma=1}^{2} (\vec{f}_\gamma \sqrt{a\, a^{\gamma\gamma}})_{,\gamma} + \vec{p}\sqrt{A} = 0 \tag{1.20}$$

$$\sum_{\gamma=1}^{2} \left[(\vec{m}_\gamma \sqrt{a\, a^{\gamma\gamma}})_{,\gamma} + \vec{a}_\gamma \times (\vec{f}_\gamma \sqrt{a\, a^{\gamma\gamma}}) \right] = 0$$

for forces and moments on the face γ denoted by

$$\vec{f}_\gamma = \left[f^{\gamma\alpha} \frac{\vec{a}_\alpha}{\sqrt{a^{(\gamma\gamma)}}} + q^\gamma \frac{\vec{a}_3}{\sqrt{a^{(\gamma\gamma)}}} \right] \tag{1.21}$$

$$\vec{m}_\gamma = \left[m^{\gamma\alpha} \frac{1}{\sqrt{a^{(\gamma\gamma)}}} (\vec{a}_3 \times \vec{a}_\alpha) \right] = e_{\alpha\lambda}\, m^{\gamma\alpha} \frac{1}{\sqrt{a^{(\gamma\gamma)}}} \vec{a}^\lambda$$

on which the indices in parenthesis are not summed.

Substitution of (1.21) into (1.20) yields

$$(f^{\gamma\alpha} \vec{a}_\alpha \sqrt{a})_{,\gamma} + (q^\gamma \vec{a}_3 \sqrt{a})_{,\gamma} + \vec{p}\sqrt{A} = 0 \tag{1.22}$$

$$\left[m^{\gamma\alpha} (\vec{a}_3 \times \vec{a}_\alpha) \sqrt{a} \right]_{,\gamma} + \vec{a}_\gamma \times (f^{\gamma\alpha} \vec{a}_\alpha + q^\gamma \vec{a}_3) \sqrt{a} = 0$$

A virtual displacement $\delta\vec{r}$ is given to the deformed position such that $\delta\vec{r} = \delta\vec{U}$. The corresponding virtual rotation conforming to the definition for the moment forces is

$$\delta\vec{\theta} = \vec{a}_3 \times \delta\vec{a}_3 \tag{1.23}$$

Since the equations of equilibrium (1.22) have been obtained by deleting a common factor $dx^1 dx^2$, a virtual work expression for the entire deformed surface Ω_o (with contour c_o) has the form

$$\iint_{\Omega_o} \left\{ (f^{\gamma\alpha} \vec{a}_\alpha \sqrt{a})_{,\gamma} + (q^\gamma \vec{a}_3 \sqrt{a})_{,\gamma} + \vec{p}\sqrt{A} \right\} \cdot \delta\vec{r}\, \frac{d\Omega_o}{\sqrt{a}} +$$

$$+ \iint_{\Omega_o} \left\{ \left[m^{\gamma\alpha} (\vec{a}_3 \times \vec{a}_\alpha) \sqrt{a} \right]_{,\gamma} + \vec{a}_\gamma \times \vec{a}_3\, q^\gamma \sqrt{a} + f^{\gamma\alpha} (\vec{a}_\gamma \times \vec{a}_\alpha) \sqrt{a} \right\} \cdot$$

$$\cdot \frac{\delta\vec{\theta}\, d\Omega_o}{\sqrt{a}} = 0 \tag{1.24}$$

where in order to satisfy the geometrical boundary conditions $\delta\vec{r} = 0$ on C_2.

Since

$$[(f^{\gamma\alpha}\vec{a}_\alpha\sqrt{a})\cdot\delta\vec{r}]_{,\gamma} = (f^{\gamma\alpha}\vec{a}_\alpha\sqrt{a})_{,\gamma}\cdot\delta\vec{r} + f^{\gamma\alpha}\vec{a}_\alpha\sqrt{a}\cdot\delta\vec{r}_{,\gamma}$$

and similar expressions for the remainding terms in (1.24) exist, Green's formula (1.14) transforms (1.24) into

$$-\iint_{\Omega_o}[f^{\gamma\alpha}\vec{a}_\alpha\cdot\delta\vec{a}_\gamma + m^{\gamma\alpha}(\vec{a}_3\times\vec{a}_\alpha)\cdot\delta\vec{\theta}_{,\gamma} + q^\gamma\vec{a}_3\cdot\delta\vec{a}_\gamma - (\vec{a}_\gamma\times\vec{a}_3)q^\gamma\cdot\delta\vec{\theta}]d\Omega_o$$
$$+\oint_{C_o}[(f^{\gamma\alpha}\vec{a}_\alpha + q^\gamma\vec{a}_3)\cdot\delta\vec{r} + (m^{\gamma\alpha}\vec{a}_3\times\vec{a}_\alpha)\cdot\delta\vec{\theta}]n_\gamma\, dc_o + \iint_\Omega\vec{P}\cdot\delta\vec{r}\, d\Omega = 0 \qquad (1.25)$$

having used $d\Omega = \sqrt{A/a}\, d\Omega_o$ in the last integral and the equation

$$f^{\gamma\alpha}(\vec{a}_\gamma\times\vec{a}_\alpha)\cdot\delta\vec{\theta} = f^{\gamma\alpha}(\vec{a}_\gamma\times\vec{a}_\alpha)\cdot\vec{a}_3\times\delta\vec{a}_3 = f^{\gamma\alpha}(\vec{a}_\gamma\times\vec{a}_\alpha)\times\vec{a}_3\cdot\delta\vec{a}_3 = 0$$

The sum of the second and third integral in (1.25) is equal to $\delta\pi_o$, the virtual work of the prescribed external loads, and which by (1.18) can be written

$$\delta\pi_o = \iint_\Omega\vec{P}\cdot\delta\vec{r}\, d\Omega + \oint_{C_o}[\vec{f}_{(n)}\cdot\delta\vec{r} + \vec{m}_{(n)}\cdot\delta\vec{\theta}]\, dc_o \qquad (1.26)$$

Substituting (1.23) and (1.26) into (1.25)

$$\iint_{\Omega_o} f^{\gamma\alpha}\delta\mu_{\gamma\alpha}\, d\Omega_o + \iint_{\Omega_o} m^{\gamma\alpha}\,\delta\eta_{\gamma\alpha}\, d\Omega_o = \delta\pi_o \qquad (1.27)$$

where

$$\delta\mu_{\gamma\alpha} \equiv \vec{a}_\alpha\cdot\delta\vec{a}_\gamma \qquad (1.28)$$

$$\delta\eta_{\gamma\alpha} \equiv -\delta b_{\gamma\alpha} + b_\gamma^{\ \rho}(\vec{a}_\rho\cdot\delta\vec{a}_\alpha) = \vec{a}_\alpha\cdot\delta\vec{a}_{3,\gamma} = -\delta b_{\gamma\alpha} + b_\gamma^{\ \rho}\,\delta\mu_{\alpha\rho}$$

and where $b_{\gamma\alpha}$ is the tensor corresponding to the second fundamental form of the deformed surface, which is given by

$$b_{\gamma\alpha} = -\vec{a}_\gamma \cdot \vec{a}_{3,\alpha} \tag{1.29}$$

It is noticed that terms involving q^γ do not appear in (1.27) since the third and fourth terms of the first integral in (1.25) cancel each other. There will now be introduced simplifications in the geometry which lead to the use of a linear bending measure. As approximation to (1.21), moments and shearing forces are now defined in the direction of the undeformed coordinate system, as follows:

$$\vec{f}_\gamma = f^{\gamma\alpha} \frac{\vec{a}_\alpha}{\sqrt{a^{(\gamma\gamma)}}} + q^\gamma \frac{\vec{A}_3}{\sqrt{a^{(\gamma\gamma)}}} \tag{1.30}$$

$$\vec{M}_\gamma = M^{\gamma\alpha} \frac{1}{\sqrt{a^{(\gamma\gamma)}}} (\vec{A}_3 \times \vec{A}_\alpha)$$

and from the equation of equilibrium of moments (1.22),

$$f^{\gamma\alpha} (\vec{a}_\gamma \times \vec{a}_\alpha) = 0$$

i.e.

$$f^{\gamma\alpha} = f^{\alpha\gamma} \tag{1.31}$$

The rotation vector is approximated

$$\delta\vec{\theta} = \vec{A}_3 \times \delta\vec{a}_3 \tag{1.32}$$

Using (1.30), (1.25) is transformed to

$$-\iint_{\Omega_o} [f^{\gamma\alpha}\vec{a}_\alpha \cdot \delta\vec{a}_\gamma + m^{\gamma\alpha}(\vec{A}_3 \times \vec{A}_\alpha) \cdot \delta\vec{\theta}_{,\gamma} + q^\gamma \vec{A}_3 \cdot \delta\vec{a}_\gamma - (\vec{a}_\gamma \times \vec{A}_3) q^\gamma \cdot \delta\vec{\theta}] d\Omega_o +$$

$$+ \delta\pi_o = 0 \tag{1.33}$$

with

$$\delta\pi_o = \oint_{c_o} [(f^{\gamma\alpha}\vec{a}_\alpha + q^\gamma \vec{A}_3)\cdot\delta\vec{r} + m^{\gamma\alpha}(\vec{A}_3\times\vec{A}_\alpha)\cdot\delta\vec{\theta}]n_\gamma dc_o + \iint_\Omega \vec{P}\cdot\delta\vec{r}d\Omega \tag{1.34}$$

Eq. (1.34) can be written as

$$\delta\pi_o = \iint_{\Omega_o} [f^{\gamma\alpha}\delta\epsilon_{\gamma\alpha} + m^{\gamma\alpha}\,\delta\xi_{\gamma\alpha} + q^\gamma(\vec{A}_3\cdot\delta\vec{a}_\gamma + \vec{a}^*_\gamma\cdot\delta\vec{a}_3)]d\Omega_o \tag{1.35}$$

where

$$\delta\epsilon_{\gamma\alpha} \equiv \delta(\vec{a}_\gamma\cdot\vec{a}_\alpha) \tag{1.36}$$

$$\delta\xi_{\gamma\alpha} \equiv \delta(\vec{A}_\alpha\cdot\vec{a}_{3,\gamma})$$

$$\vec{a}^*_\gamma \equiv (A_{\rho\gamma} + U_\rho|_\gamma)\vec{A}^\rho \tag{1.37}$$

having made use of identities obtained from (1.32) and $(1.16)_3$ such as

$$(\vec{A}_\gamma\times\vec{A}_3)\cdot\vec{A}_3\times\delta\vec{a}_3 = -(\vec{A}_3\times\vec{a}_\gamma)\times\vec{A}_3\cdot\delta\vec{a}_3 = -\vec{a}^*_\gamma\cdot\delta\vec{a}_3$$

$$(\vec{A}_3\times\vec{A}_\alpha)\cdot\delta\vec{\theta}_{,\gamma} = (\vec{A}_3\times\vec{A}_\alpha)\cdot\vec{A}_3\times\delta\vec{a}_{3,\gamma} = (\vec{A}_3\times\vec{A}_\alpha)\times\vec{A}_3\cdot\delta\vec{a}_{3,\gamma}$$

$$= \vec{A}_\alpha\cdot\delta\vec{a}_{3,\gamma} = \delta(\vec{A}_\alpha\cdot\vec{a}_{3,\gamma})$$

In order to define the bending measure, the following condition appears from (1.35),

$$\vec{A}_3\cdot\delta\vec{a}_\gamma + \vec{a}^*_\gamma\cdot\delta\vec{a}_3 = 0 \tag{1.38}$$

Since by $(1.16)_3$

$$\vec{a}^*_\gamma\cdot\delta\vec{a}_3 = -\delta\omega_{,\gamma} = \delta\theta_\gamma$$

then (1.38) becomes

$$\delta\vec{a}_3 = \vec{a}^{*\lambda}\ \delta\theta_\lambda + (\delta\vec{a}_3 \cdot \vec{A}_3)\ \vec{A}_3 \tag{1.39}$$

so that

$$\delta\vec{a}_{3,\gamma} = \vec{a}^{*\lambda}\ \delta\theta_\lambda|_\gamma + (\delta\vec{a}_3 \cdot \vec{A}_3)_{,\gamma}\vec{A}_3$$

$$\delta\xi_{\gamma\alpha} = \vec{A}_\alpha \cdot \delta\vec{a}_{3,\gamma} = (\vec{A}_\alpha \cdot \vec{a}^{*\lambda})\ \delta\theta_\lambda|_\gamma \tag{1.40}$$

Adopting the approximation in nonlinear terms

$$\vec{a}^{*\lambda} \simeq \vec{A}^\lambda \tag{1.41}$$

using $(1.16)_1$ the approximation is shown to be equivalent to

$$\vec{a}_\gamma \simeq \vec{d}_\gamma \tag{1.42}$$

with

$$\vec{d}_\gamma = \vec{A}_\gamma - \theta_\gamma \vec{A}_3 \tag{1.43}$$

The linear bending measure, denoted by $\delta\varkappa_{\gamma\alpha}$, and after indtroducing the approximation (1.41) into $(1.39)_3$, results in

$$\delta\varkappa_{\gamma\alpha} = \delta(\vec{d}_\gamma \cdot \vec{a}_{3,\alpha}) = \delta\theta_\gamma|_\alpha = -\ \delta\omega|_{\gamma\alpha} \tag{1.44}$$

Eq (1.30), the equations of equilibrium (1.22) and (1.25) can be modified introducing the approximations (1.42) and (1.44). Denoting the new components of the stress tensor, moment tensor and shearing forces respectively as $F^{\gamma\alpha}$, $M^{\gamma\alpha}$, Q^γ (with respect to the $\vec{d}_\gamma$ axes), the corresponding equations are

$$\vec{F}_\gamma = \left[\ F^{\gamma\alpha}\ \frac{\vec{d}_\alpha}{\sqrt{d^{(\gamma\gamma)}}} + \frac{Q^\gamma\ \vec{A}_3}{\sqrt{d^{(\gamma\gamma)}}}\ \right]\sqrt{\frac{A}{d}} \tag{1.45}$$

$$\vec{M}_\gamma = \left[\ M^{\gamma\alpha}\ \frac{(\vec{A}_3 \times \vec{A}_\alpha)}{\sqrt{d^{(\gamma\gamma)}}}\ \right]\sqrt{\frac{A}{d}}$$

$$(F^{\gamma\alpha}\vec{d}_\alpha\sqrt{A})_{,\gamma} + (Q^\gamma\vec{A}_3\sqrt{A})_{,\gamma} + \vec{P}\sqrt{A} = 0 \tag{1.46}$$

$$[M^{\gamma\alpha}(\vec{A}_3 \times \vec{A}_\alpha)\sqrt{A}]_{,\gamma} + \vec{d}_\gamma \times \vec{A}_3 q^\gamma \sqrt{A} = 0$$

$$F^{\gamma\alpha}(\vec{d}_\gamma \times \vec{d}_\alpha) = 0 \qquad \text{i.e. } F^{\gamma\alpha} = F^{\alpha\gamma}$$

$$\iint_\Omega [F^{\gamma\alpha}\,\delta\epsilon_{\gamma\alpha} + M^{\gamma\alpha}\,\delta\kappa_{\gamma\alpha}]\,d\Omega = \delta\pi_o \tag{1.47}$$

$$\delta\pi_o = \iint_\Omega \vec{P}\cdot\delta\vec{r}\,d\Omega + \int_C [\vec{F}_{(n)}\cdot\delta\vec{r} + \vec{M}_{(n)}\cdot\delta\vec{\theta}]\,dC$$

where

$$\vec{M}_{(n)} = M^{\alpha\beta}N_\alpha(\vec{A}_3 \times \vec{A}_\beta) \tag{1.48}$$

$$\vec{F}_{(n)} = F^{\alpha\beta}N_\alpha\vec{d}_\beta + Q\vec{A}_3$$

$$Q = Q^\alpha N_\alpha$$

$$2\delta\epsilon_{\gamma\alpha} = \vec{d}_\gamma\cdot\delta\vec{a}_\alpha + \vec{d}_\alpha\cdot\delta\vec{a}_\gamma$$

$$= \delta U_\gamma|_\alpha + \delta U_\alpha|_\gamma + \theta_\alpha\delta\theta_\gamma + \theta_\gamma\delta\theta_\alpha \tag{1.49}$$

$$2\epsilon_{\gamma\alpha} = U_\gamma|_\alpha + U_\alpha|_\gamma + \theta_\alpha\theta_\gamma$$

$$\kappa_{\gamma\alpha} = \theta_\gamma|_\alpha = -\omega|_{\gamma\alpha}$$

In order to clarify (1.40), the displacement $\vec{U}$ will be interpreted as the variation of the vector $\vec{R}$ (Fig. 1.2) so that an approximate expression for the normal to the surface, $\vec{a}_3$, is found, i.e.

$$\hat{\delta}\vec{R} \equiv \vec{U} = U_\alpha\vec{A}^\alpha + w\vec{A}_3 \tag{1.50}$$

$$\vec{a}_3 \simeq \vec{A}_3 + \hat{\delta}\vec{A}_3$$

Since $\vec{A}_3$ is a unit vector, the following formulas hold

$$\vec{A}_3 \cdot \vec{A}_3 = 1$$

$$\hat{\delta}\vec{A}_3 \cdot \vec{A}_3 = 0$$

$$\hat{\delta}\vec{A}_3 = (\vec{A}_\alpha \cdot \hat{\delta}\vec{A}_3)\,\vec{A}^\alpha \qquad (1.51)$$

$$\hat{\delta}\vec{A}_\gamma = \hat{\delta}\vec{R}_{,\gamma} = \vec{U}_{,\gamma} = U_\alpha|_\gamma\,\vec{A}^\alpha + \omega_{,\gamma}\vec{A}_3$$

The base vectors $\vec{A}_\gamma$ being normal to $\vec{A}_3$ validate

$$\vec{A}_\gamma \cdot \vec{A}_3 = 0$$

$$\vec{A}_\gamma \cdot \hat{\delta}\vec{A}_3 = -\hat{\delta}\vec{A}_\gamma \cdot \vec{A}_3 = -\omega_{,\gamma} = \theta_\gamma \qquad (1.52)$$

From (1.51) and (1.52)

$$\hat{\delta}\vec{A}_3 = \theta_\gamma\,\vec{A}^\gamma$$

$$\vec{a}_3 \simeq \vec{A}_3 + \theta_\gamma\,\vec{A}^\gamma \qquad (1.53)$$

which is the same as (1.40).

The change in the fundamental tensor $B_{\gamma\alpha}$ foran initially flat plate is

$$B_{\gamma\alpha} = -\vec{A}_\gamma \cdot \vec{A}_{3,\alpha} = 0$$

$$\hat{\delta}B_{\gamma\alpha} = -\vec{A}_\gamma \cdot (\hat{\delta}\vec{A}_3)_{,\alpha} = -\theta_\gamma|_\alpha \qquad (1.54)$$

Nielsen [5] uses as the bending measure $-\hat{\delta}B_{\gamma\alpha}$, which is the same linear bending measure (1.44) derived in this report by starting from a general nonlinear measure and following by introducing simplifications in the geometry. In the approach presented here, it has been observed that adopting (1.54) implies linearization of the in-plane measure $\varepsilon_{\gamma\alpha}$ in the terms

involving the displacement U^{α}. However $\epsilon_{\gamma\alpha}$ remains nonlinear in the terms involving the normal displacement w.

Governing Differential Equations and Virtual Work Principles

The substitution of (1.43) into the equations of equilibrium (1.46), reads

$$F^{\gamma\alpha}{}_{,\gamma}\sqrt{A}\,(\vec{A}_{\alpha}-\theta_{\alpha}\vec{A}_{3})+F^{\gamma\alpha}(\sqrt{A})_{,\gamma}(\vec{A}_{\alpha}-\theta_{\alpha}\vec{A}_{3})+$$

$$+F^{\gamma\alpha}\sqrt{A}\,(\vec{A}_{\alpha,\gamma}-\theta_{\alpha,\gamma}\vec{A}_{3})+Q^{\gamma}{}_{,\gamma}\vec{A}_{3}+(\sqrt{A})_{,\gamma}Q^{\gamma}\vec{A}_{3}+\vec{P}\sqrt{A}=0$$

$$M^{\gamma\alpha}{}_{,\gamma}\sqrt{A}\,(\vec{A}_{3}\times\vec{A}_{\alpha})+M^{\gamma\alpha}(\sqrt{A})_{,\gamma}(\vec{A}_{3}\times\vec{A}_{\alpha})+M^{\gamma\alpha}\sqrt{A}\,(\vec{A}_{3}\times\vec{A}_{\alpha,\gamma})+$$

$$+\sqrt{A}\,(\vec{A}_{\alpha}\times\vec{A}_{3})\,Q^{\alpha}=0 \qquad (1.55)$$

when the applied load per unit undeformed area is expressed as

$$\vec{P}=P^{\alpha}\vec{A}_{\alpha}+P^{3}\vec{A}_{3} \qquad (1.56)$$

and use is made of the known formulas

$$(\sqrt{A})_{,\gamma}=\sqrt{A}\begin{Bmatrix}\lambda\\ \lambda\ \ \gamma\end{Bmatrix}$$

$$\vec{A}_{\alpha,\gamma}=\begin{Bmatrix}\lambda\\ \alpha\ \ \gamma\end{Bmatrix}\vec{A}_{\lambda}$$

equations (1.55) become

$$\sqrt{A}\left[F^{\gamma\alpha}{}_{,\gamma}+\begin{Bmatrix}\lambda\\ \lambda\ \ \gamma\end{Bmatrix}F^{\gamma\alpha}+\begin{Bmatrix}\alpha\\ \lambda\ \ \gamma\end{Bmatrix}F^{\gamma\lambda}+P^{\alpha}\right]\vec{A}_{\alpha}+$$

$$\sqrt{A}\left(-\left[F^{\gamma\alpha}{}_{,\gamma}+\begin{Bmatrix}\lambda\\ \lambda\ \ \gamma\end{Bmatrix}F^{\gamma\alpha}+\begin{Bmatrix}\alpha\\ \lambda\ \ \gamma\end{Bmatrix}F^{\gamma\lambda}\right]\theta\alpha-\right.$$

$$-\left[\theta_{\lambda,\gamma} - \left\{\begin{matrix}\alpha\\ \lambda\gamma\end{matrix}\right\}\theta_\alpha\right]F^{\gamma\lambda} + \left[Q^\gamma{}_{,\gamma} + \left\{\begin{matrix}\lambda\\ \lambda\ \gamma\end{matrix}\right\}Q^\gamma\right] + P^3\Big)\vec{A}_3 = 0$$

$$\sqrt{A}\ (\vec{A}_3\times\vec{A}_\alpha)\left[M^{\gamma\alpha}{}_{,\gamma} + \left\{\begin{matrix}\lambda\\ \lambda\ \gamma\end{matrix}\right\}M^{\gamma\alpha} + \left\{\begin{matrix}\alpha\\ \lambda\ \gamma\end{matrix}\right\}M^{\gamma\lambda} - Q^\alpha\right] = 0$$

from which the governing differential equations are

$$F^{\gamma\alpha}\big|_\gamma + P^\alpha = 0 \qquad (1.57)$$

$$-(F^{\gamma\alpha}\,\theta_\alpha)\big|_\gamma + Q^\gamma\big|_\gamma + P^3 = 0$$

$$M^{\gamma\alpha}\big|_\gamma - Q^\alpha = 0$$

Substitution of $(1.57)_3$ into $(1.57)_2$ results in

$$M^{\gamma\alpha}\big|_{\gamma\alpha} - (F^{\gamma\alpha}\,\theta\alpha)\big|_\gamma + P^3 = 0 \qquad (1.58)$$

Using the values of the strain measures (1.49) in (1.47), the virtual work of the internal forces becomes

$$\delta\pi_o = \iint_\Omega \left(M^{\gamma\alpha}\,\delta\kappa_{\gamma\alpha} + F^{\gamma\alpha}\,\delta\epsilon_{\gamma\alpha}\right)d\Omega$$

thus

$$\delta\pi_o = \iint_\Omega \left(-M^{\gamma\alpha}\,\delta\omega\big|_{\gamma\alpha} + F^{\gamma\alpha}\,\delta U_\gamma\big|_\alpha + F^{\gamma\alpha}\,\omega_{,\gamma}\,\delta\omega_{,\alpha}\right)d\Omega$$

but since

$$(F^{\gamma\alpha}\,\delta U_\gamma)\big|_\alpha = F^{\gamma\alpha}\big|_\alpha\,\delta U_\gamma + F^{\gamma\alpha}\,\delta U_\gamma\big|_\alpha$$

$$-(M^{\gamma\alpha}\,\delta\omega_{,\gamma})\big|_\alpha = -M^{\gamma\alpha}\big|_\alpha\,\delta\omega_{,\gamma} - M^{\gamma\alpha}\,\delta\omega\big|_{\gamma\alpha}$$

$$= -(M^{\gamma\alpha}\big|_\alpha\,\delta\omega)\big|_\gamma + M^{\gamma\alpha}\big|_{\alpha\gamma}\,\delta\omega - M^{\gamma\alpha}\,\delta\omega\big|_{\gamma\alpha}$$

$$(F^{\gamma\alpha}\,\omega,_{\gamma}\,\delta\omega)\big|_{\alpha} = (F^{\gamma\alpha}\,\omega,_{\gamma})\big|_{\alpha}\,\delta\omega + F^{\gamma\alpha}\,\omega,_{\gamma}\,\delta\omega\big|_{\alpha}$$

then

$$\delta\pi_o = -\iint_{\Omega} F^{\gamma\alpha}\big|_{\alpha}\,\delta U_{\gamma}\,d\Omega - \iint_{\Omega}\left(M^{\gamma\alpha}\big|_{\alpha\gamma} + (F^{\gamma\alpha}\,\omega,_{\gamma})\big|_{\alpha}\right)\delta\omega\,d\Omega +$$

$$+\iint_{\Omega}\left(F^{\gamma\alpha}\,\delta U_{\gamma} - M^{\gamma\alpha}\,\delta\omega,_{\gamma} + M^{\gamma\alpha}\big|_{\gamma}\,\delta\omega + F^{\gamma\alpha}\,\omega,_{\gamma}\,\delta\omega\right)\big|_{\alpha} d\Omega \qquad (1.59)$$

Substituting (1.57) and (1.58) into (1.59), using Green's formula (1.14) in the resulting expression, and keeping $\delta\vec{r} = 0$ on C_2, the internal virtual work becomes

$$\delta\pi_o = \iint_{\Omega}\left|P^{\alpha}\delta U_{\alpha} + P^{3}\delta\omega\right| d\Omega + \int_{C_1}\left(F^{\gamma\alpha}\,\delta U_{\gamma} + M^{\gamma\alpha}\,\delta\theta_{\gamma} + Q^{\alpha}\,\delta\omega - F^{\gamma\alpha}\theta_{\gamma}\,\delta\omega\right)N_{\alpha}\,dC \qquad (1.60)$$

which by recurring to $(1.47)_2$ is seen to equate the work of the external loads, the latter written as

$$\delta\pi_o = \iint_{\Omega}\vec{P}\cdot\delta\vec{r}\,d\Omega + \int_{C_1}\left(\vec{F}^{*}_{(n)}\cdot\delta\vec{r} + \vec{M}^{*}_{(n)}\cdot\delta\vec{\theta}\right)dC \qquad (1.61)$$

Physical Components of Forces and Moments

The use of (1.43) leads to

$$d_{\gamma\alpha} = \vec{d}_{\gamma}\cdot\vec{d}_{\alpha} = (\vec{A}_{\gamma} - \theta_{\gamma}\vec{A}_{3})\cdot(\vec{A}_{\alpha} - \theta_{\alpha}\vec{A}_{3}) = A_{\gamma\alpha} + \theta_{\gamma}\theta_{\alpha} \qquad (1.62)$$

$$d = (A_{11}+\theta_1{}^2)(A_{22}+\theta_2{}^2) - (A_{12}+\theta_1\theta_2)^2$$

Eq. (1.45), (1.47) and the unit normal vector can be written

$$\vec{F}_{\gamma} = \sum_{\alpha=1}^{2}\left|F^{\gamma\alpha}\sqrt{\frac{A\,d_{\alpha\alpha}}{d\,d^{\gamma\gamma}}}\right|\frac{\vec{d}_{\alpha}}{\sqrt{d_{\alpha\alpha}}} + \left|Q^{\gamma}\sqrt{\frac{A}{d\,d^{\gamma\gamma}}}\right|\vec{A}_{3} \qquad (1.63)$$

(no sum γ, α)

$$\vec{M}_\gamma = \sum_{\alpha=1}^{2} \left[M^{\gamma\alpha} \sqrt{\frac{A\,A_{\alpha\alpha}}{d\,d^{\gamma\gamma}}} \right] \frac{(\vec{A}_3 \times \vec{A}_\alpha)}{\sqrt{A_{\alpha\alpha}}} \qquad \text{(no sum } \gamma,\alpha\text{)}$$

$$\vec{F}_{(n)} = \sum_{\beta=1}^{2} \left[F^{\alpha\beta} N_\alpha \sqrt{d_{\beta\beta}} \right] \frac{\vec{d}_\beta}{\sqrt{d_{\beta\beta}}} + \left[Q^\alpha N_\alpha \right] \vec{A}_3 \qquad \text{(no sum } \beta\text{)}$$

$$\vec{M}_{(n)} = \sum_{\beta=1}^{2} \left[M^{\alpha\beta} N_\alpha \sqrt{A_{\beta\beta}} \right] \frac{(\vec{A}_3 \times \vec{A}_\beta)}{\sqrt{A_{\beta\beta}}} \qquad \text{(no sum } \beta\text{)}$$

$$\vec{N} = N_\lambda \vec{A}^\lambda = \sum_{\alpha=1}^{2} \left[N_\alpha \sqrt{A^{\alpha\alpha}} \right] \frac{\vec{A}^\alpha}{\sqrt{A^{\alpha\alpha}}} \qquad \text{(no sum } \alpha\text{)}$$

where the physical components are the terms in square brackets.

Stress-Strain Relationship-Elastic Case

Following Nielsen [5], a linear stress-strain relationship is written

$$\begin{aligned} F^{\gamma\alpha} &= C^{\gamma\alpha\beta\mu}\, \epsilon_{\beta\mu} \\ M^{\gamma\alpha} &= D^{\gamma\alpha\beta\mu}\, \varkappa_{\beta\mu} \end{aligned} \qquad (1.64)$$

For an isotropic material it may be shown that the elastic constants must be of the form

$$\begin{aligned} C^{\gamma\alpha\beta\mu} &= K_1 \,(A^{\gamma\beta}\, A^{\alpha\mu} + A^{\gamma\mu}\, A^{\alpha\beta} + K_2\, A^{\gamma\alpha}\, A^{\beta\mu}) \\ D^{\gamma\alpha\beta\mu} &= K_3 \,(A^{\gamma\beta}\, A^{\alpha\mu} + A^{\gamma\mu}\, A^{\alpha\beta} + K_4\, A^{\gamma\alpha}\, A^{\beta\mu}) \end{aligned} \qquad (1.65)$$

The constants K_1, K_2, K_3, K_4 are found by considering (1.64) to be valid for the limiting case of a plate subjected to appropriate loads where the exact solution according to linear elasticity is known.

$$K_1 = \frac{Eh}{2(1+\nu)}$$

$$K_3 = \frac{E h^3}{24(1+\nu)}$$

$$K_2 = K_4 = \frac{2\nu}{1-\nu}$$

where h is the plate's thickness, E Young's modulus and ν Poisson's ratio. Substitution of the value of the constants into (1.65) and (1.64) gives

$$F_{\gamma\alpha} = \frac{Eh}{(1+\nu)} \left(\epsilon_{\gamma\alpha} + \frac{\nu}{1-\nu} A_{\gamma\alpha}\ \epsilon^{\beta}_{\beta}\right) \tag{1.66}$$

$$M_{\gamma\alpha} = \frac{E h^3}{12(1+\nu)} \left(\varkappa_{\gamma\alpha} + \frac{\nu}{1-\nu} A_{\gamma\alpha}\ \varkappa^{\beta}_{\beta}\right)$$

$$\frac{E h^3}{12} \varkappa_{\gamma\alpha} = (1+\nu)\ M_{\gamma\alpha} - \nu A_{\gamma\alpha} M^{\beta}_{\beta}$$

$$E h\, \epsilon_{\gamma\alpha} = (1+\nu)\ F_{\gamma\alpha} - \nu A_{\gamma\alpha} F^{\gamma}_{\gamma}$$

Boundary Conditions

The principle of virtual work (1.59) and (1.61) can be written

$$-\iint_{\Omega} \left[\left| F^{\gamma\alpha} \right|_{\alpha} + P^{\gamma} \right] \delta U_{\gamma}\ d\Omega - \iint_{\Omega} \left[\left| M^{\gamma\alpha} \right|_{\alpha\gamma} + \left(F^{\gamma\alpha}\omega_{,\gamma}\right)\Big|_{\alpha} + P^{3} \right] \delta\omega\ d\Omega +$$

$$+\int_{C_1} \left[F^{\gamma\alpha} N_{\alpha} - F^{*\gamma}_{(n)} \right] \delta U_{\gamma}\ dC + \int_{C_1} \left[M^{\gamma\alpha} \delta\theta_{\gamma} + Q^{\alpha} \delta\omega - F^{\gamma\alpha} \theta_{\gamma} \delta\omega \right] N_{\alpha}\, dC -$$

$$-\int_{C_1} \left[F^{*3}_{(n)} \delta\omega + \vec{M}^{*}_{(n)} \cdot \delta\vec{\theta} \right] dC = 0 \tag{1.67}$$

where the components of the prescribed force on C_1 are

$$\vec{F}^{*}_{(n)} = F^{*\gamma}_{(n)}\ \vec{A}_{\gamma} + F^{*3}_{(n)}\ \vec{A}_{3} \tag{1.68}$$

It is assumed that the displacements in (1.67) satisfy on C_2 the geometrical boundary conditions, namely

$$\begin{aligned} U^\gamma &= U^{*\gamma} \\ \omega &= \omega^* \\ \omega_{,\gamma} &= \omega^*_{,\gamma} \end{aligned} \tag{1.69}$$

The normal vector $\vec{N}$ and tangential vector $\vec{T}$ to the undeformed contour is given as

$$\begin{aligned} N_\gamma &= \frac{\partial N}{\partial X^\gamma} = e_{\gamma\lambda}\, T^\lambda \\ N^\lambda &= e^{\lambda\gamma}\, T_\gamma \\ T_\gamma &= \frac{\partial C}{\partial X^\gamma} = -\, e_{\gamma\lambda}\, N^\lambda \\ T^\lambda &= -\, e^{\lambda\gamma}\, N_\gamma \end{aligned} \tag{1.70}$$

with a parameter N (without indices) measured along the normal to the contour C.

The derivatives of the displacement ω transform as

$$\omega_{,\gamma} = \frac{\partial \omega}{\partial N} N_{,\gamma} + \frac{\partial \omega}{\partial C} C_{,\gamma} = N_\gamma \frac{\partial \omega}{\partial N} + T_\gamma \frac{\partial \omega}{\partial C} \tag{1.71}$$

From the definition (1.32) and equation (1.53),

$$\delta\vec{\theta} = \vec{A}_3 \times \delta\theta_\gamma \vec{A}^\gamma = e^{\gamma\lambda}\, \vec{A}_\lambda\, \delta\theta_\gamma = -\, e^{\gamma\lambda} \vec{A}_\lambda \left(N_\gamma \frac{\partial \delta\omega}{\partial N} + T_\gamma \frac{\partial \delta\omega}{\partial C}\right)$$

$$\begin{aligned} \delta\vec{\theta} &= \left(e^{\lambda\gamma} N_\gamma \frac{\partial \delta\omega}{\partial N} + e^{\lambda\gamma} T_\gamma \frac{\partial \delta\omega}{\partial C}\right) \vec{A}_\lambda \\ &= \left(-\, T^\lambda \frac{\delta\partial\omega}{\partial N} + N^\lambda \frac{\delta\partial\omega}{\partial C}\right) \vec{A}_\lambda = -\, \vec{T} \frac{\delta\partial\omega}{\partial N} + \vec{N} \frac{\delta\partial\omega}{\partial C} \end{aligned} \tag{1.72}$$

where (1.71) and (1.70) have been applied. Furthermore

$$\int_{C_1} \vec{M}^*_{(n)} \cdot \delta\vec{\theta}\, dC = -\int_{C_1} \vec{M}^*_{(n)} \cdot \vec{T}\, \frac{\delta\partial\omega}{\partial N}\, dC + \int_{C_1} \vec{M}^*_{(n)} \cdot \vec{N}\, \frac{\delta\partial\omega}{\partial C}\, dC$$

$$= -\int_{C_1} \vec{M}^*_{(n)} \cdot \vec{T}\, \frac{\delta\partial\omega}{\partial N}\, dC - \int_{C_1} \frac{\partial}{\partial C}(\vec{M}^*_{(n)} \cdot \vec{N})\, \delta\omega\, dC + \sum_{i=1}^{m_1} \left[\vec{M}^*_{(n)} \cdot \vec{N}\, \delta\omega \right]_{C_1(i)} \tag{1.73}$$

with the contour C_1 having m_1 discontinuities and $[\cdots]_{C_1(i)}$ designating the jump of the quantity in brackets at the point labeled i.

In a similar manner using (1.71)

$$\int_{C_1} M^{\gamma\alpha} N_\alpha\, \delta\theta_{\gamma,}\, dC = -\int_{C_1} M^{\gamma\alpha} N_\alpha\, \delta\omega_{,\gamma}\, dC = -\int_{C_1} M^{\gamma\alpha} N_\alpha \left(N_\gamma \frac{\delta\partial\omega}{\partial N} + T_\gamma \frac{\delta\partial\omega}{\partial C}\right) dC$$

$$= -\int_{C_1} M^{\gamma\alpha} N_\alpha N_\gamma\, \frac{\delta\partial\omega}{\partial N}\, dC + \int_{C_1} \frac{\partial}{\partial C}(M^{\gamma\alpha} N_\alpha T_\gamma)\, \delta\omega dC - \sum_{i=1}^{m1} \left[M^{\gamma\alpha} N_\alpha T_\gamma \delta\omega \right]_{C_1(i)} \tag{1.74}$$

Substitution of (1.73) and (1.74) into (1.67) yields

$$-\int_\Omega \int \left[F^{\gamma\alpha}\big|_\gamma + P^\gamma \right] \delta U_\gamma\, d\Omega - \int_\Omega \int \left[M^{\gamma\alpha}\big|_{\alpha\gamma} + (F^{\gamma\alpha}\omega_{,\gamma})\big|_\alpha + P^3 \right] \delta\omega\, d\Omega +$$

$$+\int_{C_1} \left[F^{\gamma\alpha} N_\alpha - F^{*\gamma}_{(n)} \right] \delta U_\gamma\, dC + \int_{C_1} \Big[\left(-M^{\gamma\alpha} N_\gamma \frac{\delta\partial\omega}{\partial N} + Q^\alpha \delta\omega - \right.$$

$$\left. - F^{\gamma\alpha}\theta_\gamma\, \delta\omega \right) N_\alpha + \frac{\partial}{\partial C}(M^{\gamma\alpha} N_\alpha T_\gamma)\, \delta\omega \Big] dC - \sum_{i=1}^{m1} \left[M^{\gamma\alpha} N_\alpha T_\gamma\, \delta\omega \right]_{C_1(i)} -$$

$$-\int_{C_1} \left[F^{*3}_{(n)}\, \delta\omega - \vec{M}^*_{(n)} \cdot \vec{T}\, \frac{\delta\partial\omega}{\partial N} - \frac{\partial}{\partial C}(\vec{M}^*_{(n)} \cdot \vec{N})\, \delta\omega \right] dC -$$

$$- \sum_{i=1}^{m1} \left[\vec{M}^*_{(n)} \cdot \vec{N}\, \delta\omega \right]_{C_1(i)} = 0 \tag{1.75}$$

The following boundary conditions on C_1, by assuming continuous displacements w and slopes $\frac{\partial w}{\partial N}$ in (1.75), result in

$$F^{\gamma\alpha} N_\alpha = F^{*\gamma}_{(n)} \tag{1.76}$$

$$- M^{\gamma\alpha} N_\gamma N_\alpha = - \vec{M}^*_{(n)} \cdot \vec{T}$$

$$Q^\alpha N_\alpha + \frac{\partial}{\partial C} (M^{\gamma\alpha} N_\alpha T_\gamma) + F^{\gamma\alpha} N_\alpha w_{,\gamma} = F^{*3}_{(n)} - \frac{\partial}{\partial C} (\vec{M}^*_{(n)} \cdot \vec{N})$$

$$- \left[M^{\gamma\alpha} N_\alpha T_\gamma \right]_{C_1(i)} = \left[\vec{M}^*_{(n)} \cdot \vec{N} \right]_{C_1(i)} \quad ; \quad i=1, \ldots, m_1$$

Application of (1.48), (1.43) and (1.70) leads to

$$M_{(NT)} \equiv \vec{M}_{(n)} \cdot \vec{N} = M^{\gamma\alpha} N_\alpha e_{\gamma\lambda} \vec{A}^\lambda \cdot N_\mu \vec{A}^\mu = M^{\gamma\alpha} N_\alpha e_{\gamma\lambda} N^\lambda = -M^{\gamma\alpha} N_\alpha T_\gamma \tag{1.78}$$

$$M_{(NN)} \equiv \vec{M}_{(n)} \cdot \vec{T} = M^{\gamma\alpha} N_\alpha e_{\gamma\lambda} \vec{A}^\lambda \cdot T_\mu \vec{A}^\mu = M^{\gamma\alpha} N_\alpha e_{\gamma\lambda} T^\lambda = M^{\gamma\alpha} N_\alpha N_\gamma$$

$$\vec{F}_{(n)} \cdot \vec{A}_3 = F^{\gamma\alpha} N_\alpha \vec{d}_\gamma \cdot \vec{A}_3 + Q^\alpha N_\alpha = F^{\gamma\alpha} N_\alpha w_{,\gamma} + Q^\alpha N_\alpha$$

$$\vec{F}_{(n)} \cdot \vec{A}^\gamma = F^{\beta\alpha} N_\alpha \vec{d}_\beta \cdot \vec{A}^\gamma = F^{\beta\alpha} N_\alpha \delta^\gamma_\beta = F^{\gamma\alpha} N_\alpha$$

Using the identities

$$F^{*\gamma}_{(n)} = \vec{F}^*_{(n)} \cdot \vec{A}^\gamma$$

$$F^{*3}_{(n)} = \vec{F}^*_{(n)} \cdot \vec{A}_3$$

together with (1.78), the boundary equations (1.77) appear in vector notation as

$$\vec{F}_{(n)} \cdot \vec{A}^\gamma = \vec{F}^*_{(n)} \cdot \vec{A}^\gamma \tag{1.79}$$

$$\vec{M}_{(n)} \cdot \vec{T} = \vec{M}^*_{(n)} \cdot \vec{T}$$

$$\vec{F}_{(n)} \cdot \vec{A}_3 - \frac{\partial}{\partial C} (\vec{M}_{(n)} \cdot \vec{N}) = \vec{F}^*_{(n)} \cdot \vec{A}_3 - \frac{\partial}{\partial C} (\vec{M}^*_{(n)} \cdot \vec{N})$$

$$[\vec{M}_{(n)} \cdot \vec{N}]_{C_1}(i) = [\vec{M}^*_{(n)} \cdot \vec{N}]_{C_1}(i); \quad i = 1,\ldots,m_1$$

The quantity $[\vec{M}_{(n)} \cdot \vec{N}]_{C_1}(i)$ may be interpreted as a generalized concentrated force in the direction of the displacement ω, since in the expression of virtual work it is multiplied by the variation $\delta\omega_{(i)}$ where i identifies the point of application. The quantity $\vec{F}_{(n)} \cdot \vec{A}_3 - \frac{\partial}{\partial C} (\vec{M}_{(n)} \cdot \vec{N})$ may be interpreted as a generalized distributed force on C_1 in the direction of the displacement ω, since in the virtual work it multiplies the variation $\delta\omega$. The component of the moment around $\vec{T}$ is given by $\vec{M}_{(n)} \cdot \vec{T}$ and around $\vec{N}$ by $\vec{M}_{(n)} \cdot \vec{N}$.

Flexural Formulas for Isotropic Plates

The application of (1.7), (1.57), (1.58), (1.77) and the fact that

$$A^{\gamma\alpha} N_\alpha T_\gamma = 0$$

$$A^{\gamma\alpha} N_\gamma N_\alpha = 1$$

validates the following formulas

$$M^{\gamma\alpha} = - D [(1 - \nu) \omega\big|^{\gamma\alpha} + \nu A^{\gamma\alpha} \omega\big|^{\lambda}_{\lambda}] \tag{1.80}$$

$$Q^\alpha = - D \omega\big|^{\gamma\alpha}_{\gamma}$$

$$- D \omega\big|^{\gamma\alpha}_{\gamma\alpha} + (F^{\gamma\alpha} \omega_{,\alpha})\big|_\gamma + P^3 = 0$$

or

$$- D \omega\big|^{\gamma\alpha}_{\gamma\alpha} + F^{\gamma\alpha} \omega\big|_{\gamma\alpha} + P^\alpha \omega_{,\alpha} + P^3 = 0$$

and on C_1 the boundary conditions

$$F^{\gamma\alpha} N_\alpha \omega|_\gamma - D\,\omega|_\gamma^{\gamma\alpha} - \frac{\partial}{\partial C}[D(1-\nu)\omega|^{\gamma\alpha} N_\alpha T_\gamma] = F^{*3}_{(n)} - \frac{\partial}{\partial C}(\vec{M}^*_{(n)} \cdot \vec{N})$$

$$[\omega|^{\gamma\alpha} N_\alpha T_\gamma]_{C_1}(i) = [\vec{M}^*_{(n)} \cdot \vec{N}]_{C_1}(i); \quad i=1,\ldots,m_1$$

$$- D[(1-\nu)\,\omega|^{\gamma\alpha} N_\gamma N_\alpha + \nu\,\omega|^{\lambda}_{\lambda}] = \vec{M}^*_{(n)} \cdot \vec{T}$$

where $D = \dfrac{E h^3}{12(1-\nu^2)}$

Large Deflection of Plates which Remain Flat

The normal deflection is assumed zero i.e.

$$\omega = 0 \tag{1.81}$$

$$\vec{U} = U^\alpha \vec{A}_\alpha$$

which transforms (1.16) to

$$\vec{a}_\alpha = \vec{A}_\alpha + U^\beta|_\alpha \vec{A}_\beta = (\delta^\beta_\alpha + U^\beta|_\alpha)\vec{A}_\beta \tag{1.82}$$

$$a_{\gamma\alpha} = \vec{a}_\gamma \cdot \vec{a}_\alpha = U_\gamma|_\alpha + U_\alpha|_\gamma + U_\beta|_\gamma U^\beta|_\alpha$$

Similarly to (1.21) and (1.18), the stress tensor and normal forces are defined by

$$\vec{f}_\gamma = \sigma^{\gamma\alpha} \frac{\vec{a}_\alpha}{\sqrt{a^{\gamma\gamma}}} \sqrt{\frac{A}{a}} = \sum_{\lambda=1}^{2} \left[\sigma^{\gamma\lambda} \sqrt{\frac{A\, a_{\lambda\lambda}}{a\, a^{\gamma\gamma}}} \right] \frac{\vec{a}_\lambda}{\sqrt{a_{\lambda\lambda}}} \tag{1.83}$$

(γ,λ not summed)

$$\vec{f}_{(n)} = \sigma^{\gamma\lambda} N_\gamma \vec{a}_\lambda = \sigma^{\gamma\lambda}(\delta^\alpha_\lambda + U^\alpha|_\lambda) N_\gamma \vec{A}_\alpha$$

where the quantities in brackets are the physical components.

By (1.82) the equations of equilibrium become

$$[\sigma^{\gamma\alpha}\,\vec{a}_\alpha\sqrt{A}]_{,\gamma} + \vec{P}\sqrt{A} = 0$$

or

$$[\sigma^{\gamma\alpha}\,(\delta^\beta_\alpha + U^\beta|_\alpha)\,\vec{A}_\beta\sqrt{A}]_{,\gamma} + P^\alpha\vec{A}_\alpha\sqrt{A} = 0 \qquad (1.84)$$

Using the formula

$$\left|[\sigma^{\gamma\alpha}\,(\delta^\beta_\alpha + U^\beta|_\alpha)]\,\vec{A}_\beta\sqrt{A}\right|_{,\gamma} = [\sigma^{\gamma\alpha}\,(\delta^\beta_\alpha + U^\beta|_\alpha)]|_\gamma\vec{A}_\beta\sqrt{A}$$

Eq. (1.84) can, after changing dummy indices, be written

$$[\sigma^{\gamma\lambda}\,(\delta^\alpha_\lambda + U^\alpha|_\lambda)]|_\gamma + P^\alpha = 0 \qquad (1.85)$$

The internal work is

$$\delta\pi_o = \int\!\!\int_\Omega \sigma^{\gamma\alpha}\,\delta\epsilon_{\gamma\alpha}\,d\Omega \qquad (1.86)$$

The strain measure defined by (1.35) becomes, for $\omega = 0$,

$$2\,\delta\epsilon_{\gamma\alpha} = \delta(a_{\gamma\alpha}) = \delta\,(U_\gamma|_\alpha + U_\alpha|_\gamma + U_\beta|_\gamma\,U^\beta|_\alpha) \qquad (1.87)$$

Combining (1.87) with (1.86)

$$\begin{aligned}\delta\pi_o &= \int\!\!\int_\Omega [\sigma^{\gamma\alpha}\,\delta U_\gamma|_\alpha + \sigma^{\gamma\lambda}\,U^\alpha|_\lambda\,\delta U_\alpha|_\gamma]\,d\Omega \qquad (1.88)\\ &= \int\!\!\int_\Omega \sigma^{\gamma\lambda}\,(\delta^\alpha_\lambda + U^\alpha|_\lambda)\,\delta\,U_\alpha|_\gamma\,d\Omega\\ &= -\int\!\!\int_\Omega [\sigma^{\gamma\lambda}\,(\delta^\alpha_\lambda + U^\alpha|_\lambda)]|_\gamma\,\delta U_\alpha\,d\Omega + \int\!\!\int_\Omega [\sigma^{\gamma\lambda}\,(\delta^\alpha_\lambda + U^\alpha|_\lambda)\,\delta U_\alpha]|_\gamma\,d\Omega\end{aligned}$$

With the help of Greens formula (1.14) and the equations of equilibrium (1.85), for arbitrary variations δU_α on C_1, the last expression is transformed to

$$\delta\pi_o = \int\int_\Omega P^\alpha \delta U_\alpha \, d\Omega + \int_{C_1} \sigma^{\gamma\lambda} \left(\delta^\alpha_\lambda + U^\alpha|_\lambda\right) N_\gamma \, \delta U_\alpha \, dC$$

$$= \int\int_\Omega \vec{P} \cdot \delta\vec{U} \, d\Omega + \int_{C_1} \vec{f}^*_{(n)} \cdot \delta\vec{U} \, dC \qquad (1.89)$$

from which

$$\sigma^{\gamma\lambda}\left(\delta^\alpha_\lambda + U^\alpha|_\lambda\right) N_\gamma = \vec{f}^*_{(n)} \cdot \vec{A}^\alpha \text{ on } C_1 \qquad (1.90)$$

For geometrically linear strain measure, (1.83), (1.85), (1.88), and (1.90) become

$$2\,\delta E_{\gamma\alpha} = \vec{A}_\gamma \cdot \delta\vec{a}_\alpha + \vec{A}_\alpha \cdot \delta\vec{a}_\gamma = U_\gamma|_\alpha + U_\alpha|_\gamma \qquad (1.91)$$

$$\vec{F}_\gamma = T^{\gamma\alpha}\vec{A}_\alpha = \sum_{\lambda=1}^{2} \left[T^{\gamma\lambda}\sqrt{A_{\lambda\lambda}}\right] \frac{\vec{A}_\lambda}{\sqrt{A_{\lambda\lambda}}} \quad (\lambda \text{ not summed}) \qquad (1.92)$$

$$\vec{F}_{(n)} = T^{\gamma\alpha}\vec{A}_\alpha N_\gamma = \sum_{\lambda=1}^{2} \left[T^{\gamma\lambda} N_\gamma \sqrt{A_{\lambda\lambda}}\right] \frac{\vec{A}_\lambda}{\sqrt{A_{\lambda\lambda}}} \quad (\lambda \text{ not summed})$$

$$T^{\gamma\alpha}|_\gamma + P^\alpha = 0 \qquad (1.93)$$

$$\delta\pi_o = \int\int_\Omega T^{\gamma\alpha} \delta E_{\gamma\alpha} \, d\Omega = \int\int_\Omega T^{\gamma\alpha} \delta U_\gamma|_\alpha \, d\Omega \qquad (1.94)$$

$$= \int\int_\Omega P^\alpha \delta U_\alpha \, d\Omega + \int_{C_1} T^{\gamma\alpha} N_\gamma \, \delta U_\alpha \, dC = \int\int_\Omega \vec{P}\cdot\delta\vec{U} d\Omega + \int_{C_1} \vec{F}^*_{(n)} \cdot \delta\vec{U} dC \qquad (1.95)$$

$$T^{\gamma\alpha} N_\gamma = \vec{F}^*_{(n)} \cdot \vec{A}^\alpha \quad \text{on } C_1 \qquad (1.96)$$

1.3 In-Plane Buckling of Plates

Plates subjected to in-plane loads may buckle laterally how-

ever, for certain cases there exists the possibility of in-plane buckling. For example, a circular arch (here idealized as a plate) subjected to uniform pressure may buckle in the plane for certain critical pressure (Timoshenko [6]). The state previous to buckling, refered here, is the nonlinear problem given by (1.81) through (1.90) of Art 1.2 and serves as a basis for the analysis termed the Euler Method of Stability.

The Euler Method of Stability concerns the problem of whether there exists at least one additional, distinct equilibrium configuration in the very close neighborhood of the original equilibrium configuration. The existance of a critical original configuration is assumed and a linearized theory developed, which determines the adjacent configuration.

The stresses, strains, displacements, body forces and prescribed boundary forces of the original configuration, respectively, are denoted by

$$\hat{\sigma}^{\gamma\alpha},\ \hat{\epsilon}_{\gamma\alpha},\ \hat{U}^{\gamma},\ \hat{P}_{\gamma},\ \hat{F}_{\gamma}$$

and those of the adjacent configuration by

$$\hat{\sigma}^{\gamma\alpha} + \tau^{\gamma\alpha},\ \hat{\epsilon}_{\gamma\alpha} + \epsilon_{\gamma\alpha},\ \hat{U}^{\gamma} + U^{\gamma},\ \hat{P}_{\gamma} + P_{\gamma},\ \hat{F}_{\gamma} + F_{\gamma}$$

where the prescribed boundary forces are acting on the boundary C_1 and the displacements $U^{\gamma} = 0$ on C_2.

The principle of virtual work applied to the adjacent configuration yields

$$\int_{\Omega}\int (\hat{\sigma}^{\gamma\alpha}+\tau^{\gamma\alpha})\,\delta(\hat{\epsilon}_{\gamma\alpha}+\epsilon_{\gamma\alpha})\,d\Omega - \int_{\Omega}\int (\hat{P}_{\gamma}+P_{\gamma})\,\delta U^{\gamma}\,d\Omega - \int_{C_1} (\hat{F}_{\gamma}+F_{\gamma})\,\delta U^{\gamma}\,dC = 0 \qquad (1.97)$$

where by (1.87)

$$2(\hat{\epsilon}_{\gamma\alpha}+\epsilon_{\gamma\alpha})=(\hat{U}_{\gamma}|_{\alpha}+U_{\gamma}|_{\alpha})+(\hat{U}_{\alpha}|_{\gamma}+U_{\alpha}|_{\gamma})+(\hat{U}_{\lambda}|_{\gamma}+U_{\lambda}|_{\gamma})(\hat{U}^{\lambda}|_{\alpha}+U^{\lambda}|_{\alpha}) \tag{1.98}$$

Let

$$2\tilde{E}_{\gamma\alpha}=U_{\gamma}|_{\alpha}+U_{\alpha}|_{\gamma}+\hat{U}_{\lambda}|_{\gamma}\,U^{\lambda}|_{\alpha}+U_{\lambda}|_{\gamma}\,\hat{U}^{\lambda}|_{\alpha} \tag{1.99}$$

which combined with (1.98) gives

$$(\hat{\epsilon}_{\gamma\alpha}+\epsilon_{\gamma\alpha})=\hat{\epsilon}_{\gamma\alpha}+\tilde{E}_{\gamma\alpha}+\tfrac{1}{2}U_{\lambda}|_{\gamma}\,U^{\lambda}|_{\alpha} \tag{1.100}$$

In order to have a linearized theory, the incremental quantities P^{γ} and F^{γ} are assumed to depend linearly on U^{γ} while the $\epsilon_{\gamma\alpha}$ and $\tau^{\gamma\alpha}$ can be approximated by linear functions of U^{γ}, such as

$$\tau^{\gamma\alpha}\,\delta\epsilon_{\gamma\alpha}\simeq\hat{T}^{\gamma\alpha}\,\delta\tilde{E}_{\gamma\alpha} \tag{1.101}$$

$$\hat{T}^{\gamma\alpha}=C^{\gamma\alpha\beta\mu}\tilde{E}_{\gamma\alpha}$$

where the $C^{\gamma\alpha\beta\mu}$ are independent of U^{γ}.

The substitution of (1.101) into (1.97) and the neglecting of nonlinear terms in the displacement U^{γ} and its derivatives, yields

$$\Big|\iint_{\Omega}\hat{\theta}^{\gamma\alpha}\,\delta\tilde{E}_{\gamma\alpha}d\Omega-\iint_{\Omega}\hat{P}_{\gamma}\delta U^{\gamma}d\Omega-\int_{C}\hat{F}_{\gamma}\,\delta U^{\gamma}dC\Big|+$$
$$+\iint_{\Omega}(\hat{T}^{\gamma\alpha}\delta\tilde{E}_{\gamma\alpha}+\hat{\sigma}^{\gamma\alpha}U_{\lambda}|_{\gamma}\,\delta U^{\lambda}|_{\alpha}-P_{\alpha}{}^{1}\delta U^{\alpha})d\Omega-\int_{C_1}F_{\alpha}\,\delta U^{\alpha}\,dC=0 \tag{1.102}$$

Taking the variation of (1.100) and changing afterwards the notation $\delta\hat{U}^{\gamma}$ to δU^{γ} gives $\delta\hat{\epsilon}_{\gamma\alpha}=\delta\tilde{E}_{\gamma\alpha}$. Consequently the first term in brackets in (1.102) can be cancelled since it is identified as the principle of virtual work applied to the original configuration, so that

$$\iint_{\Omega}(\hat{T}^{\gamma\alpha}\delta\tilde{E}_{\gamma\alpha}+\hat{\sigma}^{\gamma\alpha}U_{\lambda}|_{\gamma}\delta U^{\lambda}|_{\alpha}-P_{\alpha}\delta U^{\alpha})\,d\Omega-\int_{C_1}F_{\alpha}\delta U^{\alpha}dC=0 \tag{1.103}$$

Transforming (1.103) by Greens formula (1.14) and noticing that δU^{γ} are arbitrary on C_1 and Ω, the differential equations and boundary conditions thus derived are

$$[\tilde{T}^{\gamma\alpha}(A_{\gamma\lambda}+\hat{U}_{\lambda}|_{\gamma})+\hat{\sigma}^{\gamma\alpha}U_{\lambda}|_{\gamma}]|_{\alpha}+P_{\lambda}=0 \text{ on } \Omega \qquad (1.104)$$

$$\tilde{T}^{\gamma\alpha}(A_{\gamma\lambda}+\hat{U}_{\lambda}|_{\gamma})N_{\alpha}+\hat{\sigma}^{\gamma\alpha}U_{\lambda}|_{\gamma}N_{\alpha}=F_{\lambda} \text{ on } C_1$$

It is noticed that an adjacent position of equilibrium has been assumed to exist infinitely near a fundamental position of equilibrium and that $\omega = 0$ for both positions. This may be suspected when certain geometrical or loading symmetries are present such as in the case of an arch loaded with uniform pressure. Timoshenko [6] finds for the arch using the beam theory the pattern for fundamental configuration symmetric and the pattern for the adjacent configuration antisymmetric.

1.4 Lateral Buckling of Plates

Using a Linear Bending Measure

The problem considered is the stability of a plate of area Ω subjected to distributed forces on Ω and to boundary actions (forces and moments) on the contour C_1. The Euler Method of stability has been adopted for the analysis and the steps to follow are those of Art. 1.3.

The stress and moment tensors, the axial and bending measures, the in-plane and normal displacements, the distributed force, the boundary forces, and the boundary moments, respectively, for the fundamental state are

$$\hat{F}^{\gamma\alpha},\ \hat{M}^{\gamma\alpha},\ \hat{\epsilon}_{\gamma\alpha},\ \hat{\varkappa}_{\gamma\alpha},\ \hat{U}^{\alpha},\hat{\omega},\ \vec{P}^{**},\ \vec{F}^{**},\ \vec{M}^{**}$$

and for the adjacent state are

$$\hat{F}^{\gamma\alpha}+F^{\gamma\alpha},\hat{M}^{\gamma\alpha}+M^{\gamma\alpha},\ \hat{\epsilon}_{\gamma\alpha}+\epsilon_{\gamma\alpha},\ \hat{\varkappa}_{\gamma\alpha}+\varkappa_{\gamma\alpha},\ \hat{U}^{\alpha}+U^{\alpha},$$

$$\hat{\omega}+\omega,\ \vec{P}^{**}+\vec{P}^{*},\ \vec{F}^{**}+\vec{F}^{*}_{(n)},\ \vec{M}^{**}+\vec{M}^{*}_{(n)}$$

The principle of virtual work (1.47) applied to the adjacent configuration, with $\delta\vec{r}=\delta\vec{U}$, yields

$$\int\int_{\Omega}\Big[(\hat{F}^{\gamma\alpha}+F^{\gamma\alpha})\,\delta(\hat{\epsilon}_{\gamma\alpha}+\epsilon_{\gamma\alpha})+(\hat{M}^{\gamma\alpha}+M^{\gamma\alpha})\,\delta(\hat{\varkappa}_{\gamma\alpha}+\varkappa_{\gamma\alpha})\Big]d\Omega -$$
$$-\int\int_{\Omega}(\vec{P}^{**}+\vec{P}^{*})\cdot\delta\vec{r}\,d\Omega-\int_{C_1}\Big[(\vec{F}^{**}+\vec{F}^{*}_{(n)})\cdot\delta\vec{r}+(\vec{M}^{**}+\vec{M}^{*}_{(n)})\cdot\delta\vec{\theta}\Big]dC=0 \tag{1.105}$$

where

$$2\delta(\hat{\epsilon}_{\gamma\alpha}+\epsilon_{\gamma\alpha})=\delta(\hat{U}_{\gamma}|_{\alpha}+U_{\gamma}|_{\alpha})+\delta(\hat{U}_{\alpha}|_{\gamma}+U_{\alpha}|_{\gamma})+\delta[(\hat{\theta}_{\gamma}+\theta_{\gamma})(\hat{\theta}_{\alpha}+\theta_{\alpha})]$$
$$\delta(\hat{\varkappa}_{\gamma\alpha}+\varkappa_{\gamma\alpha}) = -\,\delta(\hat{\omega}|_{\gamma\alpha}+\omega|_{\gamma\alpha}) \tag{1.106}$$
$$\delta\vec{r} = \delta U^{\alpha}\vec{A}_{\alpha}+\delta\omega\vec{A}_{3}$$
$$\delta\vec{\theta} = \vec{A}_{3}\times\vec{A}^{\lambda}\,\delta\theta_{\lambda} = -\,\vec{A}_{3}\times\vec{A}^{\lambda}\,\delta\omega|_{\lambda}$$

Defining

$$2\delta\tilde{E}_{\gamma\alpha} = \delta U_{\gamma}|_{\alpha}+\delta U_{\alpha}|_{\gamma}+\hat{\theta}_{\gamma}\,\delta\theta_{\alpha}+\hat{\theta}_{\alpha}\,\delta\theta_{\gamma} \tag{1.107}$$

which combined with (1.106) results in

$$2\delta(\hat{\epsilon}_{\gamma\alpha}+\epsilon_{\gamma\alpha}) = 2\delta\tilde{E}_{\gamma\alpha}+\delta(\theta_{\alpha}\,\theta_{\gamma}) \tag{1.108}$$

Eq. (1.105) can be linearized assuming that the incremental quantities $\vec{P}^{*}$, $\vec{F}^{*}$, $\vec{M}^{*}$ are linear functions of the displacement $\vec{U}$ and that

$$F^{\gamma\alpha}\,\delta\epsilon_{\gamma\alpha}\simeq\tilde{F}^{\gamma\alpha}\,\delta\tilde{E}_{\gamma\alpha} \tag{1.109}$$
$$\tilde{F}^{\gamma\alpha} = C^{\gamma\alpha\beta\mu}\,\tilde{E}_{\beta\mu}$$

Introducing (1.109) and (1.108) into (1.105) and neglecting nonlinear terms in $\vec{U}$,

$$\iint_{\Omega} [\hat{F}^{\gamma\alpha}\,\delta\tilde{E}_{\gamma\alpha} + \hat{M}^{\gamma\alpha}\,\delta\varkappa_{\gamma\alpha} - \vec{P}^{**}\cdot\delta\vec{r}]\,d\Omega -$$

$$-\int_{C_1} [\vec{F}^{**}\cdot\delta\vec{r} + \vec{M}^{**}\cdot\delta\vec{\theta}]dC + \iint_{\Omega} [M^{\gamma\alpha}\,\delta\varkappa_{\gamma\alpha} + \hat{F}^{\gamma\alpha}\,\delta(\theta_\gamma\,\theta_\alpha)]\,d\Omega +$$

$$+\iint_{\Omega} \tilde{F}^{\gamma\alpha}\,\delta\tilde{E}_{\gamma\alpha}\,d\Omega - \iint_{\Omega} \vec{P}^{*}\cdot\delta\vec{r}\,d\Omega - \int_{C_1} [\vec{F}^{*}_{(n)}\cdot\delta\vec{r} + \vec{M}^{*}_{(n)}\cdot\delta\vec{\theta}]\,dC = 0 \quad (1.110)$$

Since the initial state is in equilibrium the first two integrals cancel eachother so that the principle of virtual work (1.110) becomes

$$\iint_{\Omega} [\tilde{F}^{\gamma\alpha}\,\delta\tilde{E}_{\gamma\alpha} + M^{\gamma\alpha}\,\delta\varkappa_{\gamma\alpha} + \hat{F}^{\gamma\alpha}\,\theta_\gamma\,\delta\theta_\alpha]\,d\Omega -$$

$$-\iint_{\Omega} \vec{P}^{*}\cdot\delta\vec{r}\,d\Omega - \int_{C_1} [\vec{F}^{*}_{(n)}\cdot\delta\vec{r} + \vec{M}^{*}_{(n)}\cdot\delta\vec{\theta}]\,dC = 0 \quad (1.111)$$

By virtue of

$$\tilde{F}^{\gamma\alpha}\,\delta\tilde{E}_{\gamma\alpha} = \tilde{F}^{\gamma\alpha}\,\delta U_\gamma\big|_\alpha + \tilde{F}^{\gamma\alpha}\,\hat{\omega}_{,\gamma}\,\delta\omega_{,\alpha}$$

and proceeding as in the derivation of (1.75), the principle (1.111) is transformed to

$$-\iint_{\Omega} [\tilde{F}^{\gamma\alpha}\big|_\alpha + P^{*\gamma}]\,\delta U_\gamma\,d\Omega - \iint_{\Omega} [M^{\gamma\alpha}\big|_{\alpha\gamma} + (\hat{F}^{\gamma\alpha}\,\omega_{,\gamma})\big|_\alpha + (\tilde{F}^{\gamma\alpha}\,\hat{\omega}_{,\gamma})\big|_\alpha +$$

$$+ P_3^{*}]\,\delta\omega\,d\Omega + \int_{C_1} [\tilde{F}^{\gamma\alpha}N_\alpha - F^{*\gamma}_{(n)}]\,\delta U_\gamma\,dC + \int_{C_1} [-M_{(NN)} +$$

$$+ M^{*}_{(NN)}]\,\frac{\delta\partial\omega}{\partial N}dC + \int_{C_1} [Q^{\alpha}N_\alpha - \frac{\partial M_{(NT)}}{\partial C} + \hat{F}^{\gamma\alpha}\omega_{,\gamma}N_\alpha + \tilde{F}^{\gamma\alpha}\hat{\omega}_{,\gamma}N_\alpha -$$

$$- F^{*3}_{(n)} + \frac{\partial M^{*}_{(NT)}}{\partial C}]\,\delta\omega\,dC - \sum_{i=1}^{m_1} [(M_{(NT)} - M^{*}_{(NT)})\,\delta\omega]_{c_1(i)} = 0 \quad (1.112)$$

where m_1 are the number of discontinuities in the tangent to C_1, and

$$M_{(NT)} = - M^{\gamma\alpha}\,N_\alpha\,T_\gamma$$

$$M_{(NN)} = M^{\gamma\alpha}\,N_\alpha N_\gamma$$

The field equations corresponding to (1.112) are

$$\tilde{F}^{\gamma\alpha}|_{\alpha} + P^{*\gamma} = 0 \tag{1.113}$$

$$M^{\gamma\alpha}|_{\alpha\gamma} + (\tilde{F}^{\gamma\alpha}\overset{\wedge}{\omega}_{,\gamma})|_{\alpha} + (\hat{F}^{\gamma\alpha}\omega_{,\gamma})|_{\alpha} + P^{*}_{3} = 0$$

$$\tilde{F}^{\gamma\alpha} N_{\alpha} = F^{*\gamma}_{(n)}$$

$$Q^{\alpha} N_{\alpha} - \frac{\partial M_{(NT)}}{\partial C} + \hat{F}^{\gamma\alpha}\omega_{,\gamma} N_{\alpha} + \tilde{F}^{\gamma\alpha}\overset{\wedge}{\omega}_{,\gamma} N_{\alpha} = F^{*3}_{(n)} - \frac{\partial M^{*}_{(NT)}}{\partial C}$$

$$M_{(NN)} = M^{*}_{(NN)}$$

$$[M_{(NT)}]_{C_1}(i) = [M^{*}_{(NT)}]_{C_1}(i); \quad i=1,\ldots m_1$$

with the last four expressions valid on the boundary C_1.

Initially Flat Plate

When the plate is initially flat, $\overset{\wedge}{\omega} = \overset{\wedge}{\omega}_{,\gamma} = 0$, Eq. (1.112) can be written

$$\int\int_{\Omega} [T^{\gamma\alpha}\delta E_{\gamma\alpha} + M^{\gamma\alpha}\delta\varkappa_{\gamma\alpha} + \hat{T}^{\gamma\alpha}\theta_{\gamma}\delta\theta_{\alpha}]\, d\Omega -$$

$$-\int\int_{\Omega} \vec{P}^{*}\cdot\delta\vec{r}\, d\Omega - \int_{C_1}[\vec{F}^{*}_{(n)}\cdot\delta\vec{r} + \vec{M}^{*}_{(n)}\cdot\delta\vec{\theta}]\, dC = 0 \tag{1.114}$$

where

$$E_{\gamma\alpha} = U_{\gamma}|_{\alpha} + U_{\alpha}|_{\gamma}$$

$$T^{\gamma\alpha} = C^{\gamma\alpha\beta\mu} E_{\beta\mu}$$

and where $\hat{T}^{\gamma\alpha}$ results from a geometrical linear analysis given by (1.93) and (1.96).

The field equations derived from (1.114) are

$$\left.\begin{aligned} & T^{\gamma\alpha}\big|_{\alpha} + P^{*\gamma} = 0 \\ & M^{\gamma\alpha}\big|_{\alpha\gamma} + (\hat{T}^{\gamma\alpha}\,\omega,_{\gamma})\big|_{\alpha} + P^{*}_{3} = 0 \end{aligned}\right\} \text{ on } \Omega \qquad (1.115)$$

$$\left.\begin{aligned} & T^{\gamma\alpha}\,N_{\alpha} = F^{*\gamma}_{(n)} \\ & Q^{\alpha}N_{\alpha} - \frac{\partial M_{(NT)}}{\partial C} + \hat{T}^{\gamma\alpha}\,\omega,_{\gamma}\,N_{\alpha} = F^{*3}_{(n)} - \frac{\partial M^{*}_{(NT)}}{\partial C} \\ & M_{(NN)} = M^{*}_{(NN)} \\ & [M_{(NT)}]_{C_1}(i) = [M^{*}_{(NT)}]_{C_1}(i) \;;\; i=1,\ldots,m_1 \end{aligned}\right\} \text{ on } C_1 \qquad (1.116)$$

Let

$$\hat{T}^{\gamma\alpha} \equiv P\,\hat{T}^{(o)\gamma\alpha} \qquad (1.117)$$

Taking $\hat{T}^{(o)\gamma\alpha}$ as a stress tensor corresponding to an arbitrary numerical value of the applied in-plane forces and P as an unknown parameter. Problem (1.115) may be interpreted as an <u>initial stress</u> problem where the initial stress tensor $\hat{T}^{(o)\gamma\alpha}$ is used to find the value of the parameter P which determines the critical value of the loading.

<u>Non-Conservative Systems</u>

For the analysis of the stability of non-conservative systems, Ziegler [1] has stressed the need to include the increment of inertia forces, namely

$$\begin{aligned} P^{*}_{\lambda} &= -M\ddot{U}_{\lambda} + B^{*}_{\lambda} \\ P^{*}_{3} &= -M\ddot{w} + B^{*}_{3} \end{aligned} \qquad (1.118)$$

where M is the mass of the plate per unit area and B^{*}_{λ}, B^{*}_{3} are prescribed body forces (other than inertia forces) given by linear functions of the displacements U^{λ}, w and their derivatives.

A type of follower-forces can be those forces which at the initial state were $\hat{f}^{\alpha}_{(n)}\ \vec{a}^{*}_{\alpha}$ and became $\hat{f}^{\alpha}_{(n)}\ \vec{d}_{\alpha}$ at the adjacent state. The $\hat{f}^{\alpha}_{(n)}$ are prescribed constants and the direction of the follower-forces for an initially flat plate are

$$\vec{a}^{*}_{\alpha} = \vec{R}_{,\alpha} + \hat{U}^{\beta}\big|_{\alpha}\ \vec{A}_{\beta}$$

$$\vec{d}_{\alpha} = \vec{a}^{*}_{\alpha} + \omega_{,\alpha}\ \vec{A}_{3}$$

The incremental stress on the contour C_f with normal N_γ is

$$\vec{F} = \hat{f}^{\alpha}_{(n)}\ \vec{d}_{\alpha} - \hat{f}^{\alpha}_{(n)}\ \vec{a}^{*}_{\alpha} = \hat{f}^{\alpha}_{(n)}\ \omega_{,\alpha}\ \vec{A}_{3} \tag{1.119}$$

The boundary conditions for the initial state of a flat plate are given by (1.96) as

$$\hat{f}^{\alpha}_{(n)} = \hat{T}^{\gamma\alpha}\ N_{\gamma}$$

which transforms (1.119) to

$$\vec{F} = \hat{T}^{\gamma\alpha}\ N_{\gamma}\ \omega_{,\alpha}\ \vec{A}_{3}$$

$$\text{i.e.}\quad F^{*}_{3} = \hat{T}^{\gamma\alpha}\ N_{\gamma}\ \omega_{,\alpha} \tag{1.120}$$

Combining (1.115) and (1.120) gives

$$Q^{\alpha}\ N_{\alpha} - \frac{\partial M_{(NT)}}{\partial C} = -\frac{\partial M^{*}_{(NT)}}{\partial C} \quad \text{on } C_f \tag{1.121}$$

When moments and forces in the direction of the vector $\vec{A}_3$ are zero, namely $B^{*}_{3} = F^{*3}_{(n)} = M^{*}_{(NN)} = M^{*}_{(NT)} = 0$, Eq. (1.114) and (1.115) become

$$\int\int_{\Omega} [M^{\gamma\alpha}\delta\varkappa_{\gamma\alpha} + \hat{T}^{\gamma\alpha}\omega_{,\gamma}\ \delta\omega_{,\alpha} + M\ddot{\omega}\delta\omega]d\Omega = 0 \tag{1.122}$$

$$M^{\gamma\alpha}\big|_{\alpha\gamma} + (\hat{T}^{\gamma\alpha}\omega_{,\gamma})\big|_{\alpha} - M\ddot{\omega} = 0 \quad \text{on } \Omega$$

$$M_{(NN)} = 0 \qquad \text{on } C_1$$

$$Q^{\alpha}N_{\alpha} - \frac{\partial M_{(NT)}}{\partial C} + \hat{T}^{\gamma\alpha}\,\omega_{,\gamma}\,N_{\alpha} = 0 \qquad \text{on } C_1\text{-}C_f$$

$$[M_{(NT)}]_{C_1(i)} = 0; \quad i=1,\ldots,m_1$$

$$\int_{\Omega}\int T^{\gamma\alpha}\delta E_{\gamma\alpha}\, d\Omega = \int_{\Omega}\int P^{*}_{\gamma}\delta U^{\gamma} d\Omega + \int_{C_1} F^{*}_{\gamma}\delta U^{\gamma} dC \qquad (1.123)$$

$$T^{\gamma\alpha}\big|_{\alpha} - M\ddot{U}^{\gamma} + B^{*\gamma} = 0 \qquad \text{on } \Omega$$

$$T^{\gamma\alpha}\,N_{\alpha} = F^{*\gamma}_{(n)} \qquad \text{on } C_1$$

Eq. (1.122) together with (1.121) constitute an eigenvalue problem whose solution is independent of the incremental stresses $T^{\gamma\alpha}$.

When the incremental applied forces normal to $\vec{A}_3$ are zero, i.e. $B^{*\gamma} = F^{*\gamma}_{(n)} = 0$, then

$$T^{\gamma\alpha} = U^{\gamma} = 0$$

which indicates that the eigenfunctions ω alone cause the strains of the middle surface given as $\omega_{,\gamma}\omega_{,\alpha}$

Initially Flat Plate-Nonlinear Bending Measure.

The bifurcation problem for initially flat plates, may be treated by assuming both nonlinear bending and axial strain measures.

In the notation of (1.27) and (1.28) the initial state is represented by

$$\hat{F}^{\gamma\alpha},\ \overset{\wedge}{\mu}_{\gamma\alpha},\ \hat{m}^{\gamma\alpha},\ \hat{b}_{\gamma\alpha},\ \hat{U}^{\alpha},\ \overset{\wedge}{\omega}$$

and the adjacent state

$$\hat{F}^{\gamma\alpha}+f^{\gamma\alpha},\ \overset{\wedge}{\mu}_{\gamma\alpha}+\mu_{\gamma\alpha},\ \hat{m}^{\gamma\alpha}+m^{\gamma\alpha},\ \hat{b}_{\gamma\alpha}+b_{\gamma\alpha},\ \hat{U}^{\alpha}+U^{\alpha},\ \overset{\wedge}{\omega}+\omega$$

The virtual work expression (1.27) for the adjacent configuration is

$$\delta\pi_o=\iint_{\Omega_o}[(\hat{f}^{\gamma\alpha}+f^{\gamma\alpha})\delta(\hat{\mu}_{\gamma\alpha}+\mu_{\gamma\alpha})-(\hat{m}^{\gamma\alpha}+m^{\gamma\alpha})\delta(\hat{b}_{\gamma\alpha}+b_{\gamma\alpha})+$$
$$+(\hat{m}^{\gamma\alpha}\hat{b}^{\rho}_{\gamma}+m^{\gamma\alpha}b^{\rho}_{\gamma})\delta(\hat{\mu}_{\alpha\rho}+\mu_{\alpha\rho})]d\Omega_o \qquad (1.124)$$

For an initially flat plate i.e.

$$\hat{b}^{\rho}_{\gamma} = \hat{m}^{\gamma\alpha} = P^{*}_{3} = 0$$

and applying (1.37), the nonlinear strain measures (1.28) result in

$$\delta\mu_{\gamma\alpha}=(\vec{a}^{*}_{\alpha}+U^{\lambda}|_{\alpha}\,\vec{A}_{\lambda}-\theta_{\alpha}\vec{A}_{3})\cdot(\delta U^{\rho}|_{\gamma}\vec{A}_{\rho}-\delta\theta_{\gamma}\vec{A}_{3})$$
$$=\delta\tilde{E}_{\gamma\alpha}+U_{\lambda}|_{\alpha}\delta U^{\lambda}|_{\gamma}+\theta_{\alpha}\delta\theta_{\gamma} \qquad (1.125)$$

$$\delta\tilde{E}_{\gamma\alpha}\equiv(\vec{a}^{*}_{\alpha}\cdot\vec{A}_{\rho})\delta U^{\rho}|_{\gamma} = (\vec{A}_{\alpha}+\hat{U}^{\lambda}|_{\alpha}\vec{A}_{\lambda})\cdot\vec{A}_{\rho}\,\delta U^{\rho}|_{\gamma}$$
$$=(A_{\alpha\rho}+\hat{U}_{\rho}|_{\alpha})\delta U^{\rho}|_{\alpha}$$

Adopting the notation

$$\hat{f}^{\gamma\alpha} = \hat{\sigma}^{\gamma\alpha}\sqrt{\frac{A}{a}}$$

and with the help of (1.124) and (1.125), the principle of virtual work for the adjacent configuration becomes

$$\int_{\Omega}\int[\hat{\sigma}^{\gamma\alpha}\delta\tilde{E}_{\gamma\alpha}-P^{**}_{\alpha}\,\delta U^{\alpha}]d\Omega-\int_{C_1}F^{**}_{\gamma}\,\delta U^{\gamma}dC+$$
$$+\iint_{\Omega_o}[f^{\gamma\alpha}\delta\mu_{\gamma\alpha}-m^{\gamma\alpha}\,\delta b_{\gamma\alpha}+m^{\gamma\alpha}b_{\gamma}{}^{\rho}\,\delta\mu_{\alpha\rho}+\hat{f}^{\gamma\alpha}(U_{\lambda}|_{\alpha}\delta U^{\lambda}|_{\gamma}+\theta_{\alpha}\delta\theta_{\gamma})]d\Omega_o-$$
$$-\int_{\Omega}\int\vec{P}^{*}\cdot\delta\vec{r}d\Omega-\int_{C_1}[\vec{F}^{*}_{(n)}\cdot\delta\vec{r}+\vec{M}^{*}_{(n)}\cdot\delta\vec{\theta}]dC = 0 \qquad (1.126)$$

where the external virtual work remains the same as in (1.105).

The following linearization is to be introduced in (1.126)

$$f^{\gamma\alpha}\delta\mu_{\gamma\alpha} \simeq \sqrt{\frac{A}{a}}\,\tilde{T}^{\gamma\alpha}\,\delta\tilde{E}_{\gamma\alpha} \tag{1.127}$$

$$\tilde{T}^{\gamma\alpha} \equiv C^{\gamma\alpha\beta\mu}\tilde{E}_{\beta\mu}$$

$$- m^{\gamma\alpha}\delta b_{\gamma\alpha}+m^{\gamma\alpha}b_{\gamma}{}^{\rho}\,\delta\mu_{\alpha\rho} \simeq \sqrt{\frac{A}{a}}\,M^{\gamma\alpha}\,\delta\varkappa_{\gamma\alpha}$$

$$M^{\gamma\alpha} \equiv D^{\gamma\alpha\beta\mu}\,\varkappa_{\beta\mu}$$

where the linearization with respect to the bending measures is the same carried out in Art. 1.2 from (1.30) to (1.44).

The first two integrals in (1.26) vanish since together they are equal to the expression of the virtual work principle relative to the original configuration. Therefore the introduction of the linearization (1.127) reduces (1.126) to

$$\int_{\Omega}\int[\tilde{T}^{\gamma\alpha}\delta\tilde{E}_{\gamma\alpha}+M^{\gamma\alpha}\delta\varkappa_{\gamma\alpha}+\hat{\sigma}^{\gamma\alpha}U_{\lambda}\big|_{\alpha}\delta U^{\lambda}\big|_{\gamma}+\hat{\sigma}^{\gamma\alpha}\,\theta_{\alpha}\delta\theta_{\gamma}]d\Omega-$$

$$-\int_{\Omega}\int\vec{P}^{*}\cdot\delta\vec{r}d\Omega-\int_{C_1}[\vec{F}^{*}_{(n)}\cdot\delta\vec{r}+\vec{M}^{*}_{(n)}\cdot\delta\vec{\theta}]dC = 0 \tag{1.128}$$

where $\hat{\sigma}^{\gamma\alpha}$ results from the nonlinear analysis of (1.81) through (1.90).

The principle (1.128) decouples into the expressions

$$\int_{\Omega}\int[\tilde{T}^{\gamma\alpha}\delta\tilde{E}_{\gamma\alpha}+\hat{\sigma}^{\gamma\alpha}U_{\lambda}\big|_{\alpha}\delta U^{\lambda}\big|_{\gamma}]d\Omega=\int_{\Omega}\int P^{*}_{\gamma}\delta U^{\gamma}d\Omega+\int_{C_1}F^{*\gamma}_{(n)}\delta U_{\gamma}dC \tag{1.129}$$

$$\int_{\Omega}\int[M^{\gamma\alpha}\delta\varkappa_{\gamma\alpha}+\hat{\sigma}^{\gamma\alpha}\theta_{\alpha}\delta\theta_{\gamma}]d\Omega=\int_{\Omega}\int P^{*3}\delta w d\Omega+\int_{C_1}[F^{*3}_{(n)}\delta w+\vec{M}^{*}_{(n)}\cdot\delta\vec{\theta}]dC \tag{1.130}$$

When the right hand sides of (1.129) and (1.130) vanish (no incremental loads), the two possibilities of bifurcation which arise are

a) In-plane buckling i.e. $w = 0$ and U^{α} solution to (1.129)

b) Lateral buckling i.e. $U^{\alpha} = 0$ and w solution to (1.130)

Substituting the geometrically linear $\hat{T}^{\gamma\alpha}$ of (1.93) instead of the nonlinear $\hat{\sigma}^{\gamma\alpha}$ of (1.128), the simpler but more approximate equations thus obtained coincide with (1.114).

2. TRIAL FUNCTION METHODS

2.1 Introduction

By using simplified theories or models, most practical problems in science and engineering can only be reduced to a system of complicated equations (field equations) which cannot be solved by the analytical methods available. Several approximate methods have been used, among them the trial function methods. In these methods, use is made of a trial solution which consists of a combination of known functions and unknown parameters which are to be determined according to specified criteria. When the criteria are orthogonality conditions the label is method of weighted residuals or when a functional is made stationary there is said to be a variational method.

A summary of these methods has been given by Finlayson and Scriven [7] and the main references are the books by Mikhlin [8, 9, 10] Crandall [11], Collatz [12], Ames [13], Becker [14], Sokolnikoff [15], Washizu [3], Gould [16], and Sobolev [17].

In this section a discussion of these methods is attempted. At times proofs are left to the references or presented here in a modified form. A special emphasis is made with respect to the conditions which the trial functions should satisfy. At the end of the section, a brief description is given of some of what has been done regarding the application of numerical methods to the problem of finding the critical loads for plates.

Some definitions given by Mikhlin [8] are now presented, to be used in the remainder of this section.

Two functions $U(\vec{X})$ and $V(\vec{X})$ of the position vector $\vec{X}$, and two constants a, b are given. Thus a homogenious quadratic functional J (U,V) satisfies the relationship

$$J(aU+bV,\ aU+bV)=a^2J(U,U)+2abJ(U,V)+b^2J(V,V) \qquad (2.1)$$

A linear functional satisfies the relationship

$$L(aU+bV) = aL(U) + bL(V) \tag{2.2}$$

A quadratic functional is positive when

$$\infty > J(U,U) \geq 0 \tag{2.3}$$

where the iquality sign only holds when $U \equiv 0$.

A quadratic positive functional may be used to define a norm

$$|U| = \sqrt{J(U,U)} \tag{2.4}$$

The class of functions for which the norm is finite are called functions with finite energy (with respect to the given functional). The norm itself in (2.4) may be termed norm with respect to a positive quadratic functional.

The scalar product of two functions in a domain Ω is

$$\langle U, V \rangle = \iint_{\Omega} UV d\Omega \tag{2.5}$$

the scalar product in a one dimensional domain s is

$$\langle U, V \rangle_s = \int_s UV dC \tag{2.6}$$

The norm of a function is given by

$$\|U\|^2 = \iint_{\Omega} U^2 d\Omega \tag{2.7}$$

The functions with finite $\|U\|$ are called functions with finite norm. A functional is positive definite if

$$|U|^2 \geq \nu^2 \|U\|^2 \tag{2.8}$$

where ν is a real constant.

A sequence of functions $\varphi_1, \varphi_2, \ldots \varphi_n$ with finite energy, are linearly independent when their Gram determinant is non-zero

$$\text{Det } [J(\varphi_i, \varphi_j)] \neq 0 \tag{2.9}$$

For the class of functions with finite norm, (2.9) is simplified to

$$\text{Det } [\langle \varphi_i, \varphi_j \rangle] \neq 0 \tag{2.10}$$

A sequence $\{\varphi_i\}$ is said to be complete in energy if for a given function $U(\vec{X})$ with finite energy and a number $\epsilon > 0$ it is possible to find an integer n for which

$$|U - U_n| < \epsilon \tag{2.11}$$

where $U_n = \sum_{i=1}^{n} q_i \varphi_i$ and the q_i are constants.

When (2.11) is satisfied it is then said that $U_n \xrightarrow{E} U$ converges in energy.

In a similar way a sequence of functions $\{\varphi_i\}$ with finite norm is complete when

$$\|U - U_n\| < \epsilon \tag{2.12}$$

i.e. $U_n \to U$ converges in the mean.

2.2 Variational Problems

The class of functions

It is known from the classical variational calculus that the problem of minimizing a functional (which has a minimum) is equivalent to the integration of a system of differential equations under appropriate boundary conditions.

For example on a two dimensional domain Ω delimited by the contour C, the Poisson's equation can be written as:

$$A_o U = U_{,\alpha\alpha} = - f_o(X_1, X_2) \tag{2.13}$$

$$U|_C = 0$$

which is equivalent to the problem of finding the minimum of the functional

$$F(U) = \iint_{\Omega} (U_{,\alpha}\, U_{,\alpha} - 2f_o U)\, d\Omega \tag{2.14}$$

under the same boundary conditions $U\big|_C = 0$.

In terms of the notation of Art. 2.1, (2.14) becomes

$$F(U) = J(U, U) - 2\, L\,(f_o, U) \tag{2.15}$$

$$J(U, V) = \iint_{\Omega} U_{,\alpha}\, V_{,\alpha}\, d\Omega$$

$$L(f_o, U) = \iint_{\Omega} f_o\, U\, d\Omega$$

where U and V are functions with finite energy.

In (2.15) the norm $|U|^2 = J(U, U)$ can be recognized as a positive functional for functions with finite energy and $L(f_o, U)$ as a linear functional.

It is observed that although the operator A_o in (2.13) involves derivatives of second order, the functional F(U) contains derivatives up to first order. J(U,U) has meaning even when the first derivatives have finite discontinuities (jumps) on certain finite number of curves. Therefore the class of functions which make the functional F(U) minimum may be broadened to include those functions with derivatives of first order possessing finite jumps on certain curves.

More generally, if the order of the maximum derivative in the functional to be minimized is t, the class of admissible functions may include those with finite jumps in its t th. derivative.

It is desirable to investigate properties of the t th derivative of a given function with respect to the axes $X_{\alpha_1}, X_{\alpha_2}, \ldots X_{\alpha_t}$.

Let also $\xi(X_\lambda)$ be a function which together with all its derivatives up to and including t th order are continuous inside the domain Ω and zero on the contour C, that is

$$\xi_{,\beta_1 \beta_2 \ldots \beta_k}\Big|_C = 0 \qquad K = 0,1,..,t \tag{2.16}$$

Sobolev [17] defines the operator $(-1)^t \partial^*_{\alpha_1 \alpha_2 .. \alpha_t}$ of <u>generalized differentiation</u> when, given the function $\xi(X_\lambda)$ of (2.16) and a function $V(X_\lambda)$, the following condition is satisfied:

$$\iint_\Omega V \, \xi_{,\alpha_1 \alpha_2 \ldots \alpha_t} \, d\Omega = (-1)^t \iint_\Omega \xi \, \partial^*_{\alpha_1 \alpha_2 \ldots \alpha_t} V \, d\Omega \tag{2.17}$$

The function $(-1)^t \partial^*_{\alpha_1 \alpha_2 \ldots \alpha_t} V$ is called <u>generalized derivative</u> of t th order and may have finite discontinuities at certain finite numbers of curves as shown by Smirnov [18]. When continuity is enforced the generalized derivative coincides with the usual derivative.

For the minimization of the functional F(U) of (2.14) the functions U belong to the class with generalized derivative of first order for which J(U,U) of (2.15) is finite (functions with finite energy) and satisfies the prescribed boundary conditions.

<u>Boundary conditions</u>

Let now F(U) be a quadratic functional given over the surface Ω and the function U be subjected to homogeneous boundary conditions on the boundary C. These boundary conditions are to be defined later, while the functional to be minimized is

$$F(U) = J(U,U) - 2 \left\langle f_o, U \right\rangle \tag{2.18}$$

where J(U,U) is an integral over the domain Ω whose integrand is a differential expression, and f_o is a function prescribed over the domain Ω.

The variational expression corresponding to (2.18) becomes

$$J(U, \delta U) - \langle f_o, \delta U \rangle = 0 \qquad (2.19)$$

For problems of this kind, Greens formula often provides an equivalent expression for $J(U, \delta U)$ which is made of an integral over the surface Ω and several integrals over C. When at each point of the boundary C a unique unit normal vector to the contour C can be drawn, the application of Green's formula may lead to

$$J(U, \delta U) = \langle A_o U, \delta U \rangle + \sum_{i=1}^{l} \langle A_i U, \hat{A}_i \delta U \rangle_C \qquad (2.20)$$

where A_o is a differential operator and l gives the number of linearly independent differential operators A_i, $\hat{A}_i$.

Substituting (2.20) into (2.19), it is found that

$$\langle A_o U - f_o, \delta U \rangle + \sum_{i=1}^{l} \langle A_i U, \hat{A}_i \delta U \rangle_C = 0 \qquad (2.21)$$

This last equation helps to define the boundary conditions. The <u>geometrical</u> or <u>principal</u> boundary conditions are those which verify

$$\hat{A}_i U = 0 \quad \text{on } \hat{s}_i \qquad i=1, 2, \ldots, l \qquad (2.22)$$

$\hat{s}_i$ being the parts of the boundary C for which the restriction is meant.

Now assuming that U satisfies only the geometrical boundary conditions (2.22), and using (2.21),

$$A_o U = f_o \quad \text{on } \Omega$$

$$A_i U = 0 \quad \text{on } s_i = C - \hat{s}_i \qquad i = 1,2,\ldots,l \qquad (2.23)$$

Eqs. (2.23) constitute the so-called <u>mechanical or natural</u> boundary conditions.

Mikhlin [14, P.162] states that when A_o is a differential operator of order 2t, the boundary conditions are homogeneous and the operator A_o is positive, i.e.

$$\langle A_o U, U \rangle \geq 0$$

$$\langle A_o U, U \rangle = 0 \Rightarrow U \equiv 0$$

Then the geometrical boundary conditions contain derivatives of order $\leq$ t-1, while the mechanical boundary conditions contain some terms with derivatives of order $\geq$ t.

For example in (2.13) the boundary condition is geometric (derivative of zeroth order).

For problems where the mechanical boundary conditions are inhomogeneous, the functional F(U) to be minimized may be written as:

$$F(U) = J(U, U) - 2\, L(U) \tag{2.24}$$

$$L(U) = \langle f_o, U \rangle + \sum_{i=1}^{l} \langle f_i, \hat{A}_i U \rangle_{s_i}$$

where the functions f_i are to be identified.

The variational expression corresponding to $(2.24)_1$, is

$$J(U, \delta U) - L(\delta U) = 0 \tag{2.25}$$

Substituting (2.20) into (2.25) and assuming U to satisfy only the homogeneous geometrical boundary conditions (2.22), it is found that

$$A_o U = f_o \quad \text{on } \Omega$$

$$A_i U = f_i \quad \text{on } s_i \quad i=1,2,\ldots,l \tag{2.26}$$

From (2.26) the f_i are identified as the prescribed functions needed for the statement of inhomogeneous mechanical boundary conditions.

Finally, a minimization problem with inhomogeneous geometrical boundary conditions can be transformed to another minimization problem with homogeneous boundary conditions so the results described above remain valid (Art. 2.5).

2.3 Method of Weighted Residuals

The application of this method to two problems will now be described. Both problems are defined as a domain Ω delimited by a boundary C. The boundary conditions are specified on l segments s_j; j=1,2,...,l of the boundary C, as follows:

A boundary value problem

$$H_o U = f_o \qquad \text{on } \Omega \tag{2.27}$$

$$H_j U = f_j \qquad \text{on } s_j, \quad j=1,2...,l$$

An eigenvalue problem

$$H_o U - \lambda M_o U = 0 \qquad \text{on } \Omega \tag{2.28}$$

$$H_j U - \lambda M_j U = 0 \qquad \text{on } s_j, \quad j=1,2,...,l$$

where for j=0,1,2,...,l the H_j, M_j are operators and the f_j are functions.

The residuals are defined for any function U_n by

$$R_j U_n = H_j U_n - f_j \quad j = 0,1,...,l \tag{2.29}$$

and for the eigenvalue problem

$$R_j U_n = H_j U_n - \lambda M_j U_n \qquad j=0,1,...,l \tag{2.30}$$

The method of weighted residuals consists of assuming a function

$$U_n = \sum_{i=1}^{n} q_i \varphi_i \qquad (2.31)$$

where φ_i are known functions, termed coordinate functions, and q_i are n parameters, which are determined by establishing n orthogonality conditions.

If the coordinate functions satisfy all the boundary conditions, it is only necessary to use the first residual R_o (Eq. 2.29 or 2.30) in the orthogonality conditions:

$$\left\langle R_o\, U_n,\ \psi_j \right\rangle = 0; \qquad j=1,2\ldots,n \qquad (2.32)$$

where ψ_j are arbitrary weighting functions.

When the given coordinate functions φ_i, i=1,...,n do not satisfy the boundary conditions it is then necessary to take the boundary residuals $R_j U_n$; j=1,...,l into consideration.

According to the form of the weighting functions in (2.32), the method receives different names, as follows:

a) Collocation

In this method a number of points $\vec{Y}_j$, j=1,...,n are chosen where the residual R_o is "collocated", so that the weighting functions become

$$\psi_j = \delta(\vec{X} - \vec{Y}_j) \qquad (2.33)$$

where $\vec{X}$ is an arbitrary point and $\delta(\vec{X}-\vec{Y}_j)$ the Delta Dirac function. By definition the Delta Dirac function is zero everywhere except for $\vec{X} = \vec{Y}_j$ where it has a unit value.

The equations obtained from (2.32) are

$$R_o\, U_n\, (\vec{Y}_j) = 0 \qquad j=1,\ldots,n \tag{2.34}$$

with coordinate functions which satisfy the boundary conditions.

When the available coordinate functions do not satisfy the boundary conditions everywhere then for each residual R_i there need to be established n_i orthogonality conditions, where $i=0,1,\ldots,l$, as follows:

$$\left\langle R_o\, U_n,\ \delta(\vec{X} - \vec{Y}_j) \right\rangle = 0 \quad j=1,\ldots,n_o \tag{2.35}$$

$$\left\langle R_i\, U_n,\ \delta(\vec{X} - \vec{Y}_j) \right\rangle_{s_i} = 0;\ j=1,\ldots,n_i;\ i=1,\ldots,l$$

or, which is the same,

$$R_i\, U_n\, (\vec{Y}_j) = 0 \qquad j=1,\ldots,n_i;\quad i=0,1,\ldots,l \tag{2.36}$$

where the total number of collocation points is kept equal to the number of coordinate functions.

b) Method of the Subdomain

The domain Ω is divided into n subdomains Ω_j and the weighting functions are defined

$$\left.\begin{aligned} \psi_j &= 1 \quad \text{when } \vec{X} \text{ belongs to } \Omega_j \\ \psi_j &= 0 \quad \text{when } \vec{X} \text{ does not belong to } \Omega_j \end{aligned}\right\} \quad j=1,\ldots,n$$

where $\vec{X}$ is an arbitrary point in Ω.

From (2.32) the orthogonality conditions become

$$\iint_{\Omega_j} R_o U_n d\Omega = 0 \qquad j=1,\ldots,n \tag{2.37}$$

where the coordinate functions included in U_n satisfy all the boundary conditions.

c) Method of Moments (Galerkin)

Given an operator T the weighting functions are defined as:

$$\psi_j = T\,\varphi_j \qquad j=1,\ldots,n \qquad (2.38)$$

and the orthogonality conditions by

$$\left\langle R_o\, U_n,\ T\,\varphi_j \right\rangle = 0 \qquad j=1,\ldots,n \qquad (2.39)$$

When T = 1 the method is termed Galerkin's method. Note that the coordinate functions need to satisfy the boundary conditions of the problem.

Although in this application Galerkin's method uses coordinate functions which satisfy all the boundary conditions, in Art. 2.7 an example is shown where (2.39) is first transformed by Green's formula to an equivalent expression in which several boundary residuals are substituted. As a result, the final expression only requires coordinate functions which satisfy the boundary conditions that had not been used in the transformation of (2.39). Thus, when Galerkin's method is applied to field equations for which an equivalent minimum problem exists, the rearrangement of (2.39) just mentioned brings Galerkin's method to coincidence with the RITZ method. Thereby only the geometrical boundary conditions of the minimum problem need to be considered.

Another variation of the Moment Method is called Kanterovick's method, where the parameters of the trial solution are functions (as oppossed to constants).

The trial solution is taken as

$$U_n = \sum_{i=1}^{n} q_i(X_1)\,\varphi_i$$

Denoting the domain Ω for X_1 = const. by C_x, the orthogonality

conditions become the system of differential equations

$$\int_{C_x} R_o \, U_n \, \psi_j \, dX_2 = 0 \qquad j=1,\ldots,n \tag{2.40}$$

where Ω has been taken as two dimensional and the weighting functions are given by (2.38).

For a two dimensional domain, Kerr [19] has applied a scheme termed Extended **Kanterovick's** Method, which consists of the following steps:

1) Application of Kanterovick's method using the coordinate functions $\varphi_i(X_2)$, $i=1,\ldots,n$ and solving the system (2.40) for the unknowns $q_i\ (X_1)$.

2) The functions $q_i(X_1)$, determined in the previous step are used for another application of Kanterovick's method as coordinate functions and $\overline{q}_i(X_2)$ are used as unknown parameters. The domain Ω for X_2 = const. is denoted by C_y and the system of differential equations to be solved becomes

$$\int_{C_y} R_o \, U_n \, \psi_j \, dX_1 = 0 \qquad j=1,\ldots,n$$

where

$$U_n = \sum_{i=1}^{n} \overline{q}_i(X_2)\ q_i(X_1)$$

$$\psi_j = T\, q_j(X_1) \qquad j=1,\ldots,n$$

3) More cycles may be made using as coordinate functions the solutions of the previous step. This may prove advantageous, especially when using one coordinate function at each step, because only one differential equation needs to be solved each time.

d) Least Squares Method

Define the functional

$$I(U_n) = \left\langle \overline{P}_o R_o U_n,\ R_o U_n \right\rangle + \sum_{j=1}^{l} \left\langle \overline{P}_j R_j U_n,\ R_j U_n \right\rangle_{s_j} \qquad (2.41)$$

where $\overline{P}_o$ given on Ω and $\overline{P}_j$ on s_j, $j=1,\ldots,l$ are all positive weighting functions.

The parameters q_i of (2.31) are determined from the minimum of $I(U_n)$, which yields:

$$\left\langle R_o U_n,\ \overline{P}_o \frac{\partial R_o U_n}{\partial q_k} \right\rangle + \sum_{j=1}^{l} \left\langle R_j U_n,\ \overline{P}_j \frac{\partial R_j U_n}{\partial q_k} \right\rangle_{s_j} = 0 \qquad (2.42)$$

$$k=1,\ldots,n$$

This expression (2.41) can be interpreted as an application of the method of weighted residuals, where all residuals are orthogonalized and the coordinate functions need not satisfy the boundary conditions.

One may notice that the application of the Least Squares Method to linear eigenvalue problems involves some difficulties since it makes the problem nonlinear.

2.4 Variational Methods

In these methods a functional is established whose stationary value results in an Euler equation equal to the governing equation of the problem and the so-called natural boundary conditions. Among the most important variational methods are:

a) Ritz Method

In this case a trial solution (2.31) is substituted into a functional which is being minimized. The two types of problems dealt with here are:

A boundary value problem

$$F(U) = |U|^2 - 2\,L(U) = J(U,U) - 2L(U) \tag{2.43}$$

or an eigenvalue problem

$$\lambda = \frac{|U|^2_H}{|U|^2_M} = \frac{J_H(U,U)}{J_M(U,U)} \tag{2.43}$$

where $J(U,U)$, $J_H(U,U)$ and $J_M(U,U)$ are positive quadratic functionals and $L(U)$ is a linear functional. The boundary conditions are the homogeneous geometrical boundary conditions corresponding to the minimum of the functionals in (2.43) (analogous to Eq. 2.22). Note that a minimum problem for which the geometrical boundary conditions are homogeneous can be transformed to another minimum problem where they are homogeneous (Art. 2.5).

The variational expressions for (2.43), are

$$J(U, \delta U) - L(\delta U) = 0 \tag{2.44}$$

or

$$J_H(U, \delta U) - \lambda J_M(U, \delta U) = 0 \tag{2.44}$$

Substituting the trial function (2.31) with coordinate functions φ_i, $i=1,\ldots,n$ satisfying the geometrical boundary conditions, it is found that

$$\sum_{i=1}^{n} J(\varphi_i, \varphi_j) - L(\varphi_j) = 0 \tag{2.45}$$

or

$$\sum_{i=1}^{n} \left(J_H(\varphi_i, \varphi_j) - \lambda J_M(\varphi_i, \varphi_j)\right) = 0 \quad j=1,\ldots,n \tag{2.45}$$

where the first expression constitutes a system of linear equations and the second a linear eigenvalue problem between two ma-

trices.

In order to have a solution to (2.45) the coordinate functions must be functions with finite energy, i.e.

$$J(\varphi_i, \varphi_i) < \infty \quad i = 1,\ldots,n$$

for the boundary value problem. In addition the coordinate functions must be linearly independent and thereby satisfy (2.9).

Using the approximation $U_n = \sum_{i=1}^{n} q_i(X_1)\,\varphi_i$, where the unknown parameters are functions, Eqs. (2.45) become a system of differential equations similar to those of Kanterovick's method but with the additional advantage that the coordinate functions need only satisfy the geometrical boundary conditions of the problem.

b) Courant's Method

Given a functional to be minimized, Courant has suggested a modified minimum problem which improves the convergence towards the satisfaction of the Euler equation of the original problem (Mikhlin [8, p. 95]).

Let $F(U)$ be the original functional and $A_oU = f_o$ its Euler equation. Assuming the function f_o to be defined in the two-dimensional domain Ω and to have continuous derivatives up to order K, it is possible to set

$$I_1(U) = F(U) + \sum_{p=0}^{k} \sum_{m=0}^{p} \left\| \frac{\partial^p (A_oU - f_o)}{\partial X_1^{\,m}\, \partial X_2^{\,p-m}} \right\|^2 \qquad (2.46)$$

It is observed that the minima of $I_1(U)$ and $F(U)$ coincide and are given by the exact solution U_o.

c) Adjoint Variational Methods.

Given an operator H_o, the adjoint operator H_o^* and adjoint boundary conditions are defined from the relationship

$$\langle H_o U,\ U^* \rangle = \langle H_o^*\ U^*,\ U \rangle \qquad (2.47)$$

where U and U^* are two admissible functions.

Adjoint variational methods make use of the adjoint operator (when $H_o^* \neq H_o$) for constructing a functional whose Euler equation is the governing equation of the problem at hand.

For a boundary value problem, the functional to be made stationary is the following

$$\bar{I} = \langle H_o U - f_o,\ U^* \rangle - \langle g_o, U \rangle = \langle H_o^*\ U^* - g_o, U \rangle - \langle f_o, U^* \rangle \qquad (2.48)$$

where $H_o U = f_o$ is the governing equation of the problem and the function $g_o(X_\alpha)$ is arbitrary but chosen according to the meaning desired for the functional $\bar{I}$ (Becker [14, p.86]).

For a function U which satisfies all the boundary conditions, the stationary value of (2.48) results in

$$\langle H_o U - f_o,\ \delta U^* \rangle + \langle \delta H_o U,\ U^* \rangle - \langle g_o,\ \delta U \rangle = 0 \qquad (2.49)$$

Since the function U^* satisfies the adjoint boundary conditions, (2.49) becomes

$$\langle H_o U - f_o,\ \delta U^* \rangle + \langle H_o^* U^* - g_o,\ \delta U \rangle = 0 \qquad (2.50)$$

i.e.

$$H_o U - f_o = 0$$

$$H_o^* U^* - g_o = 0$$

For an eigenvalue problem given by $H_o U - \lambda M_o U = 0$, the following functional is defined:

$$\bar{\lambda} = \frac{\langle U^*, H_o U \rangle}{\langle U^*, M_o U \rangle} \qquad (2.51)$$

The stationary value of (2.51) for a function U satisfying the boundary conditions is

$$\left\langle \delta U^*,\ H_o U - \lambda M_o U \right\rangle + \left\langle U^*, \delta H_o U - \lambda M_o U \right\rangle = 0 \qquad (2.52)$$

For a function U^* which satisfies the adjoint boundary conditions, (2.52) becomes

$$\left\langle H_o U - \lambda M_o U,\ \delta U^* \right\rangle + \left\langle H_o^* U^* - \lambda M_o^* U^*,\ \delta U \right\rangle = 0 \qquad (2.53)$$

i.e.

$$H_o U - \lambda M_o U = 0$$

$$H_o^* U - \lambda M_o^* U = 0$$

The adjoint variational method consists in substituting into (2.48) or (2.51) the trial solutions

$$U_n = \sum_{i=1}^{n} q_i \varphi_i \quad ; \quad U_n^* = \sum_{i=1}^{n} q_i^* \varphi_i^* \qquad (2.54)$$

where each φ_i satisfies all the boundary conditions and each φ_i^* satisfies all the adjoint boundary conditions. The parameters q_i, q_i^* are to be determined, the total number being 2n.

d) Involutory Transformations (Courant [20, p. 233]).

A functional which is made stationary under certain subsidiary constraints can be transformed, by introducing new variables called Lagrange parameters, to another functional for which the function and the parameters are arbitrary. It is possible to release a few of the constraints and introduce one parameter per release so that the function used in the new functional need satisfy beforehand only the constraints not having been released.

If the original problem is a minimum problem, usually the mod-

ified problem is only a stationary problem. Thereby some of the advantages characteristic of a minimum are lost. However since there is no need to satisfy the subsidiary conditions released, the coordinate functions used in a possible trial solution are subjected to less requirements.

Examples of this procedure are given in the book by Washizu [3].

2.5 Convergence Studies

Someconvergence theorems have been presented by Mikhlin [8] for the Galerkin and Least Squares methods. Mikhlin also gives the proof of convergence of the Ritz method for variational problems with homogeneous boundary conditions. In this article, Mikhlin's derivations are followed to some extent in the discussion of the convergence of the Ritz method for problems with inhomogeneous boundary conditions.

Ritz Method - Boundary Value Problem.

A quadratic functional to be minimized has the form

$$F_1(\omega) = |\omega|^2 - 2L_1(\omega) = J(\omega,\omega) - 2L_1(\omega) \qquad (2.55)$$

where $|\omega|^2$ is a positive quadratic functional and $L_1(\omega)$ a linear functional, both defined on a domain Ω with boundary C. The function ω is subjected to l geometrical boundary conditions given on parts $\hat{s}_j$; j=1,...,l of the boundary C, as follows:

$$\hat{A}_j \omega = \hat{f}_j \quad \text{on } \hat{s}_j; \quad j=1,\ldots,l \qquad (2.56)$$

where $\hat{A}_j$ are linear operators and $\hat{f}_j$ prescribed functions.

It is now assumed that there is available a function $\bar{\psi}$ which satisfies the geometrical conditions (2.56), i.e.

$$\hat{A}_j \bar{\psi} = \hat{f}_j \quad \text{on } \hat{s}_j; \quad j=1,\ldots,l \qquad (2.57)$$

Setting $\omega = U+\bar{\psi}$, from (2.57)

$$\hat{A}_j U = 0 \quad \text{on } \hat{s}_j \quad j=1,\ldots,l \tag{2.58}$$

that is, U satisfies homogeneous geometrical boundary conditions.

Substituting $\omega = U+\bar{\psi}$ into (2.55), it is found that

$$\begin{aligned} F_1(U+\bar{\psi}) &= |U|^2 + 2J(U,\bar{\psi}) + |\bar{\psi}|^2 - 2L_1(U) - 2L_1(\bar{\psi}) \\ &= |U|^2 - 2L(U) + |\bar{\psi}|^2 - 2L_1(\bar{\psi}) \end{aligned} \tag{2.59}$$

where

$$L(U) = L_1(U) - J(U,\bar{\psi}) \tag{2.60}$$

Let

$$F(U) = |U|^2 - 2L(U) \tag{2.61}$$

The stationary value of (2.59) is

$$\delta F_1(\omega) = \delta F(U)$$

From this last expression, the function U which makes F(U) minimum and satisfies the homogeneous boundary conditions (2.58) makes also the functional $F_1(U+\bar{\psi})$ a minimum. The Euler equations and mechanical boundary conditions corresponding to the minimum of F(U) are those given by (2.26).

Denoting the exact solution to the boundary value problem by U_o and by U functions which satisfy (2.58), the stationary value of F(U) in (2.61) may be written as:

$$J(U_o, U) = L(U) \tag{2.62}$$

Substitution of (2.62) into (2.61), results in

$$F(U) = |U|^2 - 2J(U,U_o) + |U_o|^2 - |U_o|^2$$

$$F(U) = |U - U_o|^2 - |U_o|^2 \qquad (2.63)$$

clearly from (2.63)

$$\bar{d}=\min F(U) = - |U_o|^2 \qquad (2.64)$$

It will be shown that when the functions V_n, V and U_o possess finite energy, the following inequality holds

$$F(V_n)-F(V) \leq \frac{K}{2} |V_n - V| \qquad (2.65)$$

where K is a positive constant.

From (2.63)

$$F(V_n) - F(V) = |V_n - U_o|^2 - |V - U_o|^2$$

$$=(|V_n - U_o| + |V - U_o|) (|V_n - U_o| - |V - U_o|) \qquad (2.66)$$

Since V_n, V and U_o have finite energy, it can be assumed that

$$|V_n - U_o| + |V - U_o| \leq K$$

Using this last expression and the triangle inequality, (2.66) is transformed to (2.65). The triangle inequality needed is:

$$|V_n - V| = |V_n - U_o - (V - U_o)| \geq |V_n - U_o| - |V - U_o|$$

Theorem: Ritz approximate solution to $A_oU=f_o$ constitutes a minimizing sequence for the functional F(U), provided that $A_oU = f_o$ has a solution with finite energy.

Since the problem to be solved has a minimum given by (2.64), a function V can always be found for which, when given $\epsilon > 0$, it is possible to have

$$F(V) < \bar{d} + \frac{\epsilon}{2} \tag{2.67}$$

Moreover, there is assumed available a sequence of independent functions φ_i; i=1,...,n which is complete in energy (i.e. they satisfy Eq. 2.9 and Eq. 2.11). Therefore setting $V_n = \sum_{i=1}^{n} \hat{q}_i \varphi_i$ and given $\epsilon > 0$ it is possible to find an integer n and constants $\hat{q}_i$ for which

$$|V_n - V| < \frac{\epsilon}{K} \tag{2.68}$$

where V is an arbitrary function with finite energy and K is a positive constant.

From (2.68) and (2.65)

$$F(V_n) - F(V) < \frac{\epsilon}{2}$$

and from (2.67)

$$\bar{d} \leq F(V_n) \leq F(V) + \frac{\epsilon}{2} \leq \bar{d} + \epsilon \tag{2.69}$$

When trial solutions are considered, a Ritz solution $U_n = \sum_{i=1}^{n} q_i \varphi_i$ (the same coordinate functions as for V_n) provides parameters q_i which give the minimum of the functional in (2.61) i.e.

$$F(U_n) \leq F(V_n)$$

so that (2.69) may be written as

$$\bar{d} \leq F(U_n) \leq \bar{d} + \epsilon \tag{2.70}$$

$$\lim_{n \to \infty} F(U_n) = \bar{d} \tag{2.71}$$

(2.71) being the definition of a minimizing sequence.

Substitution of (2.70) into (2.63) yields

$$F(U_n) = |U_n - U_o|^2 + \bar{d} \leq \bar{d} + \epsilon$$

or

$$|U_n - U_o|^2 \leq \epsilon \tag{2.72}$$

i.e. the Ritz solution converges in energy to the exact solution.

Ritz Method - Eigenvalue Problem

The eigenvalue problem dealt with has the following form

$$\lambda = \inf \frac{|U|^2_H}{|U|^2_M} = \frac{|U_o|^2_H}{|U_o|^2_M} \tag{2.73}$$

where $|U|^2_H$, $|U|^2_M$ are two different positive quadratic functionals, U is a function which satisfies homogeneous geometrical boundary conditions and U_o is the exact solution to the minimum problem.

For any given $\epsilon > 0$, U can be chosen to satisfy

$$\lambda \leq \frac{|U|^2_H}{|U|^2_M} \leq \lambda + \epsilon \tag{2.74}$$

Setting the variables

$$\omega = \frac{U}{|U|^2_M} \; ; \quad V_o = \frac{U_o}{|U_o|^2_M} \tag{2.75}$$

i.e. $|\omega|_M = |V_o|_M = 1$

then (2.73) and (2.74) may be written respectively as

$$\lambda = \inf |\omega|^2_H = |V_o|^2_H \tag{2.76}$$

and

$$|\omega|_H \leq \sqrt{\lambda+\epsilon} \tag{2.77}$$

For a sequence ω_n complete in energy it is possible for $\epsilon > 0$ to have

$$|\omega - \omega_n|_H < \sqrt{\epsilon} \tag{2.78}$$

and by using (2.74) the last inequality becomes

$$|\omega - \omega_n|_M \leq \sqrt{\frac{\epsilon}{\lambda}} \tag{2.79}$$

Again from (2.74), the triangle inequality and equations (2.75) through (2.79)

$$\lambda \leq \frac{|\omega_n|^2_H}{|\omega_n|^2_M} \leq \left|\frac{|\omega|_H + |\omega - \omega_n|_H}{|\omega|_M - |\omega - \omega_n|_M}\right|^2 < \left|\frac{\sqrt{\lambda+\epsilon} + \sqrt{\epsilon}}{1 - \sqrt{\frac{\epsilon}{\lambda}}}\right|^2 = \lambda + \bar{\eta} \tag{2.80}$$

where $\bar{\eta} \to 0$ when $\epsilon \to 0$

Let U_n be the Ritz solution to (2.73) and λ_n the approximate eigenvalue thus obtained. The following equation results from the use of (2.80)

$$\frac{|U_n|^2_H}{|U_n|^2_M} = \lambda_n = \min \frac{|\omega_n|^2_H}{|\omega_n|^2_M} \leq \frac{|\omega_n|^2_H}{|\omega_n|^2_M} < \lambda + \bar{\eta}$$

i.e. $\lambda \leq \lambda_n < \lambda + \bar{\eta}$ (2.81)

When $\epsilon \to 0$ then $\bar{\eta} \to 0$. Thus (2.81) can also be written

$$\lim_{n \to \infty} \lambda_n = \lambda \tag{2.82}$$

or

$$\frac{|U_o|^2_H}{|U_o|^2_M} = \lim \frac{|U_n|^2_H}{|U_n|^2_M}$$

i.e. the Ritz solution tends to the exact solution.

Another form for (2.82) results from setting

$$V_n = \frac{U_n}{|U_n|^2_M} \tag{2.83}$$

i.e. $$|V_n|_M = 1$$

so that

$$\lim |V_n|_H = |V_o|_H \tag{2.84}$$

Eq. (2.84) indicates that the normalized Ritz solution converges in energy to the normalized exact solution.

2.6 Convergence of the the Plane Problem and Eigenvalue Problem of Plates.

In this section some of the convergence properties of solutions obtained by the Ritz method are discussed in the case of the plane and eigenvalue problem of plates. As the results are independent of the coordinate system, Cartesian coordinates are adopted for simplicity. The in-plane displacements of the deformed plate are denoted by U_α, and the deflection normal to the undeformed middle surface of the plate by w. The area of the plate is Ω, the contour C and the sum of both is denoted by $\bar{\Omega} = \Omega + C$. The in-plane displacements are prescribed on the contours S_α, the deflection w on the contour S_3 and the slopes $w,_\alpha$ on the contours $S_{3+\alpha}$. The boundary conditions for w and $w,_\alpha$ are homogeneous.

In-Plane Problem

Let

$$\|U_\alpha\|^2 = \iint_\Omega U_\alpha^2 \, d\Omega \tag{2.85}$$

For functions U_α with generalized first derivatives

$$\|U_\alpha\|_{L_2(1)} = \iint_\Omega (U_{\alpha,1}^2 + U_{\alpha,2}^2) \, d\Omega \tag{2.86}$$

$$\|U_\alpha\|_{W_2(1)} = \left(\int_{S_{(\alpha)}} U_\alpha dC \right)^2 + \|U_\alpha\|^2_{L_2(1)}$$

Poincare's inequality (Mikhlin [1o, p. 155]) is

$$\|U_\alpha\|^2 \leq K_1 \|U_\alpha\|^2_{W_2(1)} \tag{2.87}$$

where K_1 is a positive constant.

Let

$$\|\vec{U}\|^2 = \iint_\Omega U_\alpha U_\alpha \, d\Omega \tag{2.88}$$

$$\|\vec{U}\|^2_{L_2(1)} = \iint_\Omega U_{\alpha,\beta} U_{\alpha,\beta} \, d\Omega$$

$$\|\vec{U}\|^2_{W_2(1)} = \left(\int_{S_1} U_1 dC \right)^2 + \left(\int_{S_2} U_2 \, dC \right)^2 + \|\vec{U}\|_{L_2(1)} \tag{2.89}$$

and from Poincare's inequality

$$\|\vec{U}\|^2 \leq K_1 \|\vec{U}\|_{W_2(1)} \tag{2.90}$$

Korn's inequality, as given by Mikhlin [9, p. 127], is

$$\|\vec{U}\|^2_{L_2(1)} \leq K_2 \|\vec{U}\|^2_E \tag{2.91}$$

where K_2 is a constant and

$$\|\vec{U}\|^2_E = \iint_\Omega E_{\alpha\beta}\, E_{\alpha\beta}\, d\Omega \quad \text{with } 2E_{\alpha\beta} = U_{\alpha,\beta}+U_{\beta,\alpha} \tag{2.92}$$

Use of the notation of (1.91) and (1.66) yields

$$E^{\gamma\alpha}T_{\gamma\alpha} = \frac{Eh}{1+\nu}\left(E^{\gamma\alpha}\, E_{\gamma\alpha} + \frac{\nu}{1-\nu}\, E^{\beta}_{\beta}\, E^{\gamma}_{\gamma}\right)$$

and for a Poisson's ratio $\frac{1}{2} > \nu > 0$ the following is derived

$$E^{\gamma\alpha}\, T_{\gamma\alpha} \geq K_3\, E^{\gamma\alpha}\, E_{\gamma\alpha} \tag{2.93}$$

The integration of (2.93) produces

$$|\vec{U}|^2_T \geq K_3 \|\vec{U}\|^2_E \tag{2.94}$$

where

$$|\vec{U}|^2_T = \iint_\Omega E^{\gamma\alpha}\, T_{\gamma\alpha}\, d\Omega \tag{2.95}$$

which by Korn's inequality appears as

$$|\vec{U}|^2_T \geq K_3K_2\, \|\vec{U}\|^2_{L_2(1)} \tag{2.96}$$

It is observed that when the geometrical boundary conditions are homogeneous, the functional of the plane problem of elasticity is positive definite, since from inequalities (2.90) and (2.94) results

$$|\vec{U}|^2_T \geq K_1K_2K_3\, \|\vec{U}\|^2 \quad \text{where } \vec{U} \text{ satisfies homogeneous B.C.}$$

The Ritz solution $\vec{U}_n$ has components $U_\alpha^{(n)}$, and the exact solution $\vec{U}_o$ has components $U_\alpha^{(o)}$ in the discussion which follows.

It has been shown by (2.72) that the Ritz solution converges in energy to the exact solution i.e. given $\epsilon > 0$ it is possible to find an integer n for which

$$\left| \vec{U}_n - \vec{U}_o \right|^2_T < \epsilon \tag{2.97}$$

$\vec{U}$ being functions which satisfy the geometrical boundary conditions of the problem.

From the inequalities (2.97) and (2.94) follows

$$\left\| \vec{U}_n - \vec{U}_o \right\|^2_E < \epsilon \tag{2.98}$$

or in expanded form

$$\iint_\Omega \left[(E_{11}^{(n)} - E_{11}^{(o)})^2 + 2(E_{12}^{(n)} - E_{12}^{(o)})^2 + (E_{22}^{(n)} - E_{22}^{(o)})^2 \right] d\Omega < \epsilon$$

i.e. the strains converge in the mean

$$\iint_\Omega (E_{11}^{(n)} - E_{11}^{(o)})^2 \, d\Omega < \epsilon; \quad 2 \iint_\Omega (E_{12}^{(n)} - E_{12}^{(o)})^2 \, d\Omega < \epsilon;$$
$$\iint_\Omega (E_{22}^{(n)} - E_{11}^{(o)})^2 \, d\Omega < \epsilon$$

The stresses also converge in the mean, being linear combinations of the strains, as for example

$$\iint_\Omega (T_{11}^{(n)} - T_{11}^{(o)})^2 \, d\Omega = \frac{Eh}{1-\nu^2} \iint_\Omega \left[(E_{11}^{(n)} - E_{11}^{(o)}) + \nu (E_{22}^{(n)} - E_{22}^{(o)}) \right]^2 d\Omega$$

$$\iint_\Omega (T_{11}^{(n)} - T_{11}^{(o)})^2 d\Omega \leq \frac{Eh}{1-\nu^2} \left[\iint_\Omega (E_{11}^{(n)} - E_{11}^{(o)})^2 d\Omega + \right.$$

$$\left. + \nu^2 \iint_\Omega (E_{22}^{(n)} - E_{22}^{(o)})^2 d\Omega \right] \leq \frac{Eh}{1-\nu^2} (1+\nu^2) \, \epsilon$$

having used the triangle inequality.

The definition (2.89), for functions $\vec{U}_n$ and $\vec{U}_o$ which satisfy the geometrical bound. cond., leads to

$$\| \vec{U}_n - \vec{U}_o \|^2_{W_2(1)} = \left(\int_{S_1} (U_1^{(n)} - U_1^{(o)}) d\Omega \right)^2 + \left(\int_{S_2} (U_2^{(n)} - U_2^{(o)}) d\Omega \right)^2 +$$

$$+ \| \vec{U}_n - \vec{U}_o \|^2_{L_2(1)} = \| \vec{U}_n - \vec{U}_o \|^2_{L_2(1)} \qquad (2.99)$$

Korn's inequality (2.96) and (2.97) results in

$$\| \vec{U}_n - \vec{U}_o \|^2_{L_2(1)} < \varepsilon \qquad (2.100)$$

or

$$\| \vec{U}_n - \vec{U}_o \|^2_{W_2(1)} < \varepsilon$$

The inequalities (2.90) and (2.100) give

$$\| \vec{U}_n - \vec{U}_o \|^2 < \varepsilon \qquad (2.101)$$

i.e. the displacements converge in the mean.

Eigenvalue Problem of Plates

Let

$$\| \omega \|_{L_q} = \left(\iint_\Omega | \omega |^q \, d\Omega \right)^{\frac{1}{q}} \qquad 0 < q < \infty \qquad (2.102)$$

and for functions ω with generalized derivatives of second order

$$\| \omega \|^2_{L_2(2)} = \iint_\Omega \omega_{,\alpha\beta} \, \omega_{,\alpha\beta} \, d\Omega \qquad (2.103)$$

$$\| w \|^2_{W_2(2)} = \left(\int_{S_3} w dC \right)^2 + \left(\int_{S_4} w_{,1} \, dC \right)^2 + \left(\int_{S_5} w_{,2} \, dC \right)^2 + \| w \|^2_{L_2(2)}$$

$$\| w \|_C = \max_{\bar{\Omega}} | w |$$

Sobolev inequalities [17, p. 69] include

$$\| w_{,\alpha} \|_{L_q} \leq K_4 \| w \|_{W_2(2)} \qquad 0 < q < \infty \qquad (2.104)$$

$$\| w \|_C \leq K_5 \| w \|_{W_2(2)} \qquad (2.105)$$

From the definition in (2.103), follows

$$| w | \leq \| w \|_C$$

or

$$w^2 \leq \| w \|^2_C$$

which leads to

$$\iint_{\Omega} w^2 \, d\Omega \leq \| w \|^2_C \; \Omega$$

which from (2.105) becomes

$$\| w \|^2 \leq K_3^2 \, \Omega \, \| w \|^2_{W_2(2)} \qquad (2.106)$$

According to (1.66)

$$\varkappa_{\gamma\alpha} = - \omega |_{\gamma\alpha}$$

$$\varkappa^{\gamma\alpha} M_{\gamma\alpha} = \frac{h^2}{12} \frac{Eh}{1+\nu} \left(\varkappa^{\gamma\alpha} \varkappa_{\gamma\alpha} + \frac{\nu}{1-\nu} \varkappa^{\beta}_{\beta} \varkappa^{\gamma}_{\gamma}\right)$$

$$\varkappa^{\gamma\alpha} M_{\gamma\alpha} \geq \frac{h^2}{12} K_3 \varkappa^{\gamma\alpha} \varkappa_{\gamma\alpha} \qquad (2.107)$$

(2.107) being analogous to (2.93).

The integration of (2.107) may be written as

$$|\omega|^2 \geq K_6 \|\omega\|^2_{\varkappa} \qquad (2.108)$$

where

$$\|\omega\|^2_{\varkappa} = \iint_{\Omega} \varkappa^{\gamma\alpha} \varkappa_{\gamma\alpha} \, d\Omega \qquad (2.109)$$

$$|\omega|^2 = \iint_{\Omega} \varkappa^{\gamma\alpha} M_{\gamma\alpha} \, d\Omega$$

When the function ω satisfies homogeneous geometrical boundary conditions, from inequalities (2.108), (2.107) and definition (2.103), it is seen that the functional $|\omega|$ is positive definite, i.e.

$$|\omega|^2 \geq \gamma^2 \|\omega\|^2$$

where $\gamma^2 = K_6 K_3^2 \, \Omega$

The eigenvalue problem for plates is defined as the minimum of

$$\lambda = \frac{|\omega|^2}{|\omega|^2_M} \qquad (2.110)$$

for functions ω which satisfy homogeneous boundary conditions.

With ω_n as the Ritz solution and ω_o as the exact solution,

$$V_n \equiv \frac{\omega_n}{|\omega_n|_M^2} \qquad V_o \equiv \frac{\omega_o}{|\omega_o|_M^2} \tag{2.111}$$

Eq. (2.98) is written in terms of the functions V_n and V_o as

$$\lim_{n \to \infty} |V_n| = |V_o| \tag{2.112}$$

The inequality (2.108) and the expression (2.112) yield

$$\lim_{n \to \infty} \|V_n\|_\kappa = \|V_o\|_\kappa \tag{2.113}$$

i.e. the bending measures of the normalized Ritz solution converge in the mean. The bending moments $M^{\gamma\alpha}$ corresponding to the normalized Ritz solution also converge in the mean to the exact values, since they are defined as linear combinations of the bending measures.

From inequalities (2.104), (2.105) and expression (2.113)

$$\lim_{n \to \infty} \|V_{n,\alpha}\|_{L_q} = \|V_{o,\alpha}\|_{L_q} \qquad 0 < q < \infty \tag{2.114}$$

$$\lim_{n \to \infty} \|V_n\|_C = \|V_o\|_C$$

i.e. the slopes of the normalized Ritz solution converge in the mean with an arbitrarily large exponent to the slopes of the exact solution. The normalized Ritz solution converges uniformly to the normalized exact solution.

2.7 An example of application of Galerkin's Method

The eigenvalue problem of plates subjected to in-plane loads varying with time and follower-forces, as given by (1.122) and (1.121), can be restated:

$$M^{\gamma\alpha}\big|_{\alpha\gamma} + (\hat{T}^{\gamma\alpha}\,\omega,_{\gamma})\big|_{\alpha} - M\ddot{\omega} = 0 \quad \text{on } \Omega \tag{2.115}$$

$$M_{(NN)} = 0 \quad \text{on } \bar{C}_1$$

$$[M_{(NT)}]_{C_1}(K) = 0 \qquad K=1,\ldots,m_1$$

$$Q^{\alpha}N_{\alpha} - \frac{\partial M_{(NT)}}{\partial C} + \hat{T}^{\gamma\alpha}\,\omega,_{\gamma}N_{\alpha} = 0 \quad \text{on } C_1\text{-}C_f$$

$$Q^{\alpha}N_{\alpha} - \frac{\partial M_{(NT)}}{\partial C} = 0 \quad \text{on } C_f$$

and with homogeneous geometrical boundary conditions

$$\omega_{C_2} = 0 \tag{2.116}$$

$$\frac{\partial \omega}{\partial N}_{\bar{C}_2} = 0$$

where ω = deflection of the plate in direction of X^3 axis (perpendicular to the plate)

$$\varkappa_{\gamma\alpha} = -\,\omega\big|_{\gamma\alpha} \tag{2.117}$$

$$M^{\gamma\alpha} = \frac{h^2}{12}\,C^{\gamma\alpha\,\beta\mu}\,\varkappa_{\beta\mu} = -\frac{h^2}{12}\,C^{\gamma\alpha\,\beta\mu}\,\omega\big|_{\beta\mu}$$

$$M_{(NN)} = M^{\gamma\alpha}N_{\alpha}N_{\gamma}$$

$$M_{(NT)} = -M^{\gamma\alpha}N_{\alpha}T_{\gamma}$$

$$Q^{\alpha} = M^{\gamma\alpha}\big|_{\gamma}$$

$C^{\gamma\alpha\,\beta\mu}$ = tensor of elastic constants defined by (1.165)

N^γ = components of the outward normal to the contour C

T^γ = components of the tangent unit vector to the contour C

m_1 = number of discontinuities of the tangent to the contour C_1.

The plate of thickness h has been subjected to in-plane loads which are represented by the stress tensor $\hat{T}^{\gamma\alpha}$. The applied bending moments on the boundary and the normal load to the middle plane of the plate are zero. Follower-forces as defined by (1.120) are prescribed on the contour C_f resulting in the component $F^*_3 = \hat{T}^{\gamma\alpha} N_\gamma w_{,\alpha}$ in the direction of the X^3 axis. The in-plane stresses are assumed to be given as

$$\hat{T}^{\gamma\alpha} = S^{\gamma\alpha} P(t) + T^{\gamma\alpha}_{(o)} P_o \qquad (2.118)$$

where the stress tensors $S^{\gamma\alpha}$ and $T^{\gamma\alpha}_{(o)}$ do <u>not</u> depend on time and have been obtained by linear analysis.

Given the coordinate functions $\varphi_i(X^\alpha)$, i=1,...,n and using the trial function $w_n = \sum_{i=1}^{n} q_i(t)\varphi_i$, the Galerkin method (or Kantorovick) yields

$$0 = -\frac{h^2}{12}\iint_\Omega (C^{\gamma\alpha\beta\mu} w_n|_{\beta\mu})|_{\gamma\alpha} \varphi_j \, d\Omega + P(t) \iint_\Omega (S^{\gamma\alpha} w_{n,\gamma})|_\alpha \varphi_j d\Omega +$$
$$+ P_o \iint_\Omega (T^{\gamma\alpha}_{(o)} w_{n,\gamma})|_\alpha \varphi_j d\Omega - \iint_\Omega M\ddot{w}_n \varphi_j d\Omega \quad j=1,...n \qquad (2.119)$$

The orthogonality conditions (2.119) may be used when the coordinate functions satisfy all the boundary conditions exactly. However it will be shown that transforming these equations it is possible to use coordinate functions which satisfy only the homogeneous geometrical boundary conditions.

For any two functions φ_i and φ_j which satisfy the homogeneous geometrical boundary conditions, integration by parts gives

$$- \frac{h^2}{12} \iint_\Omega (C^{\gamma\alpha\beta\mu} \varphi_i|_{\beta\mu})|_{\gamma\alpha} \varphi_j \, d\Omega = - \frac{h^2}{12} \iint_\Omega C^{\gamma\alpha\beta\mu} \varphi_i|_{\beta\mu} \varphi_j|_{\gamma\alpha} d\Omega +$$

$$+ \frac{h^2}{12} \int_{\bar{C}_1} C^{\gamma\alpha\beta\mu} \varphi_i|_{\beta\mu} N_\alpha N_\gamma \frac{\partial \varphi_j}{\partial N} \, dC - \sum_{K=1}^{m_1} [C^{\gamma\alpha\beta\mu} \varphi_i|_{\beta\mu} N_\alpha N_\gamma \varphi_j]_{C_1}(K) -$$

$$- \frac{h^2}{12} \int_{C_1} \left[(C^{\gamma\alpha\beta\mu} \varphi_i|_{\beta\mu})|_\gamma + \frac{\partial}{\partial C} (C^{\gamma\alpha\beta\mu} \varphi_i|_{\beta\mu} N_\alpha N_\gamma) \right] \varphi_j \, dC \qquad (2.120)$$

$$\iint_\Omega (T^{\gamma\alpha}_{(o)} \varphi_{i,\gamma})|_\alpha \varphi_j d\Omega = - \iint_\Omega T^{\gamma\alpha}_{(o)} \varphi_{i,\gamma} \varphi_{j,\alpha} \, d\Omega +$$

$$+ \int_{C_1} T^{\gamma\alpha}_{(o)} \varphi_{i,\gamma} N_\alpha \varphi_j \, dC \qquad (2.121)$$

(these last two equations may be obtained from (1.111) and (1.112) by substituting $\omega = \varphi_i$ and $\delta\omega = \varphi_j$, by making some obvious changes in notation, and by considering the fact that the prescribed bending moments and normal loads to the plate are zero)

With the help of (2.120) and (2.121), the orthogonality conditions (2.119) become

$$- \frac{h^2}{12} \iint_\Omega C^{\gamma\alpha\beta\mu} \omega_n|_{\beta\mu} \varphi_j|_{\gamma\alpha} \, d\Omega + \frac{h^2}{12} \int_{\bar{C}_1} C^{\gamma\alpha\beta\mu} \omega_n|_{\beta\mu} N_\alpha N_\gamma \frac{\partial \varphi_j}{\partial N} dC -$$

$$- \frac{h^2}{12} \int_{C_1} \left[(C^{\gamma\alpha\beta\mu} \omega_n|_{\beta\mu})|_\gamma + \frac{\partial}{\partial C} (C^{\gamma\alpha\beta\mu} \omega_n|_{\beta\mu} N_\alpha N_\gamma \right] \varphi_j \, dC -$$

$$- \sum_{K=1}^{m_1} [C^{\gamma\alpha\beta\mu} \omega_n|_{\beta\mu} N_\alpha N_\gamma \varphi_j]_{C_1}(K) + P(t) \Big[\iint_\Omega S^{\gamma\alpha} \omega_{n,\gamma} \varphi_{j,\alpha} \, d\Omega +$$

$$+ \int_{C_1} S^{\gamma\alpha} \omega_{n,\gamma} N_\alpha \varphi_j \, dC \Big] +$$

$$+ P_o \left| \iint_\Omega T^{\gamma\alpha}_{(o)}\ \omega_{n,\gamma}\ \varphi_{j,\alpha}\ d\Omega + \int_{C_1} T^{\gamma\alpha}_{(o)} \omega_{n,\gamma} N_\alpha\ \varphi_j\ dC \right| -$$

$$- \iint_\Omega M\ddot{\omega}_n\ \varphi_j\ dC = 0 \qquad\qquad j=1,\ldots,n$$

or

$$\iint_\Omega \left| - \frac{h^2}{12} C^{\gamma\alpha\beta\mu}\ \omega_n\big|_{\beta\mu}\ \varphi_j\big|_{\gamma\alpha} - (P(t)S^{\gamma\alpha}+P_oT^{\gamma\alpha}_{(o)})\omega_{n,\gamma}\ \varphi_{j,\alpha} - M\ddot{\omega}_n\varphi_j \right| d\Omega +$$

$$+ \frac{h^2}{12} \int_{C_1} C^{\gamma\alpha\beta\mu}\ \omega_n\big|_{\beta\mu} N_\alpha N_\gamma \frac{\partial\varphi_j}{\partial N}\ dC - \sum_{K=1}^{m_1} \left[\omega_n\big|_{\beta\mu} N_\alpha N_\gamma \varphi_j \right]_{C_1}(K) +$$

$$+ \int_{C_1} \left| - \frac{h^2}{12} \left| (C^{\gamma\alpha\beta\mu}\ \omega_n\big|_{\beta\mu})\big|_\alpha + \frac{\partial}{\partial C} (C^{\gamma\alpha\beta\mu}\ \omega_n\big|_{\beta\mu} N_\alpha N_\gamma) + \right.\right.$$

$$\left.\left. + (P(t)\ S^{\gamma\alpha} + P_oT^{\gamma\alpha}_{(o)})\ \omega_{n,\gamma} N_\alpha \right| \varphi_j \right| dC = 0 \qquad (2.122)$$

$$j=1,\ldots,n$$

Using the mechanical boundary conditions, (2.122) becomes:

$$\iint_\Omega \left| \frac{h^2}{12} C^{\gamma\alpha\beta\mu}\ \omega_n\big|_{\beta\mu}\ \varphi_j\big|_{\gamma\alpha} + (P(t)\ S^{\gamma\alpha} + P_o\ T^{\gamma\alpha}_{(o)})\omega_{n,\gamma}\ \varphi_{j,\alpha} + \right.$$

$$\left. + M\ddot{\omega}_n\ \varphi_j \right| d\Omega - \int_{C_f} \left[P(t)S^{\gamma\alpha}+P_oT^{\gamma\alpha}_{(o)} \right] \omega_{n,\gamma} N_\alpha \varphi_j\ dC = 0$$

$$j=1,\ldots,n \qquad (2.123)$$

This system of ordinary differential equations (2.123) involves an approximation for the mechanical boundary conditions in an average sense and the coordinate functions need only satisfy the geometrical boundary conditions. Denoting the vectors of the functions $q_j(t)$, $j=1,\ldots,n$ as $\underset{\sim}{q}$, an equivalent form of (2.123) in matrix form is

$$\left| \iint_{\Omega} \frac{h^2}{12} C^{\gamma\alpha\beta\mu} \varphi_i|_{\beta\mu} \varphi_j|_{\gamma\alpha} d\Omega \right| \underset{\sim}{q} + P(t) \left| \iint_{\Omega} S^{\gamma\alpha} \varphi_{i,\gamma} \varphi_{j,\alpha} d\Omega - \right.$$

$$- \int_{C_f} S^{\gamma\alpha} \varphi_{i,\gamma} N_\alpha \varphi_j dC \left| \underset{\sim}{q} + P_o \right| \iint_{\Omega} T^{\gamma\alpha}_{(o)} \varphi_{i,\gamma} \varphi_{j,\alpha} d\Omega -$$

$$- \int_{C_f} T^{\gamma\alpha}_{(o)} \varphi_{i,\gamma} N_\alpha \varphi_j dC \left| \underset{\sim}{q} + \right.$$

$$+ \left| \iint_{\Omega} M \varphi_i \varphi_j d\Omega \right| \ddot{\underset{\sim}{q}} = 0 \qquad (2.124)$$

In the absence of follower-forces (i.e. $C_f = 0$) the problem is called dynamic buckling of plates. When $C_f = 0$ and $P(t) = 0$ it is called the static lateral buckling of plates. If only follower-forces are prescribed on the boundary (i.e. $C_1 = C_f$), (2.123) may be simplified by (2.121) to

$$\iint_{\Omega} \left| \frac{h^2}{12} C^{\gamma\alpha\beta\mu} \omega_n|_{\beta\mu} \varphi_j|_{\gamma\alpha} + M\omega_n \varphi_j - [(P(t) S^{\gamma\alpha} + \right.$$

$$\left. + P_o T^{\gamma\alpha}_{(o)}) \omega_{n,\gamma}] |_{\alpha} \varphi_j \right| d\Omega = 0 \qquad j=1,\ldots,n$$

2.3 Selection of the Coordinate Functions

Requirements for the Coordinate Functions

The following functional is being minimized

$$F(U) = |U|^2 - 2\, L(U) = J(U,U) - 2\, L(U) \qquad (2.43)$$

where $|U|^2$ is a quadratic functional and $L(U)$ a linear functional. The quadratic functional $|U|^2$ is defined for functions U with generalized derivative of order t. The geometrical (or principal) boundary conditions contain derivatives of U of order $\leq t-1$ while the mechanical boundary conditions have at least one derivative of U of order $\geq t$. It is also supposed that the Euler equation cor-

responding to the minimum of F(U) is

$$A_o U = f_o$$

f_o being a function prescribed on the domain Ω, and A_o being an operator.

The coordinate functions φ_K; K=1,...,n used in the trial solution must

a) Be linearly independent and make $|\varphi_K|$ finite for any K=1,...,n. (Functions with finite energy).

b) Be complete in energy. i.e. for any $\varepsilon > 0$ and any U

$$|U - U_n| < \varepsilon \qquad (2.11)$$

c) Have generalized derivative of order t.

d) Satisfy the geometrical (principal) boundary conditions.

Under these conditions the solution U_n given by the Ritz method tends in energy to the exact solution U_o

$$|U_n - U_o| \underset{n \to \infty}{\longrightarrow} 0$$

Nodal Coordinate Functions

There will now be described a special sequence of coordinate functions called nodal coordinate functions. The domain Ω is divided into an arbitrary number n_e of subdomains Ω_j and on each of them a different trial function $U^{(j)}$ is assigned. For any point $\vec{X}$ referred to a fixed reference system, the global trial function is

$$U_n(\vec{X}) = U^{(j)}(\vec{X}) \qquad \text{when } \vec{X} \text{ belongs to } \Omega_j$$

The local trial function is assumed composed of e coordinate functions such as

$$U^{(j)} = \sum_{i=1}^{e} q_i^{(j)} \varphi_i^{(j)} \qquad (2.125)$$

where

$q_i^{(j)}$ are e unknown <u>local</u> parameters which represent quantities of physical significance at selected points on the contour of the subdomain Ω_j termed nodal points. Usually at the <u>nodal points</u> (or nodes), the function $U^{(j)}$ and its derivatives are chosen as parameters.

$\varphi_i^{(j)}$ are <u>local</u> coordinate functions valid only within the subdomain Ω_j. Usually polynomials are taken as these local coordinate functions.

The <u>global</u> trial function is a linear combination of n <u>nodal</u> coordinate functions, as follows

$$U_n = \sum_{K=1}^{n} q_K \varphi_K \qquad (2.126)$$

where the sequence $\{q_K\}$ is made by the local parameters which are linearly independent. There exist certain continuity conditions at the nodes, through which local parameters of one subdomain are equated to other local parameters of adjacent subdomains. In turn all the local parameters which are equal at a node are identified by one global parameter. Therefore if in a subdomain Ω_j a global parameter q_K is equal to a local parameter $q_i^{(j)}$, the <u>nodal</u> coordinate function φ_K is defined as being equal to the coordinate function φ_i which corresponds to the local parameter mentioned i.e.

$$\text{if } q_K = q_i^{(j)} \Rightarrow \varphi_K = \varphi_i \quad \text{on } \Omega_j \qquad (2.127)$$

When for such subdomain Ω_j the condition (2.127) cannot be satisfied for any local parameter,

$$\varphi_K \equiv 0 \quad \text{on} \quad \Omega_j$$

When the trial function U_n and its derivatives of order $\leq$ t-1 are continuous at the nodes but not throughout Ω, the function is said to be non-conforming. On the other hand a function U_n is conforming when all its derivatives of order $\leq$ t-1 are continuous in Ω.

Olivera [21] has shown that the completeness criteria can be satisfied by using polynomials to make a conforming or non-conforming function U_n which can take arbitrary constant values in each subdomain. The last condition is fulfilled if the function $U^{(j)}$ contains a complete polynomial of t degree, all the terms of which are affected by arbitrary coefficients, and also contains higher order polynomial terms, which can vanish whatever the value taken by the coefficients of the t th. degree polynomial.

The special case of the Ritz method which uses conforming trial functions will be termed Ritz-Subdomain method.

The Finite Element method employs non-conforming trial functions which are input in the functional to be minimized. Olivera [21] has shown that if the prescribed distributed function $f_o = 0$, the Finite Element method converges in energy to the exact solution as the size of the element (subdomain) is decreased. When $f_o \neq 0$ several Finite Element analyses must be carried out, increasing the number of elements and observing the convergence if any. Since the t-1 derivative is not continuous for non-conforming functions, the convergence to the exact solution is not assured as in the case of the Ritz-Subdomain method (examples in Zienkiewicz [22]).

Convergence of the Parameters of the Trial Solution

Given a sequence of independent coordinate functions $\{\varphi_K\}$ it is possible to define a new set of functions

$$\psi_i = \sum_{K=1}^{i} d_{iK}\, \varphi_K; \quad d_{ii} \neq 0; \quad i=1,\ldots,n \tag{2.128}$$

where the constants d_{iK} are determined from an orthogonalization process, as described by Mikhlin [8], by setting the conditions

$$J(\psi_i, \psi_j) = \begin{cases} 0 & i \neq j \\ 1 & i = j \end{cases} \tag{2.129}$$

taking the functional to be that of (2.43).

For the trial function $U_n = \sum_{i=1}^{n} \bar{\alpha}_i\, \psi_i$, the variational statement corresponding to (2.43) becomes

$$J(U_n, \psi_i) = L(\psi_i) \qquad i=1,\ldots,n$$

or by (2.129)

$$\bar{\alpha}_i = L(\psi_i) \qquad i=1,\ldots,n \tag{2.130}$$

and the trial solution can be written as

$$U_n = \sum_{i=1}^{n} L(\psi_i)\, \psi_i \tag{2.131}$$

Remembering that Ritz's and sometimes the Finite Element's solution converge in energy to the exact solution U_o, it is seen from (2.131) that U_o can be written as:

$$U_o = \sum_{i=1}^{\infty} L(\psi_i)\, \psi_i \tag{2.132}$$

which indicates that the Ritz solution consists in writting in short the exact solution expanded in orthonormal functions.

Moreover from (2.128)

$$U_n = \sum_{i=1}^{n} \bar{\alpha}_i \sum_{K=1}^{i} d_{iK}\, \varphi_K = \sum_{K=1}^{n} \varphi_K \sum_{i=K}^{n} d_{iK}\, \bar{\alpha}_K = \sum_{K=1}^{n} \varphi_K\, q_{nK}$$

where $q_{nK} = \sum_{i=K}^{n} d_{iK}\, \bar{\alpha}_K$ (2.133)

Similarly from (2.132) and (2.128)

$$U_o = \sum_{K=1}^{\infty} \varphi_K\, q_K$$

where $q_K = \sum_{i=1}^{\infty} d_{iK}\, \bar{\alpha}_K$ (2.134)

Obviously from (2.133) and (2.134)

$$\lim_{n \to \infty} q_{nK} = q_K \qquad K=1,\ldots,n \tag{2.135}$$

i.e. if the approximate solution $U_n = \sum_{K=1}^{n} q_{nK}\, \varphi_K$ converges in energy to the exact solution $U_o = \sum_{K=1}^{\infty} q_K\, \varphi_K$, the parameters of U_n converge uniformly to the coefficients of an expansion of the exact solution where the coordinate functions expand U_o.

The last statement indicates that for the Ritz-Subdomain method and for the cases where the Finite Element converges to the exact solution, the quantities of U_n represented by the global parameters tend uniformly to their exact values.

For example, for the plane stress problem (1.89), a function with generalized first derivative may be used as a trial function for each of the components of the displacement vector U_α. For triangular subdomains (Zienkiewicz [22]) it is sufficient to take as parameters the displacements U_α at the nodes, and as the local coordinate functions polynomials of first degree. Thus in this case, according to (2.135), U_α of the Ritz solution tends uniformly to the exact values at the nodes.

2.9 Critical Loads for Plates: Existing Solutions.

The steps in the determination of critical loads for elastic flat plates under conservative in-plane loads are (a) investigating a plane elastic problem, and (b) solving a linear eigenvalue problem.

Adopting Cartesian coordinates, the governing differential equations (1.93) can be satisfied identically by the Airy stress function ψ (see Wang [23, p. 93]). The stress function ψ, for a given stress tensor $T_{\gamma\alpha}$ and zero body forces, is defined by

$$\psi_{,\gamma\alpha\gamma\alpha} = 0 \tag{2.136}$$

$$T_{11} = \psi_{,22} \tag{2.137}$$

$$T_{22} = \psi_{,11}$$

$$T_{12} = -\psi_{,12}$$

The stresses for a plate of area Ω and flexural rigidity D are described immediately prior to buckling by the tensor $PT_{\gamma\alpha}$. The unknown parameter P is determined solving (1.122) i.e.

$$-D\,\omega_{,\gamma\alpha\gamma\alpha} + P(T_{\gamma\alpha}\,\omega_{,\gamma\alpha})_{,\alpha} = 0 \tag{2.138}$$

under appropiate boundary conditions for the normal deflection ω.

Problem (2.138) is equivalent to finding the minimum of the functional

$$P = \frac{\frac{1}{2}\iint_{\Omega} D[\omega_{,\alpha\alpha}\,\omega_{,\gamma\gamma} - 2(1-\nu)(\omega_{,11}\,\omega_{,22} - \omega_{,12}^2)]\,d\Omega}{-\frac{1}{2}\iint_{\Omega} T_{\gamma\alpha}\,\omega_{,\gamma}\,\omega_{,\alpha}\,d\Omega} \tag{2.139}$$

In general buckling investigations have been reported in the literature for 2 broad cases: (1) where the exact solution to the plane problem is known; (2) where an approximate solution to the plane problem is found before setting up the eigenvalue analysis.

(1) exact solution to the plane problem is known.

For this case, solutions have been presented by Timoshenko [6], Bleich [24], Bürgermeister, Steup and Kretzchmar [25], Pflüger [26], and Gerard and Becker [27].

Exact solutions are available for rectangular plates when $T_{\alpha\alpha}$ = const., $T_{12} = 0$ and two opposite edges of the plate are simply supported (in Shulesko [28] or the above references). Timoshenko [6] reports exact solutions for circular plates with or without holes where the boundaries are subjected to normal constant stresses so that the distribution of stresses prior to buckling is given by Lame's formulas.

A problem which has been solved by diverse approximate methods involves in-plane stresses of the form

$$T_{11} = e_1 + e_2 X_2 \qquad (2.140)$$

$$T_{22} = e_3 + e_4 X_1$$

$$T_{12} = e_5$$

where X_α are the Cartesian coordinates and e_1, e_2, e_3, e_4, e_5 are constants. Salvadori [29] has used the ordinary finite difference discretization for solving (2.138) when the stresses are (2.140) and the plates are rectangular. For a similar plate simply supported on the boundary, Klöppel and Sheer [30] use the Ritz method, assuming the deflection w given by a double Fourier series. Klöppel and Sheer introduce longitudinal and transverse ribs (maximum number three in each direction parallel to the axes).

Each rib carries an axial stress equal to that of the plate at the point in contact with the rib, and the rib's torsional rigidity is negligible.

Note that for square plates with stresses of the form (2.140) and with uniform edges simply supported, clamped or free, solutions to (2.139) can be found by the Ritz method using vibrating beam functions as coordinate functions. This procedure has already been used by **Webster** [31] in the analysis of free vibration of rectangular plates.

(2) Approximate solutions for both the plane elastic and eigenvalue problems.

For solving the plane elastic problem, the finite element, finite difference and integral methods have been presented, respectively, by Zienkiewicz [22], Fox [32] and Oliveira [33]. Griffin and Varga [34] have given a simple scheme for finite differences which can take care of complicated contours, though it is restricted to boundary conditions expressed in term of stresses.

Conways, Chow and Morgan [35] produce an accurate solution to the symmetric problem of Fig. 2.1 (a), where all boundary conditions are in terms of stresses. Firstly they use Filon's solution to satisfy the differential equation (2.136) and boundary conditions at the longitudinal edges. Subsequently the normal stresses on the transversal edges, which arise from Filon's solution, are approximately cancelled by a Ritz solution. The coordinate functions of the trial function are polynomials which do not affect stresses at the longitudinal edges.

Sommerfield [36] in 1906 and Timoshenko [6] in 1910 provide an approximate solution to the problem of Fig. 2.1 (a), assuming a double Fourier series as a trial function in the Ritz method. Timoshenko assumes the denominator of (2.139) in the form

$$\tfrac{1}{2}\int_0^{\hat{a}_2} (w_{,2})^2 \Big|_{X_1=0} dX_2 \qquad (2.141)$$

Let ϵ be a small distance to each side of the line $X_1 = 0$. The stresses represented by

$$T_{11} = T_{12} = 0 \qquad (2.142)$$

$$T_{22} = 0 \qquad \text{except at } X_1 = 0$$

$$P = -\lim_{\epsilon \to 0} \int_{-\epsilon}^{\epsilon} T_{22} \Big|_{X_1=0} dX_1$$

when subtituted in (2.139) give the expression (2.141) employed by Timoshenko. Therefore Timoshenko's solution corresponds to stresses represented by (2.142).

Legget [37] in 1937 shows that Timoshenko's solution to the problem of Fig. 2.1 (a) was at least 12.5% below the exact value. Legget expands the load in Fourier series and applies Filon's analysis. He observes that the stresses on the transversal edges, which result from Filon's analysis, are self-equilibrating, i.e. the force and moment resultants of the stresses on each transversal edge are zero. Thus Legget concludes by Saint-Venant's principle that the solution gives accurate stresses except near the transversal edges and that for long plates ($\hat{a}_1/\hat{a}_2 > 2$) the error diminishes.

Legget assumes a buckling shape

$$w = \sum_{i=1}^{\infty} \sum_{j=1}^{\infty} \bar{q}_{ij} \sin \frac{\pi i}{\hat{a}_1} X_1 \quad \sin \frac{\pi j}{\hat{a}_2} X_2 \qquad (2.143)$$

Substituting (2.143) into (2.138) and expanding the hyperbolic functions included in the stresses of Filon's solution, Legget arrives at the expression

$$\sum_{r=1}^{\infty} \sum_{s=1}^{\infty} K^{*}_{rs} \sin \frac{\pi r}{\hat{a}_1} X_1 \quad \sin \frac{\pi s}{\hat{a}_2} X_2 = 0$$

where the K^*_{rs} are linear functions of the set of parameters $\bar{q}_{ij}$.

The conditions

$$K^*_{rs} = 0$$

can be identified as a system of linear homogeneous equations, which has non-zero solutions when the infinite determinant is zero

$$\det [K^*_{rs}] = 0$$

Legget solves the determinant, restricting the order to 8 terms for several ratios $\hat{a}_1/\hat{a}_2$.

Zetlin [38] in 1957 analyses, by the Ritz method, the symmetrical problem of Fig. 2.1 (b) and presents graphs of the results.

White and Cottinghan [39] in 1962 study the problems represented by Fig. 2.2, using the ordinary finite difference method for both the plane and eigenvalue problems. They discreticize (2.136) in terms of finite differences of Airy stress function and restrict the analysis to stresses prescribed on the boundary, as in Timoshenko's book [40]. White and Cottinghan present graphs of the results obtained for clamped or simply supported plates along the boundary. They obtain, for control problems with a uniform compression as the stress field, an error on the order of 2%.

Peklov [41] in 1966 solves the plane problem corresponding to Fig. 2.3 by the "Load Compensating Method". He approximates the eigenvalue problem both by finite differences and by the Ritz method (with a double Fourier series as a trial solution). The Ritz method yields results 0.7% above the finite difference results. Peklov gives tables of critical loads for different ratios $\hat{a}_1/\hat{a}_2$.

Rockey and Bagchi [42] in 1969 apply the finite element method to the plane and eigenvalue problem of plates with ribs as in Fig. 2.1 (c). They use functions with discontinuous slopes for the in-plane displacements and deflection w of the plate. Rockey and Bagchi present graphs of critical loads for different rib sizes.

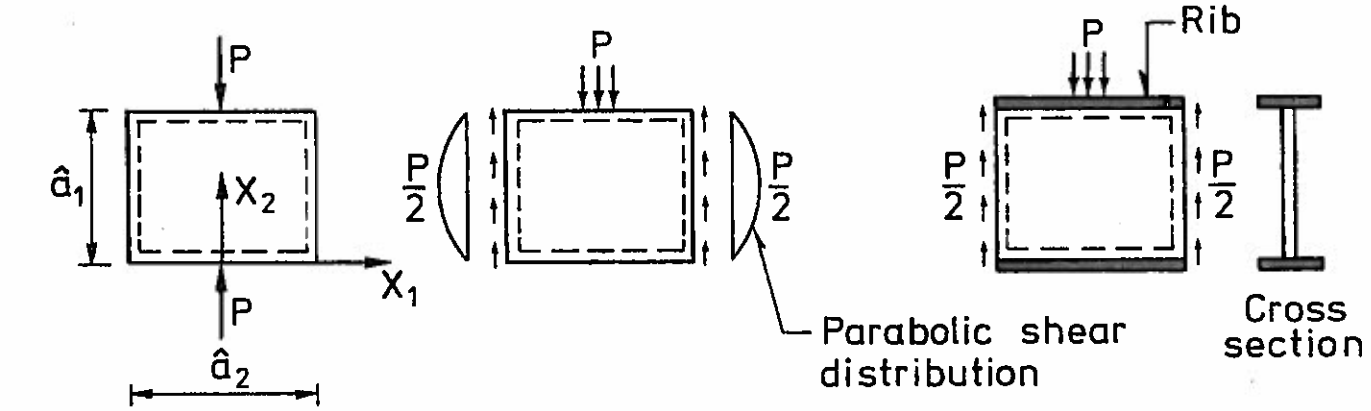

Fig. 2.1. Simply supported plates.

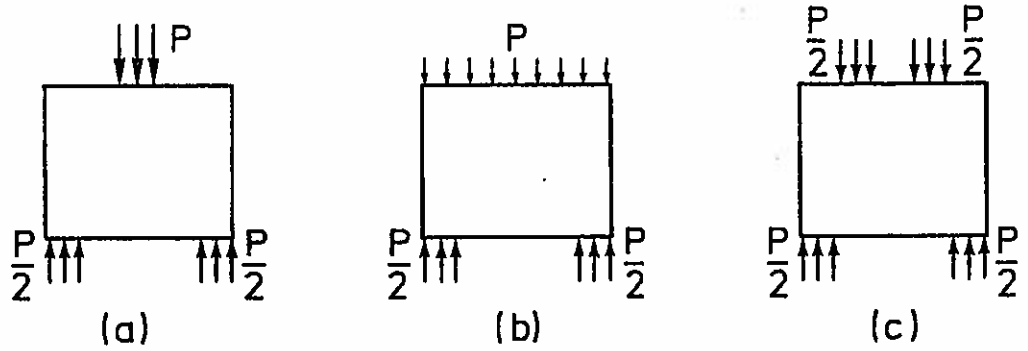

Fig. 2.2. Clamped and simply supported plates.
(White & Cottinghan)

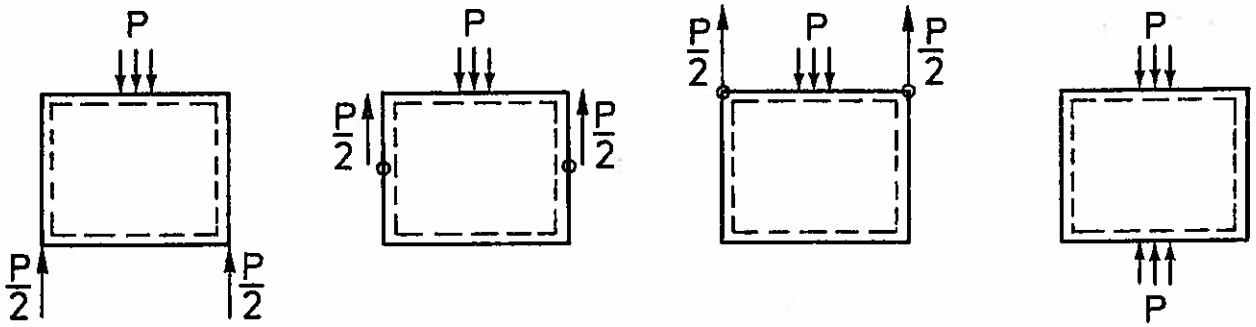

Fig. 2.3. Simply supported plates.
(Peklov)

3. LATERAL BUCKLING OF RECTANGULAR PLATES BY THE RITZ-SUBDOMAIN METHOD

3.1 Statement of the Problem of Lateral Buckling of Plates.

Let Ω, h and C be the area, thickness and contour, respectively, of a flat plate. The plate is subjected to in-plane conservative body forces $\vec{P}$ on Ω, to prescribed in-plane conservative forces $\vec{F}^{*}_{(n)}$ on the boundary C_1, and to prescribed displacements on the boundary C_2. A Cartesian coordinate system is adopted and the displacement components of the plate's middle surface at the adjacent position of equilibrium are denoted by PU_α, ω. The factor P is to be determined in the analysis. U_α are displacement components parallel to the unbuckled middle surface of the plate, and ω is the lateral deflection which is normal to U_α.

The investigation of the lateral buckling of plates can be simplified (according to Art 1.4) to solving two linear problems

a) a linear plane elastic problem, which consists of finding the U_α which satisfy the geometric boundary conditions on C_2 and turn the functional $\hat{\pi}_o$ into a minimum, where

$$\hat{\pi}_o = \tfrac{1}{2} \iint_{\Omega} \frac{Eh}{1-\nu^2} \left[E_{11}^2 + E_{22}^2 + 2(1-\nu)E_{12}^2 + 2\nu E_{11}\, E_{22}\right] d\Omega - \iint_{\Omega} \vec{P} \cdot \vec{U}\, d\Omega - \int_{C_1} \vec{F}^{*}_{(n)} \cdot \vec{U}\, dC \qquad (3.1)$$

$$E_{\gamma\alpha} = U_{\gamma,\alpha} + U_{\alpha,\gamma} \qquad (3.2)$$

as previously expressed by (1.94), (1.95) and (1.91) (although the circumflex accent has not been used here).

b) a linear eigenvalue problem, which consists of finding the w which satisfies homogeneous geometrical boundary conditions on C_2 and gives the minimum of P, where

$$P = \frac{-\frac{1}{2}\iint_{\Omega} D'\left[w_{,\alpha\alpha}\, w_{,\gamma\gamma} - 2(1-\nu)(w_{,11}\, w_{,22} - w^2_{,12}\right] d\Omega}{-\frac{1}{2}\iint_{\Omega} T_{\gamma\alpha}\, w_{,\gamma}\, w_{,\alpha}\, d\Omega} \qquad (3.3)$$

Previously denoted as (2.139). The flexural rigidity is given by

$$D = \frac{Eh^3}{12(1-\nu^2)} \qquad (3.4)$$

and the stresses $T_{\gamma\alpha}$ as

$$T_{11} = \frac{Eh}{1-\nu^2}\,(E_{11} + \nu\, E_{22}) \qquad (3.5)$$

$$T_{22} = \frac{Eh}{1-\nu^2}\,(E_{22} + \nu\, E_{11})$$

$$T_{12} = \frac{Eh}{1-\nu^2}\,(1-\nu)\, E_{12}$$

3.2 Coordinate Functions* of the Ritz-Subdomain Method.

The Ritz-Subdomain Method (see Art. 2.8) consists of dividing the domain of definition of a given minimum

*name given to the trial functions used in the Ritz Method.

problem into subdomains. Local coordinate functions continuous inside each subdomain are grouped to form global coordinate functions (valid for the entire domain) and the latter in turn are used in a trial solution for the minimum problem at hand. In the case of problem (3.1), continuous functions with piecewise continuous first derivatives are needed for U_α. On the other hand (3.3) requires for w continuous functions with continuous first derivatives $w_{,\alpha}$ and piecewise continuous second order derivatives $w_{,\alpha\beta}$.

Rectangular subdomains can be used for studying plates with parallel edges, as in Fig. 3.1(a), although in this report only rectangular plates, as in Fig. 3.1(b), are treated by means of rectangular subdomains. Moreover, two kinds of subdivisions are employed, the uniform mesh of Fig. 3.1(c) and the variable mesh of Fig. 3.1(d).

Let V be the function to be represented inside the rectangular subdomain of Fig. 3.1(b) and V_i be the value of V at the corner i (i=1,2,3,4). The following functions may be constructed using nondimensional coordinates ξ, η.

Pyramidal function (piecewise continuous) - The rectangular subdomain is divided into two triangles as in Fig. 3.2(a). The function V inside the triangle of Fig. 3.2(b) becomes

$$V = (1-\xi-\eta)\ V_1 + \xi V_2 + \eta V_3 \tag{3.6}$$

Hyperbolic Paraboloidal function (first derivatives piecewise continuous).

Let
$$\xi = \frac{X_1}{a_1} \qquad \eta = \frac{X_2}{a_2} \tag{3.7}$$

in Fig. 3.2(c) be nondimensional coordinates and (ξ_i, η_i) the coordinates of the corner i. The value of the function V inside the subdomain results, using Hermite polynomials of Zeroth degree (see Holland and Bell [43, p. 386]), as follows

$$V = \sum_{i=1}^{4} \tfrac{1}{4}(1+4\ \xi_i\xi)(1+4\ \eta_i\eta)\ V_i \qquad (3.8)$$

Bicubic function (second derivatives piecewise continuous) - With the help of Hermite polynomials of first degree

$$H_o(\xi,\xi_i) = 4(\xi+\tfrac{1}{2})^2\ (1-\xi)\xi_i + \tfrac{1}{2} - \xi_i \qquad (3.9)$$

$$H_1(\xi,\xi_i) = (\xi+\tfrac{1}{2})\ (\xi-\tfrac{1}{2})\ (\xi + \xi_i)$$

The function V inside the subdomain of Fig. 3.2(c) can be expressed as (Hansteen [44] presents V in expanded form)

$$V = \sum_{i=1}^{4} [H_o(\xi,\xi_i)H_o(\eta,\eta_i)V_i + H_1(\xi,\xi_i)H_o(\eta,\eta_i)V_{i,1}a_1 +$$

$$+ H_o(\xi,\xi_i)H_1(\eta,\eta_i)V_{i,2}a_2 + H_1(\xi,\xi_i)H_1(\eta,\eta_i)V_{i,12}a_1a_2] \qquad (3.10)$$

The continuity conditions for the Ritz method are satisfied taking hyperbolic paraboloidal functions for each of the displacements U_α and taking a bicubic function for the displacement w. In this form, cases where stiffeners and line loads are internal (not belonging to the contour C) and parallel to the edges of the plate can be treated with no additional complications. On the other hand when bicubic functions are used for U_α for plates with such type of stiffeners, special modifications are needed in the computational scheme.

In this report bicubic functions for all displecements U_α, w have been chosen for the following reasons:

- It is desirable to investigate problems with high stress gradient as in the case of plates subjected to in-plane concentrated loads. A bicubic function seems to be more able to approximate a complicated shape than a hyperbolic paraboloidal function. Furthermore, uniform plates subjected to in-plane forces on the contour C_1 are likely to have continuous stress fields. A good function for approximating a continuous exact stress field probably is a function which gives a continuous stress field. Bicubic functions for U_α produce functions $U_{\alpha,\beta}$ which are continuous, and consequently by (3.5) the resulting stresses are also continuous.
- The requirements for computer storage are two global matrices for the eigenvalue analysis and one global matrix for the plane stress analysis. Thus for a given computer's capacity the order of the plane stress global matrix should be higher than the order of the matrices included in the eigenvalue computations. For uniform plates with U_α given by bicubic functions it is necessary to have 8 unknowns per node (4 for each U_α) when determining the plane stress distribution. The eigenvalue analysis made using a bicubic function for w requires 4 unknowns per node and consequently involves matrices of lower order than the order of the plane stress global matrix.

- The choice of bicubic functions for U_α, w suggests that a more accurate treatment is to be given to the plane stress problem than to the eigenvalue problem. This appearance is so because U_α need only to be functions with piecewise continuous first derivatives and the actual functions employed have piecewise continuous second derivatives. However, the integrands of (3.3) depend quadratically on w while the integrand of the denominator in (3.3) depends only linearly on U_α. Therefore P is more sensible to errors in U_α than to errors in w, making the use of efficient functions for U_α advisable.

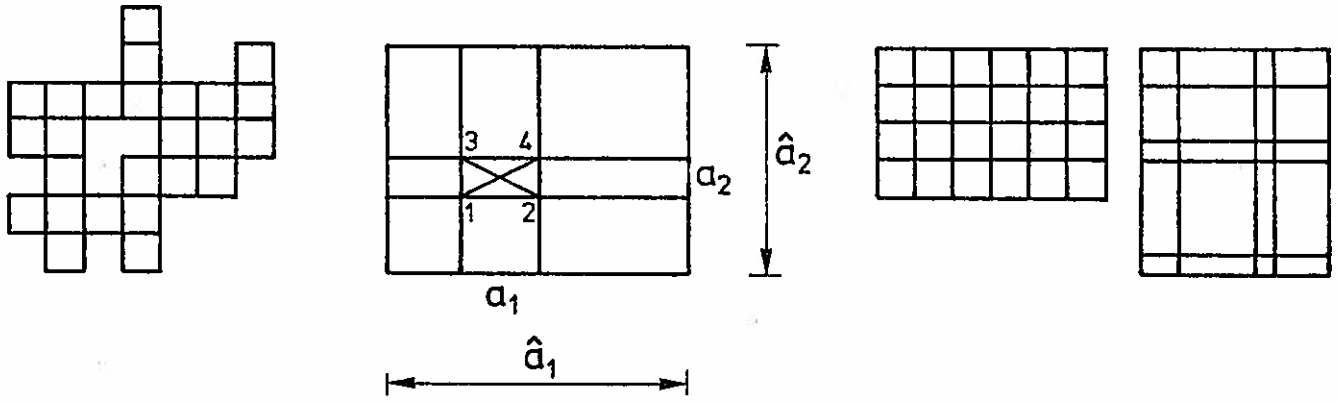

(a) Plate with parallel edges and with a hole (b) Plate showing a subdomain (c) Uniform mesh (d) Variable mesh

Fig. 3.1. Plates subdivided into rectangles

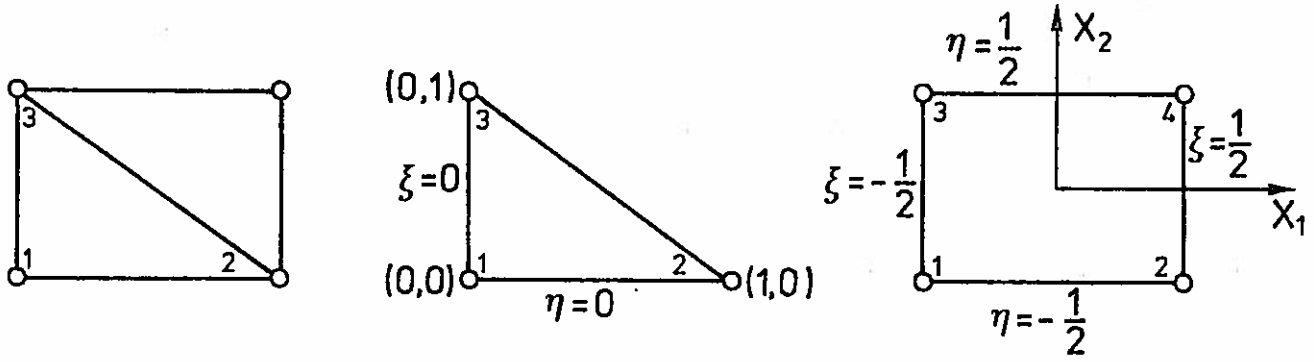

(a) Rectangular subdomain made of two triangles (b) Triangular subdomain (c) Rectangular subdomain

Note: (ξ, η) are non-dimensional coordinates

Fig. 3.2. Some types of subdomains

3.3 Discretization of Energy Integrals for Subdomains.

In this section the energy integrals (3.1) and (3.3) of plates are discretizated using the Ritz-Subdomain methods with trial functions of the form (3.10). In addition, energy integrals for stiffeners are presented and discretizated in a similar way according to functions of the form (3.10).

The derivatives of (3.9) with respect to the variable ξ become

$$H_o'(\xi,\xi_i) = -12\,\xi_i\,\xi^2 + 3\,\xi_i \tag{3.11}$$

$$H_o''(\xi,\xi_i) = -24\,\xi_i\,\xi$$

$$H_1'(\xi,\xi_i) = 3\,\xi^2 + 2\,\xi_i\,\xi - \tfrac{1}{4}$$

$$H_1''(\xi,\xi_i) = 6\,\xi + 2\,\xi_i$$

Derivatives of V in (3.10) can be obtained by using (3.11)

$$\frac{\partial V}{\partial \xi} = \sum_{i=1}^{4} [H_o'(\xi,\xi_i)H_o(\eta,\eta_i)V_i + H_1'(\xi,\xi_i)H_o(\eta,\eta_i)V_{i,1}a_1 +$$

$$+H_o'(\xi,\xi_i)H_1(\eta,\eta_i)V_{i,2}a_2 + H_1'(\xi,\xi_i)H_1(\eta,\eta_i)V_{i,12}a_1a_2]$$

$$\frac{\partial V}{\partial \eta} = \sum_{i=1}^{4} [H_o(\xi,\xi_i)H_o'(\eta,\eta_i)V_i + H_1(\xi,\xi_i)H_o'(\eta,\eta_i)V_{i,1}\,a_1 +$$

$$+H_o(\xi,\xi_i)H_1'(\eta,\eta_i)V_{i,2}a_2 + H_1(\xi,\xi_i)H_1'(\eta,\eta_i)V_{i,12}a_1a_2] \tag{3.12}$$

and similar expressions for $\frac{\partial^2 V}{\partial \xi^2}$, $\frac{\partial^2 V}{\partial \eta^2}$ and $\frac{\partial^2 V}{\partial \xi \partial \eta}$.

It is noticed that each of the five derivatives $\frac{\partial V}{\partial \xi}$, $\frac{\partial V}{\partial \eta}$, $\frac{\partial^2 V}{\partial \xi^2}$ $\frac{\partial V}{\partial \eta^2}$ and $\frac{\partial^2 V}{\partial \xi \partial \eta}$ has 16 terms of the form

$$(b_o + b_1\xi + b_2\xi^2 + b_3\xi^3)(d_o + d_1\eta + d_2\eta^2 + d_3\eta^3) \quad (3.13)$$

where the constants b_o, b_1, b_2, b_3, d_o, d_1, d_2, d_3 are readily obtained from (3.11) (the total number of constants is $8 \times 16 \times 5 = 640$).

Plane Elastic Problem (subdomain integrals)

For convenience the displacements U_α are also denoted by

$$V = U_1 \qquad (3.14)$$
$$V^* = U_2$$

Let

$$\hat{\underset{\sim}{V}}_i = [V_i \quad V_{i,1}\, a_1 \quad V_{i,2}\, a_2 \quad V_{i,12}\, a_1 a_2]^T \qquad (3.15)$$

$$\hat{\underset{\sim}{V}}^*_i = [V^*_i \quad V^*_{i,1}\, a_1 \quad V^*_{i,2}\, a_2 \quad V^*_{i,12}\, a_1 a_2]^T$$

from which $\hat{\underset{\sim}{V}}_i$ and $\hat{\underset{\sim}{V}}^*_i$ are identified as vectors containing the parameters corresponding to node i for the variables V and V^* respectively. The parameters (3.15) for the four corners of the subdomain in Fig. 3.2(c) can be grouped as

$$\hat{\underset{\sim}{h}}^*_1 = \begin{Bmatrix} \hat{\underset{\sim}{V}}_1 \\ \hat{\underset{\sim}{V}}_2 \\ \hat{\underset{\sim}{V}}_3 \\ \hat{\underset{\sim}{V}}_4 \end{Bmatrix} \qquad \hat{\underset{\sim}{h}}^*_2 = \begin{Bmatrix} \hat{\underset{\sim}{V}}^*_1 \\ \hat{\underset{\sim}{V}}^*_2 \\ \hat{\underset{\sim}{V}}^*_3 \\ \hat{\underset{\sim}{V}}^*_4 \end{Bmatrix} \qquad (3.16)$$

such that $\hat{\underset{\sim}{h}}^*_\alpha$ are the local parameters which correspond to the displacements U_α inside the subdomain. For each displacement U_α a function of the form (3.10) results in

$$U_\alpha = \underset{\sim}{\varphi}^T \hat{\underset{\sim}{h}}^*_\alpha \tag{3.17}$$

with $\underset{\sim}{\varphi}$ given by (3.10).

The first derivatives of the displacements U_α inside the subdomain can be written as

$$\begin{Bmatrix} \frac{\partial U_\alpha}{\partial \xi} \\ \\ \frac{\partial U_\alpha}{\partial \eta} \end{Bmatrix} = [\hat{D}_{ij}] \hat{\underset{\sim}{h}}^*_\alpha \tag{3.18}$$

where the matrix $[\hat{D}_{ij}]$ is 2 x 16 and each of its elements $\hat{D}_{ij}$ (32 in total) is of the form (3.13) with 8 constants given by (3.11). It is clear from (3.18) and (3.17) that

$$\begin{Bmatrix} \frac{\partial \underset{\sim}{\varphi}^T}{\partial \xi} \\ \\ \frac{\partial \underset{\sim}{\varphi}^T}{\partial \eta} \end{Bmatrix} = [\hat{D}_{ij}] \tag{3.19}$$

The integrand of the strain energy integral in (3.1) is

$$U^2_{1,1} + \frac{1-\nu}{2} U^2_{1,2} + \frac{(1-\nu)}{2} 2U_{1,2}U_{2,1} + 2\nu U_{1,1}U_{2,2} + U^2_{2,2} + \frac{1-\nu}{2} U^2_{2,1} \tag{3.20}$$

The strain energy corresponding to the subdomain in Fig. 3.1(b) is denoted by $\Delta\hat{\pi}_o$. Introducing (3.17) into (3.20), the variation of the energy for the subdomain becomes

$$\delta\Delta\hat{\pi}_o = \int_{\Delta\Omega}\int \frac{Eh}{1-\nu^2} \begin{Bmatrix} \delta\hat{h}_1^* \\ \delta\hat{h}_2^* \end{Bmatrix}^T \left[\begin{array}{c|c} \underset{\sim}{\varphi}_{,1}\underset{\sim}{\varphi}_{,1}^T + \frac{1-\nu}{2}\,\underset{\sim}{\varphi}_{,2}\underset{\sim}{\varphi}_{,2}^T & \nu\underset{\sim}{\varphi}_{,1}\underset{\sim}{\varphi}_{,2}^T + \frac{1-\nu}{2}\,\underset{\sim}{\varphi}_{,2}\underset{\sim}{\varphi}_{,1}^T \\ \hline \frac{1-\nu}{2}\,\underset{\sim}{\varphi}_{,1}\underset{\sim}{\varphi}_{,2}^T + \nu\underset{\sim}{\varphi}_{,2}\underset{\sim}{\varphi}_{,1}^T & \underset{\sim}{\varphi}_{,2}\underset{\sim}{\varphi}_{,2}^T + \frac{1-\nu}{2}\,\underset{\sim}{\varphi}_{,1}\underset{\sim}{\varphi}_{,1}^T \end{array}\right] \begin{Bmatrix} \hat{h}_1^* \\ \hat{h}_2^* \end{Bmatrix} d\Omega \tag{3.21}$$

$\Delta\Omega$ being the area of the subdomain in Fig. 3.2(c). Let ΔC_1 be the portion of the contour C_1 included in the subdomain's boundary (ΔC_1 may be zero). In addition, the following quantities are prescribed

$$\hat{\gamma} = \frac{\hat{a}_2}{\hat{a}_1} \tag{3.22}$$

$$\alpha_\lambda = \frac{a_\lambda}{\hat{a}_\lambda} \qquad \text{(no sum)}$$

$$\gamma = \frac{a_2}{a_1} = \frac{\alpha_2}{\alpha_1}\,\hat{\gamma}$$

where $\hat{\gamma}$ defines the relative size of the plate and α_λ depends on the mesh selected.

Let

$$Y_1 = \xi \tag{3.23}$$

$$Y_2 = \eta$$

and

$$\underset{\sim}{\hat{\xi}}_{\alpha\beta} = \int_{\Delta\Omega}\int \frac{\partial\underset{\sim}{\varphi}}{\partial Y_\alpha}\frac{\partial\underset{\sim}{\varphi}^T}{\partial Y_\beta}\, d\xi d\eta \tag{3.24}$$

$$\hat{\zeta}_{\alpha\beta} = \hat{\zeta}^{T}_{\beta\alpha}$$

From (3.24) and (3.19)

$$\hat{\zeta}_{\alpha\beta} = [\int_{\Delta\Omega}\int \hat{D}_{\alpha i}\hat{D}_{\beta j}\, d\xi d\eta] \tag{3.25}$$

where α, β = 1,2 have been used in the integrand since the matrix in (3.19) is 2 x 16.

Each $\hat{D}_{\alpha i}$ in the integrand of (3.25) is of the form (3.13), more precisely

$$\hat{D}_{\alpha i} = (\sum_{k=0}^{3} \hat{b}_{K\alpha i}\, \xi^{K})\,(\sum_{l=0}^{3} \hat{d}_{l\alpha i}\, \eta^{l}) \tag{3.26}$$

Using (3.26)

$$\begin{aligned}\int_{\Delta\Omega}\int \hat{D}_{\alpha i}\hat{D}_{\beta j}\,d\xi d\eta = (&\hat{b}_{o\alpha i}\hat{b}_{o\beta j} + \frac{\hat{b}_{o\alpha i}\hat{b}_{2\beta j}+\hat{b}_{1\alpha i}\hat{b}_{1\beta j}+\hat{b}_{2\alpha i}\hat{b}_{o\beta j}}{12} + \\ &+\frac{\hat{b}_{1\alpha i}\hat{b}_{3\beta j}+\hat{b}_{2\alpha i}\hat{b}_{2\beta j}+\hat{b}_{3\alpha i}\hat{b}_{1\beta j}}{80} + \frac{\hat{b}_{3\alpha i}\hat{b}_{3\beta j}}{448}) \times \\ &\times(\hat{d}_{o\alpha i}\hat{d}_{o\beta j} + \frac{\hat{d}_{o\alpha i}\hat{d}_{2\beta j} + \hat{d}_{1\alpha i}\hat{d}_{1\beta j} + \hat{d}_{2\alpha i}\hat{d}_{o\beta j}}{12} + \\ &+\frac{\hat{d}_{1\alpha i}\hat{d}_{3\beta j}+\hat{d}_{2\alpha i}\hat{d}_{2\beta j} + \hat{d}_{3\alpha i}\hat{d}_{1\beta j}}{80} + \frac{\hat{d}_{3\alpha i}\hat{d}_{3\beta j}}{448})\end{aligned} \tag{3.27}$$

Since the coefficients of the right hand side of (3.26) are known, the matrices $\hat{\zeta}_{11}$, $\hat{\zeta}_{22}$ and $\hat{\zeta}_{12}$ can be calculated. The use of an electronic computer reduces the chances of errors.

By the chain rule of differentiation

$$U_{\alpha,\beta} = \frac{1}{\alpha_{\beta}}\,\frac{\partial U_{\alpha}}{\partial Y_{\beta}} \qquad \text{(no sum)} \tag{3.28}$$

and (3.24), the expression (3.21) becomes

$$\delta\hat{\Delta\pi}_o = \frac{Eh}{1-\nu^2} \begin{Bmatrix} \delta\hat{\underset{\sim}{h}}^*_1 \\ \delta\hat{\underset{\sim}{h}}^*_2 \end{Bmatrix}^T \hat{\underset{\sim}{k}}^* \begin{Bmatrix} \hat{\underset{\sim}{h}}^*_1 \\ \hat{\underset{\sim}{h}}^*_2 \end{Bmatrix} \tag{3.29}$$

where the plate thickness h has been considered constant and the elements of the 2e x 2e matrix $\hat{\underset{\sim}{k}}^*$ are given by

$$\hat{k}^*_{ij} = \hat{\zeta}_{11ij}\,\gamma + \frac{1-\nu}{2}\,\hat{\zeta}_{22ij} \times \frac{1}{\gamma} \tag{3.30}$$

$$\hat{k}^*_{i+e;j+e} = \hat{\zeta}_{22ij}\,\frac{1}{\gamma} + \frac{1-\nu}{2}\,\hat{\zeta}_{11ij}\,\gamma$$

$$\hat{k}^*_{i;j+e} = \nu\,\hat{\zeta}_{12ij} + \frac{1-\nu}{2}\,\hat{\zeta}_{21ij} = \nu\hat{\zeta}_{12ij} + \frac{1-\nu}{2}\,\hat{\zeta}_{12ji}$$

$$\hat{k}^*_{i+e;j} = \frac{1-\nu}{2}\,\hat{\zeta}_{12ij} + \nu\hat{\zeta}_{21ij} = \frac{1-\nu}{2}\,\hat{\zeta}_{12ij} + \nu\hat{\zeta}_{12ji}$$

$$i=1,2,\ldots,e$$

$$j=1,2,\ldots,e$$

e = number of local coordinate functions for each variable U_α in the subdomain = 16 (for bicubic functions).

Introducing (3.17) into (3.1), the virtual work of the external forces for the subdomain results in

$$\delta\hat{\Delta\pi}_o = \int_{\Delta\Omega}\int \delta\hat{\underset{\sim}{h}}^{*T}_\alpha\ \underset{\sim}{\varphi}\ p^\alpha d\Omega + \int_{\Delta C_1} \delta\hat{\underset{\sim}{h}}^{*T}_\alpha\ \underset{\sim}{\varphi}\ F^{*\alpha}_{(n)} dC = \delta\hat{\underset{\sim}{h}}^{*T}_\alpha\ \hat{\underset{\sim}{f}}^*_\alpha \tag{3.31}$$

where

$$\hat{f}^*_\alpha = \int_{\Delta\Omega}\int \underset{\sim}{\varphi}\ p^\alpha\, d\Omega + \int_{\Delta C_1} \underset{\sim}{\varphi}\ F^{*\alpha}_{(n)}\, dC \tag{3.32}$$

Eigenvalue problem (Subdomain Integrals)

Let $\Delta\pi_o$ be the bending energy in the denominator of (3.3) corresponding to the subdomain in Fig. 3.2(c). The virtual work $\delta\Delta\pi_o$ can be discretizated following the procedure used for $\delta\Delta\hat{\pi}_o$ in the plane stress problem. To that effect let

$$\bar{W}_i = [\omega_i \quad \omega_{i,1}a_1 \quad \omega_{i,2}a_2 \quad \omega_{i,12}a_1a_2]^T \tag{3.33}$$

$$Z^{*T} = [\bar{W}_1^T \quad \bar{W}_2^T \quad \bar{W}_3^T \quad \bar{W}_4^T] \tag{3.34}$$

$$\omega = \Psi^T Z^* \tag{3.35}$$

$$\begin{Bmatrix} \frac{\partial^2 \omega}{\partial \xi^2} \\ \frac{\partial^2 \omega}{\partial \eta^2} \\ \frac{\partial^2 \omega}{\partial \xi \partial \eta} \end{Bmatrix} = \begin{bmatrix} \frac{\partial^2 \Psi^T}{\partial \xi^2} \\ \frac{\partial^2 \Psi^T}{\partial \eta^2} \\ \frac{\partial^2 \Psi^T}{\partial \xi \partial \eta} \end{bmatrix} \qquad Z^* = [D_{ij}]\, Z^* \tag{3.36}$$

$$D_{ij} = \left(\sum_{K=1}^{3} b_{Kij}\, \xi^K\right) \left(\sum_{l=0}^{3} d_{lij}\, \eta^l\right) \tag{3.37}$$

$$\zeta_{\alpha\beta} = \int\int_{\Delta\Omega} \frac{\partial^2 \Psi}{\partial Y_\alpha^2} \frac{\partial^2 \Psi^T}{\partial Y_\beta^2}\, d\xi d\eta = \left[\int\int_{\Delta\Omega} D_{\alpha i} D_{\beta j}\, d\xi d\eta\right] \tag{3.38}$$

$$\zeta_{33} = \int\int_{\Delta\Omega} \frac{\partial^2 \Psi}{\partial Y_1 \partial Y_2} \frac{\partial^2 \Psi^T}{\partial Y_1 \partial Y_2}\, d\xi d\eta = \left[\int\int_{\Delta\Omega} D_{3i} D_{3j}\, d\xi d\eta\right]$$

where the matrix $[D_{ij}]$ is 3 x 16. Substituting $D_{\alpha i}\, D_{\beta j}$ for $\hat{D}_{\alpha i}\, \hat{D}_{\beta j}$ in (3.27) the formula for computing $\zeta_{\alpha\beta}$ is obtained. In the same way ζ_{33} is obtained by using $D_{3i} D_{3j}$.

From (3.3) and (3.35)

$$\delta\Delta\pi_o = \int_{\Delta\Omega}\int D(\delta w_{,11}\, w_{,11}+\nu\delta w_{,11}\, w_{,22}+\nu\delta w_{,22}\, w_{,11}+\delta w_{,22} w_{,22}+ 2(1-\nu)\,\delta w_{,12}\, w_{,12})d\Omega$$

$$\delta\Delta\pi_o = \delta\underset{\sim}{Z}^{*T}\int_{\Delta\Omega}\int D(\underset{\sim}{\varphi}_{,11}\underset{\sim}{\varphi}_{,11}^{T}+\nu\underset{\sim}{\varphi}_{,11}\,\underset{\sim}{\varphi}_{,22}^{T}+\nu\underset{\sim}{\varphi}_{,22}\,\underset{\sim}{\varphi}_{,11}^{T}+\underset{\sim}{\varphi}_{,22}\underset{\sim}{\varphi}_{,22}^{T}+ 2(1-\nu)\,\underset{\sim}{\varphi}_{,12}\,\underset{\sim}{\varphi}_{,12}^{T})\,d\Omega\,\underset{\sim}{Z}^{*}$$

Using (3.22) and (3.38) in the last expression and considering the flexural rigidity D constant

$$\delta\Delta\pi_o = \frac{D}{\hat{a}_1^2}\,\delta\underset{\sim}{Z}^{*T}\,[k^*_{ij}]\,\underset{\sim}{Z}^{*} \qquad (3.39)$$

$$[k^*_{ij}] = [\zeta_{11ij}\gamma^2+\zeta_{22ij}\frac{1}{\gamma^2}+\nu(\zeta_{12ij}+\zeta_{12ji})+2(1-\nu)\zeta_{33ij}]\frac{1}{a_1^2\gamma}$$

For plates with uniform mesh (Fig. 3.1(b)), it turns out convenient to use

$$\delta\Delta\pi_o = \frac{D}{\hat{a}_1 a_1}\,\delta\underset{\sim}{Z}^{*T}\,[k^*_{ij}]\,\underset{\sim}{Z}^{*} \qquad (3.40)$$

$$[k^*_{ij}] = [\zeta_{11ij}\gamma^2+\zeta_{22ij}\frac{1}{\gamma^2}+\nu(\zeta_{12ij}+\zeta_{12ji})+2(1-\nu)\zeta_{33ij}]\frac{1}{a_1\gamma}$$

The variation of the integral in the denominator of (3.3) is expressed using (3.5) and (3.2) by

$$\int_\Omega\int T_{\gamma\alpha}w_{,\gamma}\delta w_{,\alpha}d\Omega = \int_\Omega\int\frac{Eh}{1-\nu^2}(U_{1,1}+\nu U_{2,2})w_{,1}\delta w_{,1}+ + \frac{1-\nu}{2}(U_{1,2}+U_{2,1})(w_{,1}\delta w_{,2}+w_{,2}\delta w_{,1})+ + (U_{2,2}+\nu U_{1,1})w_{,2}\,\delta w_{,2}]\,d\Omega \qquad (3.41)$$

Considering the expression (3.41) for the subdomain of area $\Delta\Omega$, (3.35) and (3.17) lead to

$$\int_{\Delta}\int_{\Omega} T_{\gamma\alpha}\,\omega_{,\gamma}\,\delta\omega_{,\alpha}\,d\Omega = \delta\underset{\sim}{Z}^{*T}\iint_{\Delta\Omega}\frac{Eh}{1-\nu^2}\Big[\underset{\sim}{\varphi}_{,1}\underset{\sim}{\varphi}^{T}_{,1}\underset{\sim}{\varphi}_{,1}+\frac{1-\nu}{2}\big(\underset{\sim}{\varphi}_{,1}\underset{\sim}{\varphi}^{T}_{,2}+\underset{\sim}{\varphi}_{,2}\underset{\sim}{\varphi}^{T}_{,1}\big)\underset{\sim}{\varphi}^{T}_{,2}+\nu\underset{\sim}{\varphi}_{,2}\underset{\sim}{\varphi}^{T}_{,2}\underset{\sim}{\varphi}_{,1}\Big]\hat{\underset{\sim}{h}}^{*}_{1}+\Big[\nu\underset{\sim}{\varphi}_{,1}\underset{\sim}{\varphi}^{T}_{,1}\underset{\sim}{\varphi}^{T}_{,2}+\frac{1-\nu}{2}\big(\underset{\sim}{\varphi}_{,1}\underset{\sim}{\varphi}^{T}_{,2}+\underset{\sim}{\varphi}_{,2}\underset{\sim}{\varphi}^{T}_{,1}\big)\underset{\sim}{\varphi}^{T}_{,1}+\underset{\sim}{\varphi}_{,2}\underset{\sim}{\varphi}^{T}_{,2}\underset{\sim}{\varphi}^{T}_{,2}\Big]\hat{\underset{\sim}{h}}^{*}_{2}\,\Big]d\Omega\,\underset{\sim}{Z}^{*} \tag{3.41}$$

Using the chain rule of differentiation, (3.36), (3.18) and (3.22) the virtual work expression (3.41) is transformed to

$$\int_{\Delta}\int_{\Omega} T_{\gamma\alpha}\omega_{,\gamma}\delta\omega_{,\alpha}d\Omega = \frac{1}{\hat{a}_1}\,\delta\underset{\sim}{Z}^{*T}[s^{*}_{ij}]\,\underset{\sim}{Z}^{*} \tag{3.42}$$

where

$$s^{*}_{ij} = \sum_{k=1}^{e}\Big[\Big(G_{ijk}\gamma+H_{ijk}\frac{1}{\gamma}\Big)\hat{h}_{ik}+\Big(I_{ijk}\frac{1}{\gamma^2}+J_{ijk}\Big)\hat{h}_{2K}\Big]\frac{1}{\alpha_1} \tag{3.43}$$

$$G_{ijK} = \int_{\Delta}\int_{\Omega}\hat{D}_{1i}\hat{D}_{1j}\hat{D}_{1K}d\xi d\eta \tag{3.44}$$

$$H_{ijK} = \frac{1-\nu}{2}\int_{\Delta}\int_{\Omega}\hat{D}_{1i}\hat{D}_{2j}\hat{D}_{2K}d\xi d\eta+\frac{1-\nu}{2}\int_{\Delta}\int_{\Omega}\hat{D}_{2i}\hat{D}_{1j}\hat{D}_{2K}d\xi d\eta$$

$$I_{ijK} = \int_{\Delta\Omega}\int\hat{D}_{2i}\,\hat{D}_{2j}\,\hat{D}_{2K}\,d\xi d\eta$$

$$J_{ijK} = \nu\iint_{\Delta\Omega}\hat{D}_{1i}\hat{D}_{1j}\hat{D}_{2K}\,d\xi d\eta+\frac{1-\nu}{2}\iint_{\Delta\Omega}\hat{D}_{1i}\hat{D}_{2j}\hat{D}_{1K}d\xi d\eta+$$

$$+\frac{1-\nu}{2}\iint_{\Delta\Omega}\hat{D}_{2i}\hat{D}_{1j}\hat{D}_{1K}d\xi d\eta$$

e = number of local coordinate functions used for each displacement U_α (for bicubic functions e=16)

$\hat{h}_{\alpha K}$ = components of the vector $\underset{\sim}{h}_\alpha$

$$\hat{\underset{\sim}{h}}_\alpha = \frac{Eh}{1-\nu^2}\hat{\underset{\sim}{h}}^*_\alpha \tag{3.45}$$

For plates where a uniform mesh is adopted (Fig. 3.1(c)), it turns out convenient to express (3.42) as

$$\int_\Delta \int_\Omega T_{\gamma\alpha}\omega_{,\gamma}\delta\omega_{,\alpha}d\Omega = \frac{1}{a_1}\ \delta\underset{\sim}{Z}^{*T}[s^*_{ij}]\underset{\sim}{Z}^* \tag{3.46}$$

where

$$s^*_{ij} = \sum_{K=1}^{e}[(G_{ijK}\gamma + H_{ijK}\frac{1}{\gamma})\hat{h}_{iK} + (I_{ijK}\frac{1}{\gamma^2} + J_{ijK})\hat{h}_{2K}] \tag{3.47}$$

The integrals G_{ijK}, H_{ijK}, I_{ijK} and J_{ijK} are symmetric with respect to the indices i,j. Since any index can take values from 1 to 16, the symmetry conditions reduce the number of quantities to be computed to 136 x 16 x 4 = 8704. Quantities Q_{lKn}, which occupy a storage in an electronic computer of (136, 16, 4) can be defined as follows

$$[Q_{lK1}\ \ Q_{lK2}\ \ Q_{lK3}\ \ Q_{lK4}] = [G_{ijK}\ \ H_{ijK}\ \ I_{ijK}\ \ J_{ijK}] \tag{3.48}$$

$$i=1,\ldots,16$$
$$j=1,\ldots,i$$
$$l=16(j-1)-\langle((j-1)j)/2\rangle + i$$

where the real number inside the symbol $\langle\ldots\rangle$ is truncated to its maximum integer.

The integrals (3.44) are made of terms of the form

$$\int_\Delta \int_\Omega \hat{D}_{\alpha i}\ \hat{D}_{\beta j}\ \hat{D}_{\gamma K}d\xi d\eta = \int_{-\frac{1}{2}}^{\frac{1}{2}}(\sum_{l=0}^{3}\hat{b}_{l\alpha i}\xi^l)(\sum_{m=0}^{3}\hat{b}_{m\beta j}\xi^m)(\sum_{n=0}^{3}\hat{b}_{n\gamma K}\xi^n)d\xi \times$$

$$\times \int_{-\frac{1}{2}}^{\frac{1}{2}} \left(\sum_{P=0}^{3} \hat{d}_{P\alpha i}\eta^P\right)\left(\sum_{q=0}^{3} \hat{d}_{q\beta j}\eta^q\right)\left(\sum_{s=0}^{3} \hat{d}_{s\gamma K}\eta^s\right)d\eta \tag{3.49}$$

where (3.26) has been used.

The line integral along the variable ξ in (3.49) results in

$$\int_{-\frac{1}{2}}^{\frac{1}{2}} \left(\sum_{l=0}^{3} \hat{b}_{l\alpha i}\xi^l\right)\left(\sum_{m=0}^{3} \hat{b}_{m\beta j}\xi^m\right)\left(\sum_{n=0}^{3} \hat{b}_{n\gamma K}\xi^n\right)d\xi = \sigma_o \hat{b}_{o\gamma K} +$$

$$+ \frac{\sigma_o \hat{b}_{2\gamma K}+\sigma_1 \hat{b}_{1\gamma K}+\sigma_2 \hat{b}_{o\gamma K}}{12} + \frac{\sigma_1 \hat{b}_{3\gamma K}+\sigma_2 \hat{b}_{2\gamma K}+\sigma_3 \hat{b}_{1\gamma K}+\sigma_4 \hat{b}_{o\gamma K}}{80} +$$

$$+ \frac{\sigma_3 \hat{b}_{3\gamma K}+\sigma_4 \hat{b}_{2\gamma K}+\sigma_5 \hat{b}_{1\gamma K}+\sigma_6 \hat{b}_{o\gamma K}}{448} + \frac{\sigma_5 \hat{b}_{3\gamma K}+\sigma_6 \hat{b}_{3\gamma K}}{2304} \tag{3.50}$$

where

$$\sigma_o = \hat{b}_{o\alpha i}\hat{b}_{o\beta j} \tag{3.51}$$

$$\sigma_1 = \hat{b}_{o\alpha i}\hat{b}_{1\beta j}+\hat{b}_{1\alpha i}\hat{b}_{o\beta j}$$

$$\sigma_2 = \hat{b}_{o\alpha i}\hat{b}_{2\beta j}+\hat{b}_{1\alpha i}\hat{b}_{1\beta j}+\hat{b}_{2\alpha i}\hat{b}_{o\beta j}$$

$$\sigma_3 = \hat{b}_{o\alpha i}\hat{b}_{3\beta j}+\hat{b}_{1\alpha i}\hat{b}_{2\beta j}+\hat{b}_{2\alpha i}\hat{b}_{1\beta j}+\hat{b}_{3\alpha i}\hat{b}_{o\beta j}$$

$$\sigma_4 = \hat{b}_{1\alpha i}\hat{b}_{3\beta j}+\hat{b}_{2\alpha i}\hat{b}_{2\beta j}+\hat{b}_{3\alpha i}\hat{b}_{1\beta j}$$

$$\sigma_5 = \hat{b}_{2\alpha i}\hat{b}_{3\beta j}+\hat{b}_{3\alpha i}\hat{b}_{2\beta j}$$

$$\sigma_6 = \hat{b}_{3\alpha i}\hat{b}_{3\beta j}$$

The integration along the variable η in (3.49) can be carried out simply by substituting the coefficients $\hat{d}\ldots$ for the coefficients $\hat{b}\ldots$ in (3.50). Since the coefficients in (3.50)

have been given by (3.12) and (3.11), the integrals (3.44) can be evaluated using an electronic computer.

Energy integrals for stiffeners

Several energy expressions for a stiffener placed from node 1 to node 2 in Fig. 3.2(c) will be considered. Then analogous energy expressions will be given for stiffeners placed on the boundary of the subdomain in Fig. 3.2(c). The stiffener from node 1 to node 2 has a constant cross section of area S^*, modulus of inertia I^* and torsional constant J^*. The stiffener is elastic with a material of Young's modulus E^* and shear modulus G^*.

Since the displacements U_α (also denoted by (3.14)) are given by (3.17) and the deflection w by (3.35), it follows that

$$V\Big|_{\eta = -\frac{1}{2}} = \underset{\sim}{\chi}^T \hat{\underset{\sim}{1}} \tag{3.52}$$

$$w\Big|_{\eta = -\frac{1}{2}} = \underset{\sim}{\chi}^T \bar{\underset{\sim}{Y}}$$

$$\frac{\partial w}{\partial \eta}\Big|_{\eta=-\frac{1}{2}} = \underset{\sim}{\chi}^T \bar{\underset{\sim}{Y}}^*$$

where

$$\underset{\sim}{\chi} = [2\xi^3 - \tfrac{3}{2}\xi + \tfrac{1}{2} \;\vdots\; \xi^3 - \tfrac{\xi^2}{2} - \tfrac{\xi}{4} + \tfrac{1}{8} \;\vdots\; -2\xi^3 + \tfrac{3\xi}{2} + \tfrac{1}{2} \;\vdots\; \xi^3 + \tfrac{\xi^2}{2} - \tfrac{\xi}{4} - \tfrac{1}{8}]^T \tag{3.53}$$

$$\hat{\underset{\sim}{1}} = [V_1 \quad a_1 V_{1,1} \quad V_2 \quad a_1 V_{2,1}]^T \tag{3.54}$$

$$\bar{\underset{\sim}{Y}} = [w_1 \quad a_1 w_{1,1} \quad w_2 \quad a_1 w_{2,1}]^T$$

$$\underset{\sim}{\bar{Y}}^{*T} = [a_2\omega_{1,2} \quad a_1a_2\omega_{1,12} \quad a_2\omega_{2,2} \quad a_1a_2\omega_{2,12}]$$

Furthermore

$$\underset{\sim}{\chi}' = \frac{\partial \underset{\sim}{\chi}}{\partial \xi} = [6\xi^2 - \tfrac{3}{2} \mid 3\xi^2 - \xi - \tfrac{1}{4} \mid -6\xi^2 + \tfrac{3}{2} \mid 3\xi^2 + \xi - \tfrac{1}{4}]^T \quad (3.55)$$

$$\underset{\sim}{\chi}'' = \frac{\partial \underset{\sim}{\chi}'}{\partial \xi} = [12\xi \mid 6\xi - 1 \mid -12\xi \mid 6\xi + 1]^T$$

$$\left.\frac{\partial V}{\partial \xi}\right|_{\eta=-\frac{1}{2}} = \underset{\sim}{\chi}'^T \underset{\sim}{\hat{1}} \quad (3.56)$$

$$\left.\frac{\partial \omega}{\partial \xi}\right|_{\eta=-\frac{1}{2}} = \underset{\sim}{\chi}'^T \underset{\sim}{\bar{Y}}$$

$$\left.\frac{\partial^2 \omega}{\partial \eta \partial \xi}\right|_{\eta=-\frac{1}{2}} = \underset{\sim}{\chi}'^T \underset{\sim}{\bar{Y}}^*$$

$$\left.\frac{\partial^2 \omega}{\partial \xi^2}\right|_{\eta=-\frac{1}{2}} = \underset{\sim}{\chi}''^T \underset{\sim}{\bar{Y}}$$

Let

$$\underset{\sim}{t}^* = \int_{-\frac{1}{2}}^{\frac{1}{2}} \underset{\sim}{\chi}' \underset{\sim}{\chi}'^T \, d\xi \quad (3.57)$$

$$\underset{\sim}{b}^* = \int_{-\frac{1}{2}}^{\frac{1}{2}} \underset{\sim}{\chi}'' \underset{\sim}{\chi}''^T d\xi$$

$$\underset{\sim}{\overline{i}} = \int_{-\frac{1}{2}}^{\frac{1}{2}} \chi_i \underset{\sim}{\chi}' \underset{\sim}{\chi}'^T d\xi \qquad ; \; i=1,2,3,4$$

$$\underset{\sim}{g}^* = \sum_{i=1}^{4} \hat{1}_i \, \underset{\sim}{\overline{i}} \quad (3.58)$$

From (3.56), (3.57) and (3.58)

$$\int_{-\frac{1}{2}}^{\frac{1}{2}} \left(\frac{\partial V}{\partial \xi}\right)^2 \Big|_{\eta=-\frac{1}{2}} d\xi = \underset{\sim}{\hat{1}}^T \; \underset{\sim}{t}^* \; \underset{\sim}{\hat{1}} \tag{3.59}$$

$$\int_{-\frac{1}{2}}^{\frac{1}{2}} \left(\frac{\partial^2 \omega}{\partial \xi \partial \eta}\right)^2 \Big|_{\eta=-\frac{1}{2}} d\xi = \underset{\sim}{\bar{Y}}^{*T} \; \underset{\sim}{t}^* \; \underset{\sim}{\bar{Y}}^*$$

$$\int_{-\frac{1}{2}}^{\frac{1}{2}} \left(\frac{\partial^2 \omega}{\partial \xi^2}\right)^2 \Big|_{\eta=-\frac{1}{2}} d\xi = \underset{\sim}{\bar{Y}}^T \; \underset{\sim}{b}^* \; \underset{\sim}{\bar{Y}}$$

$$\int_{-\frac{1}{2}}^{\frac{1}{2}} \frac{\partial V}{\partial \xi} \left(\frac{\partial \omega}{\partial \xi}\right)^2 \Big|_{\eta=-\frac{1}{2}} d\xi = \underset{\sim}{\bar{Y}}^T \; \underset{\sim}{g}^* \; \underset{\sim}{\bar{Y}}$$

The use of (3.55) into the integrals (3.57) gives

$$\underset{\sim}{t}^* = \begin{bmatrix} \frac{6}{5} & \frac{1}{10} & -\frac{6}{5} & \frac{1}{10} \\ & \frac{2}{15} & -\frac{1}{10} & -\frac{1}{30} \\ \text{Symm.} & & \frac{6}{5} & -\frac{1}{10} \\ & & & \frac{2}{15} \end{bmatrix} \tag{3.60}$$

$$\underset{\sim}{b}^* = \begin{bmatrix} 12 & 6 & -12 & 6 \\ & 4 & -6 & 2 \\ \text{Symm.} & & 12 & -6 \\ & & & 4 \end{bmatrix}$$

$$\underset{\sim}{\boxed{1}} = \underset{\sim}{\boxed{3}} = \frac{1}{70}\begin{bmatrix} -108 & -12 & 108 & -12 \\ & -6 & 12 & 1 \\ \text{Symm.} & & -108 & 12 \\ & & & -6 \end{bmatrix}$$

$$\underset{\sim}{\boxed{2}} = \frac{1}{70}\begin{bmatrix} -12 & -6 & -12 & 1 \\ & 4 & 6 & -2/3 \\ \text{Symm.} & & -12 & -1 \\ & & & -2/3 \end{bmatrix}$$

$$\underset{\sim}{\boxed{4}} = \frac{1}{70}\begin{bmatrix} -12 & 1 & 12 & -6 \\ & -2/3 & -1 & -2/3 \\ \text{Symm.} & & -12 & 6 \\ & & & 4 \end{bmatrix}$$

Let

$$S^*_\lambda = \frac{S^* E^* (1-\nu^2)}{h \hat{a}_\lambda E} \qquad (3.61)$$

$$I^*_\lambda = \frac{I^* E^*}{D \hat{a}_\lambda}$$

$$J^*_\lambda = \frac{J^* G^*}{D \hat{a}_\lambda}$$

E and ν being, respectively, Young's modulus and Poisson's ratio for the plate of thickness h.

Several energy integrals defined below are transformed according to $(3.7)_1$ to expressions containing formulae (3.59), (3.22) and (3.61), i.e.

Axial energy

$$\tfrac{1}{2}\int_{-\frac{a_1}{2}}^{\frac{a_1}{2}} S^* E^* (U_{1,1})^2 \Big|_{\eta=-\frac{1}{2}} dX_1 = \tfrac{1}{2}\frac{Eh}{(1-\nu^2)}\frac{S_1^*}{a_1}\hat{\underset{\sim}{1}}^T \underset{\sim}{t}^* \hat{\underset{\sim}{1}} \qquad (3.62)_1$$

Flexural energy

$$\tfrac{1}{2}\int_{-\frac{a_1}{2}}^{\frac{a_1}{2}} I^* E^* w_{,11}^2 \Big|_{\eta=-\frac{1}{2}} dX_1 = \frac{D}{2}\frac{I_1^*}{a_1^2}\frac{1}{\hat{a}_1 a_1}\bar{\underset{\sim}{Y}}^T \underset{\sim}{b}^* \bar{\underset{\sim}{Y}} \qquad (3.62)_2$$

Torsional energy

$$\tfrac{1}{2}\int_{-\frac{a_1}{2}}^{\frac{a_1}{2}} J^* G^* w_{,12}^2 \Big|_{\eta=-\frac{1}{2}} dX_1 = \frac{D}{2}\frac{J_1^*}{\gamma^2 a_1^2}\frac{1}{\hat{a}_1 a_1}\bar{\underset{\sim}{Y}}^{*T} \underset{\sim}{t}^* \bar{\underset{\sim}{Y}}^* \qquad (3.62)_3$$

Geometrical energy

$$\tfrac{1}{2}\int_{-\frac{a_1}{2}}^{\frac{a_1}{2}} S^* E^* U_{1,1} w_{,1}^2 \Big|_{\eta=-\frac{1}{2}} dX_1 = \tfrac{1}{2}\frac{1}{a_1}\frac{1}{a_1}\bar{\underset{\sim}{Y}}^T \underset{\sim}{g}^* \bar{\underset{\sim}{Y}} \qquad (3.62)_4$$

The axial energy $(3.62)_1$ is to be added to the right hand side of (3.1) while the flexural energy $(3.62)_2$ and torsional energy $(3.62)_3$ are to be added to the numerator of (3.3). The effect of the axial force in the stiffener due to the change in geometry from the fundamental to the adjacent state of equilibrium of the plate, represented by $(3.62)_4$, is to be included in the denominator of (3.3) with a negative sign.

When a variable mesh (as in Fig. 3.1(d)) has been selected for the analysis, the vectors (3.54) are more conveniently substituted for the constant vectors

$$\hat{\underset{\sim}{1}}_o = [V_1 \quad \hat{a}_1 V_{1,1} \quad V_2 \quad \hat{a}_1 V_{2,1}]^T \qquad (3.63)$$

$$\bar{\underset{\sim}{Y}}_o = [\omega_1 \quad \hat{a}_1 \omega_{1,1} \quad \omega_2 \quad \hat{a}_1 \omega_{2,1}]^T$$

$$\bar{\underset{\sim}{Y}}_o^* = [\hat{a}_2 \omega_{1,1} \quad \hat{a}_1 \hat{a}_2 \omega_{1,12} \quad \hat{a}_2 \omega_{2,2} \quad \hat{a}_1 \hat{a}_2 \omega_{2,12}]^T$$

Both set of vectors (3.54) and (3.63) are related bytthe matrix

$$\hat{\underset{\sim}{\alpha}}_1 = \begin{bmatrix} 1 & 0 & 0 & 0 \\ & \alpha_1 & 0 & 0 \\ & & 1 & \\ \text{Symm.} & & & \alpha_1 \end{bmatrix} \tag{3.64}$$

as follows

$$\begin{aligned} \hat{\underset{\sim}{l}} &= \hat{\underset{\sim}{\alpha}}_1 \hat{\underset{\sim}{l}}_o \\ \bar{\underset{\sim}{Y}} &= \hat{\underset{\sim}{\alpha}}_1 \bar{\underset{\sim}{Y}}_o \\ \bar{\underset{\sim}{Y}}^* &= \alpha_2 \underset{\sim}{\alpha}_1 \bar{\underset{\sim}{Y}}_o^* \end{aligned} \tag{3.65}$$

Using (3.65) and (3.58)

$$\hat{\underset{\sim}{l}}^T \underset{\sim}{t}^* \hat{\underset{\sim}{l}} = \underset{\sim}{l}_o^T [\hat{\underset{\sim}{\alpha}}_1 \underset{\sim}{t}^* \hat{\underset{\sim}{\alpha}}_1] \underset{\sim}{l}_o \tag{3.66}$$

$$\bar{\underset{\sim}{Y}}^{*T} \underset{\sim}{t}^* \bar{\underset{\sim}{Y}}^* = \bar{\underset{\sim}{Y}}_o^{*T} [\alpha_2^2 \hat{\underset{\sim}{\alpha}}_1 \underset{\sim}{t}^* \hat{\underset{\sim}{\alpha}}_1] \bar{\underset{\sim}{Y}}_o^*$$

$$\bar{\underset{\sim}{Y}}^T \underset{\sim}{b}^* \bar{\underset{\sim}{Y}} = \bar{\underset{\sim}{Y}}_o^T [\hat{\underset{\sim}{\alpha}}_1 \underset{\sim}{b}^* \hat{\underset{\sim}{\alpha}}_1] \bar{\underset{\sim}{Y}}_o$$

$$\bar{\underset{\sim}{Y}}^T \underset{\sim}{g}^* \bar{\underset{\sim}{Y}} = \bar{\underset{\sim}{Y}}_o^T [\hat{\underset{\sim}{\alpha}}_1 \underset{\sim}{g}^* \hat{\underset{\sim}{\alpha}}_1] \bar{\underset{\sim}{Y}}_o$$

$$g^* = \hat{l}_{o1} \sqrt{\underset{\sim}{1}} + \hat{l}_{o3} \sqrt{\underset{\sim}{3}} + \alpha_1 (\hat{l}_{o2} \sqrt{\underset{\sim}{2}} + \hat{l}_{o4} \sqrt{\underset{\sim}{4}})$$

The new expressions (3.66) are used for calculating the energy integrals (3.62). It is noticed that the matrices included in brackets in (3.66) can all be expressed by the function

$$\underset{\sim}{Q}_o(\underset{\sim}{t}^{**}, b_o, \beta) = b_o \begin{bmatrix} t_{11}^{**} & \beta t_{12}^{**} & t_{13}^{**} & \beta t_{14}^{**} \\ & \beta^2 t_{22}^{**} & \beta t_{23}^{**} & \beta^2 t_{24}^{**} \\ & \text{Symm.} & t_{33}^{**} & \beta t_{34}^{**} \\ & & & \beta^2 t_{44}^{**} \end{bmatrix} \qquad (3.67)$$

provided that proper values are given to the symmetric 4 x 4 matrix $\underset{\sim}{t}^{**}$ and to the constants b_o and β.

Energy integrals for stiffeners located at any of the edges of the subdomain in Fig. 3.2(c) can be calculated in analogous manner. Table 3.1 presents the analysis of the integrals

$$\hat{\pi}_{(1)\lambda} = \tfrac{1}{2} \int_{-\frac{a_\lambda}{2}}^{\frac{a_\lambda}{2}} S^* E^* U_{\lambda,\lambda}^2 \Big|_{\text{edge}} dX_\lambda \qquad \text{(no summation)} \quad (3.68)$$

$$\pi_{(2)\lambda} = \tfrac{1}{2} \int_{-\frac{a_\lambda}{2}}^{\frac{a_\lambda}{2}} I^* E^* \omega_{,\lambda\lambda}^2 \Big|_{\text{edge}} dX_\lambda$$

$$\pi_{(3)\lambda} = \tfrac{1}{2} \int_{-\frac{a_\lambda}{2}}^{\frac{a_\lambda}{2}} J^* G^* \omega_{,12}^2 \Big|_{\text{edge}} dX_\lambda$$

$$\pi_{(4)\lambda} = \tfrac{1}{2} \int_{-\frac{a_\lambda}{2}}^{\frac{a_\lambda}{2}} S^* E^* U_{\lambda,\lambda} \omega_{,\lambda}^2 \Big|_{\text{edge}} dX_\lambda$$

Likewise an approximation to (2.14) requires the computation

$$\pi_{(5)\lambda} = \tfrac{1}{2}\int_{-\frac{a_\lambda}{2}}^{\frac{a_\lambda}{2}} \omega_{,\lambda}^2 \Big|_{\text{edge}} dX_\lambda = \frac{1}{2a_\lambda}\,\bar{\underset{\sim}{Y}}^T \underset{\sim}{Q}_o\left(t^*, \frac{1}{\alpha_\lambda}, \beta_\lambda\right)\bar{\underset{\sim}{Y}} \quad \text{(no sum.)} \quad (3.68)_5$$

where $\beta_\lambda = \alpha_\lambda$ in a variable mesh, $\beta_\lambda = 1$ in a uniform mesh and $\bar{\underset{\sim}{Y}}$ taken as shown in item (2) of table 3.1.

	Uniform mesh							Variable mesh*		
	b_1	b_2	Energy	$\hat{Y}$ or $\hat{1}$ 1 2	3 4	3 1	4 2	b_1	b_2	Energy
(1) AXIAL	$\frac{S_1^*}{a_1}$	$\frac{S_2^*}{a_2}$	$\frac{1}{2}\frac{Eh}{1-\nu^2}\hat{1}^T Q_o(t^*, b_\lambda, 1)\hat{1}$	V_1	V_3	V_1^*	V_4	$\frac{S_1^*}{a_1}$	$\frac{S_2^*}{a_2}$	$\frac{1}{2}\frac{Eh}{1-\nu^2}\hat{1}^T Q_o(t^*, b_\lambda, a_\lambda)\hat{1}$
				$a_1 V_{1,1}$	$a_1 V_{3,1}$	$a_2 V_{1,2}^*$	$a_2 V_{4,2}^*$			
				V_2	V_4	V_3^*	V_4^*			
				$a_1 V_{2,1}$	$a_1 V_{4,1}$	$a_2 V_{3,1}^*$	$a_2 V_{4,2}^*$			
(3) TORSION	$\frac{J_1^*}{\gamma^2 a_1^2}$	$\frac{J_2^*}{a_1 a_2}$	$\frac{D}{2}\frac{1}{\hat{a}_1 a_1}\bar{Y}^T Q_o(t^*, b_\lambda, 1)\bar{Y}$	$a_2 \varpi_{1,2}$	$a_2 \varpi_{3,2}$	$a_1 \varpi_{1,1}$	$a_1 \varpi_{2,1}$	$\frac{J_1^*}{a_1 \hat{a}_2}$	$\frac{J_2^*}{a_1 a_2}$	$\frac{D}{2}\frac{1}{\hat{a}_1^2}\bar{Y}^T Q_o(t^*, b_\lambda, a_\lambda)\bar{Y}$
				$a_1 a_2 \varpi_{1,12}$	$a_1 a_2 \varpi_{3,12}$	$a_1 a_2 \varpi_{1,12}$	$a_1 a_2 \varpi_{2,12}$			
				$a_2 \varpi_{2,2}$	$a_2 \varpi_{4,2}$	$a_1 \varpi_{3,1}$	$a_1 \varpi_{4,1}$			
				$a_1 a_2 \varpi_{2,12}$	$a_1 a_2 \varpi_{4,12}$	$a_1 a_2 \varpi_{3,12}$	$a_1 a_2 \varpi_{4,12}$			
(2) FLEXURE	$\frac{I_1^*}{a_1^2}$	$\frac{I_2^*}{a_2 \gamma^2 a_1}$	$\frac{D}{2}\frac{1}{\hat{a}_1 a_1}\bar{Y}^T Q_o(b^*, b_\lambda, 1)\bar{Y}$	ϖ_1	ϖ_3	ϖ_1	ϖ_2	$\frac{I_1^*}{a_1^3}$	$\frac{I_2^*}{a_2 \gamma^2 a_1^2}$	$\frac{D}{2}\frac{1}{\hat{a}_1^2}\bar{Y}^T Q_o(b^*, b_\lambda, a_\lambda)\bar{Y}$
				$a_1 \varpi_{1,1}$	$a_1 \varpi_{3,1}$	$a_2 \varpi_{2,1}$	$a_2 \varpi_{2,2}$			
				ϖ_2	ϖ_4	ϖ_3	ϖ_4			
				$a_1 \varpi_{2,1}$	$a_1 \varpi_{4,1}$	$a_2 \varpi_{3,2}$	$a_2 \varpi_{4,2}$			
(4) GEOMETRIC.	$\frac{S_1^*}{a_1}$	$\frac{S_2^*}{a_2 \gamma}$	$\frac{1}{2\hat{a}_i}\bar{Y}^T Q_o(g^*, b_\lambda, 1)\bar{Y}$ where $g^* = \sum_{i=1}^{4} \hat{1}_i \lceil_i$	same as for flexure				$\frac{S_1^*}{a_1^2}$	$\frac{S_2^*}{\gamma a_1 a_1}$	$\frac{1}{2\hat{a}_1}\bar{Y}^T Q_o(g^*, b_\lambda, a_\lambda)\bar{Y}$ where $g^* = \hat{1}_1 \lceil_1 + \hat{1}_3 \lceil_3 + a_\lambda(\hat{1}_2 \lceil_2 + \hat{1}_4 \lceil_4)$

* for variable mesh $\bar{Y}$ and $\hat{1}$ of the uniform mesh case are modified by changing a_λ to $\hat{a}_\lambda$

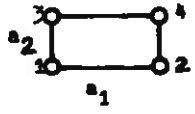

$U_1 = V$ subindex i of V_i, V_i^* or ϖ_i indicates displacement corresponding to corner i

$U_2 = V^*$

TABLE 3.1 Energy Contribution of stiffeners.

Work of external edge loads.

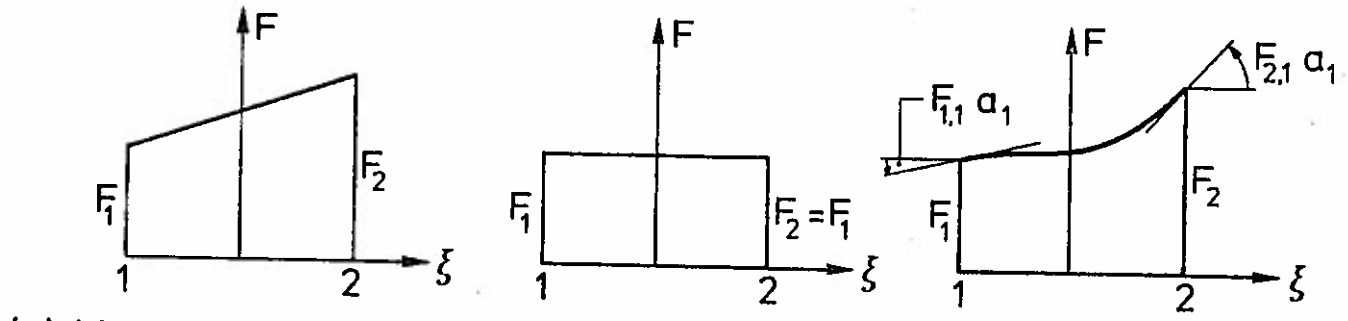

(a) Linear edge load (b) Constant edge load (c) Spline edge load

Fig. 3.3 Some types of loads on the edge 1 to 2 of a rectangular plate

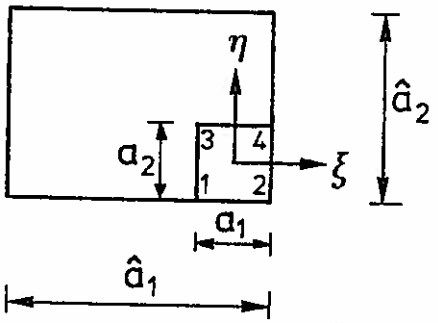

Consider a subdomain near to a boundary of a plate, for example that shown in Fig. 3.3 To simplify matters, let the prescribed external load acting on the contour of the subdomain be denoted by

$$F^{*1}_{(n)} = \bar{F} \tag{3.69}$$

$$F^{*2}_{(n)} = \bar{F}^{*}$$

and F_i (or F^{*}_i) represent the values of $\bar{F}$ (or $\bar{F}^{*}$) at the nodes $i = 1,2,3,4$.

A linear load applied on the side 1 to 2 in Fig. 3.3(a) is expressed by

$$\bar{F} = \left[\tfrac{1}{2} - \xi \;\middle|\; \tfrac{1}{2} + \xi\right] \begin{Bmatrix} F_1 \\ F_2 \end{Bmatrix} \tag{3.70}$$

The contribution of the subdomain in Fig. 3.3 to the contour integral in (3.1) is

$$\int_{-\frac{a_1}{2}}^{\frac{a_1}{2}} \bar{F}\, U_1 \Big|_{\eta=-\frac{1}{2}} dX_1 = \underset{\sim}{1}^{\wedge T} a_1 \int_{-\frac{1}{2}}^{\frac{1}{2}} F \underset{\sim}{X}\, d\xi \tag{3.71}$$

where (3.52) has been used for $U_1 = V$.

The result of introducing (3.53) and (3.70) into (3.71) is

$$\int_{-\frac{1}{2}}^{\frac{1}{2}} \underset{\sim}{\chi}\, \bar{F}\, d\xi = \frac{1}{10} \begin{bmatrix} 3 & 2 \\ 11/24 & 9/24 \\ 2 & 3 \\ -9/24 & -11/24 \end{bmatrix} \begin{Bmatrix} F_1 \\ F_2 \end{Bmatrix} \tag{3.72}$$

For a constant load as in Fig. 3.3(b), the sum of the two columns in the matrix of (3.72) gives

$$\int_{-\frac{1}{2}}^{\frac{1}{2}} \underset{\sim}{\chi}\, d\xi = \begin{Bmatrix} 1/2 \\ 1/12 \\ 1/2 \\ -1/12 \end{Bmatrix} \tag{3.73}$$

For loads distributed according to spline functions

$$\bar{F} = \underset{\sim}{\chi}^T \begin{bmatrix} F_1 & F_{1,1} a_1 & F_2 & F_{2,1} a_1 \end{bmatrix}^T \tag{3.74}$$

the integral in (3.71) becomes

$$\int_{-\frac{1}{2}}^{\frac{1}{2}} \underset{\sim}{\chi}\, \bar{F} d\xi = \int_{-\frac{1}{2}}^{\frac{1}{2}} \underset{\sim}{\chi}\, \underset{\sim}{\chi}^T d\xi \begin{Bmatrix} F_1 \\ F_{1,1}\ a_1 \\ F_2 \\ F_{2,1}\ a_1 \end{Bmatrix} \tag{3.75}$$

where

$$\int_{-\frac{1}{2}}^{\frac{1}{2}} \underset{\sim}{\chi}\,\underset{\sim}{\chi}^{T}\, d\xi = \frac{1}{420}\begin{bmatrix} 156 & 22 & 54 & -13 \\ 22 & 4 & 13 & -3 \\ 54 & 13 & 156 & -22 \\ -13 & -3 & -22 & 4 \end{bmatrix} \qquad (3.76)$$

Eq. (3.75) contains as particular cases the linear and constant load distributions, given respectively by (3.72) and (3.73).

From the definitions of $\hat{\underset{\sim}{l}}$ in (3.54) and $\hat{\underset{\sim}{h}}^{*}_{1}$ in (3.17)

$$\hat{\underset{\sim}{l}} = [\hat{h}^{*}_{\alpha 1} \quad \hat{h}^{*}_{\alpha 2} \quad \hat{h}^{*}_{\alpha 5} \quad \hat{h}^{*}_{\alpha 6}]^{T} \quad \text{with } \alpha=1$$

In the abscence of distributed loads ($P^{\alpha} = 0$) the last expression together with (3.31) validate

$$\begin{Bmatrix} \hat{f}^{*}_{\alpha 1} \\ \hat{f}^{*}_{\alpha 2} \\ \hat{f}^{*}_{\alpha 5} \\ \hat{f}^{*}_{\alpha 6} \end{Bmatrix} = \int_{-\frac{a_1}{2}}^{\frac{a_1}{2}} \bar{F}\, U_1 \Big|_{\eta=-\frac{1}{2}} dX_1 \qquad \text{with } \alpha = 1$$

and the remaining components of $\hat{\underset{\sim}{f}}^{*}_{1}$ are zero. This example illustrates how (3.62) can be computed.

In completely analogous manner the loads $\bar{F}^{*}$ of (3.69) can be distributed according to linear, constant or spline functions. The formulae obtained are (3.72), (3.73) and (3.75) with asterisks over F_i and $F_{i,1}$ $(i=1,2)$.

For loads prescribed over the transversal edges of the subdomain in Fig. 3.3, (3.71) may be written

$$\int_{-\frac{a_2}{2}}^{\frac{a_2}{2}} \bar{F}\, U_2 \Big|_{\xi=\frac{1}{2}} dX_2 = \hat{\underset{\sim}{l}}^{*T} a_2 \int_{-\frac{1}{2}}^{\frac{1}{2}} \bar{F}\, \chi^{*}\, d\eta \qquad (3.77)$$

where for the edge 2 to 4

$$\underset{\sim}{\chi}^{*} = [2\eta^3 - \tfrac{3}{2}\eta + \tfrac{1}{2} \;\vdots\; \eta^3 - \tfrac{\eta^2}{2} - \tfrac{\eta}{4} + \tfrac{1}{8} \;\vdots\; -2\eta + \tfrac{3}{2}\eta + \tfrac{1}{2} \;\vdots\; \eta^3 + \tfrac{\eta^2}{2} - \tfrac{\eta}{4} - \tfrac{1}{8}]^{T} \tag{3.78}$$

$$\underset{\sim}{\hat{1}}^{*} = [V_2 \quad a_2 V_{2,2} \quad V_4 \quad a_2 V_{4,2}]^{T}$$

Since χ^{*} has the same form as χ, it is possible to write down directly the following equations

$$\bar{F} = [\tfrac{1}{2} - \eta \;\vdots\; \tfrac{1}{2} + \eta] \begin{Bmatrix} F_2 \\ F_4 \end{Bmatrix} \tag{3.79}$$

$$\int_{-\frac{1}{2}}^{\frac{1}{2}} \underset{\sim}{\chi}^{*} \bar{F}\, d\eta = \frac{1}{10} \begin{bmatrix} 3 & 2 \\ 11/24 & 9/24 \\ 2 & 3 \\ -9/24 & -11/24 \end{bmatrix} \begin{Bmatrix} F_2 \\ F_4 \end{Bmatrix}$$

$$\int_{-\frac{1}{2}}^{\frac{1}{2}} \underset{\sim}{\chi}^{*}\, d\eta = [\tfrac{1}{2} \quad \tfrac{1}{12} \quad \tfrac{1}{2} \quad -\tfrac{1}{12}]^{T}$$

and

$$\bar{F} = \underset{\sim}{\chi}^{*T} [F_2 \quad F_{2,2}a_2 \quad F_4 \quad F_{4,2}a_2]^{T} \tag{3.80}$$

$$\int_{-\frac{1}{2}}^{\frac{1}{2}} \underset{\sim}{\chi}^{*} \bar{F}\, d\eta = \int_{-\frac{1}{2}}^{\frac{1}{2}} \underset{\sim}{\chi}^{*}\, \underset{\sim}{\chi}^{*T} d\eta \, [F_2 \quad F_{2,2}a_2 \quad F_4 \quad F_{4,2}a_2]^{T}$$

$$\int_{-\frac{1}{2}}^{\frac{1}{2}} \underset{\sim}{\chi}^{*}\, \underset{\sim}{\chi}^{*T}\, d\eta = \int_{-\frac{1}{2}}^{\frac{1}{2}} \underset{\sim}{\chi}\, \underset{\sim}{\chi}^{T} d\xi$$

The expressions derived for linear or spline distributions are useful since very often the actual distribution of edge loads can be represented accurately by such functions. Finally, for concentrated loads the computations are simpler. For example a concentrated load with components $(F_2, F_{2^*}^{*})$ placed at node 2 of Fig. 3.3 gives $F_2 \hat{1}_1 a_1$ for (3.71) and $F_2^{*} \hat{1}_1^{*} a_2$ for (3.77).

3.4 Discretization of Energy Integrals for a Plate

It has been already described how integrals of the form (3.1) and (3.3) can be calculated restricting the integration to a typical subdomain and to a typical stiffener. The sum of the energy integrals of the subdomains and stiffeners included in the plate, as shown here, can be performed by various matrix operations.

The plate of Fig. 3.1(c) is loaded on the boundary C_1 and eventually reinforced with stiffeners on C. Ritz-Subdomain bicubic trial solutions for U_α and w include the parameters

$$[U_1 \mid U_{1,1}a_1 \mid U_{1,2}a_2 \mid U_{1,12}a_1a_2 \mid U_2 \mid U_{2,1}a_1 \mid U_{2,2}a_2 \mid U_{2,12}a_1a_2] \quad (3.81)$$

and

$$[w \quad w_{,1}a_1 \quad w_{,2}a_2 \quad w_{,12}a_1a_2]$$

at each node of the plate.

Plates with stiffeners located inside of their boundary C deserve special attention. Consider that the plates of Fig. 3.4 and Fig. 3.5 include stiffeners of cross sectional area S^* which carry axial forces

$$\tau_\lambda = S^* U_{\lambda,\lambda} \qquad \text{(no summation)} \qquad (3.82)$$

From Fig. 3.4(a)

$$T_{12}^- = T_{12}^+ + S^* U_{2,22} \qquad (3.83)$$

Since the displacements U_α are continuous along the stiffener (X_2 = const,) $U_{2,22}$ is continuous and

$$U_{1,2}^- = U_{1,2}^+ = U_{1,2}$$

The last equality introduced into $(3.5)_3$ and (3.83) gives

$$U_{2,1}^- = U_{2,1}^+ + \frac{2(1+\nu)}{Eh} S^* U_{2,22} \qquad (3.84)$$

i.e. $U_{2,1}$ is discontinuous along the stiffener.

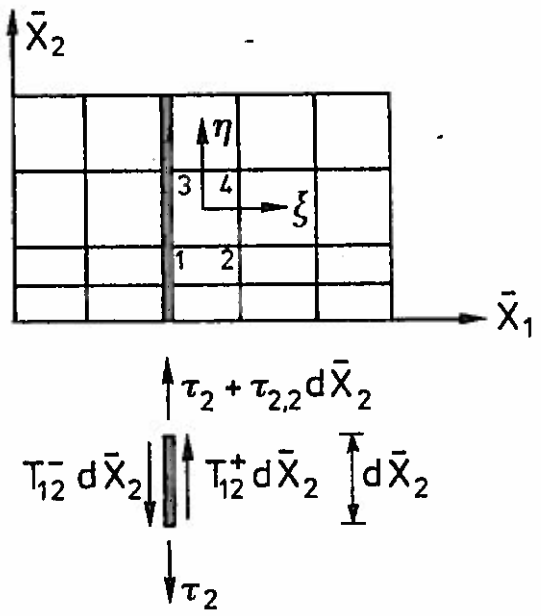

(a) Transversal stiffener

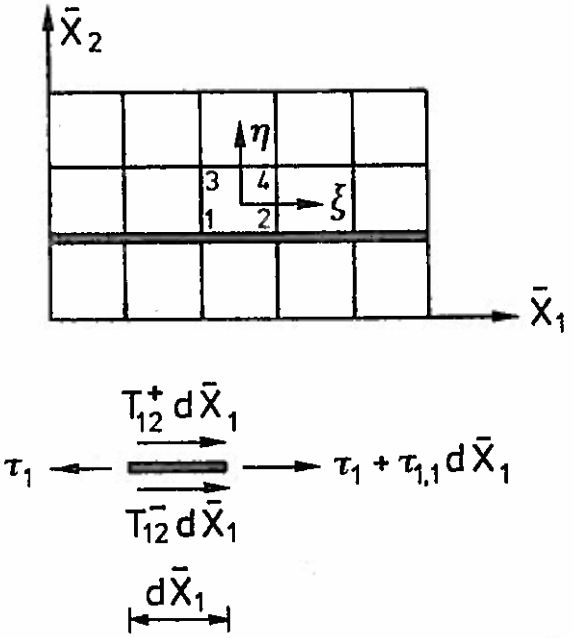

(a) Longitudinal stiffener

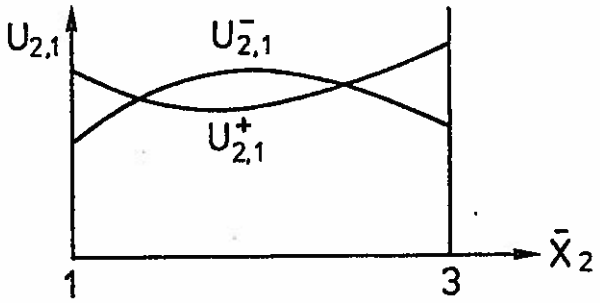

(b) $U_{2,1}$ discontinuous along the transversal stiffener

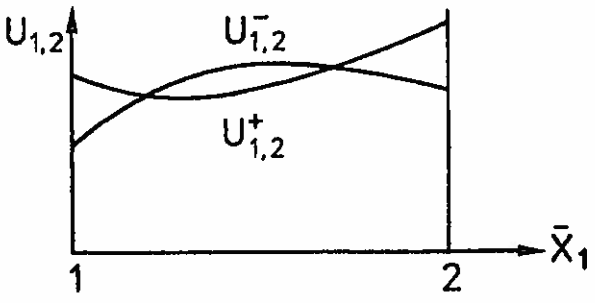

(b) $U_{1,2}$ discontinuous along the longitudinal stiffener

Fig. 3.4. Plate with transversal stiffener

Fig. 3.5. Plate with longitudinal stiffener

As shown in Fig. 3.4(b), the derivative $(U_{2,1})_{,2}$ need not be the same on both sides of the stiffener. From $(3.52)_3$ (replacing w for U_2 and η by ξ) it is observed that, for a particular η, $U_{2,1}$ in the segment between the nodes 1 and 3 of Fig. 3.4(a) depends only on the values of $U_{2,1}$ and $U_{2,12}$ at the ends of the segment. Thus, the condition (3.84) can be approximated in a

Ritz-subdomain bicubic analysis by using 10 local parameters

$$[U_1 \mid U_{1,1}{}^{a_1} \mid U_{1,2}{}^{a_2} \mid U_{1,12}{}^{a_1 a_2} \mid U_2 \mid U^-_{2,1}{}^{a_1} \mid U_{2,2}{}^{a_2} \mid U^-_{2,12}{}^{a_1 a_2} \mid$$
$$U^+_{2,1}{}^{a_1} \mid U^+_{2,12}{}^{a_1 a_2}] \qquad (3.86)$$

at each node located on the stiffener. The parameters at the remaining nodes are 8 and are given by (3.81).

Following similar development, from Fig. 3.5(a)

$$T^-_{12} = T^+_{12} + S^* U_{1,11} \qquad (3.87)$$

Since U_α are continuous along the stiffener (X_1 = const.) $U_{1,11}$ is continuous and

$$U^-_{2,1} = U^+_{2,1} = U_{2,1}$$

The last condition in $(3.5)_3$ transforms (3.87) to

$$U^-_{1,2} = U^+_{1,2} + \frac{2(1+\nu)S^*}{Eh} U_{1,11} \qquad (3.88)$$

Fig. 3.5(b) show the discontinuous $U_{1,2}$ and $U_{1,12}$ along the stiffeners. From $(3.56)_2$ it is deduced that $U_{1,2}$ depends on the coordinate $\bar{X}_1$ and the values of $U_{1,2}$ and $U_{1,12}$ at the nodes located along the stiffener. Thus along the stiffener, the vector of 10 components

$$[U_1 \mid U_{1,1}{}^{a_1} \mid U^-_{1,2}{}^{a_2} \mid U^-_{1,12}{}^{a_1 a_2} \mid U_2 \mid U_{2,1}{}^{a_1} \mid U_{2,2}{}^{a_2} \mid U_{2,12}{}^{a_1 a_2} \mid$$
$$U^+_{1,2}{}^{a_2} \mid U^+_{1,12}{}^{a_1 a_2}] \qquad (3.89)$$

replaces the vector (3.81).

Since the number of parameters per node has been determined, it is possible to define global vectors which include the parameters of all the nodes of the plate. Thus, the global vec-

tor $\hat{\underset{\sim}{q}}^*$ includes all the parameters involving U_α, $U_{\alpha,\beta}$ and $U_{\alpha,12}$ at the nodes. The global vector $\underset{\sim}{q}$ includes all the parameters involving ω, $\omega_{,\alpha}$ and $\omega_{,12}$ at the nodes. As started here, in the remaining of this chapter circumflex accents will be placed above vectors and matrices which belong more properly to the plane stress analysis.

Plane stress energy integrals (entire plate)

The vectors $\hat{\underset{\sim}{h}}^*_\alpha$ in (3.16) and (3.15) have been used for uniform mesh cases as in Fig. 3.1(c). However, for variable mesh cases as in Fig. 3.1(d) it is more convenient to use the following vectors

$$\hat{\underset{\sim}{v}}_i=[V_i \quad V_{i,1}\hat{a}_1 \quad V_{i,2}\hat{a}_2 \quad V_{i,12}\hat{a}_1\hat{a}_2] \tag{3.90}$$

$$\hat{\underset{\sim}{v}}^*_i=[V^*_i \quad V^*_{i,1}\hat{a}_1 \quad V^*_{i,2}\hat{a}_2 \quad V^*_{i,12}\hat{a}_1\hat{a}_2]$$

$$\hat{\underset{\sim}{h}}^{**}_1=[\hat{\underset{\sim}{v}}_1 \quad \hat{\underset{\sim}{v}}_2 \quad \hat{\underset{\sim}{v}}_3 \quad \hat{\underset{\sim}{v}}_4]^T$$

$$\hat{\underset{\sim}{h}}^{**}_2=[\hat{\underset{\sim}{v}}^*_1 \quad \hat{\underset{\sim}{v}}^*_2 \quad \hat{\underset{\sim}{v}}^*_3 \quad \hat{\underset{\sim}{v}}^*_4]^T$$

$(V_i;\ V^*_i)$ denoting the displacements $(U_1;\ U_2)$ at the corners $i= 1,2,3,4$ of Fig. 3.2(c).

Let

$$\left.\begin{aligned} r^*_i &= 1 \\ r^*_{i+1} &= \alpha_1 \\ r^*_{i+2} &= \alpha_2 \\ r^*_{i+3} &= \alpha_1\alpha_2 \end{aligned}\right\} \quad i=1,5,9,13 \tag{3.91}$$

$$r^*_{i+16}= r^*_i \quad ;\ i=1,\cdots,16$$

where the α_λ are given by $(3.22)_2$.

Using the diagonal matrix

$$\underset{\sim}{T} = \begin{bmatrix} r_1^* & & & \\ & r_2^* & & \\ & & \ddots & \\ & & & r_{16}^* \end{bmatrix} \tag{3.92}$$

the relationship between $\hat{\underset{\sim}{h}}_{\alpha}^{*}$ of (3.16) and $\hat{\underset{\sim}{h}}_{\alpha}^{**}$ of (3.90) becomes

$$\hat{\underset{\sim}{h}}_{\alpha}^{*} = \underset{\sim}{T}\, \hat{\underset{\sim}{h}}_{\alpha}^{**} \tag{3.93}$$

or in another form

$$\begin{Bmatrix} \hat{\underset{\sim}{h}}_1^{*} \\ \hat{\underset{\sim}{h}}_2^{*} \end{Bmatrix} = \hat{\underset{\sim}{T}} \begin{Bmatrix} \hat{\underset{\sim}{h}}_1^{**} \\ \hat{\underset{\sim}{h}}_2^{**} \end{Bmatrix} \tag{3.94}$$

where $\hat{\underset{\sim}{T}}$ is a dianonal matrix

$$\hat{\underset{\sim}{T}} = \begin{bmatrix} r_1^* & & & \\ & r_2^* & & \\ & & \ddots & \\ & & & r_{32}^* \end{bmatrix} \tag{3.95}$$

The local parameters belonging to a subdomain can be found in the global vector $\hat{\underset{\sim}{q}}^{*}$ and thus

$$\begin{Bmatrix} \hat{\underset{\sim}{h}}_1^{*} \\ \hat{\underset{\sim}{h}}_2^{*} \end{Bmatrix} = \hat{\underset{\sim}{R}}\, \hat{\underset{\sim}{q}}^{*} \quad \text{(uniform mesh)} \tag{3.96}$$

$$\begin{Bmatrix} \hat{\underset{\sim}{h}}_1^{**} \\ \hat{\underset{\sim}{h}}_2^{**} \end{Bmatrix} = \hat{\underset{\sim}{R}}\, \hat{\underset{\sim}{q}}^{*} \quad \text{(variable mesh)}$$

(the meaning of $\hat{\underset{\sim}{q}}^*$ is slightly different for uniform and variable mesh).

For a segment of stiffener the same type of relationship (3.96) exists. For example, for a segment between nodes 1 a 2 of the subdomain in Fig. 3.1(b)

$$\hat{\underset{\sim}{l}} = \hat{\underset{\sim}{R}}_1 \hat{\underset{\sim}{q}}^* \qquad \text{(uniform mesh)} \tag{3.97}$$

$$\hat{\underset{\sim}{l}}_o = \hat{\underset{\sim}{R}}_1 \hat{\underset{\sim}{q}}^* \qquad \text{(variable mesh)}$$

in accordance to $(3.54)_1$ and $(3.63)_1$.

Defining the matrices

$$\hat{\underset{\sim}{k}} = \hat{\underset{\sim}{k}}^* \qquad \text{(uniform mesh)} \tag{3.98}$$

$$\hat{\underset{\sim}{k}} = \hat{\underset{\sim}{T}}^T \hat{\underset{\sim}{k}}^* \hat{\underset{\sim}{T}} = [\hat{k}^*_{ij}\ r^*_i r^*_j] \qquad \text{(variable mesh)}$$

$$\hat{\underset{\sim}{f}} = \begin{Bmatrix} \hat{\underset{\sim}{f}}^*_1 \\ \hat{\underset{\sim}{f}}^*_2 \end{Bmatrix} \qquad \text{(uniform mesh)}$$

$$\hat{\underset{\sim}{f}} = \hat{\underset{\sim}{T}} \begin{Bmatrix} \hat{\underset{\sim}{f}}^*_1 \\ \hat{\underset{\sim}{f}}^*_2 \end{Bmatrix} \qquad \text{(variable mesh)}$$

the expressions of virtual work for a subdomain with a longitudinal stiffener segment become

$$\delta\hat{\Delta\pi}_o = \frac{Eh}{1-\nu^2}\, \delta\hat{\underset{\sim}{q}}^{*T} \hat{\underset{\sim}{R}}^T \hat{\underset{\sim}{k}} \hat{\underset{\sim}{R}} \hat{\underset{\sim}{q}}^* \tag{3.99}$$

$$\delta\hat{\pi}_{(1)1} = \frac{Eh}{1-\nu^2}\, \delta\hat{\underset{\sim}{q}}^{*T} \hat{\underset{\sim}{R}}_1^T \underset{\sim}{Q}_o\,(t^*;\ b_1;\ \beta_1)\, \hat{\underset{\sim}{R}}_1 \hat{\underset{\sim}{q}}^*$$

where $(3.96)_2$, $(3.97)_2$, (3.31) have been used. The arguments

b_1 amd β_1 take the values given in Table 3.1.

Introducing (3.98) into (3.32)

external virtual work for the subdomain = $\delta\underset{\sim}{q}^{*T}\underset{\sim}{\hat{f}}$ $\qquad (3.99)_3$

The total sums of quantities of the type (3.99) yield

$$\delta\hat{\pi}_o^* = \sum_{\Delta\Omega} \delta\Delta\hat{\pi}_o + \sum_{long} \delta\hat{\pi}_{(1)1} + \sum_{tran} \delta\hat{\pi}_{(1)2} = \frac{Eh}{1-\nu^2}\, \delta\underset{\sim}{\hat{q}}^{*T}\underset{\sim}{\hat{K}}\,\underset{\sim}{\hat{q}}^{*}$$

$$\delta\hat{\pi}_o^* = \sum_{\Delta\Omega} \delta\underset{\sim}{\hat{q}}^{*T}\,\underset{\sim}{\hat{f}} = \delta\underset{\sim}{\hat{q}}^{*T}\underset{\sim}{\hat{F}} \qquad (3.100)$$

where the symbols $\sum_{\Delta\Omega}$, $\sum_{long}$ and $\sum_{tran}$ denote total sums of strain energy for, respectively, the subdomains, the longitudinal stiffeners and the transversal stiffeners. In addition, the notation

$$\underset{\sim}{\hat{K}} = \sum_{\Delta\Omega} \underset{\sim}{\hat{R}}^T\,\underset{\sim}{\hat{k}}\,\underset{\sim}{\hat{R}} + \sum_{long} \underset{\sim}{\hat{R}}_1^T\,\underset{\sim}{Q}_o(t^*;\, b_1;\, \beta_1)\,\underset{\sim}{\hat{R}}_1 + \sum_{tran} \underset{\sim}{R}_2^T\,\underset{\sim}{Q}_o(\underset{\sim}{t}^*; b_2; \beta_2)\,\underset{\sim}{R}_2$$

$$\underset{\sim}{\hat{F}} = \sum_{\Delta\Omega} \underset{\sim}{\hat{R}}^T\,\underset{\sim}{\hat{f}} \qquad (3.101)$$

has been introduced. The arguments b_α and β_α take the values given in Table 3.1. b_α may be different for flexural, torsional or geometric contribution of virtual work. $\beta_\lambda = \alpha_\lambda$ for variable mesh cases and $\beta_\lambda = 1$ for uniform mesh cases.

From (3.101)

$$\frac{Eh}{1-\nu^2}\, \delta\underset{\sim}{\hat{q}}^{*T}\,\underset{\sim}{\hat{K}}\,\underset{\sim}{\hat{q}}^{*} = \delta\underset{\sim}{q}^{*T}\,\underset{\sim}{\hat{F}} \qquad (3.102)$$

which implies

$$\underset{\sim}{\hat{K}}\,\underset{\sim}{\hat{q}} = \underset{\sim}{\hat{F}} \qquad (3.103)$$

$$\hat{\underset{\sim}{q}} = \frac{Eh}{1-\nu^2}\,\hat{\underset{\sim}{q}}^* \tag{3.104}$$

The solution vector $\hat{\underset{\sim}{q}}$ contains the vectors $\hat{\underset{\sim}{h}}_\alpha$ defined by (3.45) which are needed for computing the geometric subdomain matrix $\hat{\underset{\sim}{s}}^*$ of (3.47). Since $\hat{\underset{\sim}{K}}$ is a symmetric band matrix, Choleski's method for band matrices can be used for solving (3.103). In this way, only half of the band of the matrix $\hat{\underset{\sim}{K}}$ needs to be stored in an electronic computer when the solution to (3.103) is to be carried out.

Eigenvalue problem integrals (entire plate).

Following a parallel development to previous plane stress analysis, the parameters corresponding to a subdomain in Fig. 3.1(d) are defined as

$$\bar{\underset{\sim}{w}}_i = [w_i \quad w_{i,1}\hat{a}_1 \quad w_{i,2}\hat{a}_2 \quad w_{i,12}\hat{a}_1\hat{a}_2] \tag{3.105}$$

$$\underset{\sim}{Z}^T = [\bar{\underset{\sim}{w}}_1 \quad \bar{\underset{\sim}{w}}_2 \quad \bar{\underset{\sim}{w}}_3 \quad \bar{\underset{\sim}{w}}_4]$$

The connection between $\underset{\sim}{Z}$ and the vector $\underset{\sim}{Z}^*$ of (3.34) is

$$\underset{\sim}{Z}^* = \bar{\underset{\sim}{T}}\,\underset{\sim}{Z} \tag{3.106}$$

with $\bar{\underset{\sim}{T}}$ given by (3.92).

The global parameters $\underset{\sim}{q}$ and the local parameters belonging either to a subdomain or to a longitudinal stiffener are related by

$$\underset{\sim}{Z}^* = \underset{\sim}{R}\,\underset{\sim}{q} \tag{3.107}$$

$$\bar{\underset{\sim}{Y}} = \underset{\sim}{R}_1\,\underset{\sim}{q}$$

$$\bar{\underset{\sim}{Y}}^* = \underset{\sim}{R}_1^*\,\underset{\sim}{q}$$

where the vectors $\underset{\sim}{\bar{Y}}$ and $\underset{\sim}{\bar{Y}}^*$ are given by (3.54). Similar relationships exist between $\underset{\sim}{q}$ and the local parameters involved in any of the expressions $(3.68)_2$, $(3.68)_3$ and $(3.68)_4$.

Defining

$$\underset{\sim}{k} = \underset{\sim}{k}^* \qquad \text{(uniform mesh)} \qquad (3.108)$$

$$\underset{\sim}{k} = \underset{\sim}{\bar{T}}^T \underset{\sim}{k}^* \underset{\sim}{\bar{T}} = [k^*_{ij} r^*_i r^*_j] \qquad \text{(variable mesh)}$$

$$\underset{\sim}{s} = \underset{\sim}{s}^* \qquad \text{(uniform mesh)}$$

$$s = \underset{\sim}{\bar{T}}^T \underset{\sim}{s} \underset{\sim}{\bar{T}} = [s^*_{ij} r^*_i r^*_j] \qquad \text{(variable mesh)}$$

the expressions (3.39) and (3.42) become

$$\delta \Delta\pi_o = \frac{D}{\underset{a_1}{\Lambda^2}} \delta \underset{\sim}{q}^T \underset{\sim}{R}^T \underset{\sim}{k} \underset{\sim}{R} \underset{\sim}{q} \qquad (3.109)$$

$$\iint_{\Delta\Omega} T_{\gamma\alpha}\, \omega_{,\gamma}\, \delta\omega_{,\alpha}\, d\Omega = \frac{1}{\underset{a_1}{\Lambda}} \delta \underset{\sim}{q}^T \underset{\sim}{R}^T \underset{\sim}{s} \underset{\sim}{R} \underset{\sim}{q}$$

Introducing (3.107) (or similar relationships between local and global parameters) into (3.109), $(3.68)_2$, $(3.68)_3$ and $(3.68)_4$, the total internal virtual work $\delta\pi^*_o$ for the stiffened plate is obtained. Taking into account that $\delta\pi^*_o$ is also equal to the total geometric virtual work, the following formulas are deduced

$$\delta\pi^*_o = \sum_{\Delta\Omega} \delta\Delta\pi_o + \sum_{long} (\delta\pi_{(2)1} + \delta\pi_{(3)1}) + \sum_{tran} (\delta\pi_{(2)2} + \delta\pi_{(3)2}) \qquad (3.110)$$

$$= \frac{D}{\underset{a_1}{\Lambda^2}} \delta \underset{\sim}{q}^T \underset{\sim}{K} \underset{\sim}{q} \qquad \text{(variable mesh)}$$

$$= \frac{D}{\underset{a_1 a_1}{\Lambda^2}} \delta \underset{\sim}{q}^T \underset{\sim}{K} \underset{\sim}{q} \qquad \text{(uniform mesh)}$$

$$\delta\pi_o^* = -P\left(\sum_{\Delta\Omega}\iint_{\Delta\Omega} T_{\gamma\alpha}\,\omega,_\gamma \delta\omega,_\alpha d\Omega + \sum_{long}\delta\pi_{(4)1} + \sum_{tran}\delta\pi_{(4)2}\right)$$

$$= -P\frac{1}{\hat{a}_1}\,\delta q^T \underset{\sim}{S}\, q \qquad \text{(variable mesh)} \tag{3.111}$$

$$= -P\frac{1}{a_1}\,\delta\, q^T \underset{\sim}{S}\, q \qquad \text{(uniform mesh)}$$

where

$$\underset{\sim}{K} = \sum_{\Delta\Omega} R^T k\, R + \sum_{long}\left[R_1^T Q_o\,(b^*, b_1, \beta_1)R_1^* + R_1^T Q_o(t^*, b_1, \beta_1)R^*\right] +$$

$$+ \sum_{tran}\left[R_2^T Q_o(b^*, b_2, \beta_2)R_2 + R_2^{*T} Q_o(t^*, b_2, \beta_2)R_2\right] \tag{3.112}$$

$$\underset{\sim}{S} = \sum_{\Delta\Omega} R^T s\, R + \sum_{long} R_1^T Q_o(q^*, b_1, \beta_1)R_1 + \sum_{tran} R_2^T Q_o(g^*, b_2, \beta_2)R_2$$

(note that b_λ and β_λ take the values given in Table 3.1)

From (3.111) and (3.112)

$$\lambda_o \underset{\sim}{K}\, q = \underset{\sim}{S}\, q \tag{3.113}$$

$$\lambda_o = -\frac{D}{P\hat{a}_1} \tag{3.114}$$

which constitutes a linear eigenvalue problem between two matrices.

3.5 Construction of Global Matrices by Electronic Computers.

An attempt will now be made to explain how an electronic computer can calculate the matrices $\hat{\underset{\sim}{K}}$, $\underset{\sim}{K}$ and $\underset{\sim}{S}$ given by (3.101) and (3.112).

The sum indicated by (3.101), can be performed, using electronic computers, by first establishing the zero matrix

$$\hat{\underset{\sim}{K}} = \underset{\sim}{0}$$

Subsequently each subdomain matrix $\hat{\underset{\sim}{k}}$ is partitioned and its parts are properly stored in the matrix $\hat{\underset{\sim}{K}}$ as shown in Fig. 3.6.

Let $\hat{L}_i^*$ be the order which V_i (see (3.14) and (3.15)) occupies in the global vector $\hat{\underset{\sim}{q}}^*$ for each of the corners i = 1,2,3,4 of a typical subdomain in Fig. 3.6. Consider a segment of the longitudinal stiffener of Fig. 3.6. The contribution

$$[Q_{oij}] = \underset{\sim}{Q}_o\,(\underset{\sim}{t}^*,\ b_1,\ 1)$$

of this segment to the half band of $\hat{\underset{\sim}{K}}$ (Fig. 3.6(d)) can be expressed by

$$\begin{aligned}
&j = 1,2,3,4 \\
&i = 1,\ldots,j \\
&k = \langle (i-1)/2 \rangle + 1 \\
&l = \langle (j-1)/2 \rangle + 1 \\
&m = \hat{L}_1^* - 1 + i - 2(k-1) \\
&n = \hat{L}_1^* + j - 2(l-1) - m \\
&\hat{K}_{mn} \rightarrow \hat{K}_{mn} + Q_{oij}
\end{aligned} \qquad (3.115)$$

where the real number included in $\langle \ldots \rangle$ is truncated to its maximum integer and the operation

$$\hat{K}_{mn} \rightarrow \hat{K}_{mn} + \ldots \qquad (3.116)$$

indicates that the variable to the right hand side is modified while its storage place in the electronic computer remains the same.

Similar schemes to (3.115) can be devised for storing the matrices $\underset{\sim}{Q}_o$ of $(3.101)_1$ in the matrix $\hat{\underset{\sim}{K}}$.

The case of plates with intermediate stiffeners (in the sense that they do not lie on the boundary) needs special consideration. In subdomains above the intermediate stiffener (Fig. 3.7(a)) instead of the local vector of parameters

$$\hat{\underset{\sim}{H}}^{*} = [\hat{\underset{\sim}{h}}_1^{*T} \quad \hat{\underset{\sim}{h}}_2^{*T}]^T \tag{3.117}$$

the following vector is used

$$\hat{\underset{\sim}{H}}^{**} = [(3.89)\text{node } 1;\ (3.89)\text{node } 2;\ (3.81)_1 \text{node } 3;\ (3.81)_1 \text{node} 4]^T \tag{3.118}$$

where the subdomains' nodes are shown in Fig. 3.2(c).

By using (3.118), the virtual work (3.29) becomes

$$\delta\hat{\Delta\pi}_o = \frac{Eh}{1-\nu^2}\, \delta\hat{\underset{\sim}{H}}^{**T}\, \hat{\underset{\sim}{k}}_o\, \hat{\underset{\sim}{H}}^{**} \tag{3.119}$$

$\hat{\underset{\sim}{k}}_o$ being a 36 x 36 matrix yet to be defined.

Since the components (notation (3.14))

$$[\hat{H}_3^{**} \quad \hat{H}_4^{**} \quad \hat{H}_{13}^{**} \quad \hat{H}_{14}^{**}] = [V_{1,2}^{-}a_2 \mid V_{1,12}^{-}a_1a_2 \mid V_{2,2}a_2 \mid V_{2,12}a_1a_2]$$

do not contribute to the virtual work (3.119) of the subdomain above the stiffener, the elements of $\hat{\underset{\sim}{k}}_o$ are

$$\hat{k}_{oij} = 0 \qquad i,j = 3,4,13,14 \tag{3.120}$$

In the same way for a subdomain to the right of a transversal stiffener as in Fig. 3.7(b), it is found that

$$\hat{\underset{\sim}{H}}^{**} = [(3.86)\text{node } 1;\ (3.81)_1 \text{ node } 2;\ (3.86)\text{node } 3;\ (3.81)\text{node } 4]^T$$

$$[\hat{H}^{**}_{6} \quad \hat{H}^{**}_{8} \quad \hat{H}^{**}_{24} \quad \hat{H}^{**}_{26}] = [V^{*-}_{1,1}a_1 \mid V^{*-}_{1,12}a_1a_2 \mid V^{*-}_{3,1}a_1 \mid V^{*-}_{3,12}a_1a_2] \tag{3.121}$$

$$k_{oij} = 0 \quad i,j=6,8,24,36$$

where the nodes are numbered as in Fig. 3.2(c) and the notation corresponds to (3.14).

The comparison between $\underset{\sim}{\hat{H}}^{**}$ and $\underset{\sim}{\hat{H}}^{*}$ of (3.117) yields

$$\hat{H}^{*}_{i} = \hat{H}^{**}_{1} \tag{3.122}$$

where $i = 1,\ldots,36$

$$1 = \hat{n}_{\alpha i} \tag{3.123}$$

$\alpha = 1$ for longitudinal intermediate stiffener

$\alpha = 2$ for transversal longitudinal stiffener

$\hat{H}^{**}_{o} = 0$ to satisfy conditions (3.120) or (3.121)

$$\underset{\sim}{\hat{n}}_1 = [1;\ 2;\ 0;\ 0;\ 17;\ 18;\ 19;\ 20;\ 3;\ 4;\ 5;\ 6;\ 0;\ 0;\ 21;$$
$$22;\ 23;\ 24;\ 7;\ 8;\ 9;\ 10;\ 11;\ 12;\ 25;\ 26;\ 27;\ 28;\ 13;$$
$$14;\ 15;\ 16;\ 29;\ 30;\ 31;\ 32]^{T}$$

$$\underset{\sim}{\hat{n}}_2 = [1;\ 2;\ 3;\ 4;\ 17;\ 0;\ 19;\ 0;\ 18;\ 20;\ 5;\ 6;\ 7;\ 8;\ 21;$$
$$22;\ 23;\ 24;\ 9;\ 10;\ 11;\ 12;\ 25;\ 0;\ 27;\ 0;\ 26;\ 28;\ 13;$$
$$14;\ 15;\ 16;\ 29;\ 30;\ 31;\ 32]^{T}$$

From the bilinear form (3.119) and (3.122) it is concluded that

$$i = 1,\ldots,36 \tag{3.124}$$

$$j = 1,\ldots,36$$

$$k = \hat{n}_{\alpha i}$$

$$1 = \hat{n}_{\alpha j}$$

$$kl = 0 \Rightarrow \hat{k}_{oij} = 0$$

$$kl \neq 0 \Rightarrow \hat{k}_{oij} = \hat{k}_{kl}$$

which constitutes the definition of $\hat{k}_o$ for a given α=1 or α=2.

Following Fig. 3.7, the upper half of the matrix $\hat{\underset{\sim}{k}}_o$ can be stored in the upper half band of the matrix $\hat{\underset{\sim}{K}}$ performing the operation

$$\hat{K}_{mn} \rightarrow \hat{K}_{mn} + \hat{k}_{oij} \qquad (3.125)$$

in Triangle 1

$$j = 1,\ldots,O_\alpha$$

$$i = 1,\ldots,j$$

$$m = \hat{L}_1^* + i - 1$$

$$n = j - i + 1$$

in Triangle 2

$$j = O_\alpha+1,\ldots,36$$

$$i = O_\alpha+1,\ldots,j$$

$$m = \hat{L}_3^* + i - O_\alpha$$

$$n = j - i + 1$$

in Rectangle 3

$$i = 1,\ldots,O_\alpha$$

$$j = O_\alpha+1,\ldots,36$$

$$m = \hat{L}_3^* + i - 1$$

$$n = \hat{L}_3^* + j - 1$$

where

$O_1 = 20$; $O_2 = 18$

α = 1 for longitudinal intermediate stiffeners

α = 2 for transversal intermediate stiffeners.

Using (3.124), the operation (3.125) can be written

$$k = n_{\alpha i} \qquad (3.126)$$

$$l = n_{\alpha j}$$

$$\text{if} \quad kl \neq 0 \quad \text{then} \quad \hat{K}_{mn} \rightarrow \hat{K}_{mn} + \hat{k}_{kl}$$

i.e. the matrix $\hat{\underset{\sim}{k}}_o$ need not be computed since $\hat{\underset{\sim}{k}}$ can be stored directly in $\hat{\underset{\sim}{K}}$.

The storage of the matrix $\underset{\sim}{k}$ in $\underset{\sim}{K}$ (or $\underset{\sim}{s}$ in $\underset{\sim}{S}$) of the eigenvalue problem can be accomplished by a partition of the matrix $\underset{\sim}{k}$ (or $\underset{\sim}{s}$) followed by a storage of the resulting submatrices in $\underset{\sim}{K}$ (or $\underset{\sim}{S}$). It can also be achieved in the following form

$$j = 1,\ldots,16 \qquad (3.127)$$

$$i = 1,\ldots,j$$

$$k = \langle (i-1)/4 \rangle + 1$$

$$l = \langle (j-1)/4 \rangle + 1$$

$$m = L^*_k - 1 + i - 4\,(k-1)$$

$$n = L^*_l + j - 4\,(l-1) - m$$

$$K_{mn} \rightarrow K_{mn} + k_{ij}$$

where L^*_k is the order which the parameter w_k of the node k (see (3.33)) occupies in the global vector $\underset{\sim}{q}$; k = 1,2,3,4.

The final representation of the matrices $\underset{\sim}{K}$ and $\underset{\sim}{S}$ is shown in Fig. 3.10. The numerical precedure adopted here (next section), justifies the use of the computer's storage pattern shown in Fig. 3.10. The matrix $\underset{\sim}{S}$ is expressed in terms of the matrices $\bar{\underset{\sim}{S}}^*$ and $\bar{\underset{\sim}{S}}^{**}$. The scheme (3.127) can be altered as follows

$$\text{if } i > 8; \text{ then } \bar{S}^*_{mn} \rightarrow \bar{S}^*_{mn} + s_{ij} \qquad (3.128)$$

otherwise

$$n = j - i$$

$$\bar{S}^{**}_{mn} \rightarrow \bar{S}^{**}_{mn} + s_{ij}$$

The plane stress distribution of the plate shown in Fig. 3.8 is considered to be similar in nature to (2.142). Since the integral (2.141) is made of integrals of the type $(3.68)_5$, the geometric virtual work (3.111) only involves nodal parameters defined along the line of action of the load. Consequently, if the nodes are numbered in the order shown, the matrix $\underset{\sim}{S}$ of $(3.112)_2$ only has nonzero elements in a small area. Imagining a stiffener placed along the line of action of the load P in Fig. 3.8 and considering a segment thereof, the expressions $(3.68)_5$ indicate that each $\underset{\sim}{Q}_o(\underset{\sim}{t}^*, \frac{1}{\alpha_\lambda}, \beta_\lambda)$ is stored in $\underset{\sim}{S}$ in exactly the same manner as the stiffener's flexural matrix $\underset{\sim}{Q}_o(\underset{\sim}{b}^*, b_\lambda, \beta_\lambda)$ is stored in $\underset{\sim}{K}$. Thus, the computation of S for the plane stress distribution (2.142) does not present new computational problems.

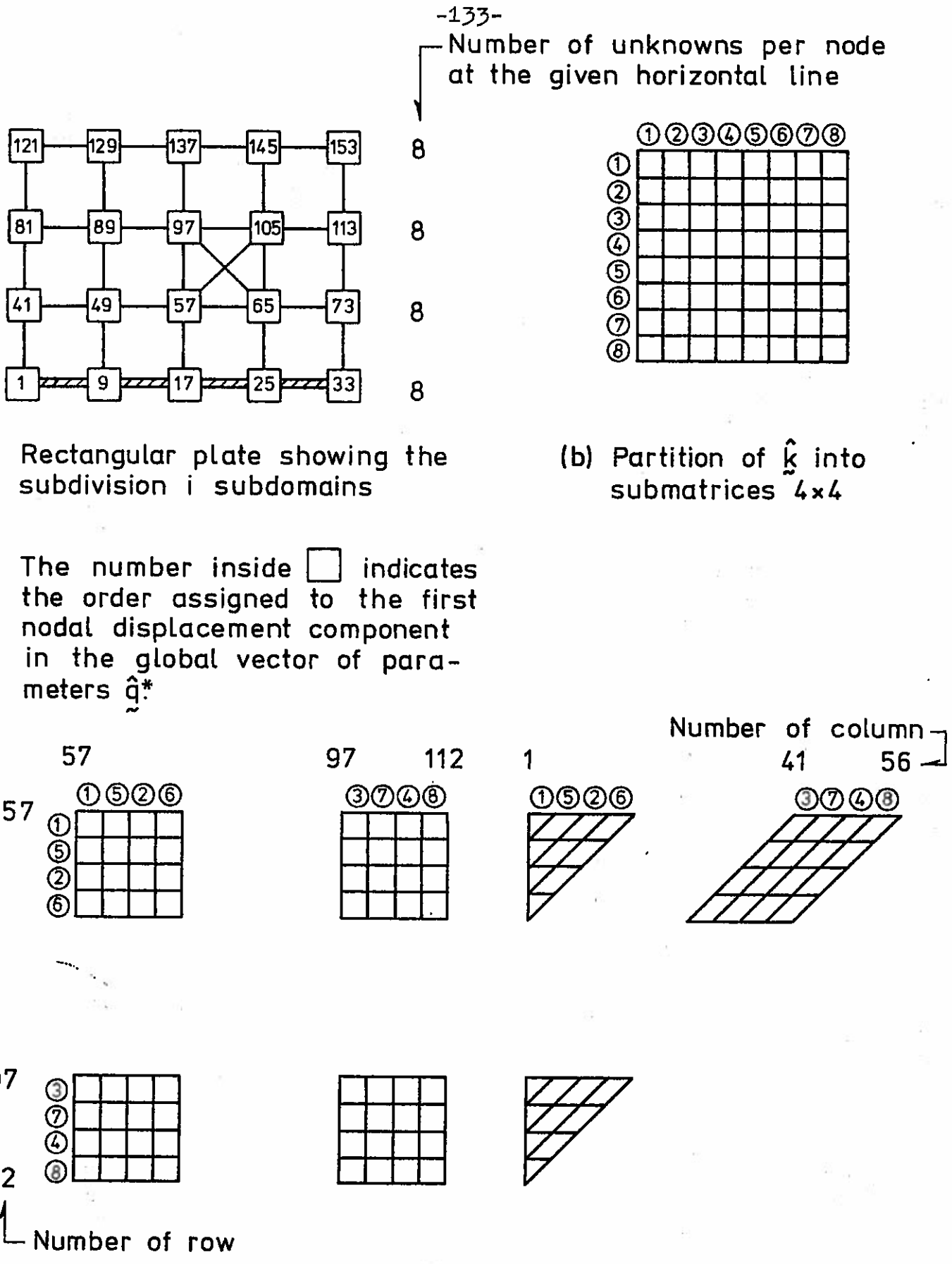

(a) Rectangular plate showing the subdivision i subdomains

(b) Partition of $\hat{\underset{\sim}{k}}$ into submatrices 4×4

(c) Global matrix $\hat{\underset{\sim}{K}}$. The storage of $\hat{\underset{\sim}{k}}$ into $\hat{\underset{\sim}{K}}$ is shown here for the subdomain marked with a cross

(d) Half-band storage of the symmetric matrix $\hat{\underset{\sim}{K}}$

Fig. 3.6. Uniform rectangular plate subjected to in-plane loads on the external boundary.

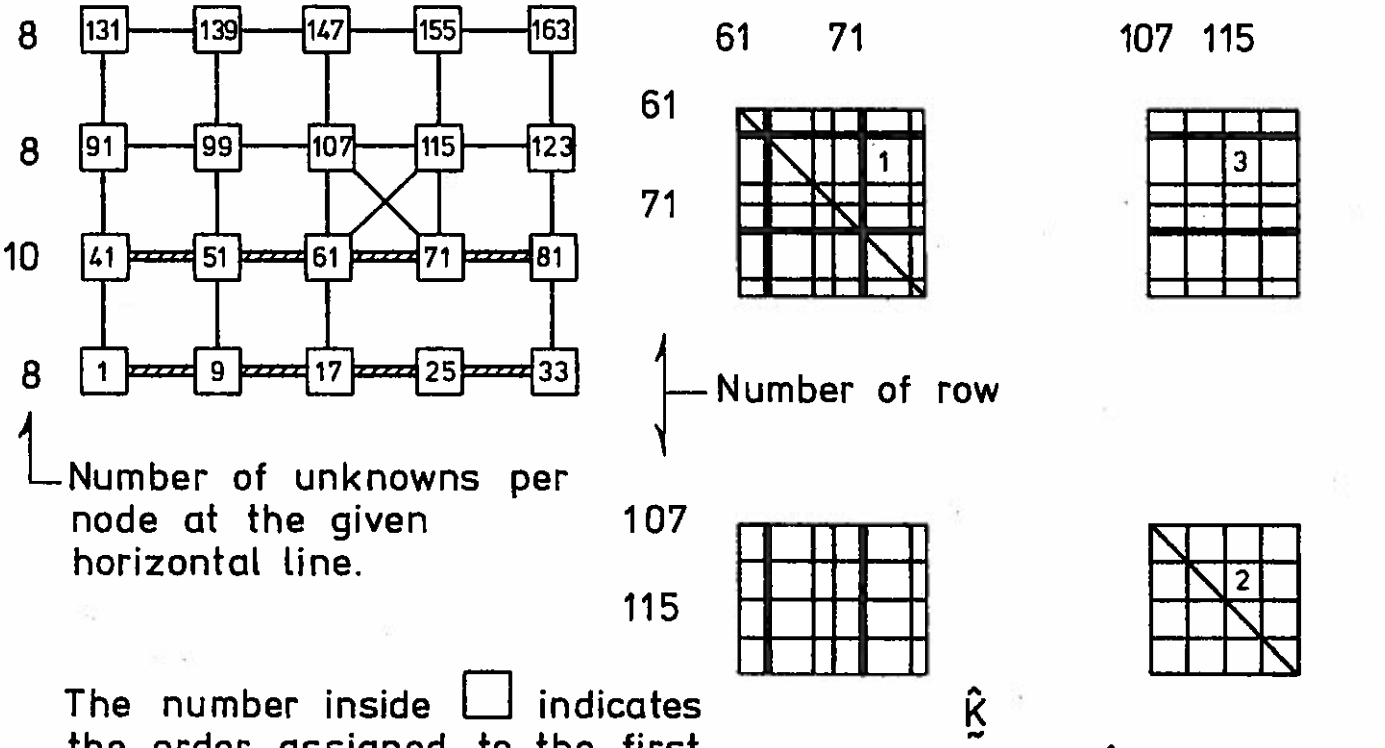

Fig. 3.7 (a). Rectangular plate with two longitudinal stiffeners.

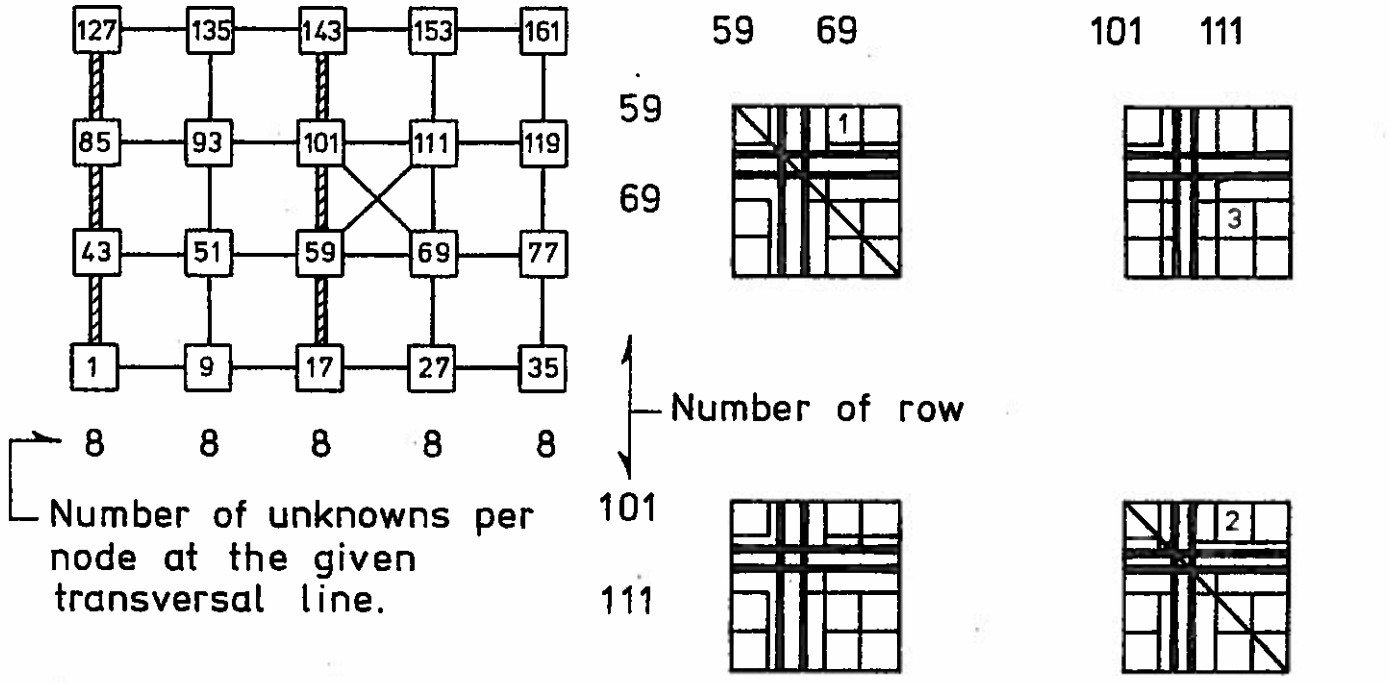

Fig. 3.7 (b). Rectangular plate with two transversal stiffeners.

After the matrices $\hat{\underset{\sim}{K}}$, $\underset{\sim}{K}$ and $\underset{\sim}{S}$ have been computed, it becomes necessary to introduce the geometrical boundary conditions' effect in such matrices.

By using the present functions, it is possible to prescribe U_α, w and $w,_\alpha$ at any segment along the boundary or inside the plate simply by sizing the subdomains properly, as is the case shown in Fig. 3.9(a). In the same figure, the following cases may be present, simultaneously or not

a) $U_\alpha = 0$ between I and II (see $(3.52)_1$)

i.e. $U_\alpha = U_{\alpha,1} = 0$ at nodes I and II (3.129)

b) $w = 0$ between I and II (see $(3.52)_1$)

i.e. $w = w,_1 = 0$ at nodes I and II

c) $w,_2 = 0$ between I and II (see $(3.52)_3$)

i.e. $w,_2 = w,_{12} = 0$ at nodes I and II

d) $U_\alpha = 0$ between III and IV (see $(3.52)_1$)

i.e. $U_\alpha = U_{\alpha,2} = 0$ at nodes III and IV

e) $w = 0$ between III and IV (see $(3.52)_2$)

i.e. $w = w,_2 = 0$ at nodes III and IV

f) $w,_1 = 0$ between III and IV (see $(3,52)_3$)

i.e. $w,_1 = w,_{12} = 0$ at nodes III and IV

The conditions above represent: b) and e) simple supports, c) and f) guided supports, b) + c) and e) + f) clamped supports.

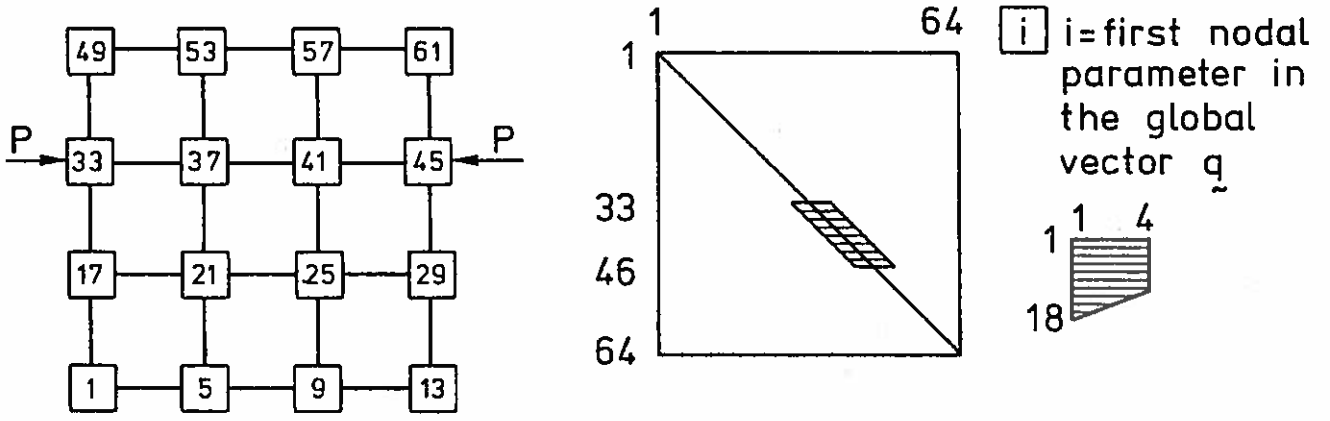

(a) Plate (b) Geometric matrix $\underset{\sim}{S}$ (c) Computer's storage

Fig. 3.8. Plate with a rigid fiber along the line of action of a force.

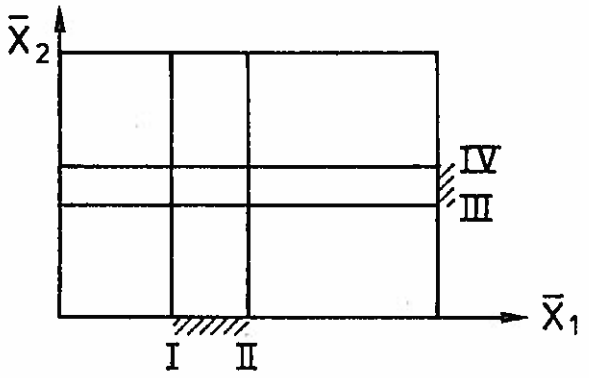

Fig. 3.9 (a). Boundary conditions for a plate

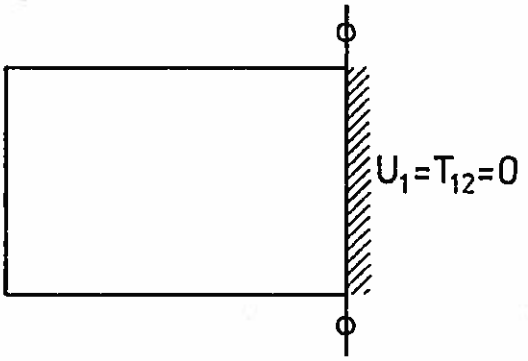

Fig. 39 (b). Half of a symmetrically loaded plate

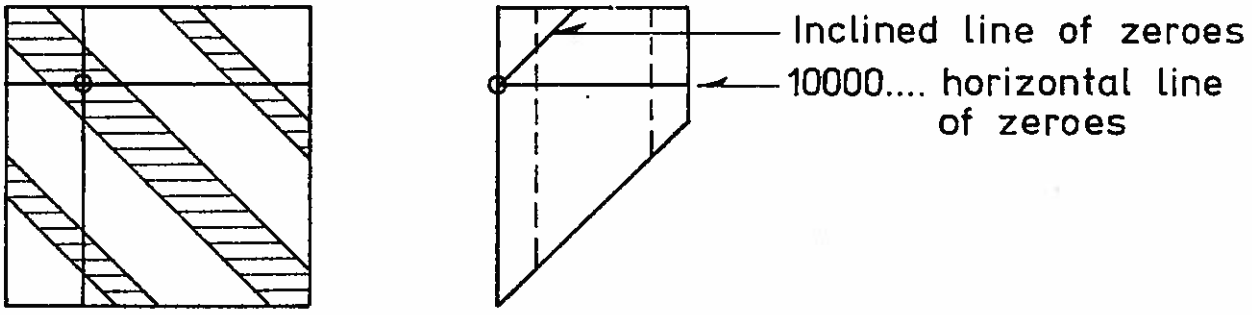

(a) Matrix $\hat{\underset{\sim}{K}}$ (b) Half band of $\hat{\underset{\sim}{K}}$

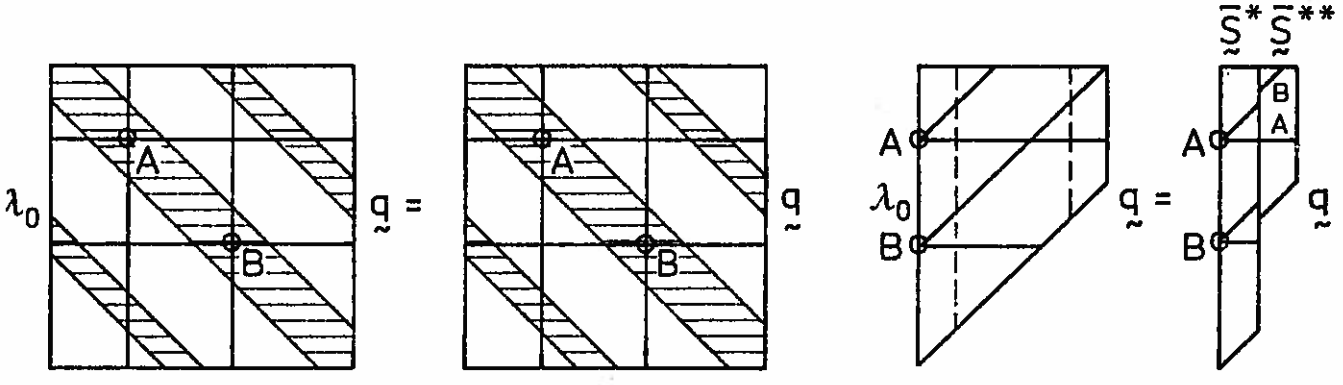

(c) $\lambda_0 \underset{\sim}{K}$ $\underset{\sim}{q}$ = $\underset{\sim}{S}$ $\underset{\sim}{q}$ (d) Computer's storage

Fig. 3.10. Sketches showing the effect of the geometrical bound. cond.

Point boundary conditions can be treated by making the point under consideration a nodal point. For example, $w = 0$ at I and II produces a deflection pattern which is only zero at the ends of the intertal I - II. Likewise, $w_{,2} = 0$ at I and II makes the normal slope $w_{,2}$ zero at the ends of the interbal I-II and not in between.

As for the symmetrically loaded plate of Fig. 3.9(b), other conditions besides the geometrical boundary conditions can sometimes be satisfied exactly. In this case the condition at the line of symmetry is $U_1 = T_{12} = 0$. The condition $U_1 = 0$ for the edge implies $U_{1,2} = 0$, which t gether with $T_{12} = 0$ produce $U_{2,1} = 0$. Finally the condition $U_1 = U_{2,1} = 0$, for the edge of symmetry, is satisfied by setting

$$U_1 = U_{1,2} = U_{2,1} = U_{2,12} = 0 \tag{3.130}$$

at the nodes located on the symmetry line of Fig. 3.9(b).

It is also necessary to pay special attention to boundaries where stiffeners end, as for $X_2 = 0$ of Fig. 3.4(a). The boundary condition $U_2 = 0$ for $X_2 = 0$ implies that at the stiffener,

$$U_2 = U^{-}_{2,1} = U^{+}_{2,1} = 0 \quad \text{for } X_2 = 0 \tag{3.131}$$

i.e. one more condition than the remaining nodes located at $\bar{X}_2 = 0$.

The boundary conditions just discussed lead to expressions of the form

$$\hat{q}_m = 0 \tag{3.132}$$

$$q_n = 0$$

where $\hat{q}_m$ is the mth. component of $\hat{q}$ and q_n is the nth. component of q. In order to represent (3.132) in the global equa-

tions (3.103) and (3.113) it becomes necessary to set

$$\hat{K}_{mn} = 1$$

the remainder of the m th. row and mth. column of $\hat{\underset{\sim}{K}} = F_m = 0$ (3.133)

$$K_{nn} = S_{nn} = 1 \tag{3.134}$$

the remainder of the n th. row and nth. column of $\underset{\sim}{K}$ and $\underset{\sim}{S} = 0$

If the eigenvalue problem is solved by an iteration procedure which employs a starting vector $\underset{\sim}{q}_{(o)}$, then

$$q_{(o)n} = 0$$

The schemes (3.133) and (3.134) have been represented in Fig. 3.10 as well as their effect on the actual matrices handled by a digital computer.

3.6 Iteration Procedure for Finding the Eigenvalue of Largest Magnitude.

The matrix eigenvalue problem (3.113) can be solved by an iteration scheme (see Faddeeva [45]) where starting from an assumed eigenvector the procedure converges to the eigenvector belonging to the eigenvalue of largest magnitude.

The positive definite symmetric band matrix $\underset{\sim}{K}$ can be expressed as a lower triangular matrix $\underset{\sim}{\bar{L}}$ multiplied by an upper triangular matrix $\underset{\sim}{\bar{U}}$. As shown by Forsythe and Moler [46, p. 28], for a given vector $\underset{\sim}{W}$, the solution to the system of linear equations

$$\underset{\sim}{K}\ \underset{\sim}{q} = \underset{\sim}{W}$$

can be obtained as follows:

a) Triangular matrix decomposition

$$\underset{\sim}{K} = \bar{\underset{\sim}{L}}\,\bar{\underset{\sim}{U}}$$

$$\bar{L}_{ij} = \bar{U}_{ji} \quad ; \; i \neq j$$

$$\bar{L}_{ii} = 1$$

i.e. $\bar{\underset{\sim}{L}}^T$ and $\bar{\underset{\sim}{U}}$ differ only in the diagonal.

b) forward elimination

$$\bar{\underset{\sim}{L}}\,\bar{\underset{\sim}{x}} = \underset{\sim}{W} \quad \text{solve for } \bar{\underset{\sim}{x}}$$

c) backward substitution

$$\bar{\underset{\sim}{U}}\,\underset{\sim}{q} = \bar{\underset{\sim}{x}} \quad \text{solve for } \underset{\sim}{q}$$

The above considerations lead to the following procedure:

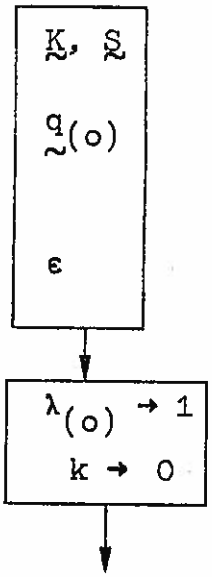

matrices stored in the digital computer as in Fig. 3.10(d))

initial vector of components $q_{(o)i}$ = { 1 unrestrained; 0 geometrical B.C. Prescribed

relative maximum difference between successive values of the largest eigenvalue's magnitude (from 10^{-4} to 10^{-6}).

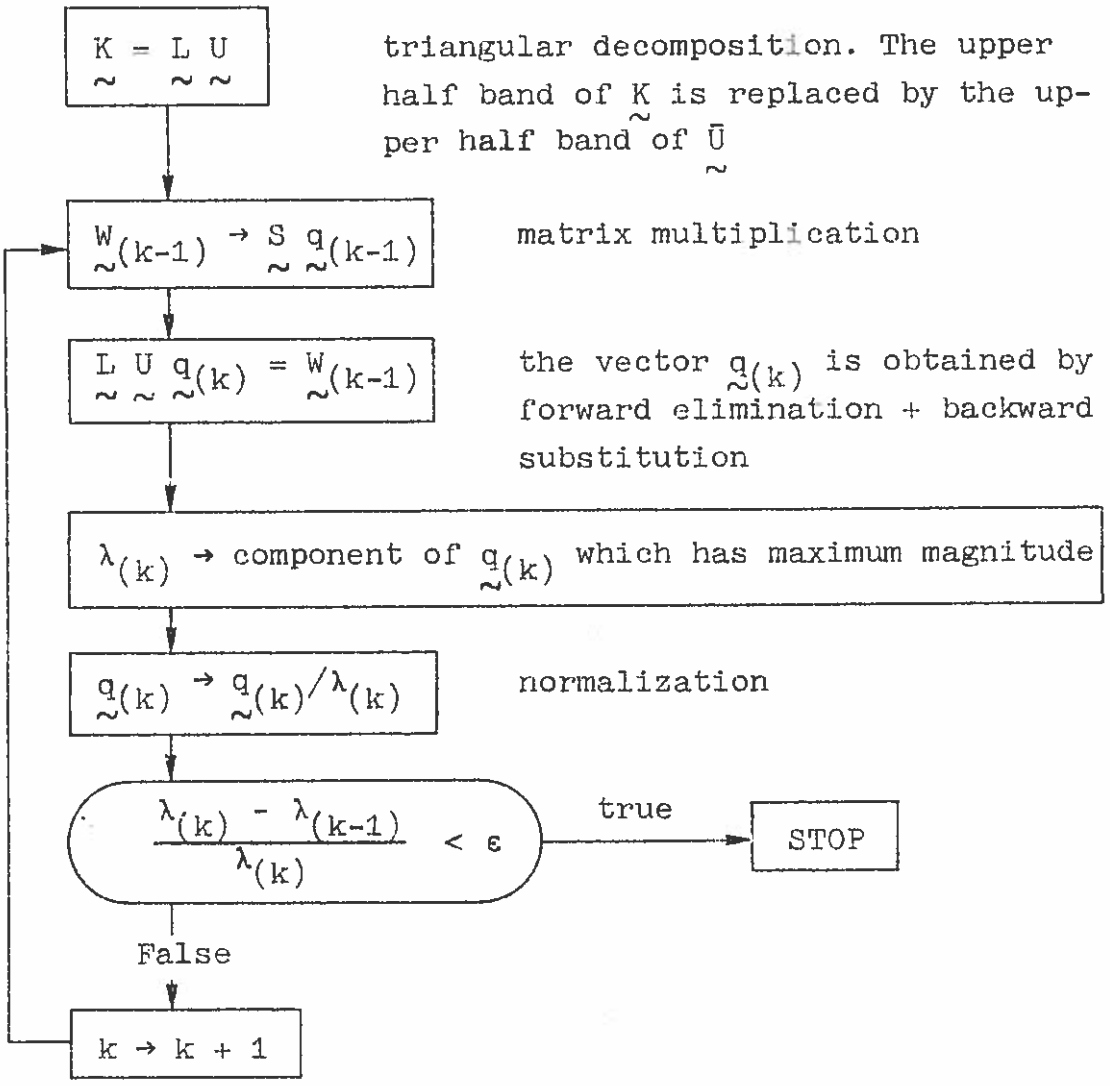

3.7 Computer Program

The computer program includes the following subroutines:

FKIJL - function corresponding to (3.27).

SPLAN - uses FKIJL for computing $\hat{\zeta}_{11}$, $\hat{\zeta}_{12}$ and $\hat{\zeta}_{22}$ of (3.25)

SEVR - from (3.30) computes $\hat{k} = \hat{k}^*$ (uniform mesh) and partitions $\hat{k}$ as in Fig. 3.6(b).

SEVRMD - from (3.30) and (3.95) computes $\hat{k} = \hat{T}^T \hat{k}^* \hat{T}$ (variable mesh) and partitions $\hat{k}$ as in Fig. 3.6(b).

ASGB2 - together with ASGBL produce a similar effect as the scheme (3.125). This subroutine is to be applied to subdomains located to the right of a transversal intermediate stiffener (Fig. 3.11(a)) or to be applied to a subdomain located above a longitudinal intermediate stiffener (Fig. 3.11(b)).

AXIAL - the stiffener's matrix (3.67) (Table 3.1) is stored according to (3.115) in a global matrix.

DIASYM - represents the effects shown in Fig. 3.10(b) produced by homogeneous geometrical boundary conditions. This subroutine is based on the scheme (3.132) which modifies a global matrix and a column vector.

CHOL - solves the system of linear equations (3.103) where $\hat{\underset{\sim}{K}}$ is stored in the computer as indicated in Fig. 3.10(b).

GIJK - function corresponding to (3.49), (3.50) and (3.51).

GMATX - computes the quantities Q_{ijk} (136, 16, 4) of (3.48) making use of GIJK in accordance to (3.44).

GMRIB - determines $\underset{\sim}{\Gamma}_1$, $\underset{\sim}{\Gamma}_2$, $\underset{\sim}{\Gamma}_3$ and $\underset{\sim}{\Gamma}_4$ of (3.60).

GEOM - $\underset{\sim}{s}^*$ is calculated using (3.42). Since for a uniform mesh $s = \underset{\sim}{s}^*$ or for a variable mesh $s = \bar{T}^T s^* \bar{T}$, the matrix $\underset{\sim}{s}$ can be established and partitioned in submatrices.

ASBK - $\underset{\sim}{s}$ is stored in $\bar{\underset{\sim}{S}}^*$ and $\bar{\underset{\sim}{S}}^{**}$ in accordance to scheme (3.128) and Fig. 3.10(d).

FORCE - the geometric matrix for stiffeners (3.58) (or $(3.66)_5$) is computed and stored in a matrix $\underset{\sim}{g}$ of an adjacent subdomain.

PART - partitions a matrix $\underset{\sim}{k}$ in submatrices.

PARTMD - given $\underset{\sim}{k}^*$, partitions the matrix $\underset{\sim}{k} = \bar{\underset{\sim}{T}}^T \underset{\sim}{k}^* \bar{\underset{\sim}{T}}$

DIABK - similar to DIASYM except for the modification to the column vector which is avoided.

ZERH - creates a row of zeros in $\underset{\sim}{S}^{**}$ (Fig. 3.10(d), line A)

ZERV - creates a diagonal of zeros in $\underset{\sim}{S}^{**}$ (Fig. 3.10(d), line B)

ZER - creates a row and a diagonal of zeros in $\underset{\sim}{S}^{**}$ (Fig. 3.10(d)).

SBUCK - uses FKIJL for computing $\underset{\sim}{\zeta}_{11}$, $\underset{\sim}{\zeta}_{12}$, $\underset{\sim}{\zeta}_{22}$, $\underset{\sim}{\zeta}_{33}$ of (3.38).

DIGZ - uses ZERH, ZERV and ZER to perform in $\underset{\sim}{S}^{**}$ all the modifications which arise from the geometrical Bound. Cond.

BOUNDY - considers the geometrical Bound. Cond. for the deflection of the plate at the external contour of the plate, which remain constant for a given edge. The matrices $\underset{\sim}{K}$ and $\underset{\sim}{q}$ are modified by DIASYM, $\underset{\sim}{S}^{*}$ is modified by DIABK and $\underset{\sim}{S}^{**}$ is modified by DIGZ.

BSYMT - multiplies a matrix by a vector when only half of the band's matrix is given (for example $\underset{\sim}{S}^{*}\ \underset{\sim}{q}$).

BMUL - the operation $\underset{\sim}{S}\ \underset{\sim}{q} = \underset{\sim}{S}^{*}\ \underset{\sim}{q} + \underset{\sim}{S}^{**}\ \underset{\sim}{q}$ is performed. $\underset{\sim}{S}^{*}$ and $\underset{\sim}{S}^{**}$ are shown in Fig. 3.10(d). The operation $\underset{\sim}{S}^{*}\ \underset{\sim}{q}$ is computed by BSYMT.

CMAX - function which determines the component of maximum magnitude in a vector.

EIGB - solves the matrix eigenvalue problem (3.113) according to the iteration procedure of Art. 3.7. The subroutines BMUL and CMAX are needed in these computations.

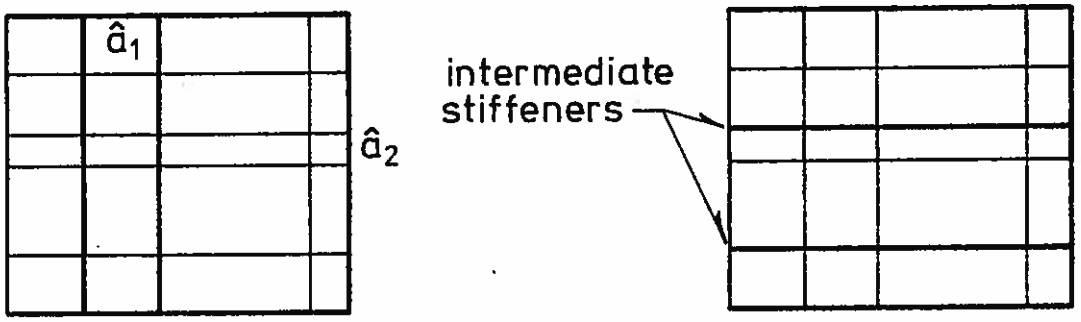

a) Longitudinal intermediate stiffeners.

b) Transversal intermediate stiffeners.

Fig. 3.11. The Plates show the two cases for which the computer program is applicable.

Loads applied on the perimeter or distributed throughout the plate (Fig. 3.11) can be handled by the computer program for a specific mesh and location of stiffeners.

For the given loading, several ratios $\hat{a}_2/\hat{a}_1$ can be analysed. By changing the bending the torsional properties of the stiffeners, it is possible to make several buckling calculations which correspond to one plane stress distribution.

The following notation

NGAM = number of plate's ratios $\hat{a}_2/\hat{a}_1$ to be analysed.
NCASE= number of buckling analysis for each ratio $\hat{a}_2/\hat{a}_1$
NE = number of subdomains
NU = 0 for a uniform mesh, otherwise NU ≠ 0 for a variable mesh.

is used in the macro-flow chart of the computer program which is given on the following page.

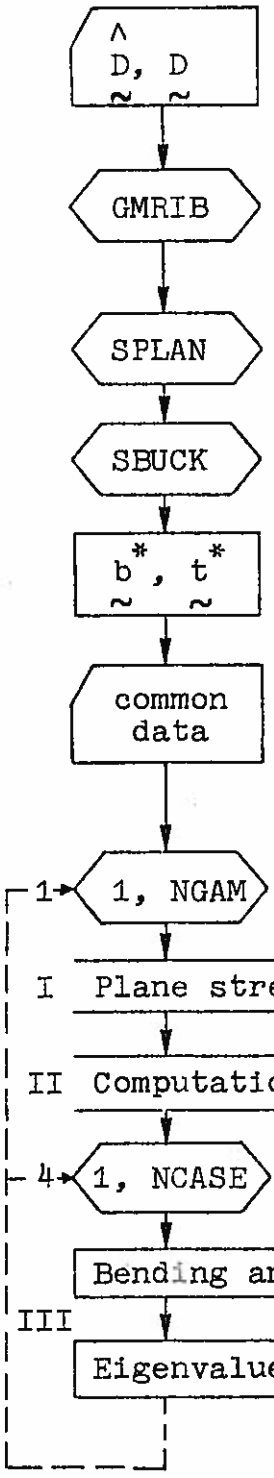

The elements of $\hat{\underset{\sim}{D}}$ (3.19) and $\underset{\sim}{D}$ (3.36) are given by coefficients of the form (3.13).

Calculation of $\underset{\sim}{\Gamma}_1, \underset{\sim}{\Gamma}_2, \underset{\sim}{\Gamma}_3, \underset{\sim}{\Gamma}_4$ as indicated by (3.57)

$\hat{\zeta}_{\alpha\beta}=,\ldots;\ \hat{\underset{\sim}{k}}^*=\ldots$ (see (3.25) and (3.30)

$\underset{\sim}{\zeta}_{\alpha\beta}=\ldots,\ \underset{\sim}{\zeta}_{33}=\ldots$ (see (3.38))

as defined by (3.60)

NU, mesh properties, ratios $\hat{a}_2/\hat{a}_1$, geometrical B.C. on the plate's edge, axial stiffener's properties $(3.61)_1$, etc.

Iteration 1

$\underset{\sim}{S}$ is the geometric global matrix.

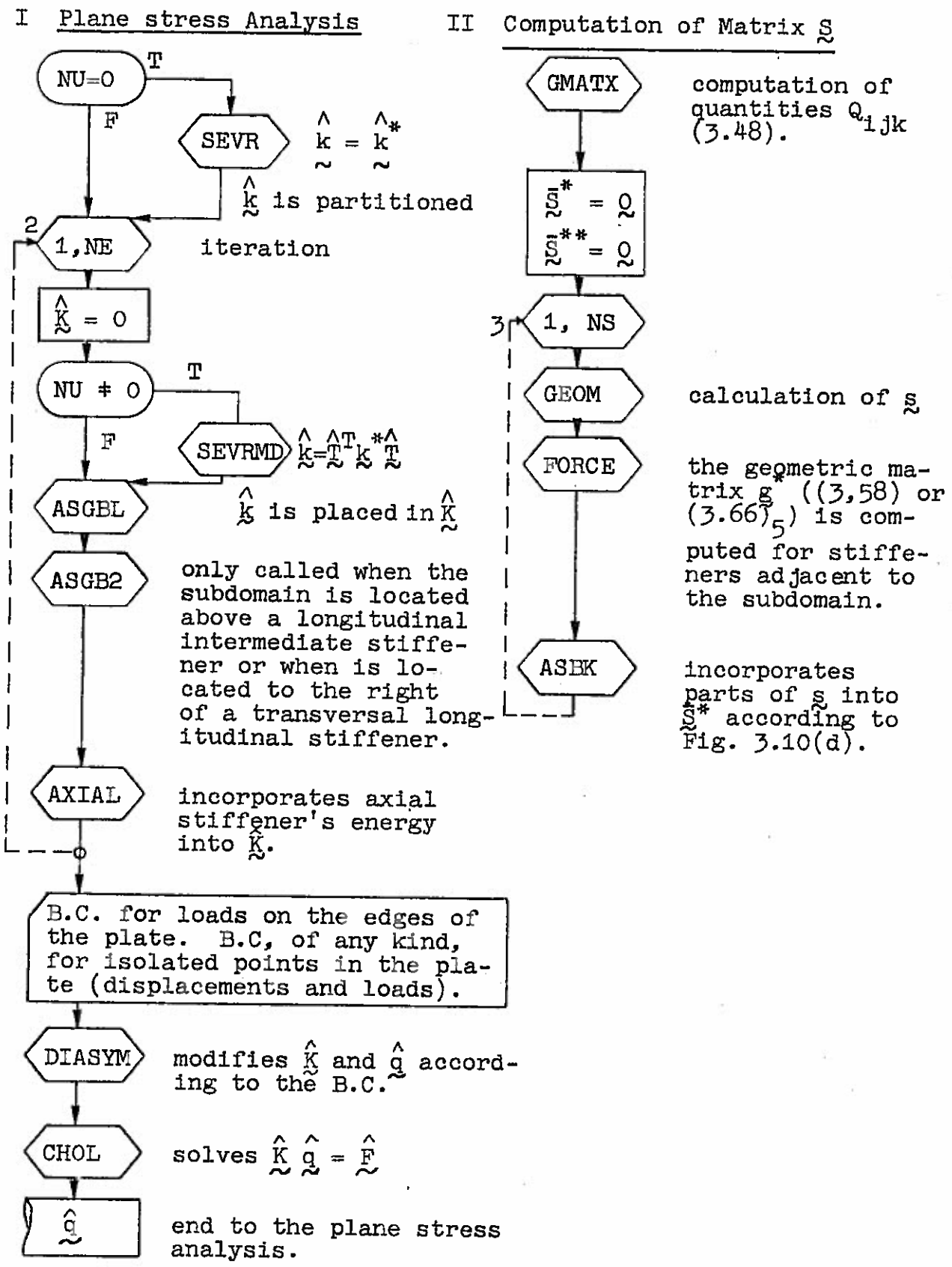
I Plane stress Analysis
NU=0
T
F
SEVR
$\hat{k} = \hat{k}^*$
$\hat{k}$ is partitioned
2
1,NE
iteration
$\hat{K} = 0$
NU ≠ 0
T
F
SEVRMD
$\hat{k} = \hat{T}^T \hat{k}^* \hat{T}$
ASGBL
$\hat{k}$ is placed in $\hat{K}$
ASGB2
only called when the subdomain is located above a longitudinal intermediate stiffener or when is located to the right of a transversal longitudinal stiffener.
AXIAL
incorporates axial stiffener's energy into $\hat{K}$.
B.C. for loads on the edges of the plate. B.C, of any kind, for isolated points in the plate (displacements and loads).
DIASYM
modifies $\hat{K}$ and $\hat{q}$ according to the B.C.
CHOL
solves $\hat{K}\,\hat{q} = \hat{F}$
$\hat{q}$
end to the plane stress analysis.
II Computation of Matrix S
GMATX
computation of quantities Q_{ijk} (3.48).
$S^* = 0$
$S^{**} = 0$
3
1, NS
GEOM
calculation of s
FORCE
the geometric matrix g^* ((3,58) or $(3.66)_5$) is computed for stiffeners adjacent to the subdomain.
ASBK
incorporates parts of s into S^* according to Fig. 3.10(d).

III Eigenvalue analysis

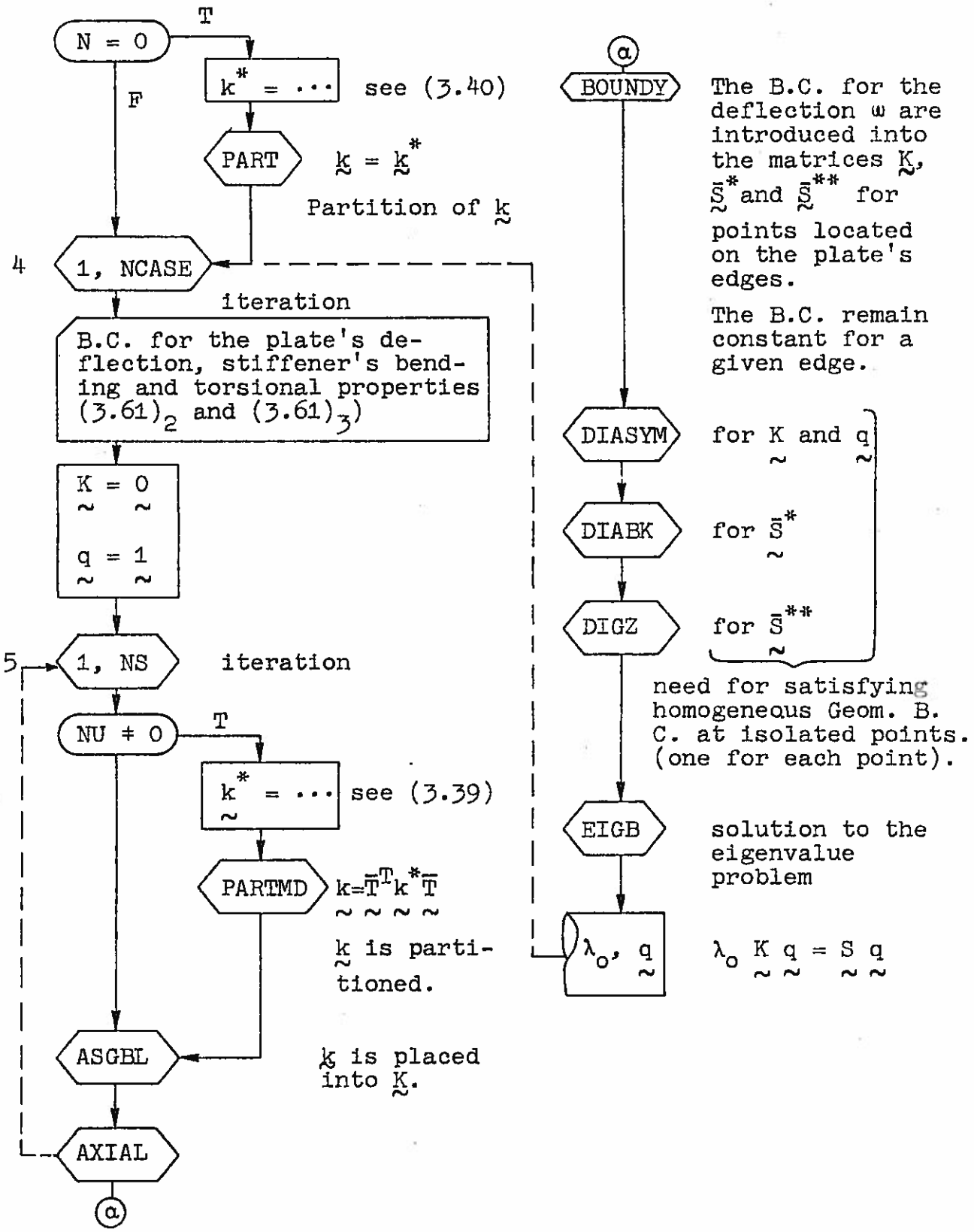

4. NUMERICAL RESULTS OBTAINED BY THE RITZ-SUBDOMAIN METHOD

4.1 Numerical and Analytical Results for Plane Stress Problems.

Fig. 4.1. shows graphs of exact stresses (defined by (3.5)) for a rectangular plate subjected to a sinusoidal load on a longitudinal edge. These stresses are exact in the sense that they solve a mathematical problem, as explained in Art. 5.1. The same figure shows as well a comparison between the exact values and results obtained using the Ritz-Subdomain method for the mesh of Fig. 4.2(a). It seems that the discontinuous stress field given by the Ritz-Subdomain method can be very close to the discontinuous exact stress field provided that the applied external forces vary in a smooth pattern. Applications of the Ritz-Subdomain method to problems with concentrated loads (not presented here) have shown accurate results when small subdomains are used near the loads. Of course the theoretical infinite stress at a concentrated load is represented in the approximate method by a distributed stress of very high value in the neighborhood of the load. Concentrated loads are commonly used when a high stress is known to exist near a point and the actual distribution of stresses around such point is unknown and of little importance.

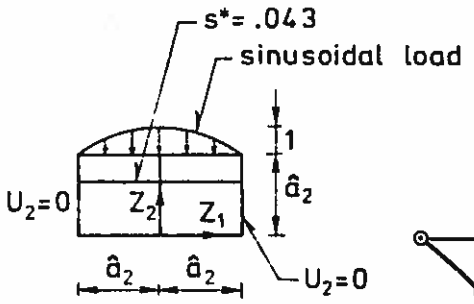

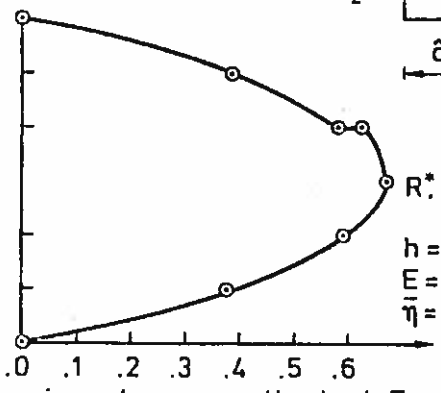

Shearing stress resultant at $Z_1 = -\hat{a}_2/2$

R^*, R^+, R^- = stiffener's axial rigidities
h = plate's thickness
E = Young's modulus of the plate
$\bar{\eta} = Z_2/\hat{a}_2$

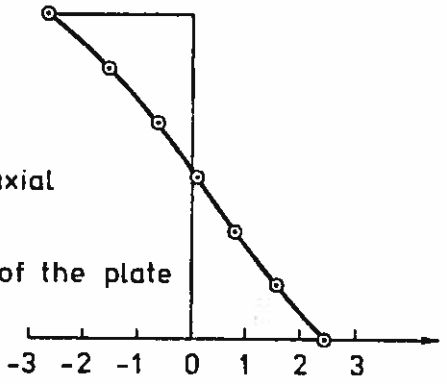

Normal stres resultant at $Z_1 = 0$

$\bar{\eta}$	Analytical	Computer
1	.0	.00063
5/6	.38407	.38423
2/3	.58042	.58003
2/3	.61974	.61999
1/2	.66943	.66943
1/3	.59034	.59031
1/6	.37637	.37653
0	.0	.00056

$$s^+ = \frac{R^+}{2Eh\hat{a}_2}$$

$s^- = \cdots$

$s^* = \cdots$

Case 1
$s^+ = s^- = 0$
$s^* = .043$

$\bar{\eta}$	Analytical	Computer
1	-2.68568	-2.68814
5/6	-1.52218	-1.52194
2/3	-0.63307	-0.63276
1/2	0.08324	0.08329
1/3	0.77667	0.77649
1/6	1.55955	1.55930
0	2.55281	2.55383

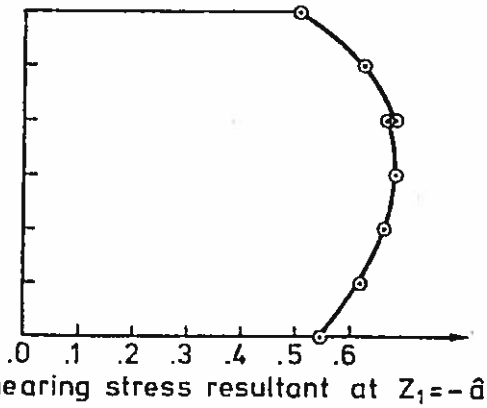

Shearing stress resultant at $Z_1 = -\hat{a}_2$

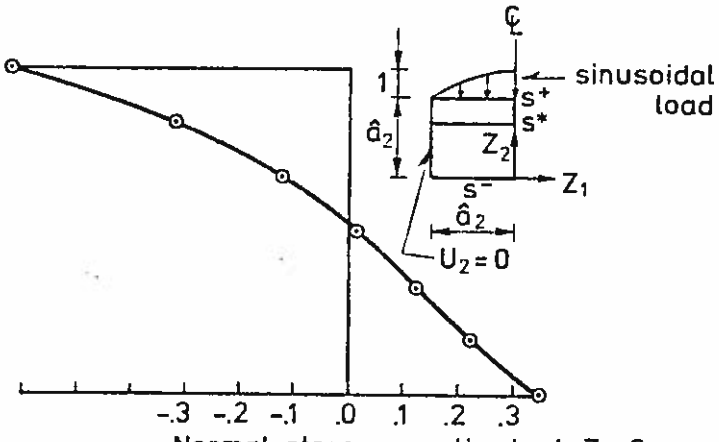

Normal stress resultant at $Z_1 = 0$

$\bar{\eta}$	Analytical	Computer
1	.505066	.505175
5/6	.625681	.625601
2/3	.682107	.681828
2/3	.671358	.671399
1/2	.684441	.684326
1/3	.665821	.665687
1/6	.620376	.620258
0	.546121	.546074

Case 2
$s^+ = s^- = .5$
$s^* = .043$

$\bar{\eta}$	Analytical	Computer
1	-0.621533	-0.622263
5/6	-0.320983	-0.321066
2/3	-0.123753	-0.123711
1/2	0.015958	0.015942
1/3	0.123233	0.123420
1/6	0.225201	0.225273
0	0.347670	0.347587

Fig. 4.1. Plane stress analyses' results.

4.2. Numerical and Analytical Results for Buckling Problems.

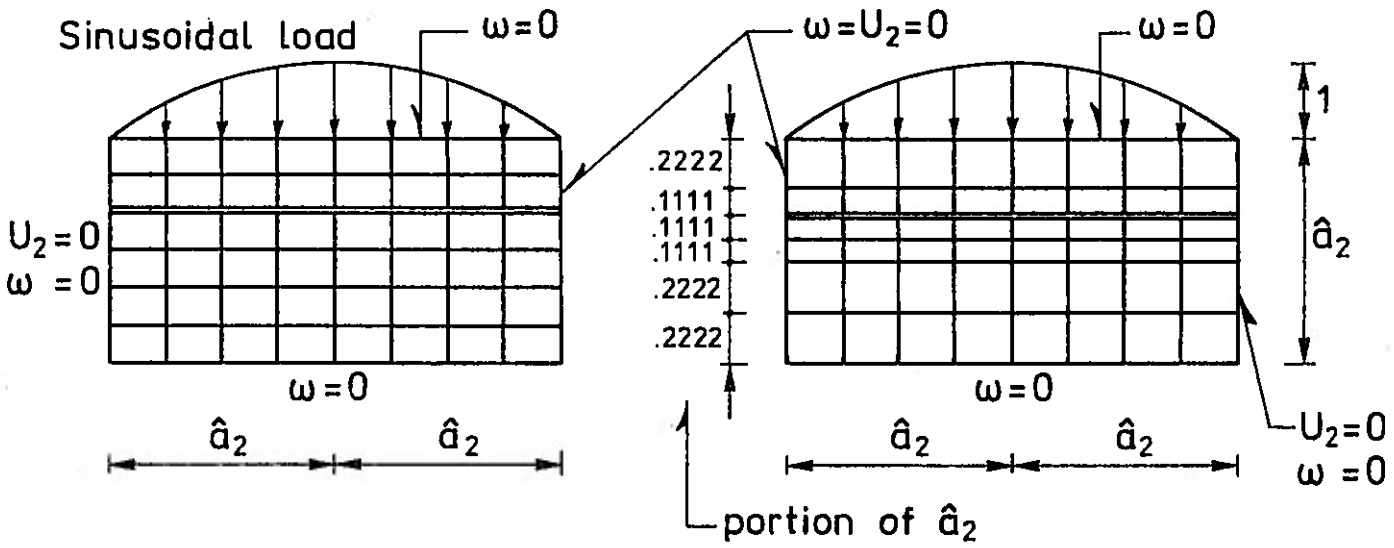

(a) Uniform mesh (b) Variable mesh

Fig. 4.2. Lateral buckling of a simply supported stiffened plate

The stiffened, simply supported plates of Fig. 4.2 have been analysed both using the Ritz-Subdomain method and the usual Ritz method. The analysis by the Ritz Method as explained in Art. 5.2 is performed by assuming a double Fourier series for the deflection ω together with the exact distribution of in-plane stresses.

The plates in Fig. 4.2 have thickness h, flexural rigidity D and Young's modulus E. In the notation of (5.14) Ehs^{+}, Ehs^{*} and Ehs^{-} are respectively the axial rigidities per unit length for the upper, intermediate and lower stiffeners. Likewise DI_1^{*} (see $(3.61)_2$) denotes the flexural rigidity per unit length of the intermediate stiffener.

Using the parameter

$$\lambda = \frac{PD}{\Lambda^2 a_2} \tag{4.1}$$

the results for various analyses of critical loads P can be written as follows:

1) $s^* = 0.043; \quad s^+ = s^- = 0; \quad I_1^* = 0$

Ritz-Subdomain $\lambda = 29.669716$

Ritz $\lambda = 29.662997$

2) $s^* = 0.043; \quad s^+ = s^- = 0; \quad I_1^* = 12.5$

Ritz-Subdomain $\lambda = 70.196128$

Ritz $\lambda = 72.016434$

3) $s^* = 0,5; \quad s^+ = s^- = 0; \quad I_1^* = 0$

Ritz-Subdomain $\lambda = 28.509359$

Ritz $\lambda = 28.507864$

Ritz-Subdomain $\lambda = 28.518222$ (variable mesh Fig. 4.2(b))

4) $s^* = 0,5; \quad s^+ = s^- = 0; \quad I_1^* = 12.5$

Ritz-Subdomain $\lambda = 68.050357$

Ritz $\lambda = 68.952423$

5) $s^* = 0.043; \quad s^+ = s^- = 0.5; \quad I_1^* = 0$

Ritz-Subdomain $\lambda = 32.031993$

Ritz $\lambda = 32.037039$

It is observed that both the Ritz and Ritz-Subdomain methods give close results when the stiffener's flexural rigidity is negligible $I_1^* = 0$ regardless of the magnitude of the axial rigidities. When $I_1^* \neq 0$ the usual Ritz method gives a higher critical load and therefore a higher error than the Ritz-Subdomain method. Apparently the deflection pattern of the Ritz-Subdomain method which is discontinuous in its second derivatives along the interfaces of the subdomains can better approximate the exact deflection pattern. The latter is discontinuous in some of its second derivatives at the places were the flexural action of the stiffeners is considered.

The buckling load obtained in 3) for the variable mesh shown in Fig. 4.2(b) is slightly higher than the one obtained for a uniform mesh. This probably occurred because the plane stress analysis for the uniform mesh involved smaller subdomains adjacent to the load which have been observed to lead to a better approximation. For example the normal stress at the upper edge on the center of the plate results in 1.006442 for the uniform mesh and 1.006522 for the variable mesh (the exact value is 1.).

One Possible conclusion after examination of the previous examples is that the Ritz-Subdomain method gives accurate answers for cases where only stiffeners having axial rigidity are considered. The effect of flexural and torsional rigigities of the stiffeners remain to be considered in more detail.

Fig. 4.3. shows several analyses performed by the Ritz-Subdomain method and an analytic method described in Art. 5.3. In the figure the flexural and torsional rigidities of the stiffener have been denoted respectively by I_2^* and J_2^* (see (3.61)). The fiber which connects the points of applications of the loads has been assumed of infinite axial rigidity and the geometric energy has been evaluated using (5.29).

The approximate results presented in Fig. 4.3 are at most 0.2%

above the exact values when one half of the plate is divided into 16 subdomains. The numerical results are equally acceptable for unstiffened plates (low buckling loads) and for plates with stiffeners of high flexural and torsional rigidities (high buckling loads).

Two or more columns (rows) of subdomains between transversal (longitudinal) stiffeners are desirable for obtaining reliable results. This factor and the capacity of the electronic computer available limit the number of stiffeners which can be considered in the analysis.

Although the effect of the stiffeners' axial, flexural and torsional rigidities have been considered separatedly, the same degree of approximation is expected when the three are considered together.

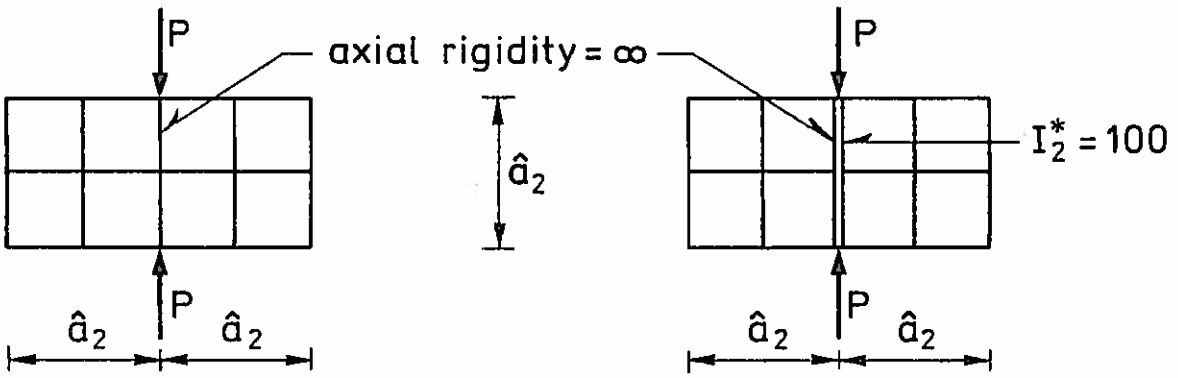

Analytical $\lambda = 12.91734$ $\lambda = 100\,\pi^2 + 12.91734 = 999.882396$

Numerical $\lambda = 13.09610$ $\lambda = 1007.489346$

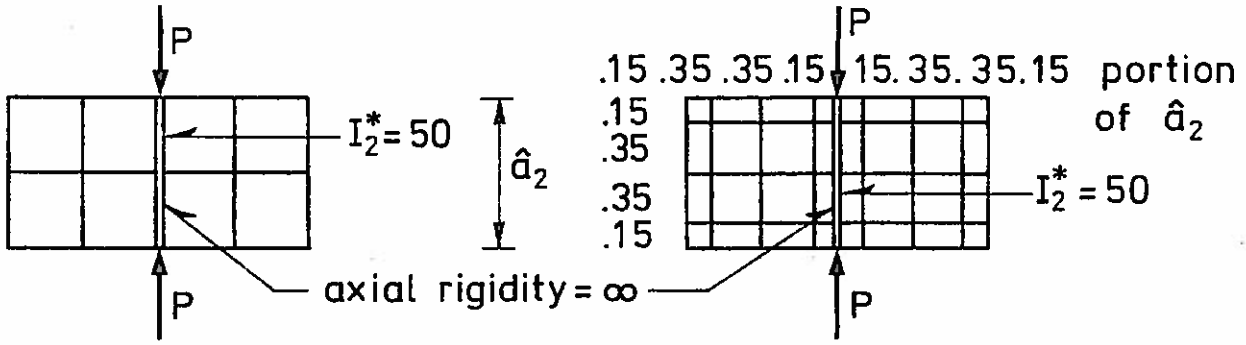

Analytical $\lambda = 506.399048$ $\lambda = 506.399048$

Numerical $\lambda = 510.328000$ $\lambda = 507.410734$

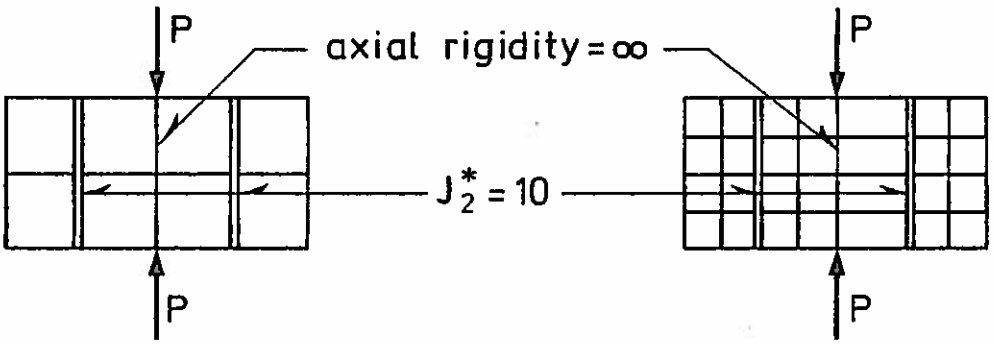

Analytical $\lambda = 16.98704$ $\lambda = 16.98704$

Numerical $\lambda = 17.14988$ $\lambda = 16.99856$

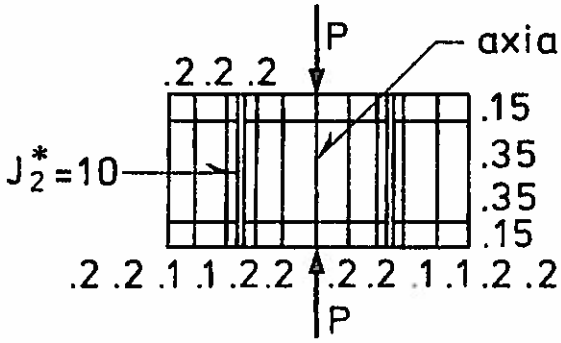

Analytical $\lambda = 16.98704$

Numerical $\lambda = 17.00666$

$$\lambda = \frac{P\hat{a}_2}{D}$$

D = the plate's flexural rigidity

Fig.4.3. Buckling of simply supported plates of ratio 1:2.

4.3 Examples Where No Solution Is Available

Fig. 4.4 has been presented for illustrating the kind of graphs or tables which can be elaborated for different loadings and boundary conditions. The case of a very long plate ($\hat{a}_1/\hat{a}_2 = 8$) may be compared with a very long plate simply supported along the longitudinal edges and clamped at the transversal edges. The buckling load for such a plate is given by $Pa_2/D = 8\pi$ which is slightly above the value obtained for the plate in Fig. 4.4 for $\hat{a}_1/\hat{a}_2 = 8$.

Fig. 4.5 shows a second example which is a beam with five transversal stiffeners. Especially for improving the plane stress results, another subdivision into subdomains should be tried. The one presented here indicates which problems can be encountered when the buckling analysis of such beams is attempted.

Fig. 4.5 gives the relative dimensions of two sets of stiffeners and the results obtained for simply supported or clamped transversal edges of the beam. The buckling modes for critical loads may be local or involving the total length of the beam. The local buckling modes may be due mainly to shear forces or mainly to compressive forces. The cases where the minimum (in absolute value) critical loads were negative indicate that a load pulling the beam downwards from the bottom flange is more "critical" than the load applied downwards on the top flange.

When the minimum parameters λ_1, were negative, the second eigenvalue λ_2 was obtained solving, instead of (3.113), the problem.

$$(\underset{\sim}{K} - |\lambda_1| \underset{\sim}{S})\, \underset{\sim}{q} = \lambda_2 \underset{\sim}{S}\, \underset{\sim}{q} \tag{4.2}$$

by applying the iteration process described in Art. 3.6. The convergence to λ_1 was slow when λ_2 was very close to λ_1 in absolute value.

The results of the Table 4.1 also show that the type of beam support may have considerable influence on the critical loads

(compare 93.48 against 24.71). It seems best to consider the beam supports carefully and to take into account the flexural and torsional properties of the stiffeners usually placed at the supports.

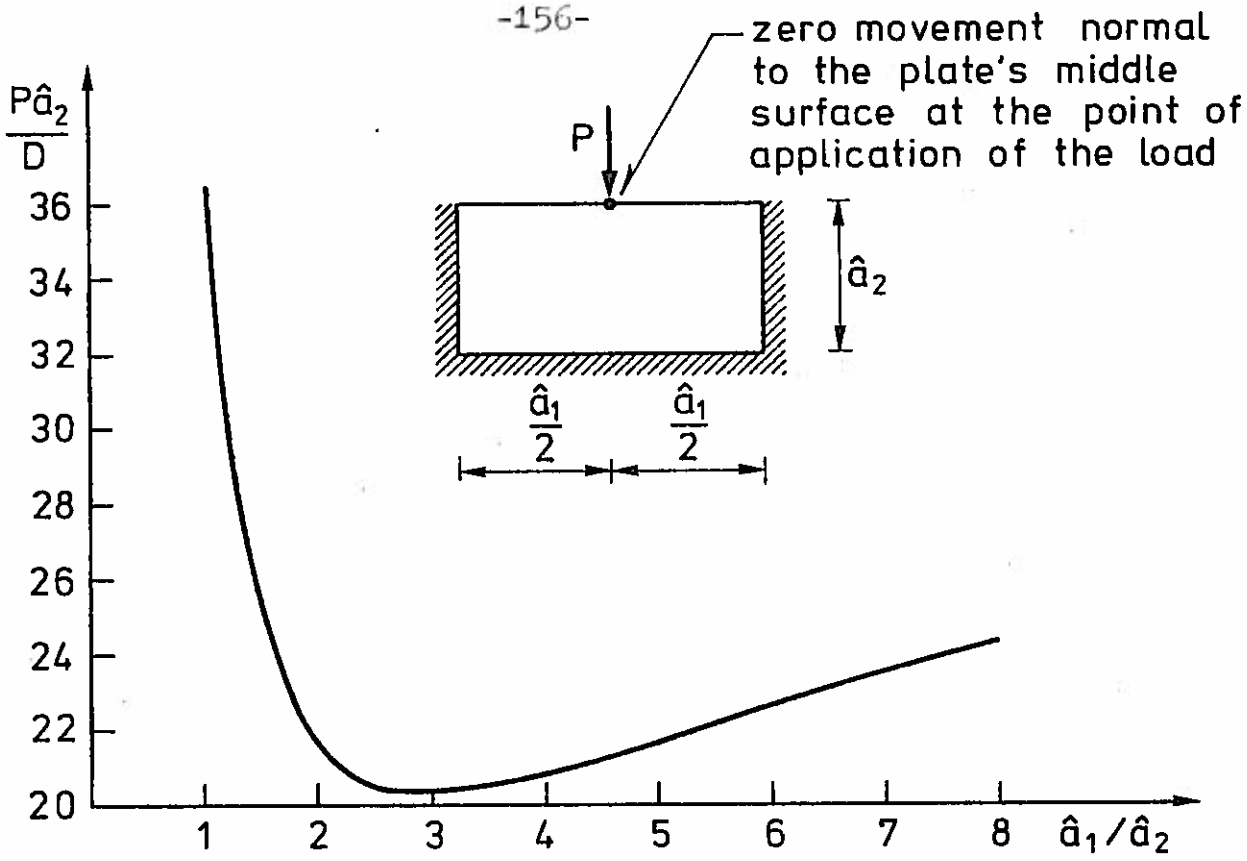

D = the plates flexural rigidity.

Results obtained using a 5×5 mesh for half a plate.

$\hat{a}_1/\hat{a}_2$	$P\hat{a}_2/D$	$\hat{a}_1/\hat{a}_2$	$P\hat{a}_2/D$
1.000	36.4976	3.636	20.6152
1.333	27.3855	4.000	20.8438
1.600	23.8381	4.444	21.1701
2.000	21.4653	5.556	22.2633
2.667	20.4248	8.000	24.3378
3.077	20.3963		

Fig.4.4. Critical load for a rectangular plate.

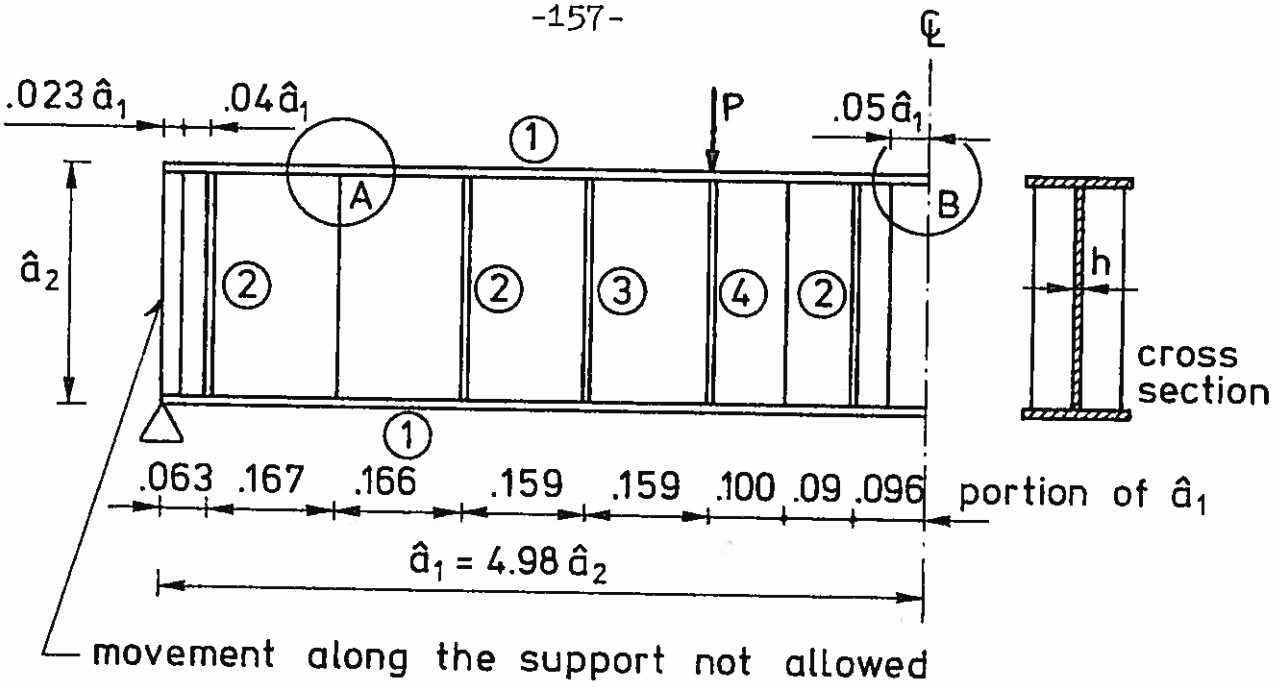

S*, I*, J* = area, modulus of inertia, torsional constant.
D = the web's flexural rigidity.

Stiffener	1 set			2 set		
	$\frac{S^*}{h\hat{a}_2}$	$\frac{EI^*}{D\hat{a}_2}$	$\frac{0.4EJ^*}{D\hat{a}_2}$	$\frac{2S^*}{h\hat{a}_2}$	$\frac{8EJ^*}{D\hat{a}_2}$	$\frac{8 \times 0.4\ EJ^*}{D\hat{a}_2}$
1	1.10461	10074.3	419.4	same numbers as set 1		
2	0.55284	2186.9	44.8			
3	0.73739	2910.1	218.8			
4	1.05341	11844.2	311.6			

Support	$\lambda_1 = \frac{P\hat{a}_2}{D}$	$\lambda_2 = \frac{P\hat{a}_2}{D}$	$\lambda_1 = \frac{P\hat{a}_2}{D}$	$\lambda_2 = \frac{P\hat{a}_2}{D}$
Clamped	-119.91 (155 cycles)	127.53 (6 cycles)	-70.43 (27 cycles)	93.48 (13 cycles)
	Local buckling due to shear in area A.		Local buckling by compression in area B.	
Simply supported	-118.97 (173 cycles)	125.42 (6 cycles)	24.71 (10 cycles)	Not computed.
	Local buckling area A		General lateral buckling*.	

* The upper flange's lateral deflection increases towards the center. The lower flange only undergoes torsion.

Fig. 4.5 Buckling Analysis of a Symmetric Beams.

5. APPENDIX TO CHAPTER 4.

5.1. Filon's Type Solution for Plates with Stiffeners.

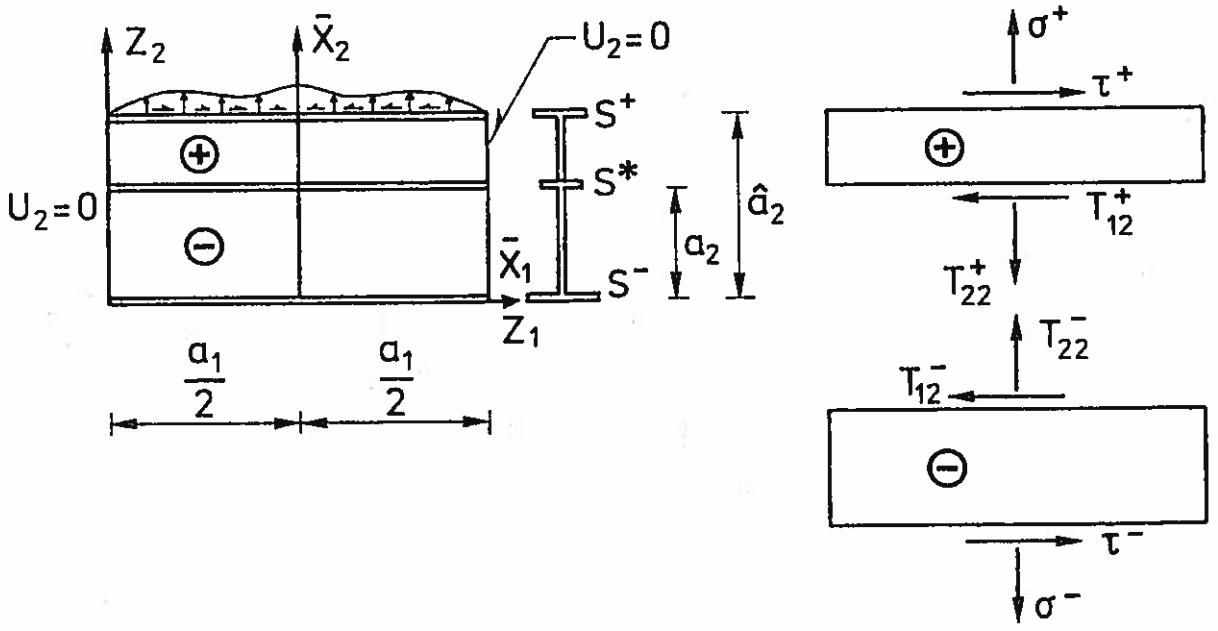

Fig. 5.1. Rectangular plate with an intermediate stiffener.

Fig. 5.1 shows a rectangular plate which has three longitudinal stiffeners with axial rigidities (area times Young's modulus) R^-, R^* and R^+. The quantities with a superscript "plus" belong to the upper part of the plate and those with superscript "minus" belong to the lower part. When equations are valid for any portion of the plate the superscript will not be written. The thickness h, Young's modulus E and Poisson's ratio ν have been chosen constant for the plate, though the formulae can be modified when such quantities differ between both parts of the plate. The stress tensor denoted by $T_{\alpha\beta}$ is given by (3,5) in terms of the strains which in turn are expressed by (3,2) in terms of the in-plane displacements U_α.

The boundary conditions at the transversal edges are

$$U_2 = T_{11} = 0 \qquad \text{at } \bar{X}_1 = \pm \frac{a_1}{2} \tag{5.1}$$

The stresses at the longitudinal edges of the plate are given by analogous Fourier series expansions such as

$$\sigma^+ = \sigma_o + \sum_{n=1}^{\infty} \sigma_n^+ \cos\nu_n \bar{X}_1 \tag{5.2}$$

$$\tau^+ = \sum_{n=1}^{\infty} \tau_n^+ \sin\nu_n \bar{X}_1$$

$$\nu_n = \frac{\pi(2n-1)}{a_1} \tag{5.3}$$

for the upper edge.

The compatibility of displacements at the interface $\bar{X}_2 = a_2$ can be expressed by

$$U^+_{1,1} = U^-_{1,1}$$

$$U^+_{2,11} = U^-_{2,11}$$

An analysis of equilibrium of the stiffeners (analogous to that of Fig. 3.5(a)) produces the following mechanical requirements

$$\left.\begin{aligned} T^+_{22} &= T^-_{22} \\ T^+_{12} &= -T^-_{12} - R^* U_{1,11} \end{aligned}\right\} \bar{X}_2 = a_2 \tag{5.6}$$

$$\left.\begin{aligned} T^+_{22} &= \sigma^+ \\ T^+_{12} - R^+ U_{1,11} &= \tau^+ \end{aligned}\right\} \bar{X}_2 = \hat{a}_2$$

and expressions at $\bar{X}_2 = 0$ similar to those of $\bar{X}_2 = \hat{a}_2$ (the sign of the shears is taken to be positive as shown in Fig. 5.1)

The equations

$$U_{1,1} = \frac{1}{Eh}(T_{11} - \nu T_{22}) = \frac{1}{Eh}(\psi_{,22} - \nu \psi_{,11}) \qquad (5.7)$$

$$U_{2,11} = \frac{1}{Eh}[(2+\nu)T_{12,1} - T_{11,2}] = -\frac{1}{Eh}[(2+\nu)\psi_{,211} + \psi_{,222}]$$

can be deduced using (3.5), (3.2), the definition of Airy's stress function ψ of (2.137) and the equilibrium equation

$$T_{12,1} + T_{22,2} = 0$$

this last equation to be used only for deducing $(5.7)_2$.

The use of (5.7) in (5.4) and of (2.137) in (5.6) leads to the expressions

$$\left.\begin{aligned} \psi^+_{,11} &= \sigma^+ \\ -\psi^+_{,12} - \frac{R^+}{Eh}(\psi^+_{,221} - \nu\psi^+_{,111}) &= \tau^+ \end{aligned}\right\} \bar{X}_2 = \hat{a}_2 \qquad (5.8)$$

$$\left.\begin{aligned} \psi^+_{,22} - \nu\psi^+_{,11} &= \psi^-_{,22} - \nu\psi^-_{,11} \\ (2+\nu)\,\psi^+_{,211} + \psi^+_{,222} &= (2+\nu)\psi^-_{,211} + \psi^-_{,222} \\ \psi^+_{,11} &= \psi^-_{,11} \\ -\psi^+_{,12} &= \psi^-_{,12} - \frac{R^*}{Eh}(\psi^-_{,221} - \nu\psi^-_{,222}) \end{aligned}\right\} \bar{X}_2 = a_2$$

$$\left.\begin{aligned} \psi^-_{,11} &= \sigma^- \\ -\psi^-_{,12} - \frac{R^-}{Eh}\left(\psi^-_{,221} - \nu\psi^-_{,111}\right) &= \tau^- \end{aligned}\right\} \bar{X}_2=0$$

where ψ^+ and ψ^- are two different stress functions.

The introduction of

$$\psi = \psi_o + \sum_{n=1}^{\infty} \psi_n \cos \nu_n \bar{X}_1 \tag{5.9}$$

Into (2.136) leads to the equations

$$\psi_{n,2222} - 2\nu_n^2 \psi_{n,22} + \nu_n^4 \psi_n = 0 \tag{5.10}$$

Whose solution in each portion of the plate is given by

$$\psi_o^+ = \psi_o^- = \sigma_o \bar{X}_1^2 \tag{5.11}$$

$$\psi_n^+ = \frac{1}{\nu_n^2} \sum_{i=1}^{4} \hat{h}_i^+ \varphi_i^+$$

$$\psi_n^- = \frac{1}{\nu_n^2} \sum_{i=1}^{4} \hat{h}_i^- \varphi_i^-$$

where for each n the constants $\hat{h}_i^+$ and $\hat{h}_i^-$ depend on the boundary conditions and where the functions φ_i^+ and φ_i^- can be written as

$$\varphi_1^+ = e^{-\nu_n(\hat{a}_2 - \bar{X}_2)} \quad ; \quad \varphi_2^+ = \nu_n(\bar{X}_2 - a_2)\varphi_1^+ \tag{5.12}$$

$$\varphi_3^+ = e^{-\nu_n(\bar{X}_2 - a_2)} \quad ; \quad \varphi_4^+ = \nu_n(\bar{X}_2 - a_2)\varphi_3^+$$

$$\varphi_1^- = e^{-\nu_n \bar{X}_2} \quad ; \quad \varphi_2^- = \nu_n(a_2 - \bar{X}_2)\varphi_1^-$$

$$\varphi_3^- = e^{-\nu_n(a_2 - X_2)} \quad ; \quad \varphi_4^- = \nu_n(a_2 - \bar{X}_2)\varphi_3^-$$

The particular form of (5.12) has been chosen for avoiding excessive growth of the exponential in the computations.

Substitution of (5.12), (5.11) and (5.9) in (5.8) results in the system of linear equations

$$\hat{\underset{\sim}{K}} \begin{Bmatrix} \hat{\underset{\sim}{h}}^{+} \\ \hat{\underset{\sim}{h}}^{-} \end{Bmatrix} = [\sigma_n^{+} \; \tau_n^{+} \; 0 \; 0 \; 0 \; 0 \; \sigma_n^{-} \; \tau_n^{-}]^T \qquad (5.13)$$

$$n = 1,2,\ldots$$

Let

$$s^{+} = \frac{R^{+}}{Eha_1} \quad ; \quad s_n^{+} = s^{+}\nu_n \qquad (5.14)$$

$$s^{*} = \frac{R^{*}}{Eha_1} \quad ; \quad s_n^{*} = s^{*}\nu_n$$

$$s^{-} = \frac{R^{-}}{Eha_1} \quad ; \quad s_n^{-} = s^{-}\nu_n$$

$$z_1 = \nu_n a_2$$

$$z_2 = \nu_n(\hat{a}_2 - a_2)$$

$$\bar{e}_1 = e^{-z_1}$$

$$\bar{e}_2 = e^{-z_2}$$

$$\upsilon_1 = 1 + \nu$$

$$\upsilon_2 = 1 - \nu$$

The elements of the matrix $\hat{\underset{\sim}{K}}$ of (5.13) are given by

$$\hat{\underset{\sim}{K}} = \begin{bmatrix} -1 & -z_2 & -\bar{e}_2 & -z_2\bar{e}_2 & 0 & 0 & 0 & 0 \\ \hat{K}_{21} & \hat{K}_{22} & \hat{K}_{23} & \hat{K}_{24} & 0 & 0 & 0 & 0 \\ -\upsilon_1 & -2 & -\upsilon_1\bar{e}_2 & 2\bar{e}_2 & \upsilon_1\bar{e}_1 & 2\bar{e}_1 & \upsilon_1 & -2 \\ \upsilon_1 & -\upsilon_2 & -\upsilon_1\bar{e}_2 & -\upsilon_1\bar{e}_2 & \upsilon_1\bar{e}_1 & -\upsilon_2\bar{e}_1 & -\upsilon_1 & -\upsilon_2 \\ -1 & 0 & -\bar{e}_2 & -\bar{e}_2 & \bar{e}_1 & 0 & 1 & 1 \\ -1 & -1 & \bar{e}_2 & -\bar{e}_2 & \hat{K}_{65} & \hat{K}_{66} & \hat{K}_{67} & \hat{K}_{68} \\ 0 & 0 & 0 & 0 & -1 & -z_1 & -\bar{e}_1 & -z_1\bar{e}_1 \\ 0 & 0 & 0 & 0 & \hat{K}_{85} & \hat{K}_{86} & \hat{K}_{87} & \hat{K}_{88} \end{bmatrix}$$

$$\hat{K}_{21} = 1 + s_n^+ \upsilon_1 \qquad (5.15)$$

$$\hat{K}_{22} = 1 + z_2 + s_n^+ (2+\upsilon_1 z_2)$$

$$\hat{K}_{23} = -\bar{e}_2 + s_n^+ \upsilon_1\bar{e}_2$$

$$\hat{K}_{24} = (1-z_2)\bar{e}_2 + s_n^+ (-2+\upsilon_1 z_2)\bar{e}_2$$

$$\hat{K}_{35} = \bar{e}_1 (-1+s_n^* \upsilon_1)$$

$$\hat{K}_{36} = \bar{e}_1 (-1+2 s_n^*)$$

$$\hat{K}_{37} = 1 + \upsilon_1 s_n^*$$

$$\hat{K}_{38} = -1 - 2 s_n^*$$

$$\hat{K}_{85} = -1 + \bar{s}_n \upsilon_1$$

$$\hat{K}_{86} = -z_1 + \bar{s}_n (2+\upsilon_1 z_1)$$

$$\hat{K}_{87} = -\bar{e}_1 + \bar{s}_n \upsilon_1 \bar{e}_1$$

$$\hat{K}_{88} = (1-z_1)\bar{e}_1 + \bar{s}_n (-2+\upsilon_1 z_1)\bar{e}_1$$

In the calculation of stresses it has been found convenient to use

$$\psi_n^+ = \sum_{i=1}^{4} \hat{q}_i^+ \hat{\zeta}_i \qquad (5.16)$$

$$\psi_n^- = \sum_{i=1}^{4} \hat{q}_i^- \hat{\zeta}_i$$

where

$$\hat{\zeta}_1 = e^{\nu_n \bar{X}_2} \; ; \; \hat{\zeta}_2 = \nu_n \bar{X}_2 \hat{\zeta}_1 \; ; \; \hat{\zeta}_3 = e^{-\nu_n \bar{X}_2} \; ; \; \hat{\zeta}_4 = \nu_n \bar{X}_2 \hat{\zeta}_3$$

$$\hat{\underset{\sim}{q}}^+ = \begin{bmatrix} \bar{e}_1\bar{e}_2 & -\nu_n a_2 \bar{e}_1\bar{e}_2 & 0 & 0 \\ 0 & \bar{e}_1\bar{e}_2 & 0 & 0 \\ 0 & 0 & 1/\bar{e}_1 & -\nu_n a_2/\bar{e}_1 \\ 0 & 0 & 0 & 1/\bar{e}_1 \end{bmatrix} \hat{\underset{\sim}{h}}^+$$

$$\hat{\underset{\sim}{q}}^- = \begin{bmatrix} 0 & 0 & \bar{e}_1 & \nu_n a_2 \bar{e}_1 \\ 0 & 0 & 0 & -\bar{e}_1 \\ 1 & \nu_n a_2 & 0 & 0 \\ 0 & -1 & 0 & 0 \end{bmatrix} \hat{\underset{\sim}{h}}^-$$

With the help of (5.16) and the notation

$$\bar{\xi} = \frac{Z_1}{a_1} \qquad \bar{\eta} = \frac{Z_2}{a_2} \tag{5.17}$$

the stresses can be written as

$$\begin{Bmatrix} T_{11} \\ T_{22} \\ T_{12} \end{Bmatrix} = \sum_{n=1}^{\infty} \begin{bmatrix} \sin\nu_n a_1 \bar{\xi} & & \\ & \sin\nu_n a_1 \bar{\xi} & \\ & & -\cos\nu_n a_1 \bar{\xi} \end{bmatrix} \underset{\sim n}{\Lambda} \begin{Bmatrix} \hat{\zeta}_1 \\ \hat{\zeta}_2 \\ \hat{\zeta}_3 \\ \hat{\zeta}_4 \end{Bmatrix} + \begin{Bmatrix} 0 \\ \sigma_o \\ 0 \end{Bmatrix} \tag{5.18}$$

where $\underset{\sim n}{\Lambda}$ in the case of the upper part of the plate becomes

$$\underset{\sim n}{\Lambda}^{+} = \begin{bmatrix} \hat{q}_1^{+} + 2\hat{q}_2^{+} & \hat{q}_2^{+} & \hat{q}_3^{+} - 2\hat{q}_4^{+} & \hat{q}_4^{+} \\ -\hat{q}_1^{+} & -\hat{q}_2^{+} & -\hat{q}_3^{+} & -\hat{q}_4^{+} \\ \hat{q}_1^{+} + \hat{q}_2^{+} & \hat{q}_2^{+} & \hat{q}_4^{+} - \hat{q}_3^{+} & -\hat{q}_4^{+} \end{bmatrix} \tag{5.19}$$

By using (5.19), the axial force carried by the intermediate stiffener results in

$$\tau^{*} = \frac{R^{*}}{Eh} (\psi_{,22} - \upsilon\psi_{,11}) = s^{*} \sum_{n=1}^{\infty} \epsilon_n \sin\nu_n a_1 \bar{\xi} \tag{5.20}$$

where

$$\epsilon_n = \sum_{j=1}^{4} (\Lambda^{-}_{n1j} - \Lambda^{-}_{n2j}) \hat{\zeta}_j \Big|_{\bar{\eta}=\alpha_2} \tag{5.21}$$

$$\alpha_2 = \frac{a_2}{\hat{a}_2} \tag{5.22}$$

Numerical Results.

The plate analysed has the following characteristics

$$\hat{a}_2/a_1 = 0.5; \quad \alpha_2 = 2/3; \quad \nu = 0.3$$

A sinusoidal load has been applied to the top edge of the plate, i.e.

$$n = 1; \quad \sigma_1^+ = 1; \quad \tau_1^+ = \sigma_1^- = \tau_1^- = 0$$

The results are given by the matrix

$$[\hat{h}^+ \quad \hat{h}^-]^T$$

as follows

1) $s^* = 0{,}043; \quad s^+ = s^- = 0{,}5$

$$\begin{bmatrix} -1.69283 & 0.883257 & 0.324864 & 0.122363 \\ 0.920436 & -0.358673 & -1.00098 & -0.526750 \end{bmatrix}$$

2) $s^* = 0.043; \quad s^+ = s^- = 0$

$$\begin{bmatrix} -2.95051 & 2.21321 & 1.00923 & 0.625182 \\ 2.90384 & -1.73015 & -1.75766 & -1.29307 \end{bmatrix}$$

3) $s^* = 0.5; \quad s^+ = s^- = 0$

$$\begin{bmatrix} -2.88251 & 2.13157 & 0.939086 & 0.677765 \\ 2.81008 & -1.68288 & -1.75462 & -1.17553 \end{bmatrix}$$

5.2 Lateral Buckling of Simply Supported Stiffened Rectangular Plates by the Ritz Method.

The lateral buckling of the plate of Fig. 5.1 is carried out assuming a double Fourier series as the deflection pattern. Considering an intermediate stiffener of bending rigidity I^*E^*, the expression of virtual work (see (3.3)) for the lateral buckling of simply supported plates becomes

$$\iint_{\Omega} D\nabla^2 w\ \delta\nabla^2 w d\Omega + \int_o^{a_1} E^* I^* w_{,11}\delta w_{,11} \Big|_{Z_2=a_2} dZ_1 =$$

$$= -P\left[\iint_{\Omega} T_{\gamma\alpha} w_{,\gamma}\delta w_{,\alpha} d\Omega + \int_o^{a_1} \tau^* w_{,1}\delta w_{,1} \Big|_{Z_2=a_2} dZ_1\right] \qquad (5.23)$$

where $T_{\gamma\alpha}$ is given by (5.18) and τ^* by (5.20).

Let

$$\hat{\gamma} = \frac{\hat{a}_2}{a_1} \quad ; \quad \gamma = \frac{a_2}{a_1} \quad ; \quad \alpha_2 = \frac{a_2}{\hat{a}_2} \qquad (5.23)$$

The deflection w is given by n_e normalized coordinate functions in the form

$$w = \sum_{i=1}^{n_e} q_i \frac{\sqrt{2}\,\varphi_i}{\gamma(\pi\mu_1)^2|\varphi_i|} \qquad (5.24)$$

where the quantity $|\varphi_i|$ is proportional to the bending energy corresponding to the function

$$\varphi_i = \sin\pi\mu_i\bar{\xi}\sin\pi\rho_i\eta \qquad (5.25)$$

Choosing an equal number of integers μ_i and ρ_i in (5.24), the expressions

$$\rho_i = \left\langle (i-1)/\sqrt{n_e} \right\rangle + 1 \qquad (5.26)$$

$$\mu_i = 2[i - (\rho_i - 1)\sqrt{n_e}] - 1$$

give a symmetric function φ_i for any $i = 1,2,\ldots, n_e$.

Substitution of (5.24) into (5.23) produces the eigenvalue problem

$$\lambda_o \underset{\sim}{K}\, \underline{q} = \underset{\sim}{S}\, \underline{q} \qquad (5.27)$$

where

$$\lambda_o = -\frac{D}{a_1 P} \qquad (5.28)$$

$$K_{ii} = 1$$

$$K_{ij} = \frac{I_o^* \sin\pi\rho_i\alpha_2 \sin\pi\rho_j\alpha_2}{|\varphi_i|\,|\varphi_j|} \qquad \text{when } \mu_i = \mu_j$$

$$K_{ij} = 0 \qquad \text{when } \mu_i \neq \mu_j$$

$$I_o^* = \frac{I^* E^*}{a_2 D}$$

$$|\varphi_i|^2 = \left[1 + \left(\frac{\rho_i}{\mu_i \gamma}\right)^2\right]^2 + I_o^* \sin^2 \pi \rho_i \alpha_2$$

$$S_{ij} = \frac{2}{(\pi\mu_i\mu_j\gamma)^2\,|\varphi_i|\,|\varphi_j|}\left[\gamma\mu_i\mu_j(*) + \frac{1}{\gamma}\rho_i\rho_j(**) - \right.$$

$$\left. - \mu_i\rho_j(***) - \rho_i\mu_j(****) + s^*\mu_i\mu_j(*****) + \frac{\sigma_o}{4}\delta_{ij}\right]$$

$$\delta_{ii} = 1$$

$$\delta_{ij} = 0 \quad \text{when } i \neq j$$

$$(*) = \sum_{n=1}^{\infty} \sum_{k=1}^{4} [\bar{\Lambda}_{n1k} \int_{o}^{\gamma} \hat{\zeta}_k \sin n\pi\rho_i \bar{\eta} \sin n\pi\rho_j \bar{\eta} d\bar{\eta} +$$

$$+ \Lambda^{+}_{n1k} \int_{\gamma}^{1} \hat{\zeta}_k \sin n\pi\rho_i \bar{\eta} \sin n\pi\rho_j \bar{\eta} d\bar{\eta}] \times$$

$$\times \int_{o}^{1} \sin n\pi(2n-1)\bar{\xi} \cos n\pi\mu_i \bar{\xi} \cos n\pi\mu_j \bar{\xi} d\bar{\xi}$$

with similar formulae for (**), (***), (****) and

$$(*****) = \sum_{n=1}^{\infty} \epsilon_n \sin n\pi\rho_i\alpha_2 \sin n\pi\rho_j\alpha_2 \int_{o}^{1} \sin n\pi(2n-1)\bar{\xi} \cos n\pi\mu_i \bar{\xi} \cdot$$

$$\cdot \cos n\pi\mu_j \bar{\xi} d\bar{\xi}$$

5.3. Lateral Buckling of Rectangular Plates with Stiffeners of Infinite Axial Rigidity.

This problem has already been mentioned in Art. 2.9. The plane stress distribution is given by (2.142) and the buckling load corresponds to the minimum of

$$P = \frac{\int\int_{\Omega} M^{\gamma\alpha} \delta\varkappa_{\gamma\alpha} d\Omega + \int_{o}^{a_2} E^* I^* w_{,22}^2 \Big|_{Z_1=a_1} dZ_2 + \int_{o}^{a_2} G^* J^* w_{,12}^2 \Big|_{Z_1=a_1} dZ_2}{\int_{o}^{a_1} w_{,2}^2 \Big|_{Z_1=a_1} dZ_2} \qquad (5.29)$$

Let $\bar{\xi}$ be given by (5.17) and let $\bar{\xi}_i$ be the coordinate $\bar{\xi}$ at point i of Fig. 5.2(a). At the point $\bar{\xi}_i$ the symbol $[\cdots]_{\bar{\xi}_i}$ will denote the jump of the quantity inside the brackets.

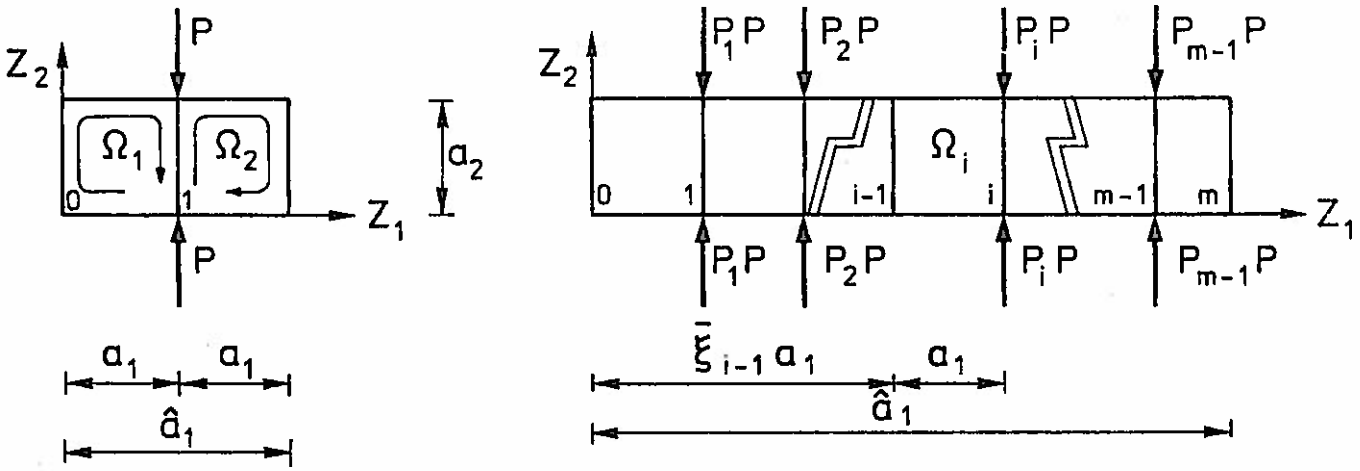

Fig. 5.2. Simply supported stiffened plates.

The minimization of (5.29) and later the application of Green's formula lead to an expression of the form *

$$\ldots \int_0^{a_2} [M_{11}]_{\bar{\xi}_1} \delta\omega_{,1} dZ_2 - \int_0^{a_2} [M_{11,1} + 2M_{12,2}]_{\bar{\xi}_1} \delta\omega dZ_2 +$$

$$+ [P\omega_{,1}\delta\omega + E^*I^*\omega_{,22}\delta\omega_{,2} - E^*I^*\omega_{,222}\delta\omega + G^*J^*\omega_{,12}\delta\omega_{,1}]_{0\bar{\xi}=\bar{\xi}_1}^{1} +$$

$$+ \int_0^{a_2} [P\omega_{,22}\delta\omega + E^*I^*\omega_{,2222}\delta\omega + G^*J^*\omega_{,122}\delta\omega_{,1}]_{\bar{\xi}=\bar{\xi}_1} dZ_2 = 0$$

---

* This form may be obtained from (1.112) considering the plate initially flat and subjected only to the forces P.

For simply supported longitudinal edges ($Z_2=0$ and $Z_2=a_2$) the conditions

$$w = w_{,1} = w_{,11} = w_{,22} = 0$$

eliminate the terms outside of the integrals in (5.30). In this manner the boundary conditions at $\bar{\xi}=\bar{\xi}_1$ become

$$- D \left[w_{,11} + \nu\, w_{,22}\right]_{\bar{\xi}_1} - G^* J^*\, w_{,221} = 0 \qquad (5.31)$$

$$- D \left[w_{,111} + (2-\nu) w_{,221}\right]_{\bar{\xi}_1} - E^* I^*\, w_{,2222} = P\, w_{,22}$$

The expression

$$w = W_n \sin n\pi\bar{\eta} \qquad (5.32)$$

satisfies the conditions for simply supported edges at $\bar{\eta}=0$ and $\bar{\eta}=1$. Substitution of (5.32) into the governing differential equation of the problem

$$- D\, w_{,\gamma\alpha\gamma\alpha} = 0 \qquad (5.33)$$

gives

$$W_{n,1111} - 2\left(\frac{n\pi}{a_2}\right)^2 W_{n,11} + \left(\frac{n\pi}{a_2}\right)^4 W_n = 0 \qquad (5.34)$$

With (5.32) the boundary conditions at $\bar{\xi} = \bar{\xi}_1$, given by (5.31), become

$$- D \left[W_{n,11} - \left(\frac{n\pi}{a_2}\right)^2 W_n\right]_{\bar{\xi}_1} + G^* J^* \left(\frac{n\pi}{a_2}\right)^2 W_{n,1} = 0 \qquad (5.35)$$

$$- D \left[W_{n,111} - \left(\frac{n\pi}{a_2}\right)^2 W_{n,1}\right]_{\bar{\xi}_1} - \left(\frac{n\pi}{a_2}\right)^2 E^* J^* W_n = -\left(\frac{n\pi}{a_2}\right)^2 P\, W_n$$

The solution ot (5.34) can be given in the form

$$W_n = (\bar{Z}_1 + \bar{Z}_2\, \varkappa_n\, \bar{\xi}) \cosh \varkappa_n \bar{\xi} + (\bar{Z}_3 + \bar{Z}_4\, \varkappa_n\, \bar{\xi}) \sinh \varkappa_n \bar{\xi} \tag{5.36}$$

where $\varkappa_n = n\pi/\gamma$ and the constants $\bar{Z}_1$, $\bar{Z}_2$, $\bar{Z}_3$ and $\bar{Z}_4$ for each n depend on the boundary conditions at the transversal edges of the plate.

The function W_n may be assumed symmetrical with respect to $\bar{\xi} = \frac{1}{2}$ when the boundary conditions at the transversal edges are identical. In this case $(5.35)_1$ is satisfied immediately and $(5.35)_2$ produces the following expression

$$P = \left(\frac{n\pi}{a_2}\right)^2 E^* I^* - 2D \left(\frac{a_2}{n\pi}\right)^2 \left.\frac{W_{,n,111}}{W_n}\right|_{\bar{\xi}=\frac{1}{2}} \tag{5.37}$$

The first term in the right hand side of (5.37) constitutes Euler's buckling load for the stiffener and the second term corresponds to the buckling load of the plate without stiffeners.

The condition

$$W_{n,1} = 0 \qquad \text{at } \bar{\xi} = \tfrac{1}{2} \tag{5.37}$$

and simply supported edges at $\bar{\xi} = 0$ and $\bar{\xi} = 1$ produces the following results

$$P = \left(\frac{n\pi}{a_2}\right)^2 E^* I^* + 4\, D \frac{n\pi}{a_2} \frac{1}{\tanh \varkappa_n - \dfrac{\varkappa_n}{\cosh^2 \varkappa_n}} \tag{5.38}$$

$$W_n = \bar{Z}_2 \left[2\varkappa_n \bar{\xi} \cosh 2\, \varkappa_n \bar{\xi} - (\varkappa_n \tanh \varkappa_n + 1) \sinh 2\, \varkappa_n\, \bar{\xi}\right]$$

The buckling of the plate without stiffeners in (5.38) coincides with the result given by Timoshenko for n = 1. Thus Timoshenko's result corresponds to the exact solution of the problem discussed here whose buckling mode is given by $(5.38)_2$.

In a similar way, (5.37) and clamped edges at $\bar{\xi} = 0$ and $\bar{\xi} = 1$ lead to

$$P = \left(\frac{n\pi}{a_2}\right)^2 E^* I^* + 2D\frac{n\pi}{a_2}\,\frac{2\varkappa_n + \sinh 2\varkappa_n}{\sinh^2 \varkappa_n - \varkappa_n^2} \tag{5.39}$$

$$W_n = \bar{Z}_2\,[2\varkappa_n \bar{\xi} \cosh 2\varkappa_n \bar{\xi} - \sinh 2\varkappa_n \bar{\xi} -$$

$$- \frac{\varkappa_n \sinh \varkappa_n}{\varkappa_n \cosh \varkappa_n + \sinh \varkappa_n}\; 2\varkappa_n \bar{\xi} \sinh 2\varkappa_n \bar{\xi}]$$

Fig. 5.2(b) shows a rectangular plate simply supported at the longitudinal sides and divided up in m subdomains. A system of loads PP_i is applied at each line $\bar{\xi} = \bar{\xi}_i$ where i = 0,1,..., m+1. A stiffener of infinite axial rigidity is assumed at the transversal lines where $P_i \neq 0$. Stiffeners with different bending and torsinal rigitities may be assumed at any of the m+1 transversal lines.

It may be observed that at each intermediate stiffener an equation of the type (5.35) exists so that each subdomain's W_n is of the form (5.36) with different constants for different subdomains.

Let the subdomain Ω_i of Fig. 5.2(b) have ratios

$$\alpha_1 = a_1/\hat{a}_1; \quad \gamma = a_2/a_1 \tag{5.40}$$

and a W_n given by (5.36), or alternatively by

$$W_n = \sum_{k=1}^{4} \bar{Z}_k \zeta_k \tag{5.41}$$

where

$$\zeta_1 = e^{-\kappa_n(\xi-1)} \quad ; \quad \zeta_2 = \kappa_n \xi \, \zeta_1 \qquad (5.42)$$

$$\zeta_3 = e^{-\kappa_n \xi} \quad ; \quad \zeta_4 = \kappa_n \xi \, \zeta_3$$

$$\kappa_n = \pi n / \gamma$$

and the coordinate ξ given by

$$\xi = (\bar{\xi} - \bar{\xi}_i) \; / \; (\bar{\xi}_i - \bar{\xi}_{i-1}) \qquad (5.43)$$

Let

$$\left.\begin{aligned} w_i &= W_n \\ w_{i,1} &= W_{n,1} \end{aligned}\right\} \quad \text{when } \bar{\xi} = \bar{\xi}_i \qquad (5.44)$$

Using (5.42), (5.44) and $\bar{\epsilon} = e^{-\kappa_n}$, the expressions are as follow

$$\begin{Bmatrix} w_i \\ w_{i,1}{}^{a_1} \\ w_{i-1} \\ w_{i-1,1}{}^{a_1} \end{Bmatrix} = \begin{bmatrix} \bar{\epsilon} & 0 & 1 & 0 \\ \kappa_n \bar{\epsilon} & \kappa_n \bar{\epsilon} & -\kappa_n & \kappa_n \\ 1 & \kappa_n & \bar{\epsilon} & \kappa_n \bar{\epsilon} \\ \kappa_n & \kappa_n(1+\kappa_n) & -\kappa_n \bar{\epsilon} & \kappa_n(1-\kappa_n)\bar{\epsilon} \end{bmatrix} \underset{\sim}{Z}$$

$$\underset{\sim}{\bar{w}} = \underset{\sim}{\bar{T}}^{-1} \underset{\sim}{Z} \qquad (5.45)$$

The contribution of the subdomain to the virtual work expression (5.29) is given by

$$\frac{D}{a_1 a_2} \; \delta \underset{\sim}{\bar{w}}^T \underset{\sim}{k} \underset{\sim}{\bar{w}} \qquad (5.46)$$

where

$$\underset{\sim}{k} = \bar{T}^T \underset{\sim}{k}^* \bar{T} \tag{5.47}$$

$$\underset{\sim}{k}^* = \frac{(n\pi)^4}{2\gamma^2 a_1} \begin{bmatrix} 2(1-\nu)B & 2(1-\nu)\varkappa_n & 0 & 0 \\ & 2B+(1-\nu)(1+2\varkappa_n) & 0 & -2(1+\nu)\bar{\epsilon} \\ & \text{Symm.} & 2(1-\nu)B & (\nu-1)(B+2\bar{\epsilon}^2) \\ & & & 2B+2(1-\nu)(1-\varkappa_n)\bar{\epsilon}^2 \end{bmatrix}$$

$$B = \frac{1-\bar{\epsilon}^2}{\varkappa_n} \tag{5.48}$$

The virtual work

$$\frac{D}{\hat{a}_1 a_2} \delta[w_i \quad w_{i,1}a_1] \begin{bmatrix} \frac{E^*I^*}{Da_2} & \frac{(n\pi)^4}{2\gamma a_1} & 0 \\ 0 & \frac{G^*J^*}{Da_2} & \frac{\gamma(n\pi)^2}{a_1} \end{bmatrix} \begin{Bmatrix} w_i \\ \\ w_{i,1}a_1 \end{Bmatrix} \tag{5.49}$$

corresponds to a stiffener located at $\bar{\xi} = \bar{\xi}_i$ with a flexural rigidity E^*I^* and a torsional rigidity G^*J^*.

The contribution of a load PP_i to the geometrical virtual work in (5.29) is given by

$$\frac{PP_i}{a_2} \frac{(n\pi)^2}{2} \delta w_i w_i \tag{5.50}$$

The total virtual work of the internal forces is obtained summing all the expressions of the type (5.46) and (5.49) In a similar way the total geometric virtual work is the sum of the expressions (5.50). These sums are expressed in matrix form by

$$\lambda_o \, \delta \underset{\sim}{q}^T \, \underset{\sim}{K} \, \underset{\sim}{q} = \delta \, \underset{\sim}{q}^T \, \underset{\sim}{S} \, \underset{\sim}{q} \qquad (5.51)$$

where $\lambda_o = D/P\hat{a}_1$ and where the vector q consists of all the quantities w_i; $w_{i,1}$ a_1 $(i=1,\ldots,m+1)$. The matrix $\underset{\sim}{S}$ is diagonal and the matrix $\underset{\sim}{K}$ is symmetric with a half band width of 4. The resulting eigenvalue problem is given by (3.113) and can be solved by the iteration process discribed in Art. 3.6.

SUMMARY

Chapter 1 contains a discussion of the buckling of plates using a two dimensional theory. The equations for the buckling of a initially flat plate include the initial nonlinear in-plane stress field in addition to flexural actions given by a linear bending measure. In the usual small bending theory of plates, the use of a linear bending measure is justified by assuming small deflections. In the case of lateral buckling, the main goal is to find a deformed state of the plate infinitely close to a flat - deformed initial state (i.e. small deformations).

In chapter 2 a discussion is given of the different known trial function methods together with the boundary and continuity conditions which the functions to be used ought to satisfy. A brief description of the application of numerical methods to buckling of plates is also given. Some convergence studies are presented which apply to the problem of plate-buckling.

In chapter 3 a particular application of the Ritz method is explained. The plate's domain is divided in subdomains (Ritz-Subdomain method) and on each subdomain different coordinate functions are assumed. The total deformation field made by the local coordinate functions must satisfy the continuity and boundary conditions of the Ritz method. Two types of problems are solved, namely, plane stress and eigenvalue problems for stiffened plates.

Chapter 4 shows the comparison between the results obtained by the Ritz-Subdomain method and other analytical or numerical results. The way of obtaining the alternative results is explained in chapter 5.

The conclusion is that the Ritz-Subdomain method gives accurate results provided that a reasonable number of subdomains are used especially near the applied loads.

REFERENCES

[1] Ziegler, H. Principles of Structural Stability. Waltham, Massachusetts, 1969.

[2] Koiter, W.T. Elastic Stability and Post-buckling Behavior. In "Nonlinear Problems", R.E. Langer (ed.), University of Wisconsin Press, 1963.

[3] Washizu, K. Variational Methods in Elasticity and Plasticity. Pergamon Press, 1968.

[4] Green A.E. & Zerna W. Theoretical Elasticity. Oxford University Press, 1954.

[5] Nielsen, M.P. On the Formulation of Linear Theories for Thin Shells. Bygningsstatiske Meddelelser. Vol. 35, 1964, 37-77.

[6] Timoshenko, S.P. & Gere, J.M. Theory of Elastic Stability. McGraw-Hill, 1961.

[7] Finlayson, B.A. & Scriven, L.E. The Method of Weighted Residuals - A Review. Applied Mechanics Reviews, Vol. 19. No. 9, Sept. 1966, 735-748.

[8] Mikhlin, S.G. Variational Methods in Mathematical Physics. Pergamon Press, 1964.

[9] Mikhlin, S.G. The Problem of the Minimum of a Quadratic Functional. Holden-Day, 1965.

[10] Mikhlin, S.G. & Smolitskiy, K.L. Approximate Methods for Solution of Differential and Integral Equations. Elsevier, 1967.

[11] Crandall, S.H. Engineering Analysis. McGraw-Hill, 1956.

[12] Collatz, L. The Numerical Treatment of Differential Equations. Springer, 1960.

[13] Ames, W.F. Nonlinear Partial Differential Equations in Engineering. Academic Press, 1965.

[14] Becker, M. Principles and Applications of Variational Methods. M.I.T. Press, 1964.

[15] Sokolnikoff, I.S. Mathematical Theory of Elasticity. McGraw-Hill, 1956.

[16] Gould, S.H. Variational Methods for Eigenvalue Problems. Oxford University Press, 1966.

[17] Sobolev, S.L. Applications of Functional Analysis in Mathematical Physics. American Mathematical Society, 1963.

[18] Smirnow, V.I. A Course of Higher Mathematics, Vol. 5. Pergamon Press, 1964.

[19] Kerr, A.D. An Extension of the Kanterovich Method. Quarterly of Applied Math. V.XXVI, No. 2, July 1968, 219-230.

[20] Courant, R. & Hilbert, D. Methods of Mathematical Physics. V.1. Interscience Pub.,1953.

[21] Oliveira, E.R. Theoretical Foundations of the Finite Element Method. Int. J. Solids Structures, 1968, Vol. 4., 929-952.

[22] Zienkiewicz, O.C. The Finite Element Method in Structural and Continuum Mechanics. McGraw-Hill, 1967.

[23] Wang, C. Applied Elasticity. McGraw-Hill, 1953.

[24] Bleich, F. Buckling Strength of Metal Structures. McGraw-Hill, 1952.

[25] Bürgermeister, G., Steup, H. & Kretzschmar, H. Stabilitätstheorie, Vols. I & II. Berlin, 1961.

[26] Pflüger, A. Stabilitätsprobleme der Elastostatik. Berlin, 1964.

[27] Gerard, G. & Becher, H. Handbook of Structural Stability: Part I-Buckling of Flat Plates. Tech. Note 3781, Natl. Advisory Comm. for Aeronautics. Washington, D.C., 1957.

[28] Shuleshko, P. Buckling of Rectangular Plates Uniformly Compressed in Two Perpendicular Directions With One Free Edge and Opposite Edge Elastically Restrained. J. Appl. Mech. Vol. 23, 1956, 359-363.

[29] Salvadori, M.G. Numerical Computation of Buckling Loads by Finite Differences. Transactions, ASCE, Vo. 116, 1951, P. 590.

[30] Klöppel, K. & Sheer, J. Beulwerte Ausgesteifter Rechteckplatten. Wilhelm Ernst, 1960.

[31] Webster, J.J. Free Vibrations of Rectangular Curved Panels, Int. J. Mech. Sci. Vol. 7, July 1968, 571-582.

[32] Fox, L. Mixed Boundary Conditions in the Relaxational Treatment of Biharmonic Problems. Proc. Roy. Soc. A, 189 (1947), 535-543.

[33] Oliveira, E.R. Plane Stress Analysis by a General Integral Method. J. Emd. Vol. 94, No. EMI, Feb. 1968, 79-101.

[34] Griffin, D.S. & Varga, R.S. Numerical Solution of Plane Elasticity Problems. J. Soc. Indust. Appl. Math. Vol. 11, No. 4, Dec. 1963, 1047-1062.

[35] Conway, H.D. Show, L. & Morgan, G.W. Analysis of Deep Beams, J. Appl. Mech. Vol. 18, 1951, 163-172.

[36] Somerfield, Z. Z. Math. Phys. 54 (1906).

[37] Leggett, D.M.A. The Effect of Two Isolated Forces on the Elastic Stability of a Flat Rectangular Plate. Proc. Cambridge Phil. Soc. Vol. 33, 325-339.

[38] Zetlin, L. Elastic Stability of Flat Plates Subjected to Partial Edge Loads. Proc. Paper 795, ASCE, Vol. 81, Sept. 1955.

[39] White, M. & Cottingham, W. Stability of Plates under Partial Edge Loads. J. Emd. Div. Proc. ASCE 85, 67 (1962).

[40] Timoshenko, S.P. & Goodier, J.N. Theory of Elasticity. McGraw-Hill, 1951.

[41] Peklov, N.A. Stability of a Hinge-Supported Rectangular Plate Loaded in its Plane with a Local Load. Clearing-house, U.S. Department of Commerce, AD. 670063 (1967).

[42] Rockey, K.C. & Baghi, D.K. Buckling of Plate Girder Webs under Partial Edge Loadings. J. Mech. Sci. 1970, Vol. 12, 61-76.

[43] Holand, I. & Bell, K. Finite Element Methods in Stress Analysis. Tapir, Norway, 1969.

[44] Hansteen, H. Finite Element Analysis of Plate Bending Based on Rectangular Elements. Int. Symposium, The Use of Elect. Computers in Civ. Eng. Univ. of Newcastle, Dept. Civ. Eng.

[45] Faddeeva, V. N. Computational Methods of Linear Algebra. Dover, 1959.

[46] Forsythe, G. & Moler, C.B. Computer Solution of Linear Algebraic Systems. Prentice-Hall, 1967.

NOTATION

A matrix is represented in the form

$$\underset{\sim}{K} = [K_{ij}]$$

where K_{ij} is the element corresponding to the ith. row and jth. column.

The transpose of the matrix $\underset{\sim}{K}$ is $\underset{\sim}{K}^{T}$.

A column vector of n components can be written as

$$\underset{\sim}{W} = [W_1 \; W_2 \; \cdots \; W_n]^T = \begin{Bmatrix} W_1 \\ W_2 \\ \vdots \\ W_n \end{Bmatrix}$$

Vectors are denoted, for example, as $\vec{P}$, $\vec{P}$.

The remaining symbols are defined in the following pages

In particular pages 3, 4, 5, 6, 40, 41, and 42 contain definitions for various symbols.

LIST OF SYMBOLS

$\vec{a}_\alpha ; \vec{a}_3$	deformed surface base vectors	6
$\vec{A}_\alpha$	undeformed surface base vectors	6
$A_{\alpha\beta} ; A_{33}$	fundamental undeformed surface tensor	6
a	determinant of $[A_{\alpha\beta}]$	6
	constant in (2.1) and (2.2)	40
$A_o ; A_i ; \hat{A}_i$	differential operators	45
$\hat{a}_\alpha$	overall dimensions of a rectangular subdomain Fig.3.116	92
a_α	dimensions of a rectangular subdomain	92
$\hat{a}_\lambda$	constant diagonal matrix (3.64)	109
$b_{\gamma\alpha}$	second fundamental tensor of the deformed surface (1.29)	11
$B_{\gamma\alpha}$	second fundamental tensor of the undeformed surface (1.54)	15
$B_\lambda^* ; B_3^*$	prescribed body forces other than inertia	34
$\hat{b}_{\gamma\alpha}$	second fundamental tensor of the deformed surface at the initial state	36
b	constant in (2.1) and (2.2)	40
$b_o ; \ldots ; b_3$	constants in (3.13)	94
$\hat{b}_{K\alpha i}$	coefficients of (3.26)	97
b_{Kij}	coefficients of (3.37)	99
$\underline{b}^*$	flexural stiffness matrix $(3.57)_2$ for ribs	105
b_o	constant in (3.67)	110
B	constant defined by (5.48)	175
C	undeformed plate's contour (1.14)	6
C_1	plate's contour where forces are prescribed	8
C_2	plate's contour where displ. are prescribed	8
c_o	deformed plate's contour	8

$C^{\gamma\alpha\beta\mu}$	tensor of elastic constants (in-plane) (1.64)	19
$C_1^{(i)}$	designates a point i of a contour C_1 where the torsional moment is discontinuous (1.73)	22
C_f	plate's contour where follower forces are prescribed (1.121)	35
C_x	domain's contour at X_1=const. (2.40)	50
C_y	domain's contour at X_2=const.	51
$\overline{C}_1$	contour where bending moments are prescribed $(2.115)_2$	71
$\overline{C}_2$	contour where rotations are prescribed $(2.116)_2$	71
ΔC_1	subdomain's contour with applied loads	96
$\vec{d}_\gamma$	vector defined by (1.43)	13
$d_{\gamma\alpha}$	$=\vec{d}_\gamma \cdot \vec{d}_\alpha$	13
d	$=\det d_{\gamma\alpha}$	13
$D^{\gamma\alpha\beta\mu}$	tensor of constants relating bending moments and bending measures	19
D	plate's flexural rigidity (1.80)	25
$\overline{d}$	minimum of a functional (2.64)	59
d_{iK}	constants to be determined from an orthogonal process (2.128)	79
$d_o;\ldots;d_3$	constants in the expression (3.13)	94
$\hat{D}_{\alpha i}$	integrands of (3.25) in the plane stress case	97
$\hat{d}_{1\alpha i}$	coefficients of the polynomial in (3.26)	97
D_{ij}	matrix element in (3.37)	99
$e_{\beta\lambda}$	surface permutation tensor $(1.16)_3$	7
E	Young's modulus of elasticity	20
$\tilde{E}_{\gamma\alpha}$	linear strain measure for the adjacent state which includes effects of a nonlinear initial state section 1.3, (1.99) section 1.4, (1.107) section 1.4, $(1.125)_2$	 29 31 37

$E^{(n)}_{\alpha\beta}$; $E^{(o)}_{\alpha\beta}$	linear in-plane strain measures corresponding respectively to a Ritz solution and to the exact solution	66
e	number of coordinate functions for each displacement in each subdomain (2.125)	77
$e_1;\ldots;e_5$	constants in (2.140)	82
E^*	modulus of elasticity for a stiffener	104
$\overline{e}_\alpha$	constants defined by (5.14)	162
$f^{\alpha\beta}$	stress tensor defined wrt. $\vec{a}_\alpha$; $\vec{a}_3$ (1.21)	9
	stress tensor defined wrt. $\vec{a}_\alpha;\vec{A}_3$ (1.30)	11
	stress tensor defined in section 1.3 wrt. $\vec{a}_\alpha;\vec{a}_3$ in (1.124) and (1.126)	37
$\vec{f}_{(n)}$	force per unit length on a face with a unit normal n_β $(1.118)_2$	8
$\vec{F}^*_{(n)}$	prescribed force per unit length of the contour C_1 in the undeformed configuration	8
$\vec{f}_\gamma$	force per unit length on a face γ in the deformed configuration (1.21)	9
$F^{\gamma\alpha}$	stress tensor defined wrt. $\vec{d}_\alpha$ (1.45)	13
$\vec{F}_\gamma$	force per unit length on the face γ in the deformed configuration (1.63)	18
$\overset{\Delta}{F}_\gamma$; F_γ	force components acting on the contour C_1 respectively for the initial and adjacent states	28
$\hat{F}^{\gamma\alpha}$	stress vector in the initial undeformed state defined wrt. $\vec{d}_\alpha$	30
$\vec{F}^{**}$	force acting on the contour C_1 of the initial configuration	30
$\widetilde{F}^{\gamma\alpha}$	related to a linear strain measure by $(1.109)_2$	31
$\hat{f}^{\alpha}_{(n)}$	components of the force per unit length of contour C_f where follower forces exist	35
f_o	function defined on a surface (2.18)	44
F(U)	functional to be minimized where U satisfies homogeneous geometrical B.C.	43

f_i	functions defined on the contour s_i (2.24)	46
$F_1(w)$	functional to be minimized where w satisfies inhomogeneous geometrical B.C. (2.55)	57
$\hat{f}_j$	functions which define homogeneous geometrical B.C. (2.56)	57
$F^{*\alpha}_{(n)}$	components of $\vec{F}^{**}_{(n)}$ in the directions $\vec{A}_\alpha$ (3.31)	98
$\hat{\underset{\sim}{f}}^*_\alpha$	subdomain's generalized loads in the direction X_α (3.32)	98
$\overline{F};\overline{F}^*$	shorthand notation in (3.69)	99
$F_1;\ldots;F_4$	value of $\overline{F}$ at the corners of a subdomain	99
F^*_2	value of $\overline{F}^*$at the corner 2	116
$\hat{\underset{\sim}{f}}$	subdomain's generalized loads	122
$\hat{\underset{\sim}{F}}$	global matrix of generalized loads (3.101)	123
$\vec{G}_I$	base vectors in the undeformed state (1.5)	5
G_{IJ}	fundamental tensor in the undeformed configuration (1.6)	5
$\vec{g}_j$	base vectors in the deformed configuration	7
g_o	arbitrary function (2.48)	55
G_{iJK}	integral in the subdomain's geometric matrix (3.44)	101
G^*	shear modulus of elasticity for a stiffener	104
$\underset{\sim}{g}^*$	geometric matrix for a stiffener (3.58)	105
h	plate's thickness	20
$H_o;H_i$	differential operators (2.27)	47
H^*_o	the adjoint of the operator H_o (2.47)	55
$H_o(\xi,\xi_i)$	cubic polynomials (3.9)	90
$H_1(\xi,\xi_i)$	cubic polynomials (3.9)	90
$H'_o;H'_1$	derivatives of the cubic polynomials (3.9) wrt. the variable ξ (3.11)	93
$\hat{\underset{\sim}{b}}^*_\alpha$	parameters in the displacement U_α corresponding to a subdomain (uniform mesh) (3.17)	95

H_{ijK}	integral in the subdomain's matrix (3.44)	101
$\hat{\underset{\sim}{h}}_{\alpha}$	vector proportional to $\hat{\underset{\sim}{h}}^{*}_{\alpha}$ (3.45)	102
$\hat{\beta}^{**}_{\alpha}$	subdomain's parameter in the displ. U_{α} for a variable mesh (3.90)	120
$\hat{\underset{\sim}{H}}^{*}$	vector which includes the parameters for the in-plane displ. in a subdomain (3.117)	128
$\hat{\underset{\sim}{H}}^{**}$	vector which includes the parameters for the in-plane displ. in a subdomain adjacent to a stiffener	128
$\hat{h}^{+}_{i};\hat{h}^{-}_{i}$	parameters of the stress functions (5.11) for a rectangular plate divided in two rectangles	161
I	functional of the Least Squares method (2.41)	52
I_1	functional of Courant's method (2.46)	54
$\bar{I}$	functional of the Adjoint Variational method (2.48)	55
I_{ijK}	integral in the subdomain's geometric matrix (3.44)	101
I^{*}	modulus of inertia for a stiffener	104
I^{*}_{λ}	ratio $(3.61)_2$: stiffener's flexural rigidity/ plate's rigidity / stiffener's length	107
I^{*}_{o}	ratio in (3.28)	168
J	quadratic functional (2.1)	40
$J_H;J_M$	quadratic functionals of an eigenvalue problem (2.28)	47
J_{ijK}	integral in the subdomain's geometric matrix (3.44)	101
J^{*}	torsion constant for a stiffener	104
J^{*}_{λ}	ratio $(3.61)_3$: stiffener's torsional rigidity/ plate's rigidity/ stiffener's length	107
K	constant in (2.68)	60
$K_1;\ldots;K_6$	constants in section 2.6	63
K^{*}_{rs}	system of linear functions	84

$\hat{\underset{\sim}{k}}^*$	subdomain's in-plane stiffness (3.30) for uniform mesh parameters	98
$\hat{k}$	subdomain's in-plane stiffness matrix (3.98)	122
$\hat{K}$	global in-plane stiffness matrix (3.112)	123
k^*	subdomain's flexural stiffness matrix for uniform mesh parameters	100
k	subdomain's flexural stiffness matrix (3.108)	125
K	global flexural stiffness matrix (3.112)	126
$\hat{k}_o$	in-plane stiffness matrix for a subdomain adjacent to an intermediate stiffener (3.119)	128
$L(\ldots)$	linear functional (2.2)	41
l	number of mechanical B.C. (2.20)	45
L_1	linear functional in (2.55)	57
$L_2^{(1)}$	index identifying the norm (2.86)	64
$L_2^{(2)}$	index identifying the norm (2.103)	67
L_q	index identifying the norm (2.102)	67
$\hat{\underset{\sim}{1}}$	nodal parameters of the displ. U_1 for a stiffener segment between nodes 1 and 2 in a uniform mesh subdivision (3.54)	104
$\hat{\underset{\sim}{1}}_o$	same as above for a variable mesh (3.63)	108
$\hat{\underset{\sim}{1}}^*$	nodal parameters of the displ. U_2 for a stiffener between nodes 2 and 4 in a uniform mesh subdivision (3.78)	116
$\hat{L}_i^*$	the order which the displ. U_1 at a node i occupies in the global vector of parameters	127
L_k^*	order which the deflection w at a node k occupies in the global vector of parameters	131
$\bar{L}$	triangular matrix	139
$m^{\gamma\beta}$	tensor of mements referred to the deformed surface (1.18)	8
$\vec{m}_{(n)}$	moment per unit length of deformed contour (1.18)	8
$\vec{m}_\gamma$	moment per unit length of deformed face γ $(1.21)_2$	9

$\vec{M}_\gamma$	moment per unit length of undeformed face γ $(1.30)_2$	11
$M^{\gamma\alpha}$	tensor moment referred to the undeformed surface $(1.30)_2$	11
$\vec{M}_{(n)}$	moment per unit length of contour C_1 (1.48)	14
m_1	number of discontinuities of the torsional moment on the contour C_1 (1.73)	22
$M_{(NT)}$	torsional moment per unit length of contour C_1 (1.78)	23
$M_{(NN)}$	bending moment per unit length of contour C_1 (1.78)	23
$\hat{M}^{\gamma\alpha}$	moment tensor at the initial state referred to the undeformed configuration (1.105)	31
$\vec{M}^{**}$	flexural moment per unit length in the initial state (1.105)	31
$\vec{M}^{*}_{(n)}$	increment of flexural moment per unit length of contour C_1 in the adjacent state (1.105)	31
$M^{*}_{(NT)}$	prescribed torsional moment per unit length of contour C_1 (1.112)	32
$M^{*}_{(NN)}$	prescribed bending moment per unit length of contour C_1 (1112)	32
M	plate's mass per unit undef. area (1.118)	34
$\hat{m}^{\gamma\alpha}$	nonlinear moment tensor at the deformed initial state (1.124)	37
$M_j; M_o$	differential operators (2.28)	47
M^{*}_o	the adjoint operator of M_o (2.53)	56
N_α	components of the unit vector normal to the undeformed plate's contour (1.14)	6
$\vec{N}$	unit normal vector with components N_α (1.70)	21
n_o	number of points collocated on the domain Ω (2.35)	49
n_i	number of points collocated on the contours s_1 (2.35)	49
n_e	number of subdomains	76
	number of coordinate functions (5.24)	167

O_α	integers O_1=20 for longitudinal stiffeners and O_2=18 for transversal stiffeners (3.125)	130
P	load parameter Fig. 1.1	1
P_c	critical load parameter Fig.1.1	1
$\vec{P}$	prescribed load per unit undeformed area (1.19)	8
$p^\alpha p^3$	components of the load per unit deformed area (1.19)	8
$P^\alpha; P$	components of the load per unit undeformed area (1.56)	16
$\hat{P}_\gamma$	prescribed load component per unit undeformed area at the initial state (1.97)	28
$\vec{P}^{**}$	prescribed load per unit undeformed area at the initial stage (1.105)	31
$\vec{P}^*$	increment of the load per unit undeformed area at the adjacent state (1.105)	31
$P^*_\gamma; P^{*3}$	components of $\vec{P}^*$ (1.130)	38
$\overline{P}_o; \overline{P}_j$	positive weighting functions (2.41)	52
$P_o; P(t)$	static and dynamic load parameters (2.118)	72
q^α	tensor of shear forces in the deformed slab (1.17)	8
q	shear force per unit length of deformed contour (1.17)	8
Q^γ	tensor of shear forces in the undef. slab(1.45)	13
q_i	parameters which multiply coordinate functions (2.31)	48
$\overline{q}_i$	second set of unknown parameters of the Extended Kanterovick's method	50
q^*_i	parameters which expand the adjoint function (2.54)	56
$\hat{q}_i$	constants in (2.68)	60
$q_i^{(j)}$	unknown subdomain's parameters included in a trial function (2.125)	77
q_{nK}	k^{th} parameter in a trial solution with n coordinate functions (2.133)	80

$\bar{q}_{ij}$	parameters in the Fourier series (2.143)	84
Q_{1ij}	the set includes all the coefficients which are necessary for calculating the subdomain's geometric matrix (3.48)	102
$\underset{\sim}{Q}_o$	matrix function used for transforming the matrices resulting from the stiffeners (3.67)	110
$\underset{\sim}{\hat{q}}^*$	global parameters in the plane stress analysis	120
$\underset{\sim}{q}$	global parameters in the eigenvalue analysis	120
$\underset{\sim}{\hat{q}}$	vector proportional to $\underset{\sim}{\hat{q}}^*$ (3.104)	124
$\underset{\sim}{q}(o)$	starting vector for an iteration solution of an eigenvalue problem	138
$\underset{\sim}{q}(k)$	vector in the k^{th} iteration in the solution of an eigenvalue problem	140
$\vec{R}$	position vector in Fig. 1.2	4
$\vec{r}$	position vector in Fig. 1.2	4
R_o	first residual defined on the domain Ω (2.28)	47
R_j	residuals on the contours s_j (2.29) and (2.30)	47
r_i^*	constants defined by (3.91)	120
$\underset{\sim}{\hat{R}}$	relates local and global parameters in the plane stress analysis (3.96)	121
$\underset{\sim}{\hat{R}}_n$	relates the local parameters of a stiffener's segment with the global parameters (3.97)	122
$\underset{\sim}{R};\underset{\sim}{R}_1;\underset{\sim}{R}_1^*$	relate local and global parameters in an eigenvalue analysis as given by (3.107)	124
$R^+;R^*;R^-$	axial rigidities of the stiffeners in Fig.5.1	158
$\hat{s}_i$	contours where geometrical B.C. are prescribed (2.22)	45
s_i	contours where mechanical B.C. are prescribed (2.22)	45
$S_1;\ldots;S_5$	contours where homogeneous geometrical B.C. are prescribed in Art. 2.6	63
$S^{\gamma\alpha}$	in-plane stress tensor for "dynamic" loads (2.118)	72

$\underset{\sim}{s}^*$	subdomain's geometric matrix in a uniform mesh subdivision (3.43)	101
S^*	stiffener's cross sectional area	104
S^*_λ	ratios (3.61): stiffener's axial rigidity/ plate's axial rigidity / stiffener's length	107
$\underset{\sim}{s}$	subdomain's geometric matrix (3.108)	125
$\underset{\sim}{S}$	global geometric matrix (3.112)	126
$\underset{\sim}{\bar{S}}^*;\underset{\sim}{\bar{S}}^{**}$	matrices which together form $\underset{\sim}{S}$ Fig.3.10	136
$s^+;s^*;s^-$	ratio of stiffener's rigidity / plate's rigidity / length (5.14)	162
$s_n^+;s_n^*;s_n^-$	quantities given by (5.14)	162
$\vec{T};T_\gamma$	tangent vector to an undeformed contour (1.72)	21
$T^{\gamma\alpha}$	in-plane geometrically linear stress tensor (1.92)	27
$\underset{\sim}{T}^{\gamma\alpha}$	in-plane geometrically linear stress tensor as given by (1.101)	29
$\overset{(o)}{T}{}^{\gamma\alpha}$	in-plane geometrically linear stress tensor corresponding to a unit load system (1.117)	34
t	maximum order of derivatives in a quadratic functional (2.16)	44
	time in (2.118)	72
$\underset{\sim}{t}^*$	matrix used for computations of torsional and geometric matrices for ribs (3.57)	105
$\underset{\sim}{t}^{**}$	any symmetric 4x4 matrix (3.67)	110
$T_{12}^-;T_{12}^+$	discontinuous shearing stresses along stiffeners (3.83)	117
$\underset{\sim}{\bar{T}}$	transformation diagonal matrix (3.92)	121
	in section 5.3, (5.45)	174
$\underset{\sim}{\hat{T}}$	transformation diagonal matrix 32x32 (3.95)	121
$T_{\alpha\beta}^-;T_{\alpha\beta}^+$	stress tensors for the stiffened plate of Fig. 5.1	158
$\vec{U}^*$	displacement vector, initial state	1

$\vec{U}$	increment of the displ. vector at the adjacent state Fig.1.1	1
U^{α}	in-plane displ. components (1.15)	6
$U^{*\gamma}$	prescribed in-plane displ. (1.69)	21
$\hat{U}^{\gamma}$	in-plane displ. at the initial state (1.98)	29
U	real function (2.1)	40
U_n	trial function (2.31)	48
U^*	the adjoint function (2.47)	55
U_n^*	the adjoint trial function (2.54)	56
U_o	exact solution of a minimum problem (2.62)	58
$U^{(j)}$	local trial function (2.125)	77
$U_\alpha^-; U_\alpha^+$	discontinuous displ. along stiffeners Art. 3.4	117
$\underset{\sim}{\overline{U}}$	triangular matrix in Art. 3.6	139
$\vec{V}$	total displ. at the adjacent state Fig.1.1	1
V^{α}	displacement functions (1.14)	6
V	real function (2.1)	40
V_n	sequence of functions with finite energy (2.65)	59
V_o	normalized exact solution to an eigenvalue problem (2.75)	61
V_i	value of the displ. U_1 at the corner i of a subdomain (3.10)	90
V_i^*	value of the displ. U_2 at the corner i of a subdomain (3.14)	94
$\underset{\sim}{\hat{V}}_i$	vector of the parameters at the corner i of a subdomain for the displ. U_1 (uniform mesh)(3.15)	94
$\underset{\sim}{\hat{V}}_i^*$	same as above for displ. U_2	94
$W_2^{(1)}$	indicates the norm in (2.99)	67
$W_2^{(2)}$	indicates the norm in $(2.103)_2$	68
$\underset{\sim}{\overline{W}}_i$	parameters at the corner i of a subdomain for the deflection w (uniform mesh) (3.34)	99

$\overline{\underset{\sim}{W}}_i$	same as above (variable mesh) (3.105)	124
$\underset{\sim}{W}$	auxiliar vector in Art. 3.6	139
$\underset{\sim}{W}_{(k)}$	value of $\underset{\sim}{W}$ at the k^{th} iteration, Art. 3.6	140
W_n	amplitude in (5.32)	171
w_i	value of W_n at nodal lines (5.44)	174
x^i	coordinate system in the deformed position Fig. 1.2	4
X^I	coordinate system, undef. position Fig. 1.2	4
$\vec{X}$	any point on a 2-dimensional domain	40
X_α	local cartesian coordinates (3.7)	89
$\overline{X}_\alpha$	global cartesian coordinates Fig. 3.4	118
$\overline{\underset{\sim}{x}}$	auxiliar vector in Art. 3.6	139
$\vec{Y}_J$	point to be "collocated" (2.35)	49
Y_α	coordinates defined by (3.23)	96
$\overline{\underset{\sim}{Y}};\overline{\underset{\sim}{Y}}^*$	vectors of local parameters for a stiffener placed between nodes 1 and 2 -- the first one is for flexural computations and the second one for torsional (unif. mesh) (3.54)	104
$\overline{\underset{\sim}{Y}}_o;\overline{\underset{\sim}{Y}}^*_o$	same as above (variable mesh) (3.63)	108
Z^I	coordinates in Fig. 1.2	4
$\underset{\sim}{Z}^*$	vector of local parameters in eigenvalue computations (unif. mesh) (3.34)	99
$\underset{\sim}{Z}$	same as above (variable mesh) (3.105)	124
Z_I	cartesian coord. system, Fig. 5.1	158
z_α	coefficients in (5.14)	162
$\overline{\underset{\sim}{Z}}$	vector of 4 constants (5.36)	172
$\alpha_1;\ldots;\alpha_t$	indices	43
$\overline{\alpha}_i$	parameters in an orthogonal expansion (2.130)	79
α_λ	subdomain's length / plate's length (3.22)	96

$\beta_1;\ldots;\beta_K$	indices in (2.16)	44
β	constant in (3.67)	110
β_λ	equal to 1 for uniform mesh and equal to α_λ for variable mesh $(3.68)_5$	111
γ	transv. length / long. length (subdomain)(3.7)	89
$\Diamond$	transv. length/long. length (plate) (3.22)	96
$\underset{\sim}{\Gamma}_i$	integrals in the geometric matrix for ribs $(3.57)_3$	105
δ	symbol of variation	2
δ^R_S	Kronecker's delta tensor (1.7)	5
$\hat{\delta}$	symbol of variation defined in (1.50)	14
$\varepsilon_{\gamma\alpha}$	nonlinear strain measure	
	section 1.2, (1.36)	12
	section 1.2, nonlinear only in w (1.49)	14
	section 1.2, nonlinear only in U^α (1.87)	26
	section 1.3, (1.98)	29
	section 1.4, (1.106)	31
ϵ	a positive small number	42
$\bar{\epsilon}$	defined in the line above (5.45)	174
$\hat{\underset{\sim}{\zeta}}_{\alpha\beta}$	matrix of the integrals (3.25)	97
$\underset{\sim}{\zeta}_{\alpha\beta};\underset{\sim}{\zeta}_{33}$	matrices of the integrals (3.38)	99
$\hat{\zeta}_i$	functions in (5.46) for the plane stress analysis of Fig. 5.1	174
ζ_i	functions (5.42) which are valid for a subdomain in Fig. 5.2	174
$\delta\eta_{\gamma\alpha}$	variation of the strain measure in $(1.28)_2$	10
$\bar{\eta}$	a small quantity	62
	nondimensional coordinate of a plate (5.17)	165
η_i	nondimensional coordinate corresponding to a corner i of the subdomain in Fig. 3.2(c)	92

$\delta\vec{\theta};\delta\theta_\gamma$	rotation vector given by (1.23)	9
	approximation in (1.32)	11
	further approximation in (1.52)	15
$\varkappa_{\gamma\sigma}$	linear bending measure (1.44)	13
$\overset{\wedge}{\varkappa}_{\gamma\alpha}$	linear bending measure for the initial state	30
$\varkappa_n$	constant defined by (5.36)	172
$\lambda(\ldots)$	eigenvalue in (2.28)	47
$\overline{\lambda}$	functional for the Adjoint Variational method (2.51)	55
λ_n	approximate eigenvalue obtained by the Ritz method using n coord. functions (2.81)	62
λ_o	proportional to the reciprocal of the critical load (3.114)	126
$\lambda_{(k)}$	k^{th} iteration in the computation of the smallest eigenvalue	140
$\lambda_1;\lambda_2$	minimum and second smallest eigenvalues (in magnitude) (4.2)	154
$\Lambda_n;\Lambda_n^+$	transformation matrices defined by (5.19)	165
$\delta\mu_{\gamma\alpha}$	nonlinear in-plane measure (1.28)	10
$\overset{\wedge}{\mu}_{\gamma\alpha}$	nonlinear in-plane measure for the initial state (1.124)	37
μ_i	integers defined by (5.26)	168
ν	Poisson's ratio (1.66)	20
ν_n	constants depending on the integer n (5.3)	159
$\varkappa\varepsilon_{\gamma\alpha}$	strain measure in (1.36)	12
ξ	defined in (2.16) for use in (2.17)	44
	nondimensional coordinate (3.7)	89
ξ_i	nondimensional coord. at the corner i of a subdomain (3.8)	90
$\overline{\xi}$	nondimensional global coord. (5.17) Fig.5.2	165
$\overline{\xi}_i$	nondimensional coord. at nodal line i, Fig.5.2	170

$\pi(\ldots)$	potential energy functional (1.1)	2
$\pi_1;\pi_2$	first and second variation of the functional π	2
$\delta\pi_o$	virtual work of external forces (1.26)	10
$\hat{\pi}_o$	potential energy of a flat plate (3.1)	87
$\Delta\hat{\pi}_o$	in-plane strain energy of a flat rectangular subdomain (3.21)	96
$\Delta\pi_o$	flexural energy of a rectangular subdomain (3.39)	100
$\pi_{(i)\lambda}$	strain energy expressions for ribs (3.68)	110
$\hat{\pi}_{(1)\lambda}$	axial strain energy expressions for ribs (3.68)	110
$\delta\hat{\pi}^*_o$	total in-plane virtual work for a stiffened plate (3.100)	123
$\delta\pi^*_o$	total flexural virtual work for a stiffened plate (3.110)	125
ρ_1	integers given by (5.26)	168
$\sigma^{\gamma\alpha}$	stress tensor for flat plates (1.83)	25
$\hat{\sigma}^{\gamma\alpha}$	stress tensor corresponding to nonlinear in-plane strain measures for the initial state (1.97)	28
$\sigma_1;\ldots;\sigma_6$	constants in (3.51)	103
$\sum_{\Delta\Omega}$	the sum is taken for all subdomains	123
$\sum_{long}$	the sum is taken for all longitudinal stiffeners (3.100)	123
$\sum_{tran}$	the sum is taken for all transversal stiffeners	123
$\sigma^+;\sigma^-$	stress at the longitudinal edges of the plate in Fig. 5.1	158
σ^+_n	terms in the Fourier expansion of σ^+ (5.2)	159
σ_o	constant term in the Fourier expansion of σ^+	159
$\tau^{\gamma\alpha}$	increment of the in-plane nonlinear stress tensor at the adjacent state (1.97)	28
τ_λ	axial force in stiffeners (3.82)	117

$\tau^+;\tau^-$	shearing stress at the top and the bottom of the plate in Fig. 5.1	158
τ_n^+	terms in the Fourier expansion of τ^+ (5.2)	159
τ^*	axial force in an intermediate longitudinal stiffener (5.20)	165
$\underset{\sim}{\hat{U}}_i$	vector of the parameters involving the displacement U_1 at a corner i of a subdomain belonging to a variable mesh (3.90)	120
$\underset{\sim}{\hat{U}}{}^*_i$	same as above for displ. U_2	120
$v_1;v_2$	constants defined by (5.14)	162
φ_i	coordinate functions (2.31)	48
$\varphi_i^{(j)}$	local coordinate functions for the subdomain Ω_j (2.125)	77
$\underset{\sim}{\varphi}$	vector of coordinate functions (3.17)	95
$\varphi_i^+;\varphi_i^-$	elements of the stress functions (5.11) for a rectangular plate divided in two rectangles	161
$\underset{\sim}{\chi}$	value of a bicubic function between nodes 1 and 2 (3.53)	104
$\underset{\sim}{\chi}{}^*$	value of a bicubic function between nodes 2 and 4 (3.78)	116
ψ_j	weighting functions in the method of weighted residuals (2.32)	48
$\bar{\psi}$	function which satisfy homogeneous geometric B.C. (2.57)	57
ψ	Airy's stress function (2.136)	81
$\psi^+;\psi^-$	Airy's stress functions (5.8) for the upper and lower regions of the plate in Fig. 5.1	158
Ω	undeformed surface (1.14)	6
Ω_o	deformed surface (1.14)	37
Ω_j	area of a subdomain (2.37)	49
$\bar{\Omega}$	area of a domain including its boundary	63
ω	normal deflection to the plate's undeformed middle surface	6

ω^*	normal deflection ω prescribed on C_2 (1.69)	21
$\hat{\omega}$	normal deflection at the initial deformed state $(1.106)_2$	31
ω_n	sequence of functions complete in energy (2.78)	62
ω_o	exact solution to a linear eigenvalue problem (2.111)	70
$\Delta\Omega$	area of a subdomain (3.21)	96

Structural Research Laboratory

Technical University of Copenhagen, Denmark

REPORTS

R 1.	Askegaard, Vagn and P. Thoft-Christensen: Spændingsoptiske lag og tøjningsmålere. 1967.	Out of print
R 2.	Møllmann, H.: The Principle of Virtual Work for Continuous Systems Derived by a Direct Method. 1968.	
R 3.	Askegaard, Vagn: Production and Application of Model Materials with Desired Physical Constants. 1968.	
R 4.	Møllmann, H.: The Analysis of Shallow Cables. 1968.	
R 5.	Dyrbye, Claës: Damped Vibrations of Slender Beams. 1968.	Out of print
R 6.	Møllmann, H.: Analysis of Plane Prestressed Cable Structures. 1969.	
R 7.	Nielsen, Leif Otto: Beregning af bjælker og rammer dynamisk påvirket ud over det elastiske område. 1968.	Out of print
R 8.	Bræstrup, Mikael W.: On the Theory of Plastic Plates. 1969.	Out of print
R 9.	Nielsen, Leif Otto: Uniqueness Problems and Minimum Principles in the Dynamic Theory of Plasticity. 1969.	Out of print
R 10.	Byskov, Esben: Two Nearly Polygonal Holes. Mathematical Crack Problems. 1969.	
R 11.	Bræstrup, Mikael W.: The Cosserat Surface and Shell Theory. 1970.	Out of print
R 12.	Askegaard, Vagn: Anvendelse af modelanalyse. 1970.	
R 13.	Solnes, Julius: The Spectral Character of Earthquake Motions. 1970.	Out of print
R 14.	Bræstrup, Mikael W.: Yield Lines in Discs, Plates and Shells. 1970.	Out of print
R 15.	Møllmann, H.: Beregning af hængekonstruktioner ved hjælp af deformationsmetoden. 1970.	Out of print
R 16.	Byskov, Esben: The Calculation of Stress Intensity Factors Using the Finite Element Method with Cracked Elements. 1970.	

R 17.	Askegaard, V.: Grundlaget for adhæsion. 1970.	
R 18.	Summaries of Lecture Notes on Experimental Stress Analysis. 1970.	
R 19.	Sørensen, Hans Christian: Forskydning i jernbetonbjælker. 1970.	
R 20.	Sørensen, Hans Christian: Forskydningsforsøg med 12 jernbetonbjælker med T-tværsnit. 1971.	
R 21.	Møllmann, H.: Analysis of Hanging Roofs Using the Displacement Method. 1971.	Out of print
R 22.	Haurbæk, Poul E.: Dæmpede svingninger i spændbetonbjælker. Svingningsforsøg med simpelt understøttede bjælker. 1971.	Publication pending
R 23.	Bræstrup, M.W.: Yield-line Theory and Limit Analysis of Plates and Slabs. 1971.	
R 24.	Dyrbye, Claës: Pendulum Vibrations. 1971.	Out of print
R 25.	Møllmann, H.: Analytical Solution for a Cable Net over a Rectangular Plan. 1971.	
R 26.	Nielsen, J.: Silotryk. 1972.	
R 27.	Askegaard, V., M. Bergholdt and J. Nielsen: Problems in connection with pressure cell measurements in silos. 1972.	
R 28.	Ramirez, H. Daniel: Buckling of plates by the Ritz method using piecewise - defined functions. 1972.	
R 29.	Thomsen, Kjeld & Henning Agerskov: Behaviour of butt plate joints in rolled beams assembled with prestressed high tensile bolts. 1972.	
R 30.	Julius Solnes and Ragnar Sigbjörnsson: Structural response to stochastic wind loading. 1972.	